GIOVANNE B. DINIZ

Morfologia comparada do sistema do hormônio concentrador de melanina

Tese apresentada ao Programa de Biologia de Sistemas do Instituto de Ciências Biomédicas da Universidade de São Paulo, para obtenção do Título de Doutor em Ciências

São Paulo
2019

GIOVANNE B. DINIZ

Comparative morphology of the melanin-concentrating hormone system

Thesis presented to the Graduate Program in Systems Biology of the Biomedical Sciences Institute of the University of São Paulo for the attainment of Ph. D. title.

São Paulo
2019

GIOVANNE B. DINIZ

Morfologia comparada do sistema do hormônio concentrador de melanina

Tese apresentada ao Programa de Biologia de Sistemas do Instituto de Ciências Biomédicas da Universidade de São Paulo, para obtenção do Título de Doutor em Ciências.

Área de concentração: Programa de Pós-Graduação em Biologia de Sistemas

Orientador: Prof. Dr. Jackson Cioni Bittencourt

Versão original.

São Paulo
2019

CATALOGAÇÃO NA PUBLICAÇÃO (CIP)
Serviço de Biblioteca e informação Biomédica
do Instituto de Ciências Biomédicas da Universidade de São Paulo

Ficha Catalográfica elaborada pelo(a) autor(a)

Diniz, Giovanne Baroni
Morfologia comparada do hormônio concentrador de melanina / Giovanne Baroni Diniz; orientador Jackson Cioni Bittencourt. -- São Paulo, 2019.
171 p.

Tese (Doutorado)) -- Universidade de São Paulo, Instituto de Ciências Biomédicas.

1. Neurociência. 2. Neuroanatomia. 3. Evolução comparada. 4. Hipotálamo. 5. MCH. I. Bittencourt, Jackson Cioni, orientador. II. Título.

UNIVERSIDADE DE SÃO PAULO
INSTITUTO DE CIÊNCIAS BIOMÉDICAS

Candidato(a): Giovanne B. Diniz

Título da Tese: Morfologia comparada do sistema do hormônio concentrador de melanina

Orientador: Prof. Dr. Jackson Cioni Bittencourt

A Comissão Julgadora dos trabalhos de Defesa da Tese de Doutorado, em sessão pública realizada a _____/_____/2019, considerou o(a) candidato(a):

( ) Aprovado(a) ( ) Reprovado(a)

Examinador(a): Assinatura: .....
Nome: .....
Instituição: .....

Examinador(a): Assinatura: .....
Nome: .....
Instituição: .....

Examinador(a): Assinatura: .....
Nome: .....
Instituição: .....

Examinador(a): Assinatura: .....
Nome: .....
Instituição: .....

Presidente: Assinatura: .....
Nome: .....
Instituição: .....

UNIVERSIDADE DE SÃO PAULO
INSTITUTO DE CIÊNCIAS BIOMÉDICAS

Cidade Universitária "Armando de Salles Oliveira"
Av. Prof. Lineu Prestes, 2415 – CEP. 05508-000 São Paulo, SP Brasil
Telefone :(55) (011) 3091.7733 – e-mail: cep@icb.usp.br

CERTIFICADO

Certificamos que o protocolo registrado sob nº **96** nas fls. **22** do livro **03** para uso de animais em experimentação, sob a responsabilidade do Prof(a) Dr(a) **Jackson Cioni Bittencourt,** Coordenador (a) da Linha de pesquisa "*Caracterização anatômica dos subtipos 1 e 2 do receptor do hormônio concentrador de melanina (MCHR) no sistema nervoso central de ratos e camundongos MCHR2-GFP-KI*" do qual participam o(s) aluno(s) **Giovanne Baroni Diniz** está de acordo com os Princípios Éticos de Experimentação Animal adotado pela Sociedade Brasileira de Ciência de Animais de Laboratório (SBCAL) e foi aprovado pela *COMISSÃO DE ÉTICA NO USO DE ANIMAIS* (CEUA) em **25.08.2014, com validade de 4 anos**.

São Paulo, 25 de agosto de 2014.

Prof. Dr. ANDERSON DE SÁ NUNES
Vice- Coordenador- CEUA- ICB/USP

Profa. Dra. ANA PAULA LEPIQUE
Secretária- CEUA - ICB/USP

ICB USP

Cidade Universitária "Armando de Salles Oliveira", Butantã, São Paulo, SP - Av. Professor Lineu Prestes, 2415 - ICB III - 05508 000
Comissão de Ética no Uso de Animais - Telefone (11) 3091-7733 - e-mail: cep@icb.usp.br

Decl. CEUA.153.2018

DECLARAÇÃO

Em adendo ao Certificado nº **96/2014/CEUA**, renovado até 25/08/2022, aprovo a inclusão dos animais abaixo indicados ao Protocolo "***Caracterização anatômica dos subtipos 1 e 2 do receptor do hormônio concentrador de melanina (MCHR) no sistema nervoso central de ratos e camundongos MCHR2-GFP-KI***", de responsabilidade do Prof. Dr. **Jackson Cioni Bittencourt**, do Departamento de Anatomia, conforme descrição da solicitação:

Espécie	Linhagem	Sexo	Idade ou peso	Quantidade
Camundongo	C57BL/6	Macho	2 meses	20
Camundongo	C57BL/6	Fêmea	2 meses	75
Rato	Sprague-Dawley	Fêmea	2 meses	20
Rato	Sprague-Dawley	Macho	2 meses	10

São Paulo, 25 de setembro de 2018.

Luciane Valéria Sita

Profa. Dra. **Luciane Valéria Sita**
Coordenadora da CEUA-ICB/USP

To Robert
Semper Fidelis

ACKNOWLEDGEMENTS

I would like to acknowledge all those who participated in this enterprise. Contributions to this Thesis came in many different shapes and sizes, some sharing knowledge and helping me grow as a professional, some providing the emotional support that an undertaking like this requires. Although they are too many to be named individually, I hope those who have touched this Thesis and my life will feel reassured of my everlasting gratitude.

First and foremost, I would like to thank the wonderful mentors I've had since I started my journey. **Prof. Jackson C. Bittencourt** has been a steady guide and friend for the past seven years. Trusting and caring, he has given me room to grow and a direction to follow, setting the example of what an academic should be. Although the completion of this Thesis represents the end of a cycle, our academic careers are inevitably intertwined, and we will continue to collaborate for many years to come. I must also thank my other supervisor, **Prof. Harry W. M. Steinbusch**, who has given me a once-in-a-lifetime opportunity to develop a second Ph.D. Thesis under his supervision at Maastricht University, the Netherlands. In addition to the fascinating cultural exchange that this opportunity allowed me, it was humbling to present my work in one of the best Universities of Europe. Another mentoring figure that must be mentioned is **Prof. Jean-Louis Nahon**, who has taken me under his wing while I was living in France and contributed so much to my personal and professional growth in that period. I would also like to thank **Prof. Anthony N. van den Pol** for his invitation to join his team at the Yale School of Medicine in the next phase of my career, challenging me to learn new methods and ask new questions. Finally, I would like to thank **Prof. Luciane V. Sita** who, although not an official supervisor, has definitely stepped up to that role, teaching me about science, ethics, and education. As a close friend, her presence is dearly missed.

This Thesis would certainly be impossible without the help of my lab colleagues. Particular gratitude goes to **Dr. Daniella S. Battagello**, with whom I've been working side by side for the past 7 years, and who is an example of work ethics, effort, and kindness. Although I haven't known **Drs. Livia C. Motta-Teixeira and Marianne O. Klein** for as long as I know Dr. Battagello, they have both been incredible colleagues and extremely accomplished researchers, with whom I'm truly honored to collaborate with. Even more important that our shared research time, however, is the fun we had together, in Brazil and abroad. Since fun has been mentioned, I would also like to thank **Ms. Erica O. Barbeiro,** who has brightened up the laboratory with her humor during her time in the lab. Other important lab colleagues whom I was lucky to work with include: **Dr. Jozélia G. P. Ferreira, Mr. Renato D. Alvisi, Ms. Jéssica C. G. Duarte, Ms. Jully Martins, Ms. Jéssica Betteto, Ms. Isis Fieri, Mr. Paulo L. Candido, and Mr. Pedro M. Cherubini.** I would also like to thank several other co-authors and collaborators who contributed directly or indirectly with our publications: **Prof. Paul E. Sawchenko** (The Salk Institute, USA), **Prof. Carol Elias** (University of Michigan, USA), **Dr. Françoise Presse** (IPMC, France), **Prof. Teresa Morales** (UNAM, Mexico), **Prof. Antoine Adamantidis** (INSELPITAL, Switzerland), **Prof. Melissa Chee** (Carleton University, Canada)**, Prof. José A. C. Horta-Junior** (UNESP), **Prof. Claudio A. Casatti** (UNESP), **Prof. Luciano F. Felicio** (FMVZ), **Prof. Gilberto F. Xavier** (IB), **Prof. Bruno F. de Souza** (FMUSP), **Prof. José Cipolla-Neto** (ICB), **Prof. Newton S. Canteras** (ICB), **Prof. Claudimara F. P. Lotfi** (ICB), **Prof. Patricia Castelucci** (ICB), **Prof. Ii-Sei Watanabe** (ICB), **Dr. Carlos A. S. Haemmerle**, **Dr. Carla M. Machado,** and **Ms. Dailiany Orechio**.

I would like to acknowledge present and past members of evaluation committees who evaluated my work, and whose suggestions and criticisms allowed many of my writings to reach the quality level necessary for publication: **Prof. Lucila L. K. Elias** (FMRP)**, Prof. Fernando R. M. Abdulkader** (ICB)**, Prof. Ruy G. Jaeger** (ICB)**, Prof. Simone C. Motta** (ICB)**, Prof. Renata Frazão** (ICB)**,** and **Prof. Camila S. Dale**

(ICB). I would also like to recognize the importance of several institutional organizations to this work: the **Graduate Program in Systems Biology**, and in particular **Prof. Maria Luiza M. Barreto-Chaves**; the **Department of Anatomy** and its clerical staff; the **Institute of Biomedical Sciences** and its clerical staff; and the **University of São Paulo**.

Last, but certainly not least, I must thank the wonderful individuals who compose my support network. My parents, **Mr. Adaberio C. Diniz** and **Ms. Isaltina B. Diniz**, whose unconditional love has inspired me to strive to be the best version of me. My interests in science and knowledge were born at home. To my friends, **Mr. João Paulo V. C. da Silva**, **Ms. Raissa F. S. Matos**, **Mr. Gabriel C. R. T. de Almeida**, **Ms. Ana Cláudia Ferreira dos Santos**, and **Mr. Ricardo P. Bindi**, I express my gratitude for the excellent time we have spent together, taking my mind away from problems when times got hard, and allowing me to see things with much more clarity. Finally, I want to thank **Mr. Robert W. Galm** for his unabating love and companionship, for giving me strength when mine falters, and shelter when it's pouring.

FINANCIAL SUPPORT

The experimental investigations and the writing of this Thesis would not be possible without financial aid from the São Paulo Research Foundation (FAPESP), grants #2016/02748-0, #2016/02224-1 and #2017/08908-2. Additional support was provided by the Brazilian Coordination for the Improvement of Higher Education Personnel (CAPES), grant CAPES/COFECUB #848/15, and by the Brazilian National Council for Scientific and Technological Development (CNPq), grant #426378/2016-4. I would also like to thank the Society for Neuroscience (SfN), the International Brain Research Organization (IBRO), and the Grass Foundation for supporting my professional development.

"Gentleman, instead of promising to satisfy your curiosity about the anatomy of the brain, I intend here to make the sincere, public confession that this is a subject on which I know nothing at all"

Opening words of the "Discours sur l'anatomie du cerveau",
delivered by **Nicolaus Steno** in 1669

RESUMO

Diniz GB. Morfologia comparada do sistema do hormônio concentrador de melanina. [Tese (Doutorado em Biologia de Sistemas)] – Instituto de Ciências Biomédicas, Universidade de São Paulo, São Paulo; 2019.

O sistema do hormônio concentrador de melanina (MCH) consiste em três genes: *Pmch, Mchr1, e Mchr2*, e nas proteínas originadas desses três genes: MCH, Neuropeptídeo E-I (NEI), Neuropeptídeo G-E, e os dois subtipos de receptores de MCH, MCHR1 e MCHR2. O sistema neuropeptidérgico do MCH tem sido implicado em diversos papéis fisiológicos, tais como a integração e promoção de comportamentos motivados, incluindo reprodução e comportamento maternal, e sono. Uma melhor compreensão dos elementos que compõem o sistema do MCH pode nos ajudar a entender melhor como ele executa essas funções. Um possível método para se obter isto é comparar diferentes espécies, identificando elementos em comum e divergências que podem nos informar sobre as correlações morfofuncionais conservadas, e sobre a evolução de neuromoduladores como um todo. No Capítulo 1, uma introdução mais extensiva sobre o MCH é providenciada. No Capítulo 2, nós conectamos o racional por trás de cada trabalho apresentado nesta tese, com um foco nas perspectivas deste campo de investigação. No Capítulo 3, empregamos imuno-histoquímica para investigar a distribuição de MCH e NEI no sistema nervoso central de três espécies diferentes de muroides: ratos (*Rattus novergicus*), camundongos (*Mus musculus*), e camundongos vulcânicos Mexicanos (*Neotomodon alstoni*). Também empregamos camundongos fêmeas em diferentes estágios do ciclo reprodutivo para identificar correlações entre a distribuição de MCH e sua função em fêmeas. No Capítulo 4, identificamos um anticorpo comercial que seletivamente marca MCHR1. Esse anticorpo foi então utilizado para mapear a distribuição de MCHR1 no prosencéfalo de ratos (machos) e camundongos (machos e fêmeas em todos os estágios do ciclo estral). Algumas áreas onde o MCHR1 foi encontrado foram utilizadas para caracterização neuroquímica. No Capítulo 5, propusemos uma normatização para a nomenclatura do MCH, e revisamos os dados disponíveis para o sistema do MCH em um grande número de espécies. Esta análise nos permitiu traçar paralelos entre a evolução do MCH e eventos genômicos de larga-escala que ocorreram na linhagem dos vertebrados. No Capítulo 6, sumarizamos os principais pontos encontrados neste trabalho. Em resumo, nossos resultados mostram que, apesar das tímidas diferenças entre machos e fêmeas, há substancial diferença entre espécies, mesmo entre espécies próximas, impossibilitando a extrapolação de dados obtidos em animais-modelo sem que haja verificação experimental prévia. Nossos resultados também sugerem que mecanismos de transmissão por volume – incluindo a liberação de MCH livre no líquor e no espaço extracelular – podem desempenhar um importante papel na função normal do sistema do MCH. Acreditamos que os dados obtidos neste trabalho avançam nossa compreensão sobre o MCH e podem ser usados como guia para outros projetos de pesquisa.

Palavras-chave: Neurociência. Neuroanatomia. Evolução comparada. Hipotálamo. MCH.

ABSTRACT

Diniz GB. Comparative morphology of the melanin-concentrating hormone system. [Thesis (Ph.D. thesis in Systems Biology)] – Instituto de Ciências Biomédicas, Universidade de São Paulo, São Paulo; 2019.

The melanin-concentrating hormone (MCH) system consists of three genes: *Pmch, Mchr1* and *Mchr2*, and the proteins originated from these three genes, namely: MCH, Neuropeptide E-I (NEI), Neuropetide G-E, and the two subtypes of MCH receptors, MCHR1 and MCHR2. The MCH neuropeptidergic system has been involved in several physiological roles, such as the integration and promotion of motivated behaviors, including reproduction and maternal behavior, and sleep. A better comprehension of the elements that comprise the MCH system may help us understand how it executes the aforementioned roles. One possible approach to achieve this is to compare different species, identifying commonalities and divergences that may inform us about conserved morphofunctional correlates, and about the evolution of neuromodulators as a whole. In Chapter 1, a more extensive introduction about the MCH system is provided. In Chapter 2, we connect the reasoning behind each work presented in this thesis, with a focus on the perspectives of the field. In Chapter 3, we employed immunohistochemistry to investigate the distribution of MCH and NEI in the central nervous system of three different species of muroids: rats (*Rattus novergicus*), mice (*Mus musculus*), and Mexican volcano mice (*Neotomodon alstoni*). We also employed female mice in different stages of the reproductive cycle to identify correlates between MCH distribution and function in females. In Chapter 4, we identified a commercial antibody that selectively labels MCHR1. This antibody was then used to map the distribution of MCHR1 in the prosencephalon of rats (male) and mice (males and females in all stages of the estrous cycle). Some areas where MCHR1 was detected were selected for further neurochemical characterization. In Chapter 5, we proposed a normalization for the nomenclature of MCH and reviewed the available data on the MCH system for a large number of species. This analysis allowed us to draw parallels between the evolution of MCH and large-scale genomic events that occurred in the vertebrate lineage. In Chapter 6, we summarize the main points of this work. In summary, our results show that, despite timid differences between males and females, there are substantial interspecies differences, even between closely related species, precluding the extrapolation of data obtained in animal models without experimental verification. Our results also suggest that volume transmission mechanisms - including the release of free MCH in the cerebrospinal fluid and extracellular space – may play an important role for the normal function of the MCH system. We believe the data obtained in this work furthers our comprehension of MCH and may be used to guide other research projects.

Keywords: Neuroscience. Neuroanatomy. Comparative evolution. Hypothalamus. MCH.

TABLE OF CONTENTS

Chapter 1

Introduction

1 INTRODUCTION

As a cornerstone of vertebrate evolution, a centralized nervous system has been a constant after the emergence of *phylum Chordata*. Among the most basal structures of this central nervous system (CNS) is the hypothalamus, as its homologous structures are found even in early-diverging chordates, such as cephalochordates and tunicates (1). The hypothalamus has been fundamentally conserved for its role in the maintenance of body homeostasis. This cardinal role cannot be executed without an enormous associated complexity since each organism finds diverse environmental challenges during their lifetime and must respond appropriately to each one of them. It is natural, therefore, that animals with a more robust hypothalamus, capable of a broader spectrum of responses, will have a fitness advantage against their peers, what resulted in a remarkable development in hypothalamic complexity regarding its spatial organization, connectivity, and chemical composition.

In the current scheme of parcellation employed by most atlas, approximately all the hypothalamus comprehended between the fornix and the internal capsule and between the optic chiasm and the mammillary bodies is considered part of the lateral hypothalamic area (LHA) (2-4), closely following the definition of lateral hypothalamus provided by Gurdjian (5). The LHA is also known as the bed nucleus of the medial forebrain bundle (mfb), the largest rostrocaudal tract of fibers in the prosencephalon (6, 7), as mfb fibers are found intermingled with LHA neurons (8, 9). This confers a remarkable connectivity to the LHA, which can send and receive projections from virtually all areas within the CNS. Although a great effort has been made to comprehend the LHA, this region still stands as one of the least understood aspects of the hypothalamus (10).

In addition to its complex hodology, the LHA contains a large number of neuronal populations characterized by different neurochemical markers (11). Various neuromodulators are synthesized by neurons within the LHA, such as melanin-concentrating hormone (MCH) (12), orexins (13), cocaine- and amphetamine-regulated transcript (14), neurokinin B (15), and galanin (16). These different neuronal populations are found intermingled with a complex population of GABAergic and glutamatergic interneurons (17). Although all these neuromodulators play essential roles in maintaining the normal function of the organism, MCH stands out for the full range of roles it has been associated with in vertebrate physiology.

1.1 Melanin-concentrating hormone

The MCH system consists of three genes: *Pmch, Mchr1* and *Mchr2*, and the proteins originated from these three genes (as reviewed in Bittencourt and Diniz (18)). The *Pmch* gene encodes the MCH precursor, which is 165 amino acids (aa)-long in rodents. This precursor contains a signal peptide of 21 aa, necessary for protein targeting, followed by a structural chain of 144 aa, and three peptides: neuropeptide G-E (NGE), a linear peptide with 19 aa; neuropeptide E-I (NEI), a linear peptide with 13 aa; and MCH, with 19 aa and cyclic structure (19, 20). The generation of the mature forms of these peptides depends on the actions of endopeptidases that act on dibasic sites, in a mechanism that is not entirely understood (21). While the synthesis of MCH and NEI has been thoroughly demonstrated (21), NGE remains as a predicted peptide, without any available evidence of its actual synthesis by neurons or biological activities. Therefore, for the purposes of this work, the term "MCH peptidergic system" refers mainly to MCH and its receptors and NEI.

The rat (*Rattus novergicus*) has been the preferred animal model for morphological studies on MCH and NEI. In this species, MCH neurons are found predominantly in the diencephalon, including the medial and lateral LHA, the incerto-hypothalamic area, the dorsomedial and posterior hypothalamic areas, and the *zona incerta*. Smaller groups are found outside the diencephalon, such as in the olfactory tubercle, pontine reticular formation, and laterodorsal tegmental nucleus (12, 18, 22). An additional group of MCH cells is observed exclusively in the preoptic hypothalamus of lactating females (23-27). Dissimilar to the exceptionally restricted pattern of MCH synthesis, MCH-ir fibers are found widespread throughout the whole CNS. Regions that contain fibers include olfactory areas, the septal nuclei, the basal nuclei, the hippocampal formation, the neocortex, several diencephalic nuclei, the mesencephalic and pontine reticular formation, the periaqueductal gray matter, and all levels of the spinal cord (12, 28-33).

While the rat has been the focus of morphological and hodological studies, mice (*Mus musculus*) have been extensively used to probe the function of MCH neurons. The most well-described roles of MCH include the integration of information to coordinate motivated behaviors (reviewed in Diniz and Bittencourt (34)) and sleep (reviewed in Ferreira et al. (35) and Gao (36)). However, MCH has also been implicated in several other functions, including emotion and stress response (37), sexual physiology (38), learning and memory consolidation (39, 40), and ventricular homeostasis (41). Despite the extensive knowledge obtained about MCH, attempts to leverage the MCH system as a pharmacological target have largely failed (42, 43). Some of the difficulties in turning the MCH system into a pharmacological option

may result from the disconnection between animal models used to obtain morphological and functional data.

An additional function has been associated with MCH: the control of skin color in vertebrates that display adaptive color change (44). Melanin-concentrating hormone released into the circulation acts as a pallor-promoting agent at melanophores in the skin (45). The development of MCH as a neurohormone in teleosts occurred concomitantly with the appearance of MCH-immunoreactive neurons in the lateral hypothalamus of those animals (46). Few attempts have been made, however, to conciliate the evolution of MCH in teleosts with other clades and, in particular, mammals. It is also unclear how MCH has originated in the vertebrate lineage.

1.2 The melanin-concentrating hormone receptors

Melanin-concentrating hormone binds to two different receptors, commonly termed MCHR1 and MCHR2 in the literature. Both receptors show typical characteristics of G protein-coupled receptors (GPCRs), such as seven transmembrane domains, a DRY motif between transmembrane domain 3 and the second intracellular loop and an Asp-linked glycosylation region near the N-terminus. Rat MCHR1 is a 353 aa-long protein, with 91% sequence identity between rats and humans (47, 48). The actions of MCHR1 are selective to $G_{i/o}$ and G_q subunits, with a predominantly inhibitory effect (49, 50). Significantly less is known about MCHR2, because this receptor was lost in the *Glires* clade (including lagomorphs – rabbits and pikas - and rodents), limiting the number of animal models available for its study (51). Through the use of MCHR1 antagonists and knockout animals, essential roles for this receptor in feeding behavior and energy expenditure have been revealed (52-54). Other works have also implicated MCHR1 in mood regulation (55) and the control of ciliary beating (41).

While the distribution of *Mchr1* expression has been investigated in both rats and mice (56-59), a single work has attempted to map immunoreactivity to MCHR1 in the CNS of male rats (56). Expression of *Mchr1* is found in several areas of the murine CNS, including olfactory areas, the cerebral cortex, striatum, hippocampal formation, amygdala, several thalamic and hypothalamic nuclei, and discreet regions of the midbrain and hindbrain, but no consensus exists among published works (56-59). Contrasting to the wealth of information obtained about *Mchr1* expression, the single mapping available for MCHR1 immunoreactivity is hard to interpret, in particular in light of recent developments in our knowledge about the subcellular localization of MCHR1.

Hervieu et al. (56) report that labeling to MCHR1 is localized to the cellular membrane. Gao and van den Pol (17) suggest that MCHR1 is found in the presynaptic membrane, based on the property of MCH to decrease the frequency of miniature glutamate-mediated postsynaptic currents in the presence of tetrodotoxin. Berbari et al. (60), on the other hand, were the first to find MCHR1 in the neuronal primary *cilia* of transfected cultured cells and slices of mice brains, observation replicated in rats using the same antibody (61) . The neuronal primary *cilium* is a sensory structure, a single non-motile *cilium* that extends from the membrane towards the extracellular space (ECS) and is often coated in receptors (62). It is believed that neuronal primary *cilia* play a major role in volume transmission (VT), a mode of communication employed by some neurons where neurochemical messengers are released in the cerebrospinal fluid (CSF) or the ECS, rather than at the synaptic cleft (63). Since MCH has been suggested to employ VT to modulate feeding behavior (64), it is important to understand what role is played by the receptor in this VT paradigm.

1.3 Aims and outline of this thesis

Given the full range of functions played by MCH in maintaining the correct function of the organism, the disconnection between animal models used to study its morphology and its physiology, the lack of a complete mapping on the distribution and subcellular localization of MCHR1, and the few attempts to conciliate the data obtained in different clades of vertebrates, we proposed in this work to study the morphology and hodology of the MCH peptidergic system in mice, in addition to the distribution of MCHR1 in both rats and mice.

In **Chapter 2**, we describe the relationship between the articles that make up this thesis, integrating the knowledge obtained in each work in a unified framework of interpretation, and applying such framework on our current knowledge about the MCH system.

In **Chapter 3**, we employed immunohistochemical methods to investigate the distribution of MCH immunoreactivity in three muroid species: *R. novergicus*, *M. musculus*, and the Mexican volcano mouse (*Neotomodon alstoni*). By identifying differences in the synthesis of MCH between rats and mice, we may better understand the functional discrepancies reported in the literature. Furthermore, the comparison between murines and a distant relative, the Mexican volcano mouse (Cricetidae), can provide us with insights on the plasticity of neuromodulatory systems, and to what extent we can extrapolate data between species.

In **Chapter 4**, we identified a commercial antibody that can be used to locate MCHR1 immunoreactivity with high specificity. Employing that antibody, we verified that MCHR1 is widely colocalized with a neuronal primary *cilium* marker in the murine CNS, and that several areas related to previously indicated functions of MCH contain ciliary MCHR1, including several distinct neurochemical populations within some of those areas. These results suggest that VT may play an important role in normal MCH function. Although no sex-linked differences were observed, we identified some differences between rats and mice, indicating that there is a certain degree of plasticity in the MCH receptors between species.

In **Chapter 5**, we systematically compare the MCH peptidergic system among vertebrates, including the genetic composition of the MCH system, amino acid sequence changes, and the morphological distribution of MCH-synthesizing neurons and their fibers, in an attempt to identify critical events in the evolution of the MCH system. We also propose a standardization for the nomenclature of elements belonging to the MCH system. By overlaying the evolution of MCH with broader genetic events, we can better understand how hypothalamic neuromodulatory systems evolved, and how they may have contributed to the increasing complexity of the nervous system in extant species.

In **Chapter 6**, we discuss the main conclusions obtained in the aforementioned works, with a focus on the perspectives of the field.

Chapter 2

The Relationship Between The Articles That Make Up This Thesis

2 THE RELATIONSHIP BETWEEN THE ARTICLES THAT MAKE UP THIS THESIS

When taken together, the articles here presented aimed to characterize several underexamined aspects of the MCH system, namely: its degree of conservation in muroid species; the existence of sexual dimorphisms; the subcellular localization of MCH, NEI, and MCHR1; the connectivity pattern of MCH|NEI neurons in mice, and how it compares to the model distribution of rats; the neurochemical structure of the lateral hypothalamic area, which harbors this peptidergic population; the distribution of ciliary MCHR1 and the neurochemical characterization of MCHR1-ir *cilia*-containing neurons; the origins of the MCH system in vertebrates; and how MCH evolved to display the current neuroanatomical organization observed in extant species.

After the orexigenic properties of MCH were discovered by Qu et al. (65), a vast effort has been poured to turn the MCH system into a reliable pharmacological target. These attempts have been mostly unsuccessful, as treatments with MCHR1 antagonists frequently result in unexpected side-effects, what severely undermined the therapeutic potential of this system (42, 43). In a natural response, a wealth of data pertinent to the MCH system has been generated, associating this peptide to an increasing number of roles; yet, several fundamental questions about this system remain unanswered. The data obtained in this work provides valuable insights into the widespread actions of MCH, which may be used as a starting point for future works to try to target specific parts of the MCH system.

2.1 Interspecies differences in MCH distribution

An interspecies analysis of the MCH system, in this work performed using members of the Muroidea superfamily, reveals an intricate pattern of evolution that combines highly conserved cellular aspects with somewhat divergent anatomical conformations. Among the conserved cellular aspects of this system we may list: 1. extensive cosynthesis between MCH and NEI; 2. the existence of multipolar/fusiform/crescent subtypes of MCH neurons; 3. the lack of colocalization between MCH|NEI and ORX; 4. the segregation of MCH and NEI in different subcellular compartments; 5. presence of abundant varicosities along axonal projections of MCH|NEI neurons; and 6. the neuronal primary *cilia* as a major site of MCHR1 localization.

In contrast to the conserved cellular characteristics, the distributions of MCH|NEI and MCHR1 are less conserved between muroid species. The differences observed in the distribution of MCH-ir cells can be grouped into extra-diencephalic and diencephalic. Rats have several extra-diencephalic groups that have not

been observed in other members of Euarchontoglires, including the olfactory tubercle, the paramedian pontine reticular formation, and the laterodorsal tegmental nucleus. Although it is possible that the synthesis of MCH in these areas was acquired after the divergence of the *Rattus* lineage, it is more likely that studies in other species did not reach the threshold for detection that Bittencourt et al. (12) obtained through the use of colchicine to interrupt axonal transport. Supporting this second possibility is the presence of cells in the paramedian pontine reticular formation of the cat (61) and the basal telencephalon of lungfish (66). Although the low synthesis of MCH in those cells would argue against the importance of MCH for their function, it is possible that MCH levels are dynamically modulated, displaying a low baseline under standard laboratory conditions, but increasing under specific scenarios. Given the roles of the olfactory tubercle and the laterodorsal tegmental nucleus in functions linked to MCH (36, 67, 68), further studies involving those two areas are necessary to better understand the role of MCH in olfactory integration and sleep.

For comparative purposes, MCH neurons within the hypothalamus can be categorized into medial or lateral, with substantial variability within each group. In rats, medial neurons are found close to the third ventricle wall, displaying a sizeable rostrocaudal distribution that includes neurons in the periventricular nucleus, third ventricle dorsal cap, incerto-hypothalamic area, posterior hypothalamic area, and dorsal tuberomammillary nucleus. The rostro-caudal extent is substantially smaller in *N. alstoni*, and even more so in *M. musculus*, where medial neurons are restricted to the anterior hypothalamic area and incerto-hypothalamic area. This medial group is likely homologous to the MCH neurons found within the paraventricular organ of cyclostomes and elasmobranchs (69, 70), or in the dorsomedial hypothalamic area of lungfish (66) and lissamphibians (71). The lateral group, although also variable in its dorsoventral and mediolateral extents, is more conserved, with neurons found in the LHA and general vicinity of the *mfb* in all mammals. This group does not have a non-mammalian homolog, however, suggesting it was acquired after the divergence of the mammalian lineage. The stronger intraclass conservation of the lateral group, when compared to the medial group, indicates a probable gain of function for it that surpassed the functions of the medial group, allowing a less strict evolutionary constraint over the latter.

The development of a sizeable lateral group of MCH neurons appears to have occurred at least twice during evolution: once in the teleost lineage, and once in the mammalian lineage. In the case of the teleost lateral migration, the duplication of *Pmch* appears to have played a significant role, with one of the newly formed paralogs becoming an important neurohormone secreted through the neurohypophysis. Accordingly, MCH neurons were positively selected to occupy a ventrolateral position towards the *nucleus lateralis tuberis*, a hypothalamic nucleus that is intimately connected with the infundibulum and the hypophysis. Mammals, however, did not undergo a specific whole genome duplication event and do not contain multiple paralogs

of *Pmch*. How to explain the lateral migration observed in this clade? Although speculative, this lateralization event may be connected with the forebrain bundle. In actinopterygians and lissamphibians, there are two major tracts connecting the olfactory bulb to the hindbrain: the lateral forebrain bundle and the *mfb* (72). In those clades, the *mfb* is found close to the third ventricle, in a similar position to MCH neurons. This potentially allows MCH neurons to receive olfactory information through the *mfb*. Furthermore, in those clades, some primary olfactory fibers bypass the olfactory bulb and project directly to the diencephalon (73), what could theoretically provide MCH neurons with another source of olfactory information. Extrabulbar olfactory pathways, however, are not observed in mammals, and there is no lateral forebrain bundle, only a *mfb* located laterally within the hypothalamus (7). It is conceivable, therefore, that the lateralization of the *mfb* in mammals created a positive pressure for MCH neurons to be found in more lateral areas, as those lateral neurons retained the ability to tap into the information stream made available by the *mfb*.

2.2 Morphofunctional correlates

The most striking difference regarding the distribution of MCH-ir neurons between rats and mice was found in the periventricular zone of the hypothalamus. This hypothalamic zone is commonly associated with the control and execution of neuroendocrine functions (74). Since MCH immunoreactivity was almost absent from the mouse periventricular zone, we hypothesized that MCH has a diminished role in neuroendocrine functions in this species. The distribution of MCHR1, however, disputes this idea. *Cilia* containing MCHR1 were found in several neurochemical populations of mice related to neuroendocrine function, including kisspeptin neurons of the preoptic hypothalamus (75), corticotropin-releasing factor neurons of the paraventricular hypothalamic nucleus (76), and tyrosine hydroxylase neurons of the arcuate nucleus (77). This indicates that the interpretation of our results is somewhat more complicated than we initially imagined. Instead of a difference in importance of MCH for neuroendocrine function, our results suggest a difference in mechanism: rats may employ both wiring transmission and VT, while mice appear to rely only on VT. Perhaps even more important for our comprehension of the hypothalamus, however, is the implication that the well-established division of functions between hypothalamic zones applies exclusively to wiring transmission.

Interspecies differences were not limited to MCH but were also found for MCHR1. Both the caudate-putamen nucleus (CPu) and the subventricular zone of the dentate gyrus showed different patterns of labeling between rats and mice. The CPu is a substantial structure in rodents, corresponding to the dorsal *striatum* of other species. It is the primary receptor of inputs among the basal nuclei, receiving dense inputs from dopaminergic nuclei of the midbrain and communicating with the cortex. These connections allow the CPu

to integrate a large amount of information, modulating motor activity, the selection of appropriate responses, and encoding reward value (78). The selective knockdown of *Mchr1* in mice results in increased motor activity (54, 79), while intraventricular injections of MCH in rats do not affect the subject's motor function (80). Given the role of the CPu in the control of motor activity, ciliary MCHR1 may play a role in those differences. Another established role of MCH in the CPu is to communicate the nutrient value of sugar, acting on the post-ingestion reward effect of glucose by modulating dopamine (DA) release in the *striatum* (81). There is not enough information about this function in rats, however, to determine if the presence of MCHR1-ir *cilia* in the caudate putamen may contribute to differences between species.

The second area where mice and rats diverged with respect to MCHR1 is the subventricular zone, area that has been thoroughly implicated in adult neurogenesis, as new neurons are originated in it and incorporated into the hippocampal circuit throughout life (82). Rats and mice are known to have different rates of newborn neuron generation, with rats displaying overall higher rates (83). Since the primary *cilium* has been implicated in the life cycle of cells, playing an essential role in signaling pathways during development (84), MCHR1 may interact with other ciliary proteins to modulate cell proliferation in the subventricular zone. Further experimental investigation is required to confirm or refute this possibility.

2.3 Volume transmission

In addition to interspecies differences, the subcellular localization of MCH and MCHR1 is highly informative about the inner workings of the MCH system. One of the major conclusions that can be drawn from our work is that VT is an integral part of MCH communication, at least in rodents. It is likely that VT in the MCH system is observed outside Rodentia, however, as the consensus sequence that targets MCHR1 to the *cilium*, first identified by Berbari et al. (60), can be found in a wide range of mammals, including humans, cows, cats, elephants, bats, platypuses and opossum. Agreeing to the idea that neuronal primary *cilia* are a strictly mammalian structure, the consensus sequence is not found in non-mammalian vertebrates. Therefore, a better understanding of VT MCH is fundamentally intertwined with our comprehension of MCH functions.

Several of our observations indicate that VT plays a role in MCH function, or help us understand how it may happen: the neuronal primary *cilium* is a sensory structure, whose primary function is to sense chemical messengers in the ECS; MCH and NEI are found in different subcellular compartments, allowing them to be released through different methods; MCH|NEI immunoreactive fibers are found in the ventricle walls and leptomeningeal space, suggesting release of MCH in the CSF; MCH/NEI fibers and ciliary MCHR1 are found in a complementary pattern within the prosencephalon.

The presence of MCHR1 in the primary *cilium* has significant repercussions for the signaling mechanism of MCH within the CNS. In addition to indicating that MCH is likely found abundantly in the ECS, the primary *cilium* is involved in two critical signaling pathways: *Hedgehog* and *Wnt*. We cannot exclude, at this point, the possibility that MCHR1 interacts with members of the *Hedgehog* and *Wnt* cascades that are located in the *cilium* (*i.e. Patched-1*, *Smoothened, Inversin*) (85). That would expand the mechanisms of action of MCH-MCHR1 interactions in the cell beyond the well-known roles in inhibiting adenylate cyclase, increasing Ca^{2+} influx, MAP kinase, and ERK activation (49, 50). More studies are necessary, however, to determine if there is a crosstalk between MCHR1 and *Hedgehog/Wnt* in the *cilium*. With the antibody identified in this work, such studies should now be possible.

If MCH is found free in the ECS around ciliary MCHR1, it must be released in a way that facilitates its access to the ECS. There are multiple pathways through which that may happen. We found the same pattern of densely varicose fibers in mice and Mexican volcano mice that has been described for rats by Bittencourt et al. (12). This pattern is similar to what has been described for other neurochemical systems, including serotonin, norepinephrine and acetylcholine in several parts of the brain (86-90), where those fibers have numerous enlargement that have no discernible synaptic specialization. To this date, there is no ultrastructural description of labeled MCH axons, what impairs our ability to know if MCH/NEI vesicles are released at the synaptic environment or the surrounding ECS.

Once released, MCH can diffuse through the ECS to reach proximal MCHR1 receptors. Although long-distance travel through the ECS is unlike due to enzymatic action, as demonstrated for other peptides (91), MCH and NEI may travel distances shorter than 1mm away from the release site. This would explain why MCH-ir fibers are observed juxtaposed to MCHR1-ir rich areas. A similar mechanism has been proposed for DA communication, consisting on the release of DA in the medial septal nucleus (MS) to reach D_1 and D_2 receptors in the shell of the *nucleus accumbens* (92). The movement between the MS and the shell of the *nucleus accumbens* appears to the facilitated by factors like concentration and temperature gradients. In particular, for the latter, immunoreactivity to uncoupling protein 2 (UCP2) is found in the MS. Given the role of UCP2 in generating heat locally, it may serve to create a temperature gradient in the area (93). One interesting question to be asked is: why not simply release MCH within the area containing MCHR1-ir *cilia*? Although there is no experimental evidence to answer this question, we may speculate that VT, in this case, adds an additional layer of control over peptide-receptor binding. The tortuosity and proteolytic activities in the ECS are dynamic parameters (94), as well as UCP2 activity, suggesting that even after peptide release, additional mechanisms may facilitate or difficult the MCH trajectory towards the MCHR1-enriched areas.

While the release of MCH in the ECS by varicosities is the most likely method of short-range release of this neuromodulator, the long-range release of MCH likely happens through the CSF, as brilliantly demonstrated by Noble et al. (64) in mice. The fibers found within the borders of the ventricular *lumen* of mice in this work are

compatible with what was described elsewhere. We also found fibers that appear to reach the subleptomeningeal space, another possible contact point between MCH and the CSF, and we extend the anatomical basis for such release to rats. Combined with the widespread distribution of ciliary MCHR1, the release of MCH in the CSF can work as a broadcast system, allowing MCH neurons to influence multiple close and distant brain areas simultaneously.

Besides an axonal release in distant sites, another possibility is that MCH and NEI are somatodendritically released in the LHA. Upon confocal visualization, it was possible to see that MCH is confined to the rough endoplasmic *reticulum* and Golgi apparatus, centered around the soma, while NEI immunoreactivity is widespread, found in the proximal dendrites of the neuron, on what may be the smooth endoplasmic *reticulum* or the cytosol itself. This opens up the possibility that NEI is somatodendritically released, in a similar fashion to DA (95), while MCH is packed and transported to be released in axons. A somatodendritical release of MCH cannot be discarded, however, as vasopressin and oxytocin are released by large core vesicles that fuse with the somatodendritical membrane (96). Another possibility is that NEI occupies the smooth endoplasmic *reticulum* along the whole neuron extension, including the axonal compartment, what may underlie two different mechanisms of release for axonal MCH and NEI: high-speed vesicle transportation for MCH and slow endoplasmic *reticulum* transport for NEI.

The exocytosis of vesicles in the somatodendritic membrane is dependent on calcium entry, associated or not to action potentials (97), and the necessary calcium current to exocytosis is 10 to 100-fold less than for vesicle release at the synaptic specialization (98). This could potentially uncouple MCH and NEI release, as NEI would be released from the somatodendritic compartment under low calcium entry conditions, while MCH could be released at the axon after high calcium conditions associated to the neuronal depolarization. This could lead to a highly-controlled release, as MCH|NEI neurons possess both sodium-calcium exchangers and voltage-dependent calcium channels that are modulated by several receptors at the membrane surface, including receptors for oxytocin, vasopressin, and opioids (99, 100). Therefore, neuromodulators can potentially increase or decrease NEI exocytosis through the modulation of calcium currents without necessarily facilitating or depressing firing in MCH|NEI neurons. That may explain why MCH|NEI neurons are mostly silent during the light phase (101, 102), as exocytosis could happen independently of the neuron's electrophysiological properties.

Chapter 3

Melanin-concentrating hormone peptidergic system: Comparative morphology between muroid species

Diniz GB[1], **Battagello** DS[1], **Cherubini** PM, **Reyes-Mendoza** JD, **Luna-Illades** C, **Klein** MO, **Motta-Teixeira** LC, **Sita** LV, **Miranda-Anaya** M, **Morales** T and **Bittencourt** JC

[1]These authors contributed equally to this work

This is the accepted version of the following article: Diniz, GB, Battagello, DS, Cherubini, PM, et al. Melanin-concentrating hormone peptidergic system: Comparative morphology between muroid species. J Comp Neurol. 2019; 1– 29**, which has been published in final form at** https://doi.org/10.1002/cne.24723**.**

Melanin-concentrating hormone peptidergic system: comparative morphology between muroid species

Giovanne B. Diniz[a,1], Daniella S. Battagello[a,b,1], Pedro M. Cherubini[a], Julio D. Reyes-Mendoza[b], Cesar Luna-Illades[b], Marianne O. Klein[a], Lívia C. Motta-Teixeira[a,c], Luciane V. Sita[a], Manuel Miranda-Anaya[d], Teresa Morales[b] and Jackson C. Bittencourt[a,e,*]

[a] Department of Anatomy, Institute of Biomedical Sciences, University of São Paulo, São Paulo, Brazil;

[b] Departamento de Neurobiología Celular y Molecular, Instituto de Neurobiología, Universidad Nacional Autónoma de México, Queretaro, México;

[c] Department of Physiology and Biophysics, Institute of Biomedical Sciences, University of São Paulo, São Paulo, Brazil;

[d] Unidad Multidisciplinaria de Docencia e Investigación, Facultad de Ciencias, Universidad Nacional Autónoma de México, Queretaro, Mexico;

[e] Center for Neuroscience and Behavior, Institute of Psychology, University of São Paulo, São Paulo, Brazil.

[1] These authors contributed equally to this work.

*Correspondence:

Jackson C. Bittencourt

jcbitten@icb.usp.br

Running Title: Comparative morphology of the MCH system

Acknowledgments

We would like to thank Maria Eugenia Ramos for technical support. Financial support for this study was provided in the form of grants from the São Paulo Research Foundation (FAPESP), grants 2016/02748-0 (GBD) and 2016/02224-1 (JCB). This work was also supported by UNAM, grants UNAM-DGAPA-PPA (DSB), UNAM-DGAPA-PAPIIT IN204718 (TM), UNAM-DGAPA-PAPIIT IN212118 (MM-A). This work was also supported by a 2017 short stay grant from the International Brain Research Organization - Latin America Regional Committee (IBRO-LARC), awarded to DSB. We are thankful for the support provided by the Brazilian Coordenação de Aperfeiçoamento de Pessoal de Nível Superior (CAPES, Office for the Advancement of Higher Education, Grant # 848/15). JCB is an Investigator with the Brazilian Conselho Nacional de Desenvolvimento Científico e Tecnológico (CNPq, National Council for Scientific and Technological Development, grant # 426378/2016-4).

Data Availability Statement

Some of the data that support the findings of this study are openly available in OSF at http://doi.org/10.17605/OSF.IO/ZRK2. The remaining data that support the findings of this study are available from the corresponding author upon reasonable request.

Conflict of Interest Statement

The authors declare no conflict of interest.

Authors Contribution

All authors had full access to all the data in the study and take responsibility for its integrity and the accuracy of its analysis. GBD, DSB, PMC, JDR-M, MOK, and LCM-T performed experiments and participated in data collection. TM and JCB designed the study and its experimental approach. CL, MM-A, and JCB provided the animals. LVS discussed results. GBD, DSB, TM and JCB analyzed the data and wrote the manuscript.

Abstract

Melanin-concentrating hormone [MCH] is a conserved neuropeptide, predominantly located in the diencephalon of vertebrates, and associated with a wide range of functions. While functional studies have focused on the use of the traditional mouse laboratory model, critical gaps exist in our understanding of the morphology of the MCH system in this species. Even less is known about the non-traditional animal model *Neotomodon alstoni* (Mexican volcano mouse). A comparative morphological study among these rodents may, therefore, contribute to a better understanding of the evolution of the MCH peptidergic system. To this end, we employed diverse immunohistochemical protocols to identify key aspects of the MCH system, including its spatial relationship to another neurochemical population of the tuberal hypothalamus, the orexins. Three-dimensional reconstructions were also employed to convey a better sense of spatial distribution to these neurons. Our results show that the distribution of MCH neurons in all rodents studied follow a basic plan, but individual characteristics are found for each species, such as the preeminence of a periventricular group only in the rat, the lack of posterior groups in the mouse, and the extensive presence of MCH neurons in the anterior hypothalamic area of *Neotomodon*. Taken together, these data suggest a strong anatomical substrate for previously described functions of the MCH system, and that particular neurochemical and morphological features may have been determinant to species-specific phenotypes in rodent evolution.

Keywords: MCH, NEI, lateral hypothalamic area, mouse, *Peromyscus*, *Neotomodon alstoni*, Mexican volcano mouse, RRID_AB_2650444, RRID_AB_2650445, RRID_AB_2315019, RRID_AB_572268.

1. Introduction

The melanin-concentrating hormone (MCH) system is comprised of several vertebrate genes, including *Pmch*, *Mchr1,* and *Mchr2* (as reviewed in Bittencourt & Diniz, 2018). The *Pmch* gene encodes a propeptide called the pre-pro-melanin-concentrating hormone, or ppMCH, which originates, in mammals, three neuropeptides: mature MCH, neuropeptide E-I (NEI), and neuropeptide G-E (NGE) (Nahon et al., 1989; Vaughan et al., 1989). The MCH system has been strongly conserved in vertebrates, with *Pmch* homologs found in a wide range of species, from lampreys to humans (Bird et al., 2001; Elias et al., 2001). The MCH structure, in particular, has been highly preserved, with an identical structure shared among all mammals, and a single conservative amino acid substitution between mammalian and elasmobranch MCH (Mizusawa et al., 2012).

The strong conservation of the MCH peptidergic system can be explained by the wide range of functions associated with MCH and NEI, which include but are not limited to: ingestive behavior (Georgescu et al., 2005; Ludwig et al., 2001; Qu et al., 1996), energy expenditure (Guesdon et al., 2009; Segal-Lieberman et al., 2003; Shimada et al., 1998), reward (Domingos et al., 2013; Karlsson et al., 2016; Mul et al., 2011), sensory integration (Adams et al., 2011; Miller et al., 1993; Sita et al., 2016), sleep (Lagos et al., 2009; Tsunematsu et al., 2014; Verret et al., 2003), stress response (Kennedy et al., 2003; Smith et al., 2006; Smith et al., 2009), learning (Adamantidis et al., 2008; Le Barillier et al., 2015; Monzon et al., 1999), sexual physiology (Gonzalez et al., 1996; Murray et al., 2000a; Murray et al., 2006), and maternal physiology (Alachkar et al., 2016; Benedetto et al., 2014; Parkes & Vale, 1993a). As a unifying theory for those functions, we recently proposed that MCH is a homeostatic maintainer, or metabolic dampener, acting to avoid large fluctuations from the baseline by integrating external and internal inputs, and organizing an appropriate response (Diniz & Bittencourt, 2017).

The large number of roles played by MCH-synthesizing neurons is supported by an extensive network of projections that reach almost all areas of the central nervous system. The first mapping of the MCH system was performed by Bittencourt et al. (1992), who described the distribution of *Pmch* expression and the immunoreactivity to MCH and NEI in male Sprague-Dawley rats. In the rat, the main site harboring MCH-immunoreactive (MCH-ir) neurons is the diencephalon, with neurons found in the lateral hypothalamic area (LHA), anterior hypothalamic area (AHA), posterior hypothalamic area (PHA), perifornical nucleus (PeF), and in the adjoining *zona incerta* (ZI) (Bittencourt & Diniz, 2018; Bittencourt et al., 1992). In the LHA, MCH neurons are intermingled with another neuropeptidergic population, the orexin neurons (Peyron et al., 1998; Swanson et al., 2005). It was later described that a subgroup of ZI neurons are actually part of a hypothalamic structure, called the incerto-hypothalamic area (IHy) (Bittencourt & Diniz, 2018; Sita et al., 2007). Outside the diencephalon, MCH neurons are found in discrete groups of weakly labeled neurons in the olfactory tubercle and the paramedian pontine reticular formation (Bittencourt et al., 1992). Exclusively in female rats, immunoreactive neurons are also found in the laterodorsal tegmental nucleus at all time points of the reproductive cycle (Rondini et al., 2007), and in the medial preoptic area (MPOA), anterior paraventricular hypothalamic nucleus (PVH), and periventricular hypothalamic nucleus exclusively in late-lactation dams (Knollema et al., 1992; Rondini et al., 2010). Contrasting to the restricted synthesis of MCH, projections of MCH neurons are found widespread in the central nervous system, ranging from the olfactory bulb to the spinal cord (Bittencourt et al., 1992).

Looking at the available data, it becomes apparent that the MCH system is sexually dimorphic, highly plastic, and strongly linked to sexual physiology, both from functional (Messina et al., 2006; Murray et al., 2000a; Murray et al., 2006; Santollo & Eckel, 2008; Wu et al., 2009) and structural viewpoints (Alvisi et al., 2016; Chiocchio et al., 2001; Costa et al., 2019; Ferreira et al., 2017; Gallardo et al., 2004; Knollema et al., 1992; Murray et al., 2000b; Santollo & Eckel, 2013). Few works, however, have thoroughly examined the dimorphisms between males and females. It is also conspicuous that most of the morphological and hodological data generated up to this point has used the rat as the preferred animal model (Bittencourt & Elias, 1998; Bittencourt et al., 1992; Elias & Bittencourt, 1997; Elias et al., 2008; Haemmerle et al., 2015; Lima et al., 2013), while

functional studies have more commonly used the laboratory mouse, resulting in a disparity between morphological and functional data concerning the MCH system. The prevalence of traditional animal models in research further limits our knowledge, with MCH morphological data available for only two other species of the *Rodentia* clade, the Siberian hamster (*Phodopus sungoros*) and the golden hamster (*Mesocricetus auratus).* Taking this lack of diversity on morphological information about the MCH system into consideration, we proposed with this work to investigate aspects of the MCH system in three rodent species, the brown rat (*Rattus norvegicus*), the house mouse (*Mus musculus*), and for the first time the Mexican volcano mouse (*Neotomodon alstoni*), in an attempt to understand neurochemical and morphological variations that may exist between phylogenetic related species.

Rodents are the most specious vertebrate clade known (Wilson & Reeder, 2005), with superfamily *Muroidea* alone being larger than any other non-rodent order. This extensive speciation reflects the geographical dominance of rodents, with species found in almost every continent, as well as their varied habitats and adaptive behaviors. This broad development of rodents is reflected in the appearance of several significant shifts in diversification rate, particularly in the cricetids and murids lineages (Fabre et al., 2012). This accelerated diversification equips us with a unique tool to investigate how neurochemical populations change and develop in response to diversified habitats, in animals who have conserved their overall brain structure and macroscopic morphology. However, this same accelerated diversity creates challenges in terms of phylogenetic classification. The phylogenetic relationship between *Rattus, Mus* and *Neotomodon* is illustrated in Fig. 1. *Neotomodon alstoni* was initially described as three species by (Merriam, 1898), *N. alstoni*, *N. orizabae*, and *N. perotensis*, and later analyses condensed into a single species, *N. alstoni* (Davis, 1944; Davis & Follansbee, 1945; Williams & Ramirez-Pulido, 1984).

The phylogenetic classification of *Neotomodon* has been greatly disputed in the literature. Although initially assigned to subfamily *Neotominae* due to the similarity with the *Neotoma* genus (Miller & Rhen, 1901), the morphological similarities between *N. alstoni* and members of the *Peromyscus* genus led others to ascribe *N. alstoni* to the *Peromyscus* radiation (Davis & Follansbee, 1945; Goldman, 1910; Williams et al., 1985; Yates et al., 1979), including references to this species as *Peromyscus alstoni*. Recent molecular works have consolidated the independence of the *Neotomodon* as a monotypic lineage and its position inside the *Peromyscus* genus (Miller & Engstrom, 2008; Platt et al., 2015; Reeder et al., 2006). The very position of the *Peromyscus* has changed over time. Simpson (1945) classified *Peromyscus* under the *Cricetinae* subfamily, while Michaux et al. (2001) classified *Peromyscus* under *Sigmodontinae*. Fabre et al. (2012), using 11 genes from 1265 species of rodents, proposed that *Peromyscus* is part of subfamily *Neotominae*, which is a sister clade to *Sigmodontinae* under the *Cricetidae* family. Regardless of the exact position of *N. alstoni*, morphological and molecular data indicate that this species is more closely related to the cricetids than to murids.

Given the importance of *Neotominae* species as animal models (Miller & Engstrom, 2008), the position of *N. alstoni* as an external comparison point to murids, and the importance of more morphological information about the MCH system in *Mus musculus* for a deeper understanding of the functional findings obtained in that species, we employed immunohistochemical methods to identify and characterize the MCH system and the spatially related ORX system in different rodent species. We believe such comparative morphology approach can provide important information about the evolution of neuropeptidergic systems and help us understand the conserved roles of MCH.

2. Materials and Methods

2.1. Animals

Adult male and female C57BL/6 house mice (*Mus musculus*, n = 30) and adult male and female Sprague-Dawley albino rats (*Rattus norvegicus*, n = 5) were bred and raised in the animal facility of the Department of Anatomy (Institute of Biomedical Sciences of the University of São Paulo). The animals were housed in a

controlled environment with a 12h light/dark cycle, constant temperature of 22ºC, and free access to chow and water. The handling of animals was always performed by one of two designated researchers and occurred under the approval of the Ethics Committee on the Animal Use of the Institute of Biomedical Sciences (CEUA089/10 and CEUA096/14) following all the appropriate national and international guidelines.

Before the experimental groups were generated, four to six animals were housed together in propylene boxes. Once females reached 8 weeks of age, their estrous cycle was verified for two weeks by the method of vaginal cytology (Byers et al., 2012). Animals that displayed a cycle without irregularities were mated with experienced males in the afternoon of the day of proestrus. In the following morning, a new vaginal collection was performed, and pregnancy was confirmed by the abundant presence of spermatozoa in the sample. The day spermatozoa were observed in the sample was designated as the first day of pregnancy. Pregnant females were transferred to a new housing cage and were kept alone for the rest of the experiment. The day of birth was designated *postpartum* day 0 (PPD0), and the litter was culled to four males and four females in PPD2. Females were randomly assigned to the following groups: 10^{th} gestational day, five days *postpartum*, twelve days *postpartum*, and nineteen days *postpartum*. The male mice used for breeding were also sacrificed to compose the male group, and virgin female mice were sacrificed in the morning of the diestrus day to compose the female control group. Three adult male and two adult female rats were sacrificed to provide an interspecies comparison point.

Adult male Mexican volcano mice (*Neotomodon alstoni*, n = 5) were bred and raised in the animal facility of the Facultad de Ciencias, Universidad Nacional Autónoma de México, individually housed in a light- and temperature-controlled environment (12h light/dark cycle, 23ºC), and with free access to chow and water. Once animals reached 6 months of age, individuals identified as non-spontaneous obese (Báez-Ruiz et al., 2014; Carmona-Alcocer et al., 2012) were used in the remaining of the experiment. All handling of *N. alstoni* animals followed the ethical guidelines of the National Research Council of the National Academy of Sciences Guide for the Care and Use of Laboratory Animals and the Official Mexican Standard NOM-062-Z00-1999.

2.2. Tissue collection

Tissue collection was performed using the method of transcardiac perfusion. Briefly, at the day of perfusion, animals were anesthetized with an excess of ketamine, xylazine, and acepromazine. Once verified the loss of reflexes, animals were thoracotomized, their hearts exposed, and a butterfly needle connected to a peristaltic pump inserted into the left ventricle. Twenty milliliters of cold 0.9% saline were used to clear the vascular bed for one minute, and then 250 ml of cold 4% formaldehyde in borate buffer (pH 9.5) were perfused in the animal for 12.5 minutes. Once the procedure was complete, animals were decapitated, and the brains were carefully removed from the skull and submerged in the same fixation solution supplemented with sucrose (20%) for 4 hours at 4º C. Brains were then transferred to potassium phosphate-buffered saline (KPBS, pH 7.4) and kept at 4º C until sectioning, which was performed within 72 hours of collection. Tissue sectioning was performed in a sliding microtome. Brains were snap frozen and sectioned in 20µm-thick frontal slices, from the olfactory bulb to the medulla oblongata. Slices were kept at -20º in antifreeze solution. For the collection of *N. alstoni* tissue, a similar procedure was performed with a few modifications to account for the larger size of these animals, as follows: 1) the fixative solution used was 4% formaldehyde in phosphate-buffered saline (pH 7.2), conforming to previously employed perfusion in *N. alstoni* (Luna-Illades et al., 2017) ; 2) brains were postfixed overnight in the same formaldehyde solution supplemented with 30% sucrose; 3) brains were sectioned in the frontal plane into 30µm-thick sections.

2.3. Immunohistochemistry

2.3.1. Antibodies

All antibodies used in this work have been previously used in other works (Table 1) and were extensively characterized. Bittencourt et al. (1992) tested the anti-MCH antiserum in an adsorption test against 8

compounds, with only rat MCH resulting in complete ablation of labeling, while salmon MCH just partially affected the ability of the antiserum to immunolabel cells. Those same authors screened the anti-NEI antiserum against 11 compounds, with only rat NEI abolishing labeling, and α-melanocyte-stimulating hormone (α-MSH) mildly reducing labeling intensity. Fronczek et al. (2005) verified the specificity of the anti-orexin antiserum by performing a dot blot test against a panel of 22 compounds, with only the orexin-A well resulting in labeling. Vaasjo et al. (2018) report that the anti-TH antibody used specifically labels neurons that are otherwise identified with several independent catecholaminergic markers, and Yew et al. (1995) performed an adsorption test with TH to show its specificity.

To ensure their specificity was unaltered when applied to mouse tissue, we performed antibody omission controls (primary and secondary), and a preadsorption panel for the anti-MCH and anti-NEI antibodies used in this work. The antisera were incubated with 4-400µM of peptides overnight at 4º C, and then used in immunohistochemical reactions as described below. All antibody omission tests resulted in no labeling, as anticipated. Each antibody was incubated in serial concentrations of MCH, NEI, NGE, α-MSH and corticotropin-releasing factor (CRF). While MCH, NEI and NGE share a common phylogenetic history, α-MSH has been previously described to be contained in MCH neurons when an antibody raised in salmon was used (Fellmann et al., 1987), and shares a C-terminal aliphatic amide motif with NEI (Bittencourt et al., 1992), while CRF immunoreactivity has been described in areas that overlap those of MCH in rats (Sakanaka et al., 1987). As expected, incubation of anti-MCH in MCH completely abolished labeling in all concentrations tested, and a similar result was obtained after the incubation of anti-NEI in NEI. Incubation of anti-MCH in NEI, NGE, α-MSH and CRF resulted in no appreciable change in labeling intensity, as did incubation of anti-NEI in MCH, NGE, α-MSH and CRF. Our results confirm that both antibodies label their intended targets with high specificity and no crossreactivity.

2.3.2. Immunoperoxidase

For the morphological description of MCH/NEI neurons and the fiber mapping, single-label immunoperoxidase was performed. The protocol used is a variation of the method presented by Hoffman et al. (2016). To that end, slices were rinsed in KPBS to wash off the antifreeze solution, incubated with a 0.3% solution of hydrogen peroxide for 15 minutes to quench endogenous peroxidase activity, rinsed in KPBS, and incubated with either anti-MCH or anti-NEI (Table 1) in KPBS supplemented with 0.3% of Triton X-100 and 3% of normal goat serum (Vector Laboratories; Burlingame, CA, USA) for approximately 16 hours at room temperature. Slices were then rinsed in KPBS and incubated with biotinylated anti-goat IgG antibody (1:800, Vector Laboratories) in KPBS supplemented with Triton X-100 for 1 hour at room temperature, followed by an incubation with avidin-biotin-horseradish peroxidase complex (1:333, Vectastain ABC Elite, Vector Laboratories) for 1 hour at room temperature. Slices were then rinsed in KPBS and transferred to a slightly acidic medium (0.2M acetate buffer, pH 6.5). Chromogen deposition was performed through incubation of the slices with 0.02% 3,3'-diaminobenzidine (DAB – Sigma-Aldrich Co.; St. Louis, MO, USA), 0.003% hydrogen peroxide, and 2.5% nickel (II) sulfate. Optimal reaction time was determined by visual observation of the reacting slices in an optical brightfield microscope. After rinses in acetate buffer and KPBS, slices were mounted in rostrocaudal order in gelatin-coated glass slides and dried in a kiln overnight. Slices were then dehydrated in graded concentrations of alcohol, cleared in xylene, covered in mounting medium (D.P.X., Sigma-Aldrich), and coverslipped.

To perform three-dimensional reconstructions of the main orexinergic populations of the rat hypothalamus we employed double peroxidase labeling. To that end, slices were labeled as described above using an anti-orexin (ORX) antibody (Table 1). After the final rinses, slices were incubated in anti-MCH antibody (Table 1). After new secondary antibody and avidin-biotin steps, chromogen deposition was performed using a red DAB commercial kit (NovaRED, Vector Laboratories). After KPBS rinses, the slices were dried in a kiln for 72º C and cleared in xylene for 1 minute, as dehydration in alcohol dissolves the red DAB precipitate, and then

coverslipped with DPX as mounting medium. In some cases, adjacent series of slices were stained using the Nissl method. To that end, slices were transferred to glass slides in rostrocaudal order and dried in a kiln for at least 24 hours. Slices were then dehydrated in graded concentrations of alcohol, cleared in xylene, rehydrated in the same battery of alcohol, and the slides were submerged in 0.25% thionin solution for 30 seconds. After washes in distilled water, the slices were once more dehydrated and coverslipped.

2.3.3. Osmium Impregnation

For a better visualization of fibers in darkfield microscopy, sections which undergone peroxidase labeling were impregnated with osmium. In these cases, immunoperoxidase was performed as previously described and slices were mounted on glass slides and dried in a kiln for at least 24 hours. Slices were then dehydrated in raising concentrations of alcohol, cleared in xylene for 30 minutes, rehydrated in decreasing concentrations of alcohol, and incubated with a 0.005% osmium tetroxide (Sigma-Aldrich) aqueous solution for 30 minutes. Slides were then washed in tap water, submerged in a 0.05% thiocarbohydrazide (Sigma-Aldrich) aqueous solution for 15 minutes, and washed on tap water once more. After extensive washes, the slides were returned to the osmium tetroxide solution, where they remained for 30 minutes. A new round of washes in tap water was performed, the slices were dehydrated in increasing concentrations of alcohol, cleared in xylene, covered in mounting medium (D.P.X.) and coverslipped.

2.3.4. Immunofluorescence

For the simultaneous visualization of multiple markers, the immunofluorescence method with or without amplification was used. To perform biotinylated tyramine signal amplification, slices were rinsed in KPBS, incubated in 0.3% hydrogen peroxidase for 15 minutes, subjected to new rinses and then incubated with primary antibody (Table 1) in KPBS supplemented with 0.3% of Triton X-100 and 3% normal donkey serum (Jackson Laboratories) for 48 or 72 hours at 4º C. This step was followed by rinses in KPBS, incubation with the appropriate biotinylated anti-IgG antibody (1:5’000) for one hour at room temperature, and incubation with avidin-biotin-horseradish peroxidase solution (1:833 - Vectastain ABC Elite, Vector Laboratories) for 30 minutes at room temperature. For the amplification step, slices were incubated with a 0.05% biotinylated tyramine (Sigma-Aldrich) solution supplemented with 0.005% hydrogen peroxide for 20 minutes at room temperature. After new rinses, labeling was performed by incubating the slices with a 1:200 fluorophore-conjugated streptavidin solution for 2 hours at room temperature. To perform multiple labeling, slices were labeled as described and then incubated with a second or third primary antibody solution (Table 1). After 48 or 72 hours incubating at 4º C, the slices were rinsed and incubated for 2 hours at room temperature with a fluorophore-conjugated secondary antibody solution (1:200). After the final washes, slices were counterstained with DAPI nuclear stain, air dried for one hour and covered with aqueous mounting media and coverslipped.

Random slices containing the tuberal hypothalamus were selected from *Mus* animals to estimate the rate of colocalization of MCH and NEI. Slides were incubated with MCH or NEI primary antiserum overnight, and then incubated for 2 hours at room temperature with a fluorophore-conjugated secondary antibody solution (1:200). After rinses, the slices were incubated with the complimentary MCH or NEI primary antiserum overnight, and then incubated for 2 hours at room temperature with a fluorophore-conjugated secondary antibody solution (1:200) of a different wavelength. The order of primary antisera and of secondary antibody was systematically varied between animals.

2.4. Microscopy and image acquisition

Brightfield and darkfield photomicrographs were obtained with a Nikon Eclipse 80i upright microscope (Nikon Co.; Tokyo, Japan) coupled to a digital camera (CX3000), operated with the Microlucida 3.03 acquisition software (MicroBrightField Inc.; Williston, VT, USA). Widefield epifluorescence photomicrographs were obtained with a Leica DMR microscope (Leica Biosystems; Wetzlar, Germany) equipped with the appropriate filters. Images were acquired with a DS-R1 CCD camera (Nikon Co.) operated with acquisition software NIS –

Elements BR 3.22 (Nikon Co.). Images were adjusted using the Adobe Photoshop CC 2015.0.0 suite (Adobe Systems Inc.; San Jose, CA, USA) to ensure uniform brightness, contrast, and sharpness, with alterations applied to every pixel in each picture and performed with care not to alter the information illustrated in the figures. Schematics were drawn using the Adobe Illustrator CC 2015.0.0 software (Adobe Systems Inc.). Multiphoton confocal fluorescence photomicrographs were obtained with an LSM-800 microscope (Carl Zeiss; Jena, Germany) equipped with four laser lines (405, 488, 565, 630) and the appropriate detectors. Images were acquired and processed using the ZEN Blue Edition software (Carl Zeiss).

To estimate the colocalization percentage between MCH and NEI, immunolabeled slices were photographed using a monochromatic camera coupled to a Leica DMR microscope. Each fluorophore was imaged individually, and then the photomicrographs were overlaid using the software NIS – Elements BR 3.22. Using the same software, each cell in one side of each randomly selected slice was then scored for its peptide complement, and the ratio of MCH/NEI cells over the total number of MCH or NEI cells was used as the colocalization rate.

2.5. Three-dimensional reconstruction

Series of slices labeled for MCH only or double labeled for MCH and ORX were used for three-dimensional reconstruction of the LHA. The whole series was analyzed by brightfield microscopy, and all slices containing labeled neurons were included in the analysis. Briefly, slices were examined under a low-magnification 10X objective lens and the main reference structures (ventricles and fiber tracts) were drawn using the three-dimensional reconstruction software Neurolucida 11.03 (MicroBrightField Inc.), as described in Diniz et al. (2018). Using high-magnification objectives, different markers were placed over the drawing for each MCH or ORX labeled cell. Once all labeled sections were drawn, they were grouped, aligned, and reconstructed in the Neurolucida 3D suite.

3. Results

3.1. Morphological subtypes of MCH neurons

Both anti-MCH and anti-NEI sera successfully labeled neurons in the major diencephalic areas containing MCH and NEI-immunoreactive neurons in the rat – the LHA, the IHy and the ZI, in a similar pattern to that described by Bittencourt et al. (1992). As also described for the rat, we confirmed that MCH and NEI have over 95% colocalization in the hypothalamus, with a negligible number of neurons labeled for only one peptide. Therefore, all descriptions for MCH or NEI are interchangeable and, otherwise stated, labeled neurons will be referred as MCH/NEI neurons for simplicity. In an attempt to define the subcellular localization of MCH and NEI in the same neurons, we investigated double-labeled slices using confocal microscopy. Although MCH and NEI are found in the same neurons, these two markers occupy different subcellular compartments (Fig. 2). Neuropeptide E-I labeling is stronger and delineates the soma, proximal dendrites, and axonal projections, while somewhat absent close to the nucleus (green labeling in Fig. 2). On the other hand, MCH is found in the soma around the nucleus, without delineating proximal processes (magenta labeling in Fig. 2). Small packets of MCH immunoreactivity can be observed all around the area, suggesting MCH is enclosed in vesicles. No subcellular colocalization was found between the two markers (Fig. 2 b1, b2).

Three main morphological subtypes of MCH/NEI neurons were observed for all animals analyzed. The first subtype, and the most numerous, was the multipolar type (Fig. 3 a1, a2). These neurons have an irregular or rounded shape, with the emergence of two to five primary dendrites, frequent ramification into secondary dendritic branching, and occasional tertiary branching. The second subtype was the fusiform type (Fig. 3 b1, b2). These neurons are elongated, with their dorsoventral dimension usually smaller than their mediolateral dimension, with the usual emergence of two primary dendrites, less frequent secondary branching, and seldom observed tertiary ramifications. The third neuronal subtype found, and the least numerous, was the crescent type (Fig. 3 c1, c2). Crescent MCH/NEI neurons are found closely associated to blood vessels in the

hypothalamus, with a curved shape that is likely secondary to the spatial displacement by the blood vessel. These neurons often have two discernible primary dendrites, and further ramification was seldom observed.

3.2. Distribution of MCH/NEI neurons in the mouse hypothalamus

The distribution of MCH/NEI neurons in *M. musculus* can be described as two major patterns of immunoreactivity: anterior and posterior. The anterior pattern starts at the end of the PVH, with cells found in the AHA, IHy, medial part of ZI and the pericapsular part of the LHA (Fig. 4 a1, b1). Despite their physical proximity, neurons from the AHA can be differentiated from neurons of the IHy due to a prevalence of multipolar neurons in the former, while labeled neurons in the later are predominantly fusiform. Likewise, neurons in the LHA are predominantly multipolar, while the adjoining ZI contains fusiform neurons. With the emergence of the dorsomedial hypothalamic nucleus, neurons in the AHA are pushed outwards, forming a new subgroup: the internuclear group (Fig. 4 c1).

At the following level, illustrated in Fig. 4 d1, a transitional pattern develops, with structures from the anterior pattern, such as the IHy and the internuclear subgroup, well developed, while there is an increase in the number of neurons in the LHA. The posterior pattern is characterized by a concentration of MCH/NEI cells in the LHA and the end of the medial groups (Fig. 4 e1, f1). Two subgroups of neurons develop in the LHA: one dorsolateral with respect to the cerebral peduncle, and one associated to the fornix and the PeF. The distribution of MCH/NEI cells in the rostrocaudal axis soon ends, with only a few scattered cells found in the medial zone of the hypothalamus, potentially invading the limits of the PHA. Only a few cells are seen bordering the dorsal tuberomammillary nucleus, but none of them appear to invade the limits of that nucleus.

The distribution of MCH/NEI neurons in *N. alstoni* can also be described in terms of two patterns separated by a transitory stage. As is the case with *M. musculus*, the anterior pattern is characterized by large numbers of labeled neurons in the AHA, IHy, ZI, and the pericapsular LHA (Fig. 5 a1, b1). The anterior pattern of *N. alstoni* differs from *M. musculus* in three critical points. The number of labeled neurons in the AHA is greatly increased in *N. alstoni*, and this group occupies a larger area in the dorsoventral axis, perhaps reflecting a larger AHA in this species. Second, a group of medial AHA neurons is slightly separated from the other neurons by an empty band of neuropil, and its dorsolateral position with respect to the third ventricle (3V) is reminiscent of the rat 3V dorsal cap (Bittencourt & Diniz, 2018). Third, there is no internuclear group. As a direct consequence of the enlarged AHA group, an IHy is virtually indistinguishable from this group. The level illustrated in Fig. 5 c1 represents the stereotypical intermediate stage, with a large number of labeled neurons in the AHA concomitant to an increase in the number of MCH/NEI neurons of the pericapsular LHA, in addition to neurons in the central LHA, where previously there were only a few.

The posterior pattern starts to consolidate at the level illustrated in Fig. 5 d1 and is fully realized at the level illustrated in Fig. 5 e1. At the posterior level, the largest number of MCH/NEI neurons is found in the LHA, in a pattern that is very reminiscent of *Mus*, with two apparent groups formed: one dorsomedial with respect to the cerebral peduncle, and the other closely associated to the PeF. The number of labeled neurons directly dorsal to the fornix, however, is considerably larger than that found in *M. musculus*. An additional group of cells found in *N. alstoni* that is not found in *M. musculus* is the PHA group, which appears right at the end of the rostrocaudal distribution of MCH/NEI in *N. alstoni* (Fig. 5 f1). This group is numerous and located medially inside this area, close to the third 3V, but without invading the boundaries of the periventricular nucleus.

Comparing the distribution of MCH/NEI neurons of *M. musculus* and *N. alstoni* with that described for the rat (Bittencourt & Diniz, 2018; Bittencourt et al., 1992), a group of neurons was conspicuously missing: the periventricular group. To confirm this interspecies difference, we compared level-matched slices of male and female rats to male and female *M. musculus* mice and we confirmed the absence of those neurons in mice, both in the third ventricle dorsal cap and in the periventricular nucleus (Fig. 6). Furthermore, several extradiencephalic sites of MCH synthesis have been described for the rat, including the olfactory tubercle, the

pedunculopontine tegmental area, and the laterodorsal tegmental area (Bittencourt et al., 1992; Rondini et al., 2007). We were not able to detect MCH or NEI immunoreactivity in any of those sites.

3.3. Three-dimensional neurochemical structure of the *Mus musculus* lateral hypothalamic area

Using immunoperoxidase labeled sections of the three species to assemble three-dimensional models of the tuberal hypothalamus revealed remarkably different patterns of organization. In *Rattus* (Fig. 7 a), immunoreactive neurons form an almost continuous band, dorsally limited by the thalamus and ventrally limited by the PeF. Neurons form a high-density zone in the lateral LHA, with particularly high numbers in the area lateral to the fornix. Several neurons are seen very close to the dorsal half of the 3V, including neurons from the 3V dorsal cap that appear to join the two sides over the third ventricle. The *Mus* hypothalamus (Fig. 7 b), on the other hand, shows an accentuated reduction in the number of labeled neurons, with the central part of the LHA (dorsal to the fornix) almost devoid of MCH neurons. Despite the presence of neurons in the medial part of the tuberal hypothalamus resulting from the AHA labeling seen in *Mus*, few neurons are proximal to the 3V. The *Neotomodon* hypothalamus (Fig. 7 c), finally, is more homogenously labeled, with a higher count of neurons found in the ventral part of the tuberal hypothalamus, ventral to the fornix. Animated comparisons of the three animals can be found in Diniz et al., 2019 (dataset).

By analyzing the distribution of MCH neurons in the *Mus* LHA, we observed that MCH/NEI neurons were mostly absent of the central portion of the LHA, where ORX neurons are concentrated in three-dimensional views of the rat hypothalamus (Diniz et al., 2018). To set the spatial relationship between MCH/NEI and ORX neurons in the LHA, we performed double immunoperoxidase labeling and reconstructed the hypothalamus with markers for each neuronal type (Fig. 8). The lack of significant colocalization between MCH and ORX had been established earlier by immunofluorescence. The distribution of ORX neurons is more restricted than that of MCH/NEI neurons. Orexin-immunoreactive neurons are concentrated in the lateral part of the medial zone and the medial part of the lateral zone, partially overlapping with the PeF, with most MCH/NEI and ORX neurons intermingling in the dorsal LHA. Despite proximity between these two populations, no clear contact or colocalization was observed. The three-dimensional reconstruction (Fig. 8 b) revealed a concentric organization, with ORX-ir cells forming a spheroid shape centered dorsally to the fornix, which we called the LHA “core”, and MCH-ir cells were found mostly at the boundaries of that core, in what we described as the LHA “shell”. An animation of the three-dimensional reconstruction in movement is available in Diniz et al., 2019 (dataset).

3.4. The *Mus musculus* incerto-hypothalamic area

Because the putative IHy of *M. musculus* mice appeared to be significantly smaller in rostrocaudal extent to the described IHy of the rat (Sita et al., 2003, 2007), we performed double immunofluorescence to identify MCH/NEI neurons and tyrosine hydroxylase (TH)-ir neurons, a marker of dopamine synthesis. Our results confirm the existence of a *Mus* IHy, where MCH/NEI neurons are found intermingled with dopaminergic neurons of the A13 group, spanning an area of approximately 300µm in the rostrocaudal axis (Fig. 9). In virtually every case analyzed we found instances of MCH/NEI neurons making apparent contact with the soma of TH-ir neurons (insets in Fig. 9). To confirm those contacts were not an artifact of perspective resulting from widefield microscopy, we analyzed IHy-containing slices with confocal microscopy, and we confirmed that, in several cases, MCH/NEI neurons make extensive soma-soma contacts with dopaminergic neurons, despite no colocalization between all three markers in any one single neuron (Fig. 10).

3.5. MCH/NEI immunoreactivity during lactation

The MPOA is among the extra-hypothalamic areas of MCH synthesis described in the literature in *Rattus*. The expression of *Pmch* mRNA in this area cannot be detected in male animals, estrous-cycling animals or during gestation, but signals appear as soon as the 5th day postpartum, increasing in intensity towards the end of the lactation period and vanishing after weaning (Alvisi et al., 2016; Costa et al., 2019; Ferreira et al.,

2017; Knollema et al., 1992; Rondini et al., 2010). To assert if a similar phenomenon is observed in *Mus*, we performed immunohistochemistry in MPOA slices to detect MCH. As described for the rat, no immunoreactivity signals could be detected in males, estrous-cycling females or gestating mice. Different of the rat, however, no immunoreactivity was detected in the 5th or 12th day postpartum, and only weak, scattered immunoreactivity was found in the MPOA of 19th day postpartum mice, with signals disappearing after weaning (Fig. 11). These results indicate that the appearance of MCH neurons in the *Mus* MPOA is delayed and less extensive than that reported for *Rattus*. Since Costa et al. (2019) also reported an increase in MCH-ir fibers in the median eminence (ME) of female rats that closely followed the dynamics of MCH detection in the MPOA, we investigated the ME of mice in different periods. Almost no MCH immunoreactivity was detected in the *Mus* ME, regardless of sex and reproductive stage (Fig. 12), suggesting there is no lactation-induced response by the MCH system in *M. musculus*.

3.6. The distribution of MCH-ir fibers

Considering there was a significant difference between rats and mice in the presence of MCH/NEI-ir fibers in the ME, we decided to investigate the whole distribution of MCH/NEI-ir fibers in the *M. musculus* nervous system. To allow for a clearer visualization of immunolabeled fibers, we uploaded a series of nine illustrative frontal sections to a publicly available repository (Diniz et al., 2019 - dataset), where the full resolution images can be accessed and downloaded. Therefore, we opted not to provide an exhaustive description of the areas that contain MCH/NEI-ir fibers, but to only highlight the most noteworthy characteristics of these projections, especially in light of the similarities to what has already been described for *Rattus* (Bittencourt et al., 1992).

3.6.1. Telencephalon

There is a relatively high heterogeneity in MCH/NEI innervation among cortical areas, regarding both fiber density and specific *laminae* distribution. The higher densities of labeled fibers were found in the cingulate cortex, chiefly on areas 32a and 32b, with a particularly high density in the anterior part of this cortical area. Another area of high density is the agranular insular cortex. Fibers were also located in the main olfactory bulb, accessory olfactory nucleus and piriform cortex with medium densities. The septal area is one of the most densely innervated areas of the *Mus musculus* brain, with a very high density of labeled fibers in the ventral limb of the diagonal band of Broca and the medial septal nucleus, which can be considered the most densely innervated area of the *Mus* brain. The ventral part of the lateral septal nucleus also received numerous fibers, while the intermediate and dorsal parts were less innervated. The high density of fibers in septal structures contrasts with the negligible amount of labeling in nucleus accumbens and the ventral pallidum, while only scattered fibers were seen in the caudate-putamen nucleus. The medial *globus pallidus* receives a medium density of fibers, and its lateral division receives a high density. The hippocampal formation is another subcortical area heavily innervated by MCH/NEI-ir fibers. The highest number of fibers is found in *stratum lacunosum moleculare*, although fewer fibers could be seen in all other strata of the CA1, CA2 and CA3 fields. A moderate number of fibers could also be seen in the polymorphic layer of the dentate gyrus, chiefly in the subgranular zone.

3.6.2. Diencephalon

The largest numbers of MCH/NEI-ir fibers in the thalamus were found in the midline nuclei, including the *reuniens* and rhomboid nuclei. The lateral habenular nucleus also receives an important amount of MCH-ir fibers, while the medial habenular nucleus has a negligible contingent. The lateral and anterior thalamic groups are also labeled, although in lesser densities. The mediodorsal nucleus, posterior group, and intralaminar nuclei have almost no fibers. The remaining thalamic areas have sparse fibers. In the subthalamus, both the subthalamic nucleus and the ZI have a significant number of MCH/NEI-ir fibers, but there is only a small number of terminal boutons in these areas, indicating that these fibers are coursing to other regions through the

subthalamus and have little synaptic activity in this region. Numerous areas of the hypothalamus contain MCH-ir fibers. A large contingent of fibers were found along the rostrocaudal axis of the lateral zone, including the lateral preoptic area, lateral hypothalamic area, and the PHA. The medial zone has an intermediate amount of fibers, including the MPOA and the dorsomedial hypothalamic nucleus. As an exception to this rule, the ventromedial hypothalamic nucleus was virtually devoid of labeled fibers. In the periventricular zone, the PVH and the arcuate nucleus receive a moderate number of fibers, while the preoptic nucleus receives a small amount. The suprachiasmatic and retrochiasmatic hypothalamic nuclei were virtually devoid of labeling.

3.6.3. Midbrain and hindbrain

The majority of immunoreactive fibers in the brainstem were found along the rostrocaudal extension of the reticular formation. In the midbrain, many fibers can be observed in the periaqueductal gray matter and the mesencephalic reticular formation. The Edinger-Westphal nucleus receives a high number of fibers, similar to the rat. There is an average number of immunolabeled fibers in the ventral tegmental area and the *pars compacta* of the *substantia nigra*. Due to the major role of dopaminergic neurons in these areas over motivation and reward, functions previously ascribed to MCH (Diniz & Bittencourt, 2017), we investigated if MCH/NEI-ir fibers contact TH-ir neurons in these areas. Although a fraction of the MCH/NEI-ir were found close to TH-ir neurons (Fig. 13), the most common occurrence was to observe the outline of cells that were not TH-ir, but which were surrounded by MCH/NEI-ir fibers, suggesting a relationship between MCH and local interneurons. A substantial number of fibers was found in the *colliculi* layers, although only a few fibers were found in the geniculate bodies. Fibers could also be found in areas linked to arousal close to the fourth ventricle, such as the laterodorsal tegmental nucleus, the dorsal raphe, and the *locus coeruleus*. In the hindbrain, sensorial (*e.g.* principal sensory trigeminal nucleus) and autonomic (*e.g.* nucleus of the solitary tract) nuclei have moderate innervation.

3.6.4. Periventricular zones and the leptomeningeal space

Recent reports have shown that MCH is released in the ventricular space as part of a volume transmission mechanism of communication (Jiang & Brüning, 2018; Noble et al., 2018). We, therefore, decided to examine the periventricular zones and the leptomeningeal space of both rats and mice. A large number of varicose fibers could be observed in the subventricular zone of the brain ventricles, with a notable high density on the subventricular zone of the lateral ventricles (Fig. 14 a1, a2). Furthermore, we also observed a high density of immunolabeled fibers close to the brain surface, with a particularly high density of fibers on the dorsal surface of the mesencephalon (Fig. 14 b1, b2).

4. Discussion

4.1. The MCH/NEI neuron

A feature of the MCH peptidergic system is the conservation of the MCH/NEI neuron in murids, especially when considering the morphological differences observed for other systems and areas in species with a stricter phylogenetic relationship, including strain-linked differences (Bachtell et al., 2002; Baker et al., 1980), between species belonging to the same genus (Shapiro et al., 1991; Young et al., 1996; Young et al., 1997), and between murine species (Lehman et al., 2013; Morin et al., 2006; Piggins et al., 2001). In both species, several similarities can be pointed out: 1. Almost all neurons that synthesize MCH also synthesize NEI; 2. MCH/NEI neurons can be classified in multipolar, fusiform and crescent shapes, with similar characteristics; 3. MCH/NEI neurons do not colocalize significantly with ORX; 4. MCH and NEI are found in different subcellular compartments, as previously suggested for the rat by Bittencourt et al. (1992) using electron microscopy. These observations are important, since they reveal that the synthesis of MCH and NEI has been maintained tethered, with these two peptides found in different subcellular compartments. Combined to the observation of numerous varicosities along the axonal projections in all three species (Bittencourt et al., 1992; this work), this data may be informative about the neuronal communication methods employed by MCH/NEI neurons.

Volume transmission has been recently proposed as a mechanism of communication in the MCH peptidergic system particularly important for feeding behavior (Jiang & Brüning, 2018; Noble et al., 2018). The varicose pattern of fibers found in MCH/NEI fibers is compatible with that observed in other systems who have been strongly associated to volume transmission, including serotonin, norepinephrine and acetylcholine (Contant et al., 1996; Descarries et al., 1975; Descarries et al., 1997; Descarries et al., 1977; Séguéla et al., 1989). The segregation of MCH in NEI in different subcellular compartments could potentially allow different mechanisms and sites of release for each neuromodulator (Jaffe et al., 1998; Patel et al., 2009; Trueta & De-Miguel, 2012), what may explain how MCH and NEI show significant functional differences (Gonzalez et al., 1998; Parkes & Vale, 1993b; Sanchez et al., 1997), despite the large degree of overlap in their synthesis. Furthermore, the presence of immunolabeled fibers in the internal and external surfaces of the brain could provide a means for MCH and NEI to reach the cerebrospinal fluid and travel to distant areas of the brain regardless of direct innervation. Further studies will be necessary to determine what are the exact mechanisms of release employed by MCH/NEI neurons and how extensive volume transmission is for this system.

Another intriguing feature of MCH/NEI neurons is their extensive somatic contacts with dopaminergic cells of the *Mus* IHy. Similar membrane juxtapositions have been described for the rat (Sita et al., 2007), but the lack of higher resolution microscopy in previous works impaired our ability to distinguish between simple focal plane artifacts or actual membrane contacts. Three-dimensional visualization of confocal photomicrographs allowed us to verify that MCH/NEI neurons and TH-ir neurons have somatic contacts in the *Mus* IHy. These membrane juxtapositions may occur due to the presence of electrical synapses between these neurons, with gap junctions allowing a communication mechanism faster than traditional synaptic mechanisms (Miller & Pereda, 2017). The existence of such contacts could indicate that the IHy acts as a tethering point between the MCH peptidergic system and the catecholaminergic system through the A13 group of dopaminergic neurons. The presence of multiple contacts in each animal and in every animal analyzed bespeaks a functional significance, especially when those contacts are conserved in at least two different genera.

4.2. Comparative morphology

In contrast to the strongly conserved cellular characteristics, the distribution of MCH/NEI neurons is less conserved, as summarized in Fig. 15. In *Mus*, MCH/NEI neurons were found exclusively in the tuberal and mammillary areas of the hypothalamus and the adjoining ZI, without any labeling detected outside the diencephalon. This distribution differs from the rat, where immunoreactive neurons are found in several extra-diencephalic areas, including the olfactory tubercle, the paramedian pontine reticular formation, and the laterodorsal tegmental nucleus (Bittencourt et al., 1992; Rondini et al., 2007). One possible explanation is methodological in nature: Bittencourt et al. (1992) report that extradiencephalic sites required extended times of exposition in the autoradiographic film, and colchicine injections were needed for those neurons to become immunodetectable. Therefore, it is possible that, in this work, our detection methods did not surpass a certain minimal threshold of detection for these neurons, even though we employed strong signal amplification techniques. This theory is supported by the recent finding of immunoreactive neurons in the pontine reticular formation of the cat (Costa et al., 2018). However, the lack of descriptions of those groups in other species, with varying phylogenetic distances to rodents, points to an acquisition that may have happened in the rat lineage alone (Bird et al., 2001; Bittencourt et al., 1998; Elias et al., 2001).

The diencephalic distribution of MCH/NEI neurons was also linked to the species examined. The AHA is a major region of variation between *Rattus*, *Mus,* and *Neotomodon*. In the rat, the density of immunolabeled neurons in this area is lower than in *Mus* and *Neotodomon*, with scattered neurons that only loosely respect the boundaries of this area, and a clear separation between the IHy, the third ventricle dorsal cap, and the AHA (Bittencourt et al., 1992). *Neotodomon*, on the other hand, has a high number of labeled neurons in the AHA, which extends dorsally and occupies the space where the putative IHy would be situated. *Mus* occupies an

intermediate position in this spectrum, with an average density of MCH/NEI neurons in the IHy, and a dorsal extension that almost reaches, but not quite intermingles with, the IHy.

Three groups of neurons described in *Rattus* could not be found in *Mus*: the periventricular group, including the 3V dorsal cap; the neurons in the dorsal part of the dorsal tuberomammillary nucleus; and the PHA group. In *Neotomodon*, neurons can be seen close to the periventricular zone, including a group of neurons inside the *N. alstoni* AHA that closely resembles the rat 3V dorsal cap. These neurons, however, are not as proximal to the 3V as those found in the rat. The *Neotomodon* PHA closely resembles that of the rat, but it does not appear to have neurons in the dorsal tuberomammillary nucleus, with this feature remaining exclusive to *Rattus*. Finally, neurons of the *Mus* LHA have a different spatial relationship with the PeF than both *Rattus* and *Neotomodon*, with fewer neurons in *Mus* and a distribution that is more dorsolateral than that of the other two rodents. The major similarity between all three species is the pericapsular portion of the LHA. Neurons were consistently found in the lateral LHA, both dorsolaterally and ventrolaterally with respect to the internal capsule and cerebral peduncle. These neurons are less numerous in the anterior pattern and become denser in the posterior tuberal hypothalamus. There is a good correspondence between these neurons and compartments *e*, *e1*, *e2* and *d* of the medial forebrain bundle (Nieuwenhuys et al., 1982), what may help explain the widespread distribution of fibers in the mice, despite less neuronal groups being present in this species. Neurons in the ZI were also consistently distributed in all three species.

Another two rodents had their MCH systems described, the golden hamster and the Siberian hamster, both cricetids. The Siberian hamster (*Phodopus sungorus*) has a diencephalic distribution of MCH-ir neurons that includes the LHA, ZI, the PHA, and the margin of the dorsomedial hypothalamic nucleus, occupying predominantly the dorsal half of the tuberal hypothalamus (Khorooshi & Klingenspor, 2005). No immunolabeled neurons were described in the periventricular zone of the Siberian hamster, further strengthening this feature as a particularity of the rat. The described fields of innervation for the Siberian hamster are mostly compatible with *Mus*, including the dorsomedial hypothalamic nucleus, LHA, ZI, posterior hypothalamic area, paraventricular thalamic nucleus, raphe nuclei, and the intergeniculate leaflet. The major disagreement between the Siberian hamster and the domestic mouse was the internal layer of the median eminence, which contains fibers in the hamster, but not in *Mus*. The presence of MCH fibers in the ME of the Siberian hamster is a common feature shared with *Rattus*, but it is likely that the function played by this innervation is completely different between these two species. Siberian hamsters undergo seasonal changes of fur color, while all other rodent species examined for MCH do not. Since Weatherhead and Logan (1981) demonstrated that α-MSH darkens the fur of Siberian hamsters, it is possible that MCH released through the posterior pituitary may antagonize the effects of α-MSH, as it does in the control of skin pigmentation in teleost fish (Kawauchi et al., 1983).

Vidal et al. (2005) reported the MCH distribution in another hamster species, the golden hamster (*Mesocricetus auratus*). The similarity between this species and *Mus* is remarkable. The authors describe the presence of immunolabeled neurons in the medial ZI, the posterior division of the PVH (likely a misidentified IHy), the pericapsular LHA, and the caudal dorsomedial AHA. The golden hamster has few MCH neurons in the PeF, which is similar to *Mus* but dissimilar to *Rattus, Neotomodon, and Phodopus*. Considering the phylogenetic relationship between these animals, and the implied role of the PeF in feeding behavior (Elias et al., 1998; Stanley et al., 1993; Stanley & Thomas, 1993), some overlap in environmental conditions or behavior may have driven a convergent reduction of MCH in the PeF in both *Mus* and *Mesocricetus*.

Looking at the five species examined here and elsewhere, a muroid basic plan starts to emerge. Neurons immunolabeled for MCH/NEI are most uniformly found in the dorsolateral hypothalamus, including the pericapsular zone of the LHA (intermingled with the medial forebrain bundle), and in the thalamic ZI, spanning a rostrocaudal distribution that ranges from the caudalmost levels of the PVH to the appearance of the mammillary complex. This basic plan appears to have been largely maintained in the *Euarchantoglires*

superorder, of which two simians had their MCH immunoreactivity described: tufted capuchin monkeys (*Sapajus spp.* – Bittencourt et al., 1998) and humans (*Homo sapiens* – Elias et al., 2001). In both species, MCH-ir neurons were described to be predominantly located in the dorsolateral LHA, to be present in the ZI, and to be distributed in a rostrocaudal extent similar to what has been escribed above for muroids. There is little evidence, however, for the presence of MCH neurons in the medial and periventricular zones of the hypothalamus of simii, including the IHy, making these areas the major discrepancy between rodents and primates. Unfortunately, little is known about MCH in non-muroid species of the *Glires* clade, including the important laboratory model guinea-pig, and rabbits and hares. Since the loss of one MCH receptor is believed to have happened at the root of the *Glires* clade (Tan et al., 2002), it would be interesting to investigate to what extent the particularities of muroids could be adaptive responses to the loss of one of the receptors.

Support for the *Euarchantoglires* basic plan is not found in the *Laurasiatheria* superorder. In the two ungulates with known MCH distributions, pigs (*Sus scrofa domesticus* – Chometton et al., 2014) and sheep (*Ovis aries* – Tillet et al., 1996), MCH neurons are found predominantly in the ventral portion of the LHA, extending from the ventrolateral part of the fornix to the internuclear space between the DMH and the VMH, only scattered presence of neurons in the ZI, and a larger rostrocaudal extent that ends at the ventral tegmental area. In the only carnivore with a described MCH distribution, the domestic cat (*Felis catus* – Torterolo et al., 2006), the results are dissimilar to species of both the *Euarchantoglires* superorder and of the *Artiodactyla* order, with the largest aggregation of neurons found in the perifornical nucleus, and additional groups found in the dorsomedial hypothalamus and the posterior hypothalamic area, but seldom found in the pericapsular LHA or caudal to the mammillary nuclei area. This is indicative of a strong diversification of the distribution of MCH-ir neurons in the *Laurasiatheria* superorder, possibly due to the dissimilar stereotypical roles played by studies carnivores and ungulates in their natural environment.

Overall, it is evident that the distribution of MCH neurons has remained notably plastic in a broad range of species. Therefore, the mapping of MCH in non-traditional laboratory models can be a useful tool for the investigation and understanding of the evolution and diversification of the mammalian hypothalamus. We expect future studies to address open questions, such as the influence of the MCHR1 loss on the *Glires* clade, functional differences between the lateral and medial groups of MCH neurons in the tuberal hypothalamus (and their implications on the transposability of rodent data to humans), and the untapped diversity of MCH distribution in species of grandorder *Laurasiatheria*.

4.3. Morphofunctional correlates

Several roles attributed to MCH and NEI in rats and mice were found to have anatomical correlates in this study. Areas linked to reward are innervated by MCH/NEI neurons, including light innervation of the caudate-putamen and moderate innervation of the ventral tegmental area, with MCH/NEI-ir fibers contacting dopaminergic neurons in the latter, supporting the circuit suggested by Domingos et al. (2013). Actions of MCH on learning, memory consolidation/retrieval, and emotion (Le Barillier et al., 2015; Monzon et al., 1999; Sita et al., 2016; Torterolo et al., 2015) also had a clear anatomical substrate in *Mus musculus* mice, with a dense innervation of the medial septal nucleus and the dorsal part of the hippocampal formation, similar to *Rattus* (Lima et al., 2013). Similar observations were made for autonomic modulation mediated by the nucleus of the solitary tract and the PVH (Abbott et al., 2003; Brown et al., 2007), sleep and arousal mediated by the dorsal raphe and the ventrolateral periaqueductal grey matter (Clément et al., 2012; Lagos et al., 2009; Lagos et al., 2011), and sensory integration through projections to olfactory areas and the medial septal nucleus (Adams et al., 2011; Miller et al., 1993).

The lack of MCH neurons in periventricular zones of *Mus*, as well as the limited number of fibers in these zones and in the ME, could be indicative of an important functional dimorphism between the two species. Smith et al. (2006) demonstrated that MCH is capable of stimulating adrenocorticotropic hormone (ACTH) and corticosterone release in mice, two essential elements of the hypothalamus-pituitary-adrenal (HPA) axis. In the

rat, this modulation has been hypothesized to occur directly at the median eminence, with MCH-ir fibers interacting through axo-axonic contacts with corticotropin-releasing factor (CRF) fibers, or indirectly through projections to the PVH and/or the arcuate nucleus. In *Mus*, the latter appears to be the favored option, as the scarcity of fibers in the external layer of the ME makes it improbable that direct fiber contact occurs.

In a similar fashion, Chiocchio et al. (2001), Gallardo et al. (2004) and Costa et al. (2019) suggested that MCH-ir fibers in the external layer of the ME participate in the endocrine modulation of the reproductive cycle, since the density of labeling in the ME changes according to the estrous cycle stage of the animal, and MCH-ir fibers are found in proximity to gonadotropin-releasing hormone (GnRH)-ir fibers. As is the case with the hypothalamus-pituitary-adrenal axis modulation, MCH actions over the hypothalamus-pituitary-gonadal axis are probably independent of the median eminence. Since Wu et al. (2009) reports a direct innervation and electrophysiological modulation of GnRH neurons in the anteroventral periventricular hypothalamic nucleus of *Mus*, that could account for the mechanism of sexual modulation performed by MCH in the absence of ME contacts. This trend of a decreased endocrine modulation by MCH in mice was also observed during the lactation period. While rat dams display MCH immunoreactivity in neurons of the MPOA as soon as the 5th day postpartum (Knollema et al., 1992; Rondini et al., 2010), mice dams had detectable MCH-ir neurons only on the 19th day. Furthermore, there was no alteration in the density of MCH-ir fibers in the median eminence, as it has been reported for the rat as a mechanism for MCH-oxytocin interaction during lactation (Costa et al., 2019). Overall, this indicates a decreased participation of MCH in neuroendocrine phenomena in the *Mus*, making the rat a more suitable experimental model for this particular line of investigation.

4.4. Neurochemical domains

The differences between the three species resulted in accentuated disparate patterns of distribution when MCH neurons were visualized in three-dimensional models. Perhaps even more important than the comparison between the three species was our observation that the *Mus musculus* LHA is concentrically organized, as observed with the simultaneous observation of MCH and ORX. While ORX neurons form a high-density spheroid located at the center of the LHA, the LHA core (LHAc), the distribution of MCH neurons results in a hemisphere that surrounds ORX neurons from the dorsal, lateral, ventral and posterior sides, leaving the anterior side mostly uncovered, the LHA shell (LHAs).

These areas of differential neuromodulator predominance, or neurochemical domains, coexist with the well described nuclear organization. While the nuclear parcellation is supported by cellular density and connectivity, in several instances the distribution of neurochemically-defined populations does not conform to the described nuclei, as it has been illustrated for MCH, NEI, and ORX in this work. Likewise, the LHAc and LHAs cannot be described in terms of projection fields, as these two neurochemical domains contain neurons with different projection patterns (Hahn, 2010; Hahn & Swanson, 2015; Swanson et al., 2005). These two organization models are, therefore, complementary, as they account for different aspects of the complex hypothalamic structure. We believe three-dimensional reconstructions are powerful tools when combined with neurochemical studies, as they may help elucidate emergent patterns that are not clearly observable in two-dimensional slices.

4.5. Conclusion

In this study, three rodent species were examined regarding the morphology of their MCH peptidergic system, including the non-traditional model species *N. alstoni*. The most thoroughly examined species in this work was the domestic mouse, as the extensive functional data present in the literature created a major need for further morphological understanding of its anatomical basis. Comparisons between the species studied in this work revealed, however, that several aspects of *Mus* were conserved in other rodents, such as the morphological types of MCH/ NEI neurons, the cosynthesis of those neuropeptides, the subcellular separation of MCH and NEI, and the existence of membrane juxtapositions between MCH/NEI and dopaminergic neurons.

Not all aspects of the MCH system, however, are conserved, with a basic plan of distribution common for all three species marked with particularities for each one of them.

The differences found for each genus may signify functional differences among these species. The well-developed perifornical nucleus of *Neotomodon* may be part of the neural substrate of the spontaneous changes in weight observed in the *N. alstoni*. The intimate relationship between MCH/NEI neurons and the periventricular zone of *Rattus* is indicative of a strong neuroendocrine function for the MCH peptidergic system in the rat. The concentrical organization of MCH neurons around ORX neurons in three-dimensional reconstructions and the profuse innervation of ventricles and the brain surface are indicative of a strong anatomical basis for volume transmission, which may play an accentuated role in *Mus*. Each one of these aspects merits further investigation, but we believe there is now a solid understanding of the underlying morphology to assist in such studies.

References

Abbott, C. R., Kennedy, A. R., Wren, A. M., Rossi, M., Murphy, K. G., Seal, L. J., . . . Bloom, S. R. (2003). Identification of hypothalamic nuclei involved in the orexigenic effect of melanin-concentrating hormone. *Endocrinology, 144*(9), 3943-3949. doi:10.1210/en.2003-0149

Adamantidis, A., Salvert, D., Goutagny, R., Lakaye, B., Gervasoni, D., Grisar, T., . . . Fort, P. (2008). Sleep architecture of the melanin‐concentrating hormone receptor 1‐knockout mice. *European Journal of Neuroscience, 27*, 1793-1800. doi:10.1111/j.1460-9568.2008.06129.x

Adams, A. C., Domouzoglou, E. M., Chee, M. J., Segal-Lieberman, G., Pissios, P., & Maratos-Flier, E. (2011). Ablation of the hypothalamic neuropeptide melanin concentrating hormone is associated with behavioral abnormalities that reflect impaired olfactory integration. *Behavioural brain research, 224*, 195-200. doi:10.1016/j.bbr.2011.05.039

Alachkar, A., Alhassen, L., Wang, Z., Wang, L., Onouye, K., Sanathara, N., & Civelli, O. (2016). Inactivation of the melanin concentrating hormone system impairs maternal behavior. *European Neuropsychopharmacology, 26*(11), 1826-1835. doi:10.1016/j.euroneuro.2016.08.014

Alvisi, R. D., Diniz, G. B., Da-Silva, J. M., Bittencourt, J. C., & Felicio, L. F. (2016). Suckling-induced Fos activation and melanin-concentrating hormone immunoreactivity during late lactation. *Life sciences, 148*, 241-246. doi:10.1016/j.lfs.2016.02.038

Bachtell, R., Tsivkovskaia, N., & Ryabinin, A. (2002). Strain differences in urocortin expression in the Edinger–Westphal nucleus and its relation to alcohol-induced hypothermia. *Neuroscience, 113*(2), 421-434. doi:10.1016/S0306-4522(02)00174-4

Báez-Ruiz, A., Luna-Moreno, D., Carmona-Castro, A., Cárdenas-Vázquez, R., Díaz-Muñoz, M., Carmona-Alcocer, V., . . . Miranda-Anaya, M. (2014). Hypothalamic expression of anorexigenic and orexigenic hormone receptors in obese females Neotomodon alstoni: effect of fasting. *Nutritional Neuroscience, 17*(1), 31-36. doi:10.1179/1476830513Y.0000000063

Baker, H., Joh, T. H., & Reis, D. J. (1980). Genetic control of number of midbrain dopaminergic neurons in inbred strains of mice: relationship to size and neuronal density of the striatum. *Proceedings of the National Academy of Sciences, 77*(7), 4369-4373. doi:10.1073/pnas.77.7.4369

Benedetto, L., Pereira, M., Ferreira, A., & Torterolo, P. (2014). Melanin-concentrating hormone in the medial preoptic area reduces active components of maternal behavior in rats. *Peptides, 58*, 20-25. doi:10.1016/j.peptides.2014.05.012

Bird, D. J., Potter, I. C., Sower, S. A., & Baker, B. I. (2001). The distribution of melanin-concentrating hormone in the lamprey brain. *General and comparative endocrinology, 121*(3), 232-241. doi:10.1006/gcen.2001.7609

Bittencourt, J. C., & Diniz, G. B. (2018). Neuroanatomical Structure of the MCH System. In *Melanin-Concentrating Hormone and Sleep* (1st ed., pp. 1-46): Springer.

Bittencourt, J. C., & Elias, C. F. (1998). Melanin-concentrating hormone and neuropeptide EI projections from the lateral hypothalamic area and zona incerta to the medial septal nucleus and spinal cord: a study using multiple neuronal tracers. *Brain research, 805*(1-2), 1-19. doi:10.1016/S0006-8993(98)00598-8

Bittencourt, J. C., Frigo, L., Rissman, R. A., Casatti, C. A., Nahon, J.-L., & Bauer, J. A. (1998). The distribution of melanin-concentrating hormone in the monkey brain (Cebus apella). *Brain research, 804*(1), 140-143. doi:10.1016/S0006-8993(98)00662-3

Bittencourt, J. C., Presse, F., Arias, C., Peto, C. A., Vaughan, J. M., Nahon, J.-L., . . . Sawchenko, P. E. (1992). The melanin-concentrating hormone system of the rat brain: an immuno- and hybridization histochemical characterization. *The Jorunal of Comparative Neurology, 319*(2), 218-245. doi:10.1002/cne.903190204

Brown, S. N., Chitravanshi, V. C., Kawabe, K., & Sapru, H. N. (2007). Microinjections of melanin concentrating hormone into the nucleus tractus solitarius of the rat elicit depressor and bradycardic responses. *Neuroscience, 150*(4), 796-806. doi:10.1016/j.neuroscience.2007.10.002

Byers, S. L., Wiles, M. V., Dunn, S. L., & Taft, R. A. (2012). Mouse estrous cycle identification tool and images. *PLoS One, 7*(4), e35538. doi:10.1371/journal.pone.0035538

Carmona-Alcocer, V., Fuentes-Granados, C., Carmona-Castro, A., Aguilar-González, I., Cárdenas-Vázquez, R., & Miranda-Anaya, M. (2012). Obesity alters circadian behavior and metabolism in sex dependent manner in the volcano mouse Neotomodon alstoni. *Physiology & Behavior, 105*(3), 727-733. doi:10.1016/j.physbeh.2011.09.022

Chiocchio, S. R., Gallardo, M. a. G. P., Louzan, P., Gutnisky, V., & Tramezzani, J. H. (2001). Melanin-concentrating hormone stimulates the release of luteinizing hormone-releasing hormone and gonadotropins in the female rat acting at both median eminence and pituitary levels. *Biology of Reproduction, 64*(5), 1466-1472. doi:10.1095/biolreprod64.5.1466

Chometton, S., Franchi, G., Houdayer, C., Mariot, A., Poncet, F., Fellmann, D., . . . Risold, P. (2014). Different distributions of preproMCH and hypocretin/orexin in the forebrain of the pig (Sus scrofa domesticus). *J Chem Neuroanat, 61*, 72-82. doi:10.1016/j.jchemneu.2014.08.001

Clément, O., Sapin, E., Libourel, P.-A., Arthaud, S., Brischoux, F., Fort, P., & Luppi, P.-H. (2012). The lateral hypothalamic area controls paradoxical (REM) sleep by means of descending projections to brainstem GABAergic neurons. *Journal of Neuroscience, 32*(47), 16763-16774. doi:10.1523/JNEUROSCI.1885-12.2012

Contant, C., Umbriaco, D., Garcia, S., Watkins, K. C., & Descarries, L. (1996). Ultrastructural characterization of the acetylcholine innervation in adult rat neostriatum. *Neuroscience, 71*(4), 937-947. doi:10.1016/0306-4522(95)00507-2

Costa, A., Castro-Zaballa, S., Lagos, P., Chase, M. H., & Torterolo, P. (2018). Distribution of MCH-containing fibers in the feline brainstem: Relevance for REM sleep regulation. *Peptides, 104*, 50-61. doi:10.1016/j.peptides.2018.04.009

Costa, H. C., Da-Silva, J. M., Diniz, G. B., Da-Silva Pereira, L., Gobbo, D. R., Da-Silva, R. J., . . . Bittencourt, J. C. (2019). Characterization and origins of melanin-concentrating hormone immunoreactive fibers of the posterior lobe of the pituitary and median eminence during lactation in Long-Evans rat. *Journal of neuroendocrinology, 00:e12723*. doi:10.1111/jne.12723

Davis, W. B. (1944). Notes on Mexican mammals. *Journal of Mammalogy, 25*(4), 370-403. doi:10.2307/137490

Davis, W. B., & Follansbee, L. A. (1945). The mexican volcano mouse, Neotomodon. *Journal of Mammalogy, 26*(4), 401-411. doi:10.2307/1375160

Descarries, L., Alain, B., & Watkins, K. C. (1975). Serotonin nerve terminals in adult rat neocortex. *Brain research, 100*(3), 563-588. doi:10.1016/0006-8993(75)90158-4

Descarries, L., Gisiger, V., & Steriade, M. (1997). Diffuse transmission by acetylcholine in the CNS. *Progress in Neurobiology, 53*(5), 603-625. doi:10.1016/S0301-0082(97)00050-6

Descarries, L., Watkins, K. C., & Lapierre, Y. (1977). Noradrenergic axon terminals in the cerebral cortex of rat. III. Topometric ultrastructural analysis. *Brain research, 133*(2), 197-222. doi:10.1016/0006-8993(77)90759-4

Diniz, G. B., & Bittencourt, J. C. (2017). The Melanin-Concentrating Hormone as an Integrative Peptide Driving Motivated Behaviors. *Frontiers in systems neuroscience, 11*, 1-32. doi:10.3389/fnsys.2017.00032

Diniz, G. B., Candido, P. L., Klein, M. O., Alvisi, R. D., Presse, F., Nahon, J.-L., . . . Bittencourt, J. C. (2018). The weaning period promotes alterations in the orexin neuronal population of rats in a suckling-dependent manner. *Brain Structure & Function, 223*(8), 3739-3755. doi:10.1007/s00429-018-1723-0

Domingos, A. I., Sordillo, A., Dietrich, M. O., Liu, Z.-W., Tellez, L. A., Vaynshteyn, J., . . . Friedman, J. M. (2013). Hypothalamic melanin concentrating hormone neurons communicate the nutrient value of sugar. *Elife, 2*, e01462. doi:10.7554/eLife.01462

Elias, C. F., & Bittencourt, J. C. (1997). Study of the origins of melanin-concentrating hormone and neuropeptide EI immunoreactive projections to the periaqueductal gray matter. *Brain research, 755*(2), 255-271. doi:10.1016/S0006-8993(97)00104-2

Elias, C. F., Lee, C. E., Kelly, J. F., Ahima, R. S., Kuhar, M., Saper, C. B., & Elmquist, J. K. (2001). Characterization of CART neurons in the rat and human hypothalamus. *Journal of Comparative Neurology, 432*(1), 1-19. doi:10.1002/cne.1085

Elias, C. F., Saper, C. B., Maratos‐Flier, E., Tritos, N. A., Lee, C., Kelly, J., . . . Barsh, G. S. (1998). Chemically defined projections linking the mediobasal hypothalamus and the lateral hypothalamic area. *Journal of Comparative Neurology, 402*(4), 442-459. doi:10.1002/(SICI)1096-9861(19981228)402:4<442::AID-CNE2>3.0.CO;2-R

Elias, C. F., Sita, L. V., Zambon, B. K., Oliveira, E. R., Vasconcelos, L. A. P., & Bittencourt, J. C. (2008). Melanin-concentrating hormone projections to areas involved in somatomotor responses. *J Chem Neuroanat, 35*(2), 188-201. doi:10.1016/j.jchemneu.2007.10.002

Fabre, P.-H., Hautier, L., Dimitrov, D., & Douzery, E. J. P. (2012). A glimpse on the pattern of rodent diversification: a phylogenetic approach. *BMC Evolutionary Biology, 12*, 88. doi:10.1186/1471-2148-12-88

Fellmann, D., Bugnon, C., & Risold, P. (1987). Unrelated peptide immunoreactivities coexist in neurons of the rat lateral dorsal hypothalamus: Human growth hormone-releasing factor1–37−, salmon melanin-concentrating hormone-and α-melanotropin-like substances. *Neuroscience Letters, 74*(3), 275-280. doi:10.1016/0304-3940(87)90309-0

Ferreira, J. G. P., Duarte, J. C. G., Diniz, G. B., & Bittencourt, J. C. (2017). Litter size determines the number of melanin-concentrating hormone neurons in the medial preoptic area of Sprague Dawley lactating dams. *Physiology & Behavior, 181*, 75-79. doi:j.physbeh.2017.08.028

Fronczek, R., Lammers, G. J., Balesar, R., Unmehopa, U. A., & Swaab, D. F. (2005). The number of hypothalamic hypocretin (orexin) neurons is not affected in Prader-Willi syndrome. *The Journal of Clinical Endocrinology & Metabolism, 90*(9), 5466-5470. doi:10.1210/jc.2005-0296

Gallardo, M. G. P., Chiocchio, S. R., & Tramezzani, J. H. (2004). Changes of melanin-concentrating hormone related to LHRH release in the median eminence of rats. *Brain research, 1030*(1), 152-158. doi:10.1016/j.brainres.2004.10.005

Georgescu, D., Sears, R. M., Hommel, J. D., Barrot, M., Bolanos, C. A., Marsh, D. J., . . . DiLeone, R. J. (2005). The hypothalamic neuropeptide melanin-concentrating hormone acts in the nucleus accumbens to modulate feeding behavior and forced-swim performance. *Journal of Neuroscience, 25*(11), 2933-2940. doi:10.1523/JNEUROSCI.1714-04.2005

Goldman, E. A. (1910). *Revision of the wood rats of the genus Neotoma*: US Government Printing Office.

Gonzalez, M. I., Baker, B. I., Hole, D. R., & Wilson, C. A. (1998). Behavioral effects of neuropeptide EI (NEI) in the female rat: interactions with α-MSH, MCH and dopamine. *Peptides, 19*(6), 1007-1016. doi:10.1016/S0196-9781(98)00045-X

Gonzalez, M. I., Vaziri, S., & Wilson, C. A. (1996). Behavioral effects of alpha-MSH and MCH after central administration in the female rat. *Peptides, 17*(1), 171-177. doi:10.1016/0196-9781(95)02092-6

Guesdon, B., Paradis, É., Samson, P., & Richard, D. (2009). Effects of intracerebroventricular and intra-accumbens melanin-concentrating hormone agonism on food intake and energy expenditure. *American Journal of Physiology Regulatory, Integrative and Comparative Physiology, 296*(3), R469-R475. doi:10.1152/ajpregu.90556.2008

Haemmerle, C. A. S., Campos, A. M. P., & Bittencourt, J. C. (2015). Melanin-concentrating hormone inputs to the nucleus accumbens originate from distinct hypothalamic sources and are apposed to GABAergic and cholinergic cells in the Long-Evans rat brain. *Neuroscience, 289*, 392-405. doi:10.1016/j.neuroscience.2015.01.014

Hahn, J. D. (2010). Comparison of melanin-concentrating hormone and hypocretin/orexin peptide expression patterns in a current parceling scheme of the lateral hypothalamic zone. *Neuroscience Letters, 468*(1), 12-17. doi:10.1016/j.neulet.2009.10.047

Hahn, J. D., & Swanson, L. W. (2015). Connections of the juxtaventromedial region of the lateral hypothalamic area in the male rat. *Frontiers in systems neuroscience, 9*(66), 1-53. doi:10.3389/fnsys.2015.00066

Hoffman, G. E., Murphy, K. J., & Sita, L. V. (2016). The importance of titrating antibodies for immunocytochemical methods. *Current Protocols in Neuroscience, 76*(1), 2.12.11-12.12.37. doi:10.1002/cpns.1

Jaffe, E. H., Marty, A., Schulte, A., & Chow, R. H. (1998). Extrasynaptic vesicular transmitter release from the somata of substantia nigra neurons in rat midbrain slices. *Journal of Neuroscience, 18*(10), 3548-3553. doi:10.1523/JNEUROSCI.18-10-03548.1998

Jiang, H., & Brüning, J. C. (2018). Melanin-Concentrating Hormone-Dependent Control of Feeding: When Volume Matters. *Cell Metabolism, 28*(1), 7-8. doi:10.1016/j.cmet.2018.06.018

Jones, K. R., Fariñas, I., Backus, C., & Reichardt, L. F. (1994). Targeted disruption of the BDNF gene perturbs brain and sensory neuron development but not motor neuron development. *Cell, 76*(6), 989-999.

Karlsson, C., Aziz, A. M. A., Rehman, F., Pitcairn, C., Barchiesi, R., Barbier, E., . . . Thorsell, A. (2016). Melanin‐Concentrating Hormone and Its MCH‐1 Receptor: Relationship Between Effects on Alcohol and Caloric Intake. *Alcoholism: Clinical & Experimental Research, 40*(10), 2199-2207. doi:10.1111/acer.13181

Kawauchi, H., Kawazoe, I., Tsubokawa, M., Kishida, M., & Baker, B. I. (1983). Characterization of melanin-concentrating hormone in chum salmon pituitaries. *Nature, 305*(5932), 321-323. doi:10.1038/305321a0

Kennedy, A. R., Todd, J. F., Dhillo, W. S., Seal, L. J., Ghatei, M. A., O'Toole, C. P., . . . Bloom, S. R. (2003). Effect of direct injection of melanin-concentrating hormone into the paraventricular nucleus: further evidence for a stimulatory role in the adrenal axis via SLC-1. *Journal of neuroendocrinology, 15*(3), 268-272. doi:10.1046/j.1365-2826.2003.00979.x

Khorooshi, R. M. H., & Klingenspor, M. (2005). Neuronal distribution of melanin-concentrating hormone, cocaine-and amphetamine-regulated transcript and orexin B in the brain of the Djungarian hamster (Phodopus sungorus). *J Chem Neuroanat, 29*(2), 137-148. doi:10.1016/j.jchemneu.2004.10.003

Knollema, S., Brown, E. R., Vale, W., & Sawchenko, P. E. (1992). Novel hypothalamic and preoptic sites of prepro-melanin-concentrating hormone messenger ribonucleic Acid and Peptide expression in lactating rats. *Journal of neuroendocrinology, 4*(6), 709-717. doi:10.1111/j.1365-2826.1992.tb00222.x

Lagos, P., Torterolo, P., Jantos, H., Chase, M. H., & Monti, J. M. (2009). Effects on sleep of melanin-concentrating hormone (MCH) microinjections into the dorsal raphe nucleus. *Brain research, 1265*, 103-110. doi:10.1016/j.brainres.2009.02.010

Lagos, P., Torterolo, P., Jantos, H., & Monti, J. M. (2011). Immunoneutralization of melanin-concentrating hormone (MCH) in the dorsal raphe nucleus: effects on sleep and wakefulness. *Brain research, 1369*, 112-118. doi:10.1016/j.brainres.2010.11.027

Le Barillier, L., Léger, L., Luppi, P. H., Fort, P., Malleret, G., & Salin, P. A. (2015). Genetic deletion of melanin‐concentrating hormone neurons impairs hippocampal short‐term synaptic plasticity and hippocampal‐dependent forms of short‐term memory. *Hippocampus, 25*(11), 1361-1373. doi:10.1002/hipo.22442

Lehman, M. N., Hileman, S. M., & Goodman, R. L. (2013). Neuroanatomy of the kisspeptin signaling system in mammals: comparative and developmental aspects. In *Kisspeptin signaling in reproductive biology* (pp. 27-62): Springer.

Lima, F. B., Sita, L. V., Oliveira, A. R., Costa, H. C., Da-Silva, J. M., Mortara, R. A., . . . Bittencourt, J. C. (2013). Hypothalamic melanin-concentrating hormone projections to the septo-hippocampal complex in the rat. *J Chem Neuroanat, 47*, 1-14. doi:0.1016/j.jchemneu.2012.10.003

Ludwig, D. S., Tritos, N. A., Mastaitis, J. W., Kulkarni, R., Kokkotou, E., Elmquist, J., . . . Maratos-Flier, E. (2001). Melanin-concentrating hormone overexpression in transgenic mice leads to obesity and insulin resistance. *The Journal of Clinical Investigation, 107*(3), 379-386. doi:10.1172/JCI10660

Luna-Illades, C., Morales, T., & Miranda-Anaya, M. (2017). Decreased food anticipatory activity of obese mice relates to hypothalamic c-Fos expression. *Physiology & Behavior, 179*, 9-15. doi:10.1016/j.physbeh.2017.05.020

Merriam, C. H. (1898). A new genus (Neotomodon) and three new species of murine rodents from the mountains of southern Mexico. *Proc. Biol. Soc. Washington, 12*, 127-129.

Messina, M. M., Boersma, G., Overton, J. M., & Eckel, L. A. (2006). Estradiol decreases the orexigenic effect of melanin-concentrating hormone in ovariectomized rats. *Physiology & Behavior, 88*(4-5), 523-528. doi:10.1016/j.physbeh.2006.05.002

Michaux, J., Reyes, A., & Catzeflis, F. (2001). Evolutionary history of the most speciose mammals: molecular phylogeny of muroid rodents. *Molecular Biology and Evolution, 18*(11), 2017-2031. doi:10.1093/oxfordjournals.molbev.a003743

Miller, A. C., & Pereda, A. E. (2017). The electrical synapse: Molecular complexities at the gap and beyond. *Developmental Neurobiology, 77*(5), 562-574. doi:10.1002/dneu.22484

Miller, C. L., Hruby, V. J., Matsunaga, T. O., & Bickford, P. C. (1993). Alpha-MSH and MCH are functional antagonists in a CNS auditory gating paradigm. *Peptides, 14*(3), 431-440. doi:10.1016/0196-9781(93)90128-4

Miller, G. S., & Rhen, J. A. G. (1901). Systematic results of the study of North American land mammals to the close of the year 1900. *Proc. Boston Soc. Nat. Hist., 30*(1), 1-352.

Miller, J. R., & Engstrom, M. D. (2008). The relationships of major lineages within peromyscine rodents: a molecular phylogenetic hypothesis and systematic reappraisal. *Journal of Mammalogy, 89*(5), 1279-1295. doi:10.1644/07-MAMM-A-195.1

Mizusawa, K., Amiya, N., Yamaguchi, Y., Takabe, S., Amano, M., Breves, J. P., . . . Takahashi, A. (2012). Identification of mRNAs coding for mammalian-type melanin-concentrating hormone and its receptors in the scalloped hammerhead shark Sphyrna lewini. *General and comparative endocrinology, 179*(1), 78-87. doi:10.1016/j.ygcen.2012.07.023

Monzon, M. E., de Souza, M. M., Izquierdo, L. A., Izquierdo, I., Barros, D. M., & de Barioglio, S. R. (1999). Melanin-concentrating hormone (MCH) modifies memory retention in rats. *Peptides, 20*(12), 1517-1519. doi:10.1016/S0196-9781(99)00164-3

Morin, L., Shivers, K.-Y., Blanchard, J., & Muscat, L. (2006). Complex organization of mouse and rat suprachiasmatic nucleus. *Neuroscience, 137*(4), 1285-1297. doi:10.1016/j.neuroscience.2005.10.030

Mul, J. D., la Fleur, S. E., Toonen, P. W., Afrasiab-Middelman, A., Binnekade, R., Schetters, D., . . . Cuppen, E. (2011). Chronic loss of melanin-concentrating hormone affects motivational aspects of feeding in the rat. *PLoS One, 6*(5), e19600. doi:10.1371/journal.pone.0019600

Murray, J. F., Adan, R. A. H., Walker, R., Baker, B. I., Thody, A. J., Nijenhuis, W. A., . . . Wilson, C. A. (2000a). Melanin-concentrating hormone, melanocortin receptors and regulation of luteinizing hormone release. *Journal of neuroendocrinology, 12*(3), 217-223. doi:10.1046/j.1365-2826.2000.00440.x

Murray, J. F., Baker, B. I., Levy, A., & Wilson, C. A. (2000b). The influence of gonadal steroids on pre-pro melanin-concentrating hormone mRNA in female rats. *Journal of neuroendocrinology, 12*(1), 53-59. doi:10.1046/j.1365-2826.2000.00425.x

Murray, J. F., Hahn, J. D., Kennedy, A. R., Small, C. J., Bloom, S. R., Haskell‐Luevano, C., . . . Wilson, C. A. (2006). Evidence for a Stimulatory Action of Melanin‐Concentrating Hormone on Luteinising Hormone Release Involving MCH1 and Melanocortin‐5 Receptors. *Journal of neuroendocrinology, 18*(3), 157-167. doi:10.1111/j.1365-2826.2005.01397.x

Nahon, J.-L., Presse, F., Bittencourt, J. C., Sawchenko, P. E., & Vale, W. (1989). The rat melanin-concentrating hormone messenger ribonucleic acid encodes multiple putative neuropeptides coexpressed in the dorsolateral hypothalamus. *Endocrinology, 125*(4), 2056-2065. doi:10.1210/endo-125-4-2056

Nieuwenhuys, R., Geeraedts, L. M. G., & Veening, J. G. (1982). The medial forebrain bundle of the rat. I. General introduction. *Journal of Comparative Neurology, 206*(1), 49-81. doi:10.1002/cne.902060106

Noble, E. E., Hahn, J. D., Konanur, V. R., Hsu, T. M., Page, S. J., Cortella, A. M., . . . Szujewski, C. C. (2018). Control of Feeding Behavior by Cerebral Ventricular Volume Transmission of Melanin-Concentrating Hormone. *Cell Metabolism, 28*(1), 55-68.e57. doi:10.1016/j.cmet.2018.05.001

Parkes, D. G., & Vale, W. W. (1993a). Contrasting actions of melanin-concentrating hormone and neuropeptide-E-I on posterior pituitary function. *Ann N Y Acad Sci, 680*(1), 588-590. doi:10.1111/j.1749-6632.1993.tb19746.x

Parkes, D. G., & Vale, W. W. (1993b). Contrasting Actions of Melanin‐Concentrating Hormone and Neuropeptide‐E‐I on Posterior Pituitary Function. *Ann N Y Acad Sci, 680*(1), 588-590. doi:10.1111/j.1749-6632.1993.tb19746.x

Patel, J. C., Witkovsky, P., Avshalumov, M. V., & Rice, M. E. (2009). Mobilization of calcium from intracellular stores facilitates somatodendritic dopamine release. *Journal of Neuroscience, 29*(20), 6568-6579. doi:10.1523/JNEUROSCI.0181-09.2009

Peyron, C., Tighe, D. K., Van Den Pol, A. N., De Lecea, L., Heller, H. C., Sutcliffe, J. G., & Kilduff, T. S. (1998). Neurons containing hypocretin (orexin) project to multiple neuronal systems. *Journal of Neuroscience, 18*(23), 9996-10015. doi:10.1523/JNEUROSCI.18-23-09996.1998

Piggins, H. D., Samuels, R. E., Coogan, A. N., & Cutler, D. J. (2001). Distribution of substance P and neurokinin‐1 receptor immunoreactivity in the suprachiasmatic nuclei and intergeniculate leaflet of hamster, mouse, and rat. *Journal of Comparative Neurology, 438*(1), 50-65. doi:10.1002/cne.1301

Platt, R. N., Amman, B. R., Keith, M. S., Thompson, C. W., & Bradley, R. D. (2015). What Is Peromyscus? Evidence from nuclear and mitochondrial DNA sequences suggests the need for a new classification. *Journal of Mammalogy, 96*(4), 708-719. doi:10.1093/jmammal/gyv067

Qu, D., Ludwig, D. S., Gammeltoft, S., Piper, M., Pelleymounter, M. A., Cullen, M. J., . . . Maratos-Flier, E. (1996). A role for melanin-concentrating hormone in the central regulation of feeding behaviour. *Nature, 380*(6571), 243-247. doi:10.1038/380243a0

Reeder, S. A., Carroll, D. S., Edwards, C. W., Kilpatrick, C. W., & Bradley, R. D. (2006). Neotomine–peromyscine rodent systematics based on combined analyses of nuclear and mitochondrial DNA sequences. *Molecular Phylogenetics and Evolution, 40*(1), 251-258. doi:10.1016/j.ympev.2006.03.016

Rondini, T. A., Donato, J., Rodrigues, B. C., Bittencourt, J. C., & Elias, C. F. (2010). Chemical identity and connections of medial preoptic area neurons expressing melanin-concentrating hormone during lactation. *J Chem Neuroanat, 39*(1), 51-62. doi:10.1016/j.jchemneu.2009.10.005

Rondini, T. A., Rodrigues, B. C., de Oliveira, A. P., Bittencourt, J. C., & Elias, C. F. (2007). Melanin-concentrating hormone is expressed in the laterodorsal tegmental nucleus only in female rats. *Brain Res Bull, 74*(1-3), 21-28. doi:10.1016/j.brainresbull.2007.04.006

Sakanaka, M., Shibasaki, T., & Lederis, K. (1987). Corticotropin releasing factor‐like immunoreactivity in the rat brain as revealed by a modified cobalt‐glucose oxidase‐diaminobenzidine method. *Journal of Comparative Neurology, 260*(2), 256-298. doi:10.1002/cne.902600209

Sanchez, M. S., Baker, B. I., & Celis, M. E. (1997). Melanin-concentrating hormone (MCH) antagonizes the effects of α-MSH and neuropeptide EI on grooming and locomotor activities in the rat. *Peptides, 18*(3), 393-396. doi:10.1016/S0196-9781(96)00327-0

Santollo, J., & Eckel, L. A. (2008). The orexigenic effect of melanin-concentrating hormone (MCH) is influenced by sex and stage of the estrous cycle. *Physiology & Behavior, 93*(4-5), 842-850. doi:10.1016/j.physbeh.2007.11.050

Santollo, J., & Eckel, L. A. (2013). Oestradiol Decreases Melanin‐Concentrating Hormone (MCH) and MCH Receptor Expression in the Hypothalamus of Female Rats. *Journal of neuroendocrinology, 25*(6), 570-579. doi:10.1111/jne.12032

Segal-Lieberman, G., Bradley, R. L., Kokkotou, E., Carlson, M., Trombly, D. J., Wang, X., . . . Maratos-Flier, E. (2003). Melanin-concentrating hormone is a critical mediator of the leptin-deficient phenotype. *Proceedings of the National Academy of Sciences of the United States of America, 100*(17), 10085-10090. doi:10.1073/pnas.1633636100

Séguéla, P., Watkins, K. C., & Descarries, L. (1989). Ultrastructural relationships of serotonin axon terminals in the cerebral cortex of the adult rat. *Journal of Comparative Neurology, 289*(1), 129-142. doi:10.1002/cne.902890111

Shapiro, L. E., Leonard, C. M., Sessions, C. E., Dewsbury, D. A., & Insel, T. R. (1991). Comparative neuroanatomy of the sexually dimorphic hypothalamus in monogamous and polygamous voles. *Brain research, 541*(2), 232-240. doi:10.1016/0006-8993(91)91023-T

Shimada, M., Tritos, N. A., Lowell, B. B., Flier, J. S., & Maratos-Flier, E. (1998). Mice lacking melanin-concentrating hormone are hypophagic and lean. *Nature, 396*(6712), 670-674. doi:10.1038/25341

Simpson, G. G. (1945). The principles of classification and a classification of mammals. *Bull. Amer. Museum Nat. History., 85*.

Sita, L. V., Diniz, G. B., Canteras, N. S., Xavier, G. F., & Bittencourt, J. C. (2016). Effect of intrahippocampal administration of anti-melanin-concentrating hormone on spatial food-seeking behavior in rats. *Peptides, 76*, 130-138. doi:10.1016/j.peptides.2015.12.007

Sita, L. V., Elias, C. F., & Bittencourt, J. C. (2003). Dopamine and melanin-concentrating hormone neurons are distinct populations in the rat rostromedial zona incerta. *Brain research, 970*(1-2), 232-237. doi:10.1016/S0006-8993(03)02345-X

Sita, L. V., Elias, C. F., & Bittencourt, J. C. (2007). Connectivity pattern suggests that incerto-hypothalamic area belongs to the medial hypothalamic system. *Neuroscience, 148*(4), 949-969. doi:10.1016/j.neuroscience.2007.07.010

Smith, D. G., Davis, R. J., Rorick-Kehn, L., Morin, M., Witkin, J. M., McKinzie, D. L., . . . Gehlert, D. R. (2006). Melanin-concentrating hormone-1 receptor modulates neuroendocrine, behavioral, and corticolimbic neurochemical stress responses in mice. *Neuropsychopharmacology, 31*(6), 1135-1145. doi:10.1038/sj.npp.1300913

Smith, D. G., Hegde, L. G., Wolinsky, T. D., Miller, S., Papp, M., Ping, X., . . . Craig, D. A. (2009). The effects of stressful stimuli and hypothalamic–pituitary–adrenal axis activation are reversed by the melanin-concentrating hormone 1 receptor antagonist SNAP 94847 in rodents. *Behavioural brain research, 197*(2), 284-291. doi:10.1016/j.bbr.2008.08.026

Stanley, B. G., Magdalin, W., Seirafi, A., Thomas, W. J., & Leibowitz, S. F. (1993). The perifornical area: the major focus of (a) patchily distributed hypothalamic neuropeptide Y-sensitive feeding system (s). *Brain research, 604*(1-2), 304-317. doi:10.1016/0006-8993(93)90382-W

Stanley, B. G., & Thomas, W. J. (1993). Feeding responses to perifornical hypothalamic injection of neuropeptide Y in relation to circadian rhythms of eating behavior. *Peptides, 14*(3), 475-481. doi:10.1016/0196-9781(93)90135-4

Swanson, L. W., Sanchez-Watts, G., & Watts, A. G. (2005). Comparison of melanin-concentrating hormone and hypocretin/orexin mRNA expression patterns in a new parceling scheme of the lateral hypothalamic zone. *Neuroscience Letters, 387*(2), 80-84. doi:10.1016/j.neulet.2005.06.066

Tan, C. P., Sano, H., Iwaasa, H., Pan, J., Sailer, A. W., Hreniuk, D. L., . . . Howard, A. D. (2002). Melanin-concentrating hormone receptor subtypes 1 and 2: species-specific gene expression. *Genomics, 79*(6), 785-792. doi:10.1006/geno.2002.6771

Tillet, Y., Batailler, M., & Fellmann, D. (1996). Distribution of melanin-concentrating hormone (MCH)-like immunoreactivity in neurons of the diencephalon of sheep. *J Chem Neuroanat, 12*(2), 135-145. doi:10.1016/S0891-0618(96)00195-0

Torterolo, P., Sampogna, S., Morales, F. R., & Chase, M. H. (2006). MCH-containing neurons in the hypothalamus of the cat: searching for a role in the control of sleep and wakefulness. *Brain research, 1119*(1), 101-114. doi:10.1016/j.brainres.2006.08.100

Torterolo, P., Scorza, C., Lagos, P., Urbanavicius, J., Benedetto, L., Pascovich, C., . . . Monti, J. M. (2015). Melanin-concentrating hormone (MCH): role in REM sleep and depression. *Frontiers in Neuroscience, 9*, 475. doi:10.3389/fnins.2015.00475

Trueta, C., & De-Miguel, F. F. (2012). Extrasynaptic exocytosis and its mechanisms: a source of molecules mediating volume transmission in the nervous system. *Frontiers in Physiology, 3*(319), 1-19. doi:10.3389/fphys.2012.00319

Tsunematsu, T., Ueno, T., Tabuchi, S., Inutsuka, A., Tanaka, K. F., Hasuwa, H., . . . Yamanaka, A. (2014). Optogenetic manipulation of activity and temporally controlled cell-specific ablation reveal a role for MCH neurons in sleep/wake regulation. *Journal of Neuroscience, 34*(20), 6896-6909. doi:10.1523/JNEUROSCI.5344-13.2014

Vaasjo, L. O., Quintana, A. M., Habib, M. R., Mendez de Jesus, P. A., Croll, R. P., & Miller, M. W. (2018). GABA‐like immunoreactivity in Biomphalaria: Colocalization with tyrosine hydroxylase‐like

immunoreactivity in the feeding motor systems of panpulmonate snails. *Journal of Comparative Neurology, 526*(11), 1790-1805. doi:10.1002/cne.24448

Vaughan, J. M., Fischer, W. H., Hoeger, C., Rivier, J., & Vale, W. (1989). Characterization of melanin-concentrating hormone from rat hypothalamus. *Endocrinology, 125*(3), 1660-1665. doi:10.1210/endo-125-3-1660

Verret, L., Goutagny, R., Fort, P., Cagnon, L., Salvert, D., Leger, L., . . . Luppi, P. H. (2003). A role of melanin-concentrating hormone producing neurons in the central regulation of paradoxical sleep. *BMC Neuroscience, 4*, 1-19. doi:10.1186/1471-2202-4-19

Vidal, L., Blanchard, J. H., & Morin, L. P. (2005). Hypothalamic and zona incerta neurons expressing hypocretin, but not melanin concentrating hormone, project to the hamster intergeniculate leaflet. *Neuroscience, 134*(3), 1081-1090. doi:10.1016/j.neuroscience.2005.03.062

Weatherhead, B., & Logan, A. (1981). Interaction of α-melanocyte-stimulating hormone, melatonin, cyclic AMP and cyclic GMP in the control of melanogenesis in hair follicle melanocytes in vitro. *Journal of Endocrinology, 90*(1), 89-96. doi:10.1677/joe.0.0900089

Williams, S. L., & Ramirez-Pulido, J. (1984). *Morphometric variation in the volcano mouse, Peromyscus (Neotomodon) alstoni (Mammalia: Cricetidae)*: Carnegie Museum of Natural History.

Williams, S. L., Ramírez-Pulido, J., & Baker, R. J. (1985). Peromyscus alstoni. *Mammalian species*(242), 1-4. doi:10.2307/3503917

Wilson, D. E., & Reeder, D. M. (2005). *Mammal species of the world: a taxonomic and geographic reference* (3rd ed. Vol. 1): JHU Press.

Wu, M., Dumalska, I., Morozova, E., van den Pol, A. N., & Alreja, M. (2009). Melanin-concentrating hormone directly inhibits GnRH neurons and blocks kisspeptin activation, linking energy balance to reproduction. *Proceedings of the National Academy of Sciences, 106*(40), 17217-17222. doi:10.1073/pnas.0908200106

Yates, T., Baker, R., & Barnett, R. (1979). Phylogenetic analysis of karyological variation in three genera of peromyscine rodents. *Systematic Biology, 28*(1), 40-48. doi:10.1093/sysbio/28.1.40

Yew, D., Luo, C., Shen, W., Chow, P., Zheng, D., & Yu, M. (1995). Tyrosine hydroxylase-and dopamine-β-hydroxylase-positive neurons and fibres in the developing human cerebellum—An immunohistochemical study. *Neuroscience, 65*(2), 453-461. doi:10.1016/0306-4522(94)00521-6

Young, L. J., Huot, B., Nilsen, R., Wang, Z., & Insel, T. R. (1996). Species differences in central oxytocin receptor gene expression: comparative analysis of promoter sequences. *Journal of neuroendocrinology, 8*(10), 777-783. doi:10.1046/j.1365-2826.1996.05188.x

Young, L. J., Winslow, J. T., Nilsen, R., & Insel, T. R. (1997). Species differences in V_1a receptor gene expression in monogamous and nonmonogamous voles: Behavioral consequences. *Behavioral neuroscience, 111*(3), 599. doi:10.1037/0735-7044.111.3.599

[dataset] Diniz, G., Battagello, D.S., Cherubini, P. M., Reyes-Mendoza, J. D., Luna-Illades, C., Klein, M. O., Motta-Teixeira, L. C., Sita, L. V., Miranda-Anaya, M., Morales, T., & Bittencourt, J. C.; 2019; Melanin-concentrating hormone peptidergic system: comparative morphology between muroid species - Dataset 1; OSF; 10.17605/OSF.IO/ZRK2V

Figure Legends

Figure 01 – Phylogenetic tree of the *Muroidea* superfamily. Diagrammatic representation of the phylogenetic relationship between members of the *Muroidea* superfamily. Species examined in this work are labeled in red, and species from which data about the MCH system is available but which were not examined in this work are labeled in green. Other species were included for reference, in black. This tree is based on the molecular data of Fabre et al. (2012) and Platt et al. (2015).

Figure 02 – MCH and NEI immunoreactivities are detected in different subcellular compartments. Confocal microscopy of frontal brain slices obtained from a male *Mus musculus* submitted to double immunofluorescence labeling. Neuropeptide E-I is pseudocolored in green and MCH in magenta. a1, a2) Neuropeptide E-I labeling results in ample labeling of somas, proximal dendrites, axons and varicosities. Melanin-concentrating hormone labeling, on the other hand, is restricted to the soma and shows less morphological variety. b1, b2) Two orthogonal stacks of the field shown in a1. Neuropeptide E-I labeling circumvents MCH staining in all four neurons shown in this field, suggesting these neurons occupy different subcellular compartments. Scale bar: a1 = 40µm; b1, b2 = 30µm; a2 = 20µm.

Figure 03 – The morphological subtypes of MCH/NEI neurons. Brightfield photomicrographs of adult male *Mus musculus* brain slices submitted to peroxidase immunohistochemistry with anti-NEI antiserum. a1, a2) Multipolar neurons are characterized by the lack of preferential orientation, proportional dorsoventral and mediolateral dimensions, and the emergence of three or more primary dendrites, with frequent branching. In the illustrated neuron, the emergence of its axon can be seen at the upper part of the neuron; b1, b2) Fusiform neurons, on the other hand, are preferentially oriented in the mediolateral axis, have a high mediolateral/dorsoventral ratio, and the emergence of two primary dendrites, with less branching; c1, c2) Crescent neurons are found in the periphery of blood vessels. These neurons have a sickle shape that follows the wall of the blood vessel, in addition to the emergence of two primary dendrites, which often also contribute to the encircling of the blood vessel. The observation of crescent neurons often occurs in tandem with the presence of immunoreactive fibers and varicosities inside the blood vessel wall. Abbreviations: 3V – third ventricle; bv – blood vessel; f – fornix; ic – internal capsule; opt – optic tract. Scale bar: A, B: 200µm; C: 50µm; A'-C': 20µm.

Figure 04 – The distribution of MCH/NEI neurons along the rostrocaudal axis of *M. musculus*. Brightfield photomicrographs of adult male *Mus musculus* brain slices submitted to peroxidase immunohistochemistry with anti-MCH antiserum and adjacent slices stained using Nissl staining for cytoarchitectonical purposes. a1 - c2) The anterior pattern of MCH immunoreactivity is marked by the even distribution of labeled neurons in the AHA, IHy, ZI, and pericapsular LHA; d1, d2) The transition from the anterior to the posterior pattern is characteristically illustrated; e1 – g2) The posterior pattern of MCH immunoreactivity is marked by a concentration of labeled neurons in the LHA, with a group located dorsomedially with respect to the cerebral peduncle and another group associated to the PeF. Abbreviations: 3V – third ventricle; AHA – anterior hypothalamic area; Arc – arcuate nucleus; cp – cerebral peduncle; DMH – dorsomedial hypothalamic nucleus; DTM – dorsal tuberomammillary nucleus; f – fornix; ic – internal capsule; LHA – lateral hypothalamic area; ME – median eminence; MeA – medial nucleus of the amygdala; mt – mammillothalamic tract; opt – optic tract; Pe – periventricular nucleus of the hypothalamus; PeF - perifornical nucleus; PHA – posterior hypothalamic area; PMV –

ventral premammillary nucleus; PVH – paraventricular hypothalamic nucleus; SOR – supraoptic nucleus, retrochiasmatic part; STh – subthalamic nucleus; VMH – ventromedial hypothalamic nucleus; ZI – *zona incerta*. Scale bar: 500µm.

Figure 05 – The distribution of MCH/NEI neurons along the rostrocaudal axis of *N. alstoni*. Brightfield photomicrographs of adult male *Neotomodon alstoni* brain slices submitted to peroxidase immunohistochemistry with anti-MCH antiserum and adjacent slices stained using Nissl staining for cytoarchitectonical purposes. a1 – b2) The anterior pattern of MCH immunoreactivity is marked by an enlarged group of neurons in the AHA, a lack of distinguishable IHy, and scattered neurons in the ZI and the pericapsular LHA; c1, c2) The transitional stage results in a shift from the medial zone to the lateral zone as the main harbor of MCH/NEI neurons; d1 – f2) The posterior pattern in characterized by a large number of neurons in the LHA and the appearance of a posterior hypothalamic area group. Abbreviations: 3V - third ventricle; AHA – anterior hypothalamic area; AHP – anterior hypothalamic area, posterior part; Arc – arcuate nucleus; cp – cerebral peduncle; DMH – dorsomedial hypothalamic nucleus; ic – internal capsule; LHA – lateral hypothalamic area; ME – median eminence; mt – mammillothalamic tract; opt – optic tract; Pe – periventricular hypothalamic nucleus; PeF – perifornical nucleus; PHA – posterior hypothalamic area; VMH – ventromedial hypothalamic nucleus; ZI – *zona incerta*. Scale bar: 500µm.

Figure 06 – Interspecies difference in the periventricular zone of the hypothalamus. Brightfield photomicrographs of adult male *Rattus norvegicus* and *Mus musculus* brain slices submitted to peroxidase immunohistochemistry with anti-NEI antiserum. a, b) In the anterior part of the rat tuberal hypothalamus, labeleded neurons are seen in great proximity to the 3V, both in the periventricular nucleus and in the third ventricle dorsal cap, medial to the IHy. There is no clear difference between male and female rats; c, d) In *Mus*, few neurons are seen medial to the AHA, and the third ventricle dorsal cap is completely devoid of cellular labeling, despite a large number of labeled fibers coursing through this area. The lack of MCH-ir neurons in the periventricular zone was common for male and female mice. Abbreviation: 3V – third ventricle. Scale bar: 200µm.

Figure 07 – Comparison of the MCH/NEI system three-dimensional structure in three rodent species. Three-dimensional reconstruction of semi-serial slices of hypothalamus from *R. norvegicus*, *M. musculus* and *N. alstoni* submitted to peroxidase immunohistochemistry with anti-MCH antiserum. Each neuron is indicated by a magenta dot. a) Three-dimensional reconstructions of the rat hypothalamus show a mediolateral band of dense immunoreactivity, including the heavily populated space between the fornix and the internal capsule/cerebral peduncle, with few open spaces observed in the medial tuberal hypothalamus resulting from scattered immunoreactivity in the rat AHA. The rostrocaudal extent of labeling in *Rattus* is larger than in other species; b) The *Mus musculus* 3D structure, on the other hand, shows a lower number of neurons, a dense band of labeled ells in the ventrolateral part of the tuberal hypothalamus and a spheroid zone almost devoid of labeling centered dorsal to the fornix. c) The tuberal hypothalamus of *N. alstoni* is more homogenously occupied by MCH neurons, including neurons ventral to the fornix, which are seldom observed in the other two species. Structures: 3V – third ventricle (orange); f – fornix (yellow); ic – internal capsule (purple); mt – mammillothalamic tract (green); opt – optic tract (blue). Structures: 3V – third ventricle (orange); f – fornix (yellow); ic – internal capsule (purple); mt – mammillothalamic tract (green); opt – optic tract (blue).

Figure 08 – Concentrical organization of the *Mus* LHA. a1, a2) Brightfield photomicrographs of adult male *Mus musculus* brain slices submitted to double peroxidase immunohistochemistry with anti-NEI (red-brown neurons) and anti-ORX (black neurons) antisera. Despite their co-habitation of the LHA, MCH and ORX neurons occupy mostly different compartments in this area. Orexin-ir neurons are concentrated in the area immediately dorsal to the fornix, while MCH neurons are located in the external part of the LHA. The laterodorsal part of the LHA is the area of highest cohabitation between MCH and ORX neurons, as shown in the higher magnification; b) Three-dimensional reconstruction of semi-serial double labeled slices of a male adult *Mus musculus* mouse. Orexin neurons are indicated as cyan dots and MCH neurons are indicated as magenta dots. The distribution of ORX neurons forms a spheroid shape centered on the central part of the LHA, dorsal to the fornix. This area with a high proportion of ORX cells was termed the LHA core. Melanin-concentrating hormone cells, on the other hand, form a semisphere around ORX neurons, occupying the pericapsular LHA, the adjoining ZI, the IHy, the AHA and the internuclear group. This area of high proportion of MCH cells was termed the LHA shell. Structures: 3V – third ventricle (orange); f – fornix (yellow); ic – internal capsule (purple); mt – mammillothalamic tract (green); opt – optic tract (blue). Scale bar: A: 500µm; A': 50µm.

Figure 09 – The *Mus musculus* incerto-hypothalamic area. Widefield fluorescence photomicrographs of adult male *Mus musculus* brain slices submitted to double fluorescence immunohistochemistry with anti-NEI (green neurons) and anti-TH (magenta neurons) antisera and adjacent slices stained using Nissl staining for cytoarchitectonical purposes. a1, a2) The *Mus musculus* IHy starts at around Bregma -1.2 with a small number of MCH/NEI intermingled with the medialmost part of the A13 dopaminergic group; b1, c2) As the A13 group moves medially, MCH/NEI neurons become predominantly intermingled with the lateral part of the A13 group. Several soma-soma contact points between MCH/NEI and TH neurons are observed, as illustrated in the insets; d1, d2) At Bregma -1.55, the IHy ends at the same level the A13 group ends. Abbreviations: 3V – third ventricle; A13 – dopaminergic group A13; AHA – anterior hypothalamic area; Arc – arcuate nucleus; DMH – dorsomedial hypothalamic nucleus; f – fornix; ic – internal capsule; LHA – lateral hypothalamic area; opt – optic tract; SubI – subincertal zone; VMH – ventromedial hypothalamic nucleus; ZI – *zona incerta*. Scale bar: A-D: 500µm; A'-D': 100µm; Inslets: 20µm.

Figure 10 – Soma-soma contacts between MCH/NEI and dopaminergic neurons of the IHy. Confocal photomicrographs of adult male *Mus musculus* brain slices submitted to triple fluorescence immunohistochemistry with anti-NEI (green labeling), anti-MCH (purple labeling), and anti-TH (red labeling) antisera. Points of contacts between MCH/NEI-ir and TH-ir neurons are highlighted with white rectangles. Note the continuity between neurons, but the lack of real colocalization between the two markers. Scale bar: A: 40µm; A': 20µm.

Figure 11 – Late synthesis of MCH in the medial preoptic area during the female reproductive cycle. Brightfield photomicrographs of adult female *Mus musculus* brain slices submitted to peroxidase immunohistochemistry with anti-MCH antiserum. a, b) Similar to the rat, no MCH immunoreactivity can be detected in the MPOA of diestrus (virgin) and pregnant females; c) Dissimilar to the rat, no immunoreactivity is observed in the MPOA of *Mus* dams 5 days after delivery; d) MCH-ir neurons can be detected in the MPOA of female *Mus* 19 days after delivery, at the final stage of lactation. In the

Mus musculus mouse, fewer neurons are found, they are weakly immunoreactive and concentrated in the ventral part of the MPOA. Abbreviation: 3V – third ventricle; ox – optic chiasm. Scale bar: 100µm.

Figure 12 – The reproductive cycle has minimal effect on MCH immunoreactivity in the *Mus musculus* median eminence. Darkfield photomicrographs of adult male and female *Mus musculus* brain slices submitted to peroxidase immunohistochemistry with anti-MCH antiserum. Both median eminence laminae are sparsely innervated by MCH-ir fibers and both sex and reproductive stage have minimal effect on the amount of MCH-ir fibers in the median eminence. White spots in panel f are due to an artifact and do not reflect an increase in the number of fibers at the median eminence proper. Abbreviation: 3V – third ventricle; PPD5 – 5th day postpartum; PPD12 – 12th day postpartum; PPD19 – 19th day postpartum. Scale bar: 100µm.

Figure 13 – NEI fibers abut cells in the mesencephalic dopaminergic groups. Widefield fluorescence photomicrographs of adult male *Mus musculus* brain slices submitted to double fluorescence immunohistochemistry with anti-NEI (green labeling) and anti-TH (magenta labeling) antisera. NEI-ir fibers are found in the *pars compacta* of the *substantia nigra* (a1, a2) and in the ventral tegmental area (b1, b2). While a few fibers are found close to TH-positive cells (white arrowheads), some fibers outline cells that are not TH-ir, likely interneurons (white arrows). Abbreviations: SNc – *substantia nigra*, *pars compacta*; VTA – ventral tegmental area. Scale bar: A, B: 200µm; A', B': 50µm.

Figure 14 – Neuropeptide E-I-ir fibers are found in the external and internal surfaces of the brain. Widefield fluorescence photomicrographs of adult male *Mus musculus* brain slices submitted to fluorescence immunohistochemistry with anti-NEI (green labeling) and counterstained with DAPI. a1) the medial part of the lateral ventricle receives a high density of innervation by MCH/NEI fibers. a2) Higher magnification of the delineated area in A. Several fibers in the medial wall of the lateral ventricle can be seen in the subventricular zone and entering the ventricle. b1) Fibers immunoreactive to NEI are found in the roof of the midbrain and in other superficial areas. b2) Higher magnification of the delineated area in b2. MCH/NEI fibers form a network of fibers that potentially reaches the subpial zone and access the cerebrospinal fluid contained in this space. Abbreviations: cc – corpus callosum; LV- lateral ventricle. Scale bar: A: 500µm; B: 200µm; A': 100µm; B': 50µm.

Figure 15 – The main aspects of the MCH peptidergic system in the three species examined in this work. Diagrammatic representation of the anatomical description of MCH-ir neurons in the tuberal hypothalamus of the three muroid species analyzed in this work. Four groups of MCH neurons are represented in the diagram: green – lateral and medial hypothalamus; red – *zona incerta*; blue – incerto-hypothalamic area; yellow – periventricular nucleus.

Abbreviations

3V - third ventricle

α-MSH - α-melanocyte-stimulating hormone

Arc - arcuate nucleus

AHA - anterior hypothalamic area

BT - biotinylated tyramine

CRF - corticotrophin-releasing factor

DAB - 3,3'-diaminobenzidine

DAPI - 4',6-diamidino-2-phenylindole

IF - immunofluorescence

IHy - incerto hypothalamic area

IP - immunoperoxidase

KPBS - potassium phosphate-buffered saline

LHA - lateral hypothalamic area

MCH - melanin-concentrating hormone

ME – median eminence

MPOA - medial preoptic area

NEI - neuropeptide E-I

NGE - neuropeptide G-E

ORX – orexin

PBS - phosphate-buffered saline

PPD - postpartum day

PeF - perifornical nucleus

PHA - posterior hypothalamic area

PVH - paraventricular hypothalamic nucleus

ZI - *zona incerta*

Tables

Table 1. Primary antibodies employed in this work

Antibody	Manufacturer	Man. Code	Reference (First author, volume: pages, year and journal)	PubMed ID	RRID	Antigen sequence	Application/ Concentration
Rabbit anti (rat) melanin-concentrating hormone (anti-MCH)	Peptide Biology Laboratory, The Salk Institute	PBL #234	Bittencourt JC, 319(2):218-245, 1992 – Journal of Comparative Neurology	1522246	RRID_AB_2650444	DFDMLRCMLGRVYRPCWQV	1:700 [IF] 1:70'000 [IP] 1:35'000 [BT]
Rabbit anti (rat) neuropeptide E-I (anti-NEI)	Peptide Biology Laboratory, The Salk Institute	PBL #237	Bittencourt JC, 319(2):218-245, 1992 – Journal of Comparative Neurology	2477226	RRID_AB_2650445	EIGDEENSAK FPI	1:1'000 [IF] 1:70'000 [IP] 1:35'000 [BT]
Rabbit anti (rat, mouse, human) orexin (anti-ORX)	Phoenix Pharma-ceuticals, Inc.	H-003-30	Fronczek R, 90(9):5466-70, 2005 – The Journal of Clinical Endocrinology & Metabolism	15985489	RRID_AB_2315019	QPLPDCCRQKTCSCRLYELLHGAG NHAAGILTL	1:2'000 [IP]
Mouse anti (rat, mouse, human) tyrosine hydroxylase (anti-TH)	ImmunoStar Inc.	#22941	Jones KR, 76(6):989-99, 1994 – Cell	8137432	RRID_AB_572268	Whole TH purified from rat PC12 cells	1:1'000 [IF]

BT – biotinylated tyramine; IF – immunofluorescence; IP – immunoperoxidase

Figure 1.tiff

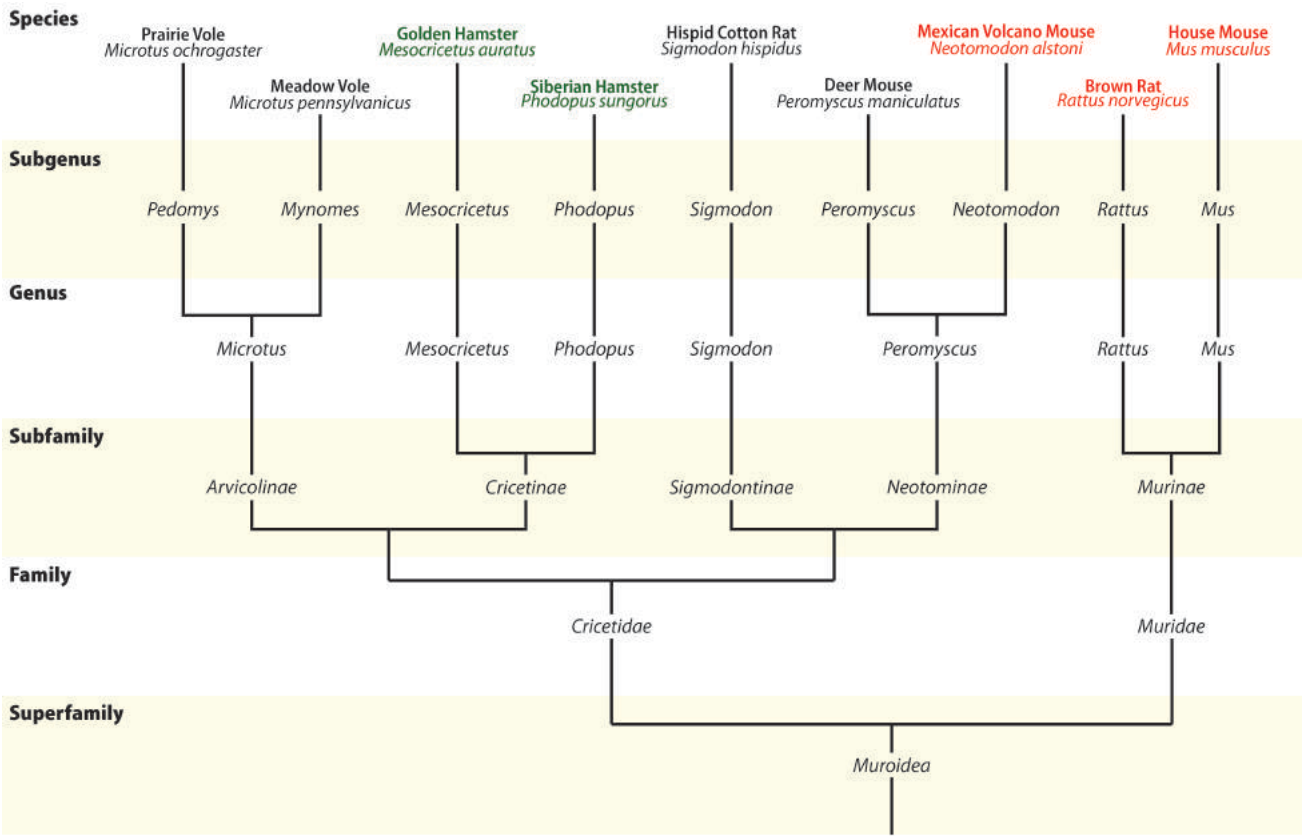

Figure 2.tiff

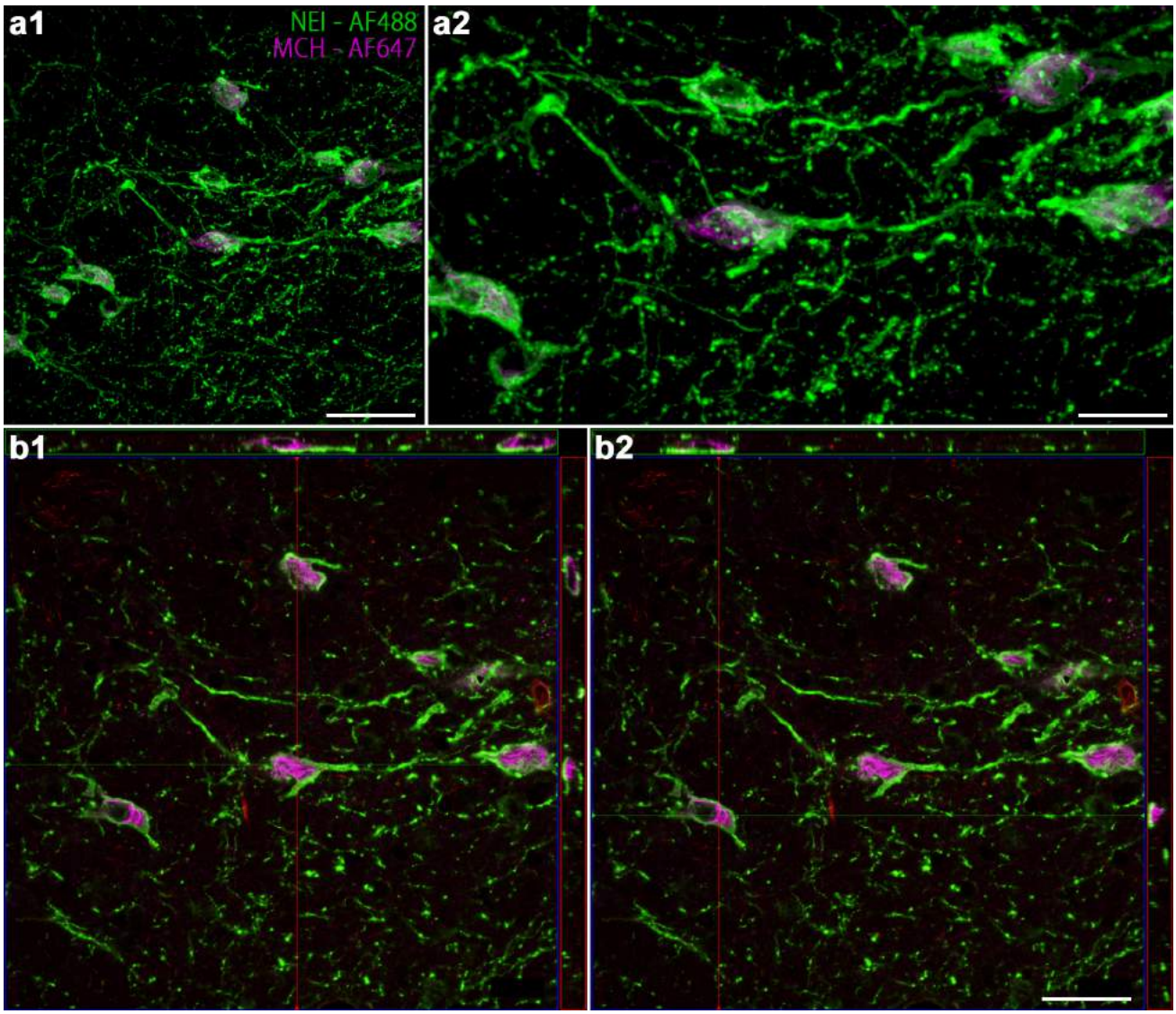

Figure 3.tiff

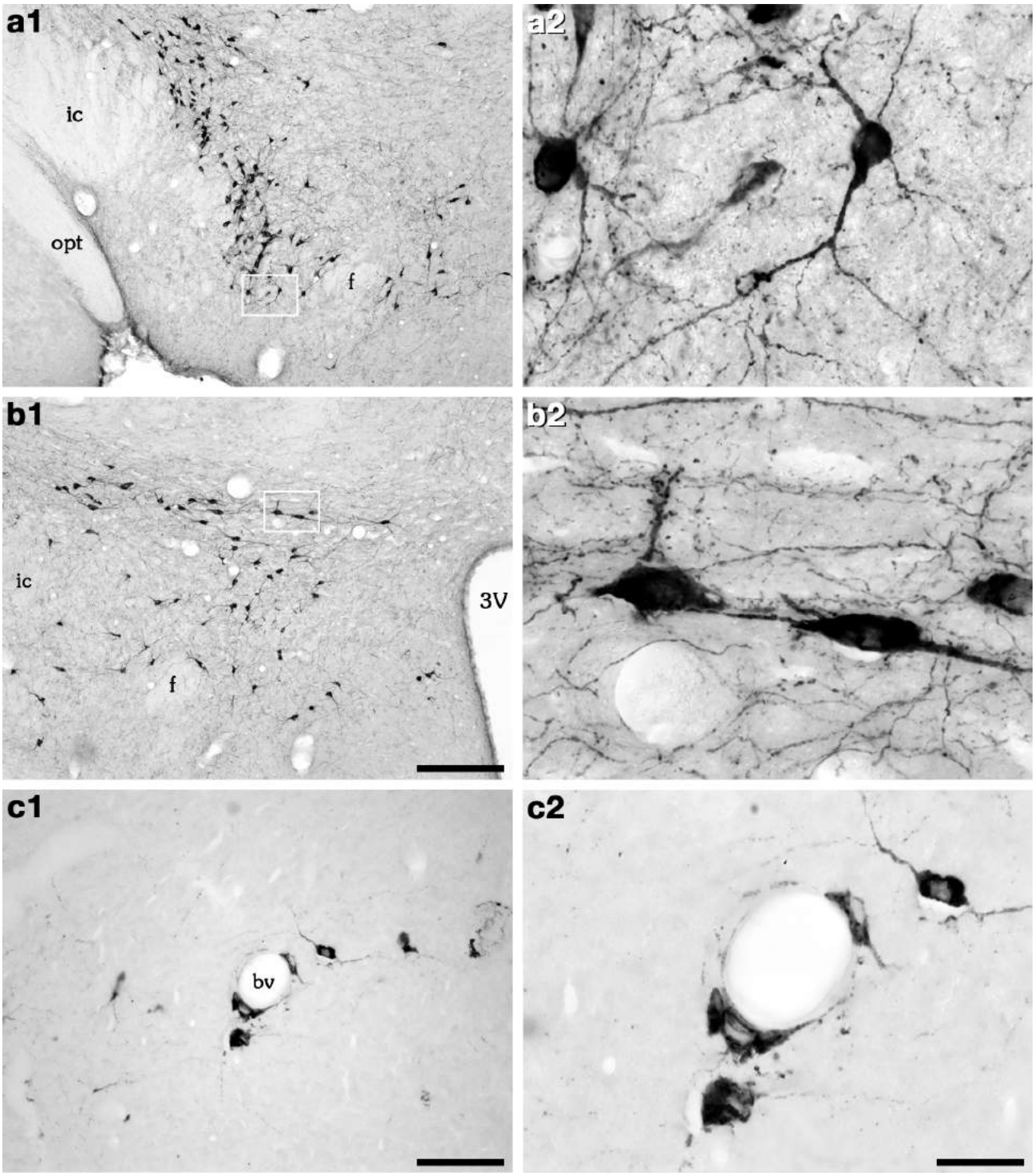

Figure 4a.tiff

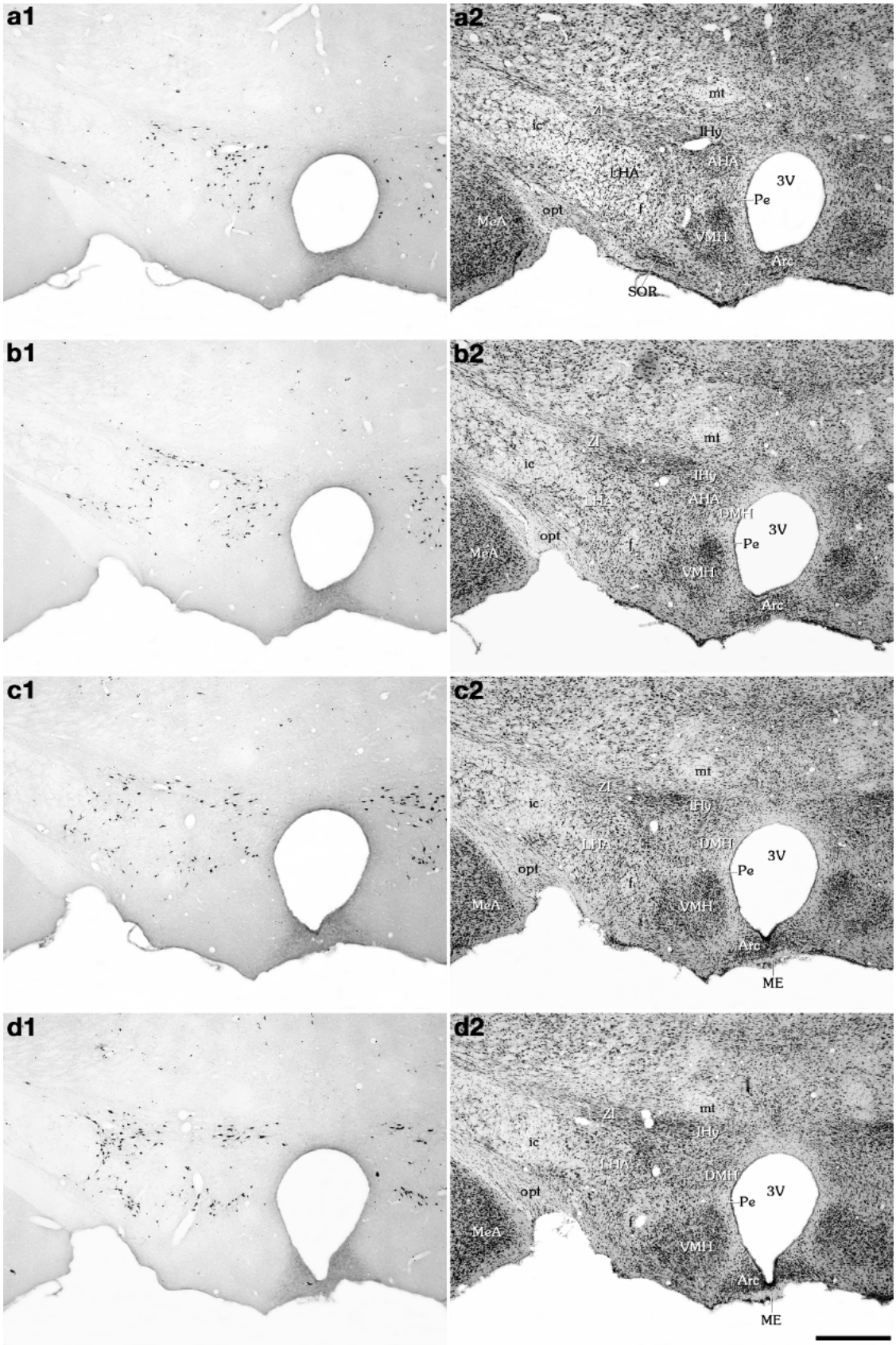

Figure 4b.tiff

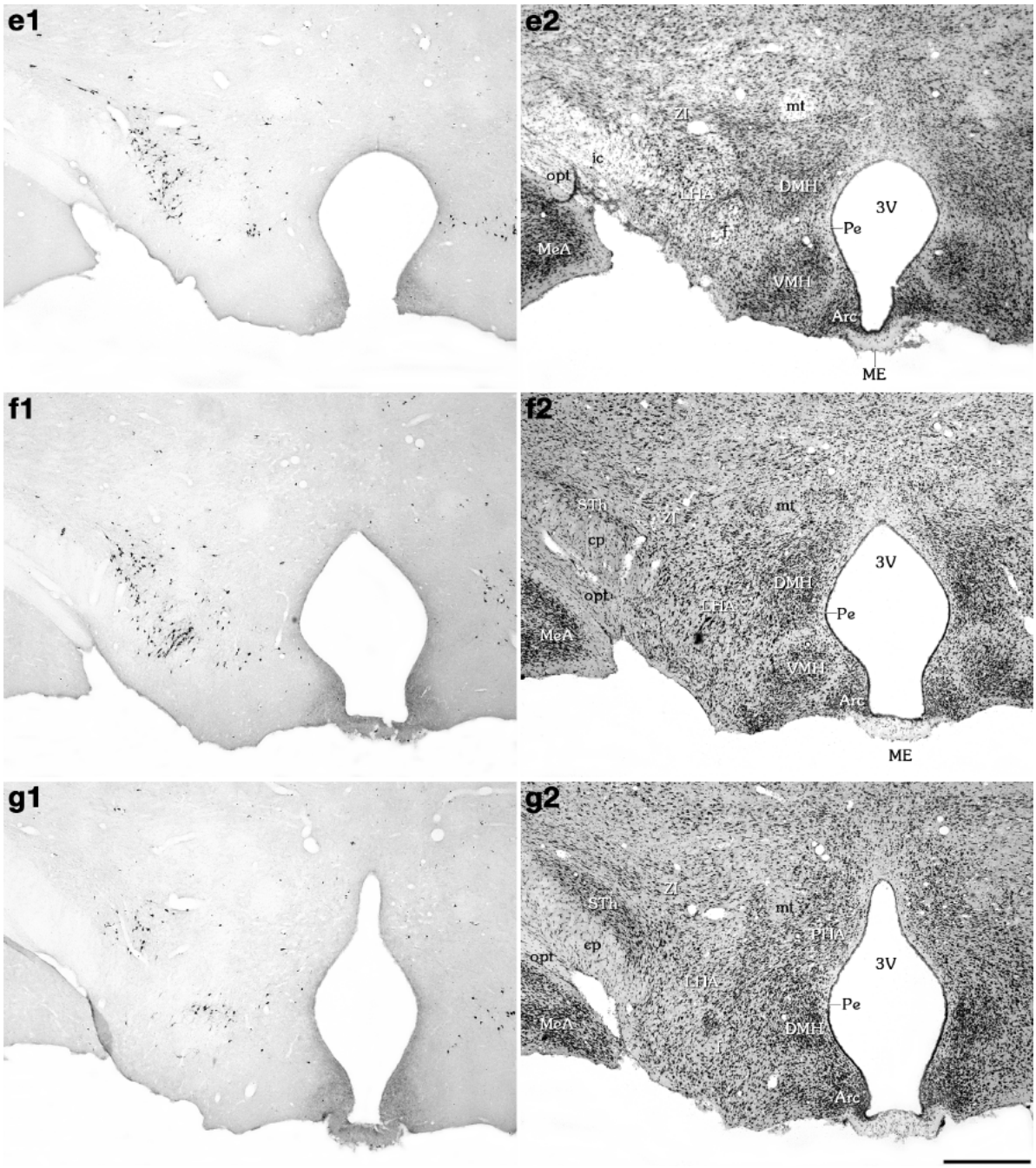

Figure 5a.tiff

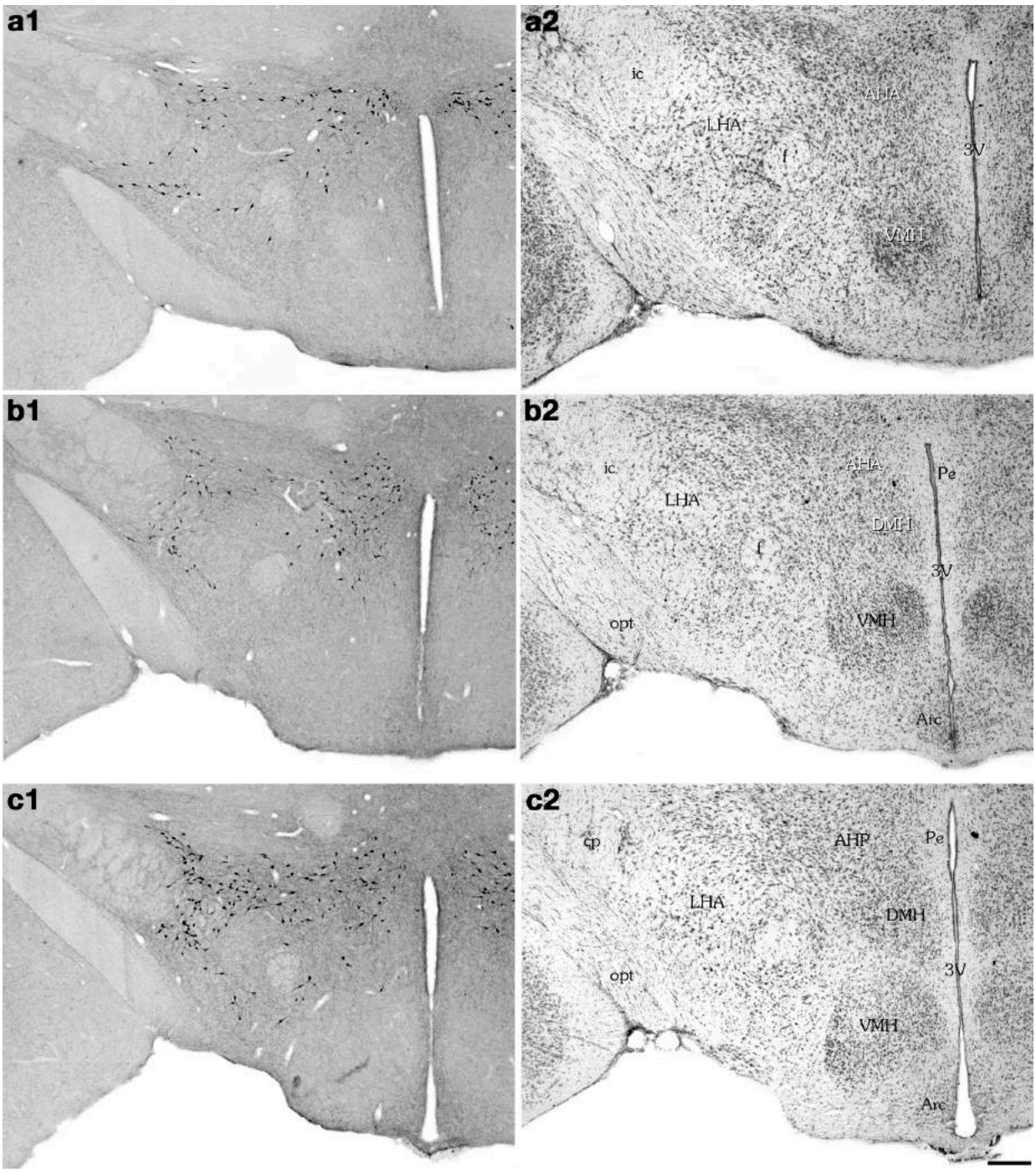

Figure 5b.tiff

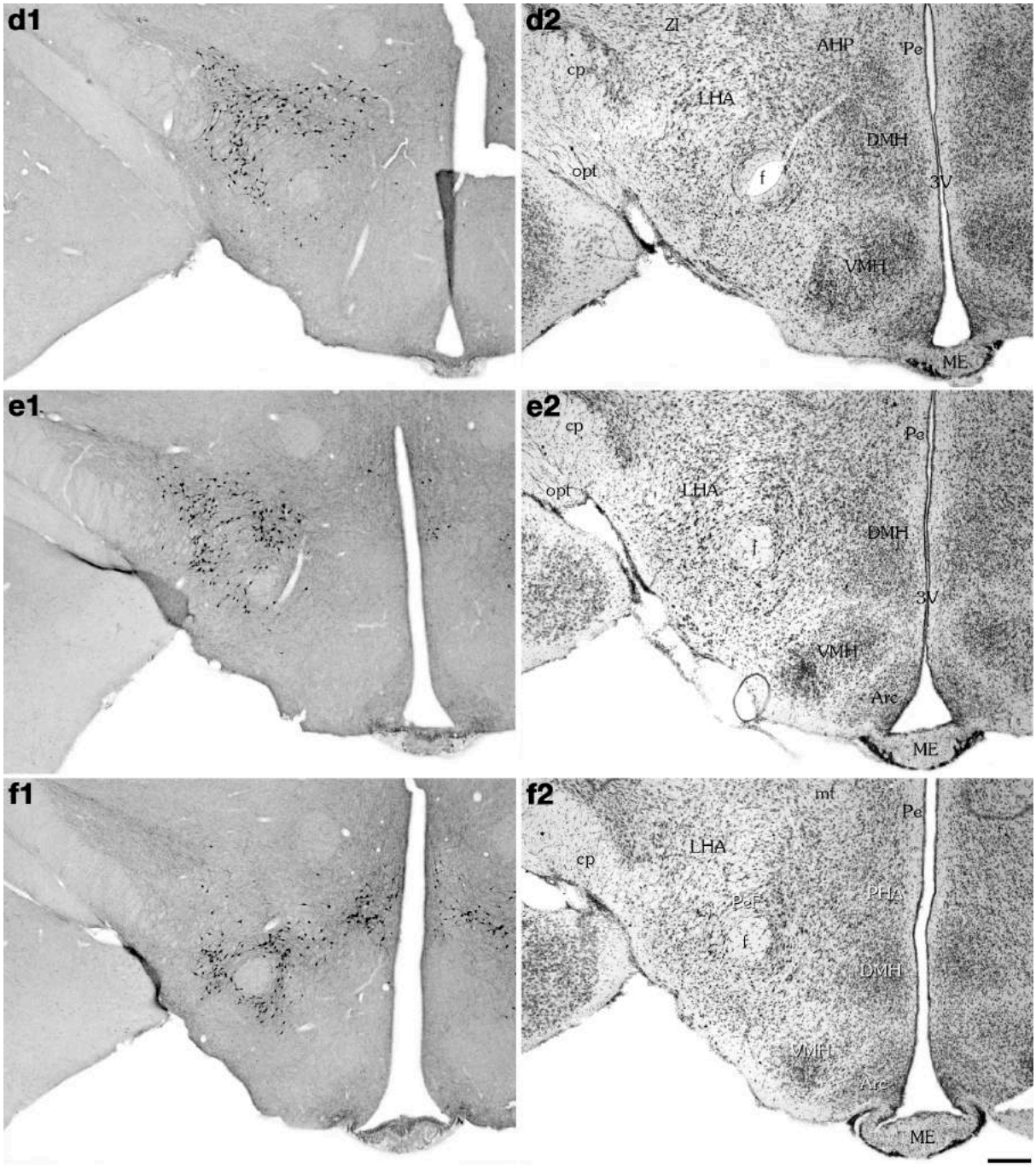

Figure 6.tiff

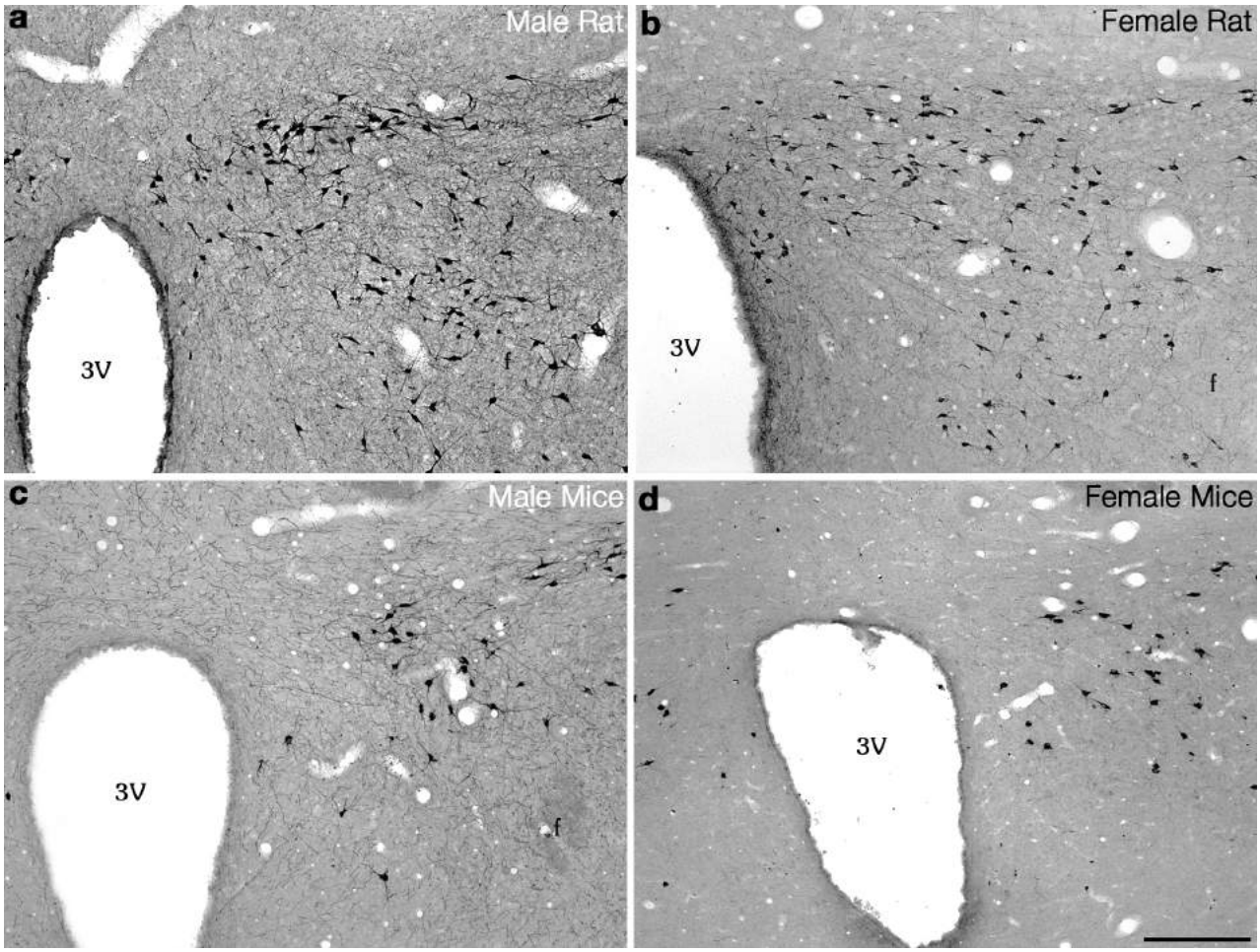

Figure 7.tiff

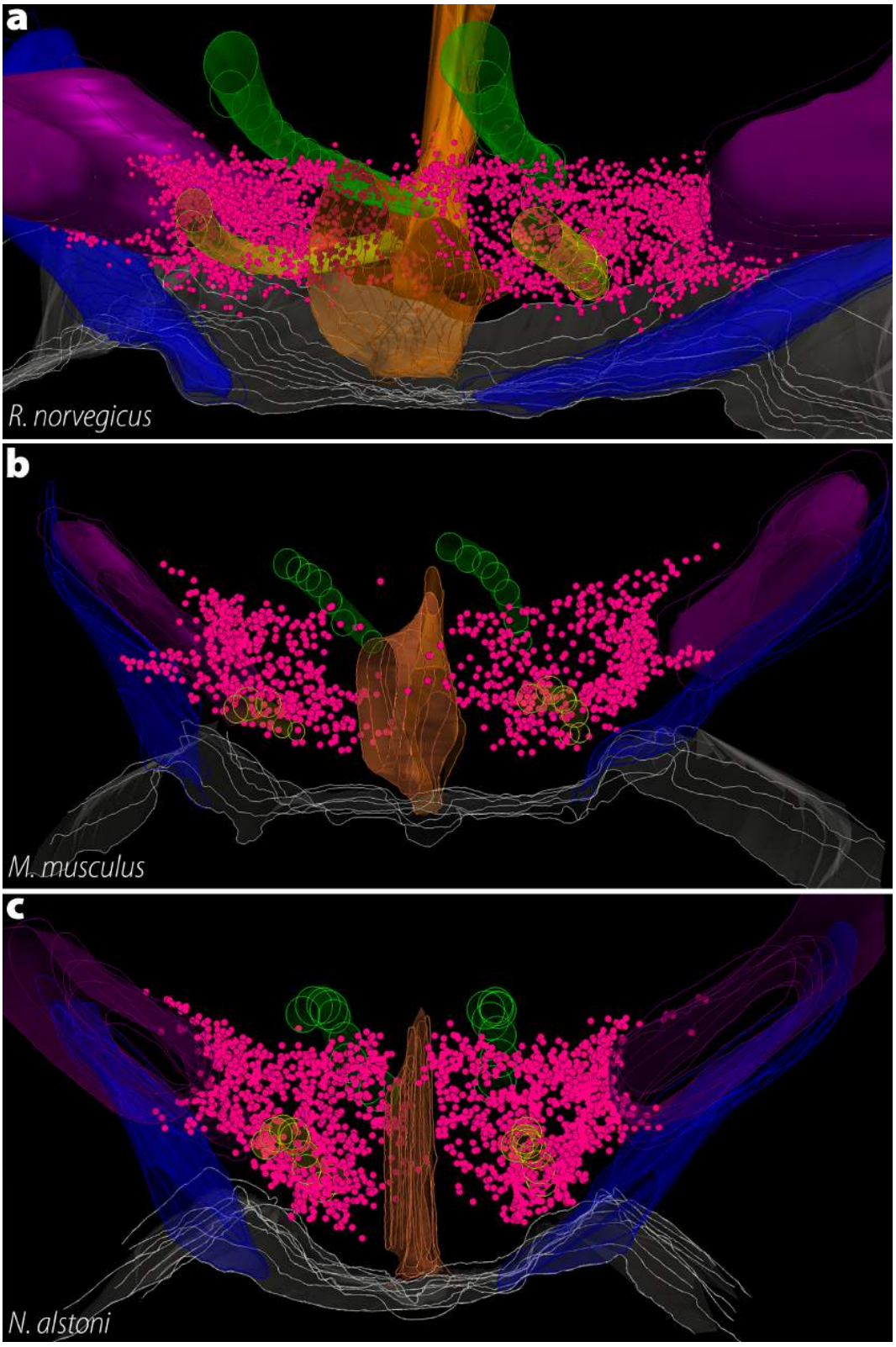

Figure 8.tiff

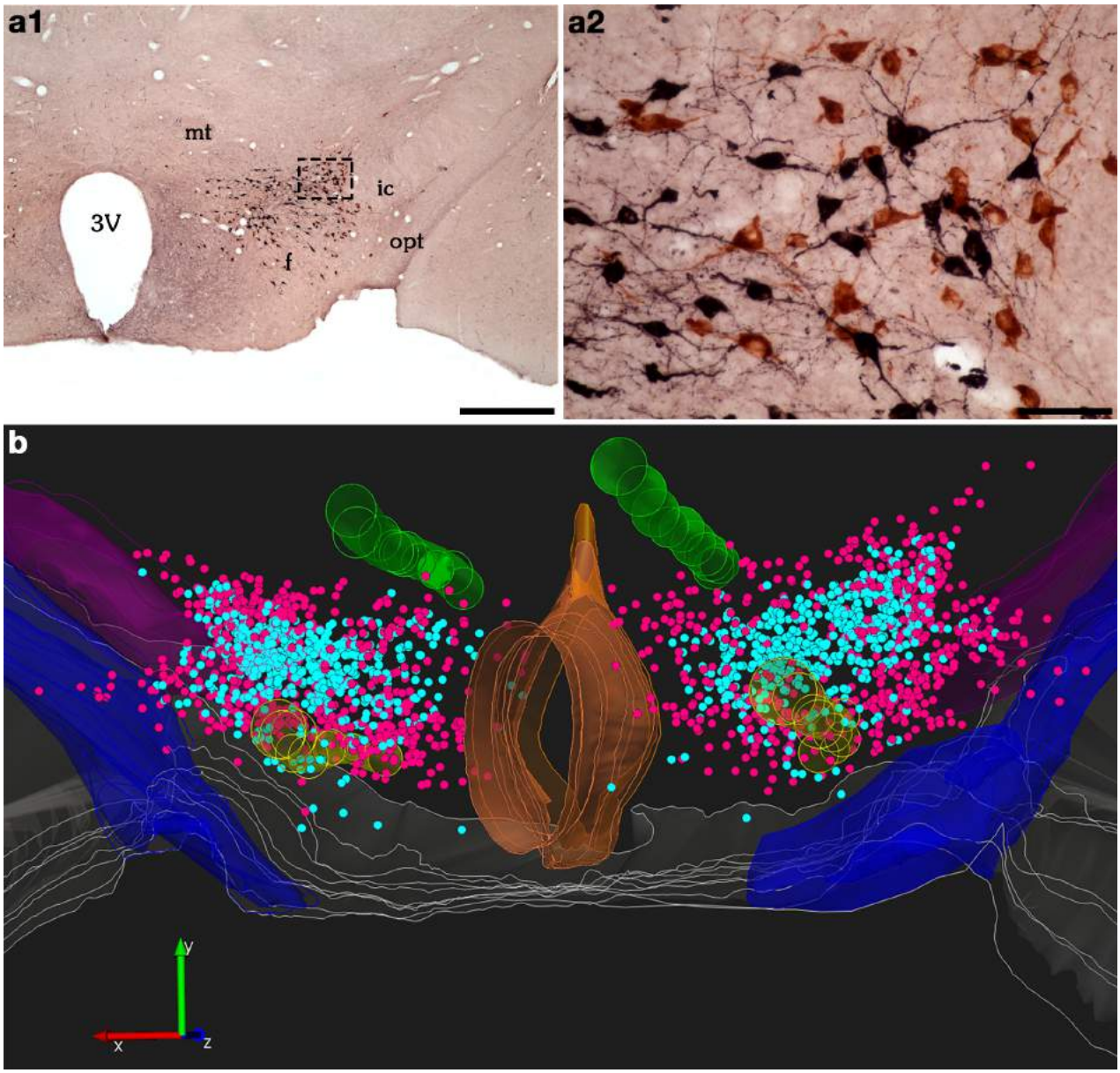

Figure 9.tiff

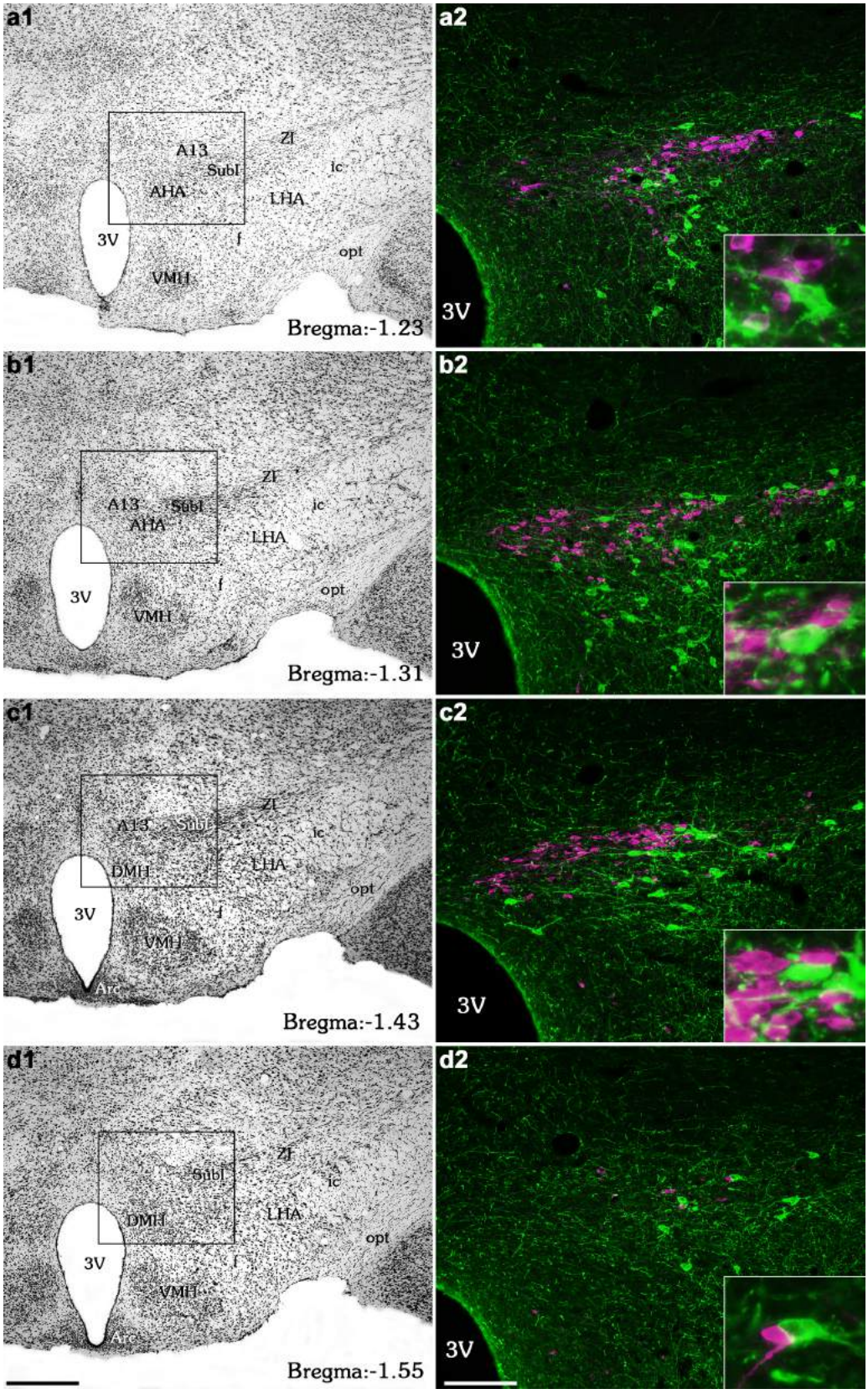

Figure 10.tiff

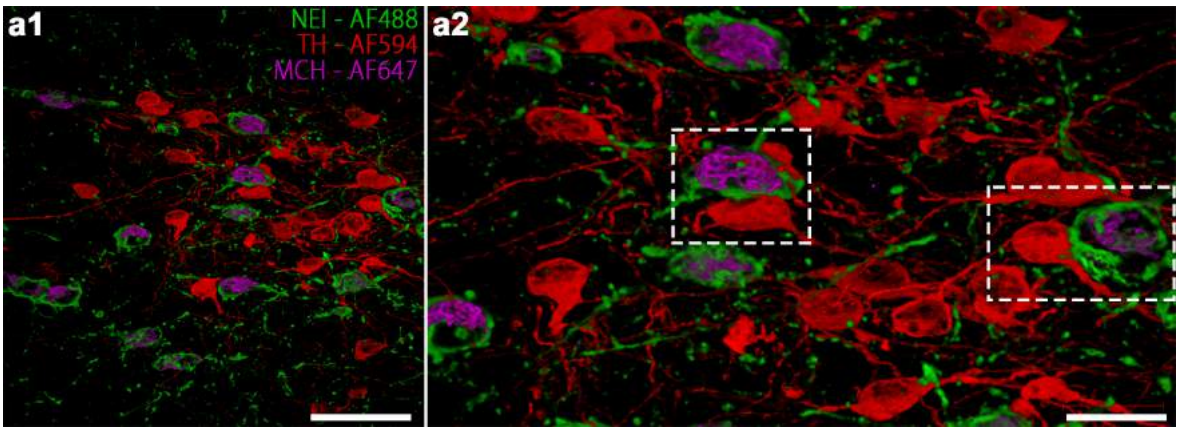

Figure 11.tiff

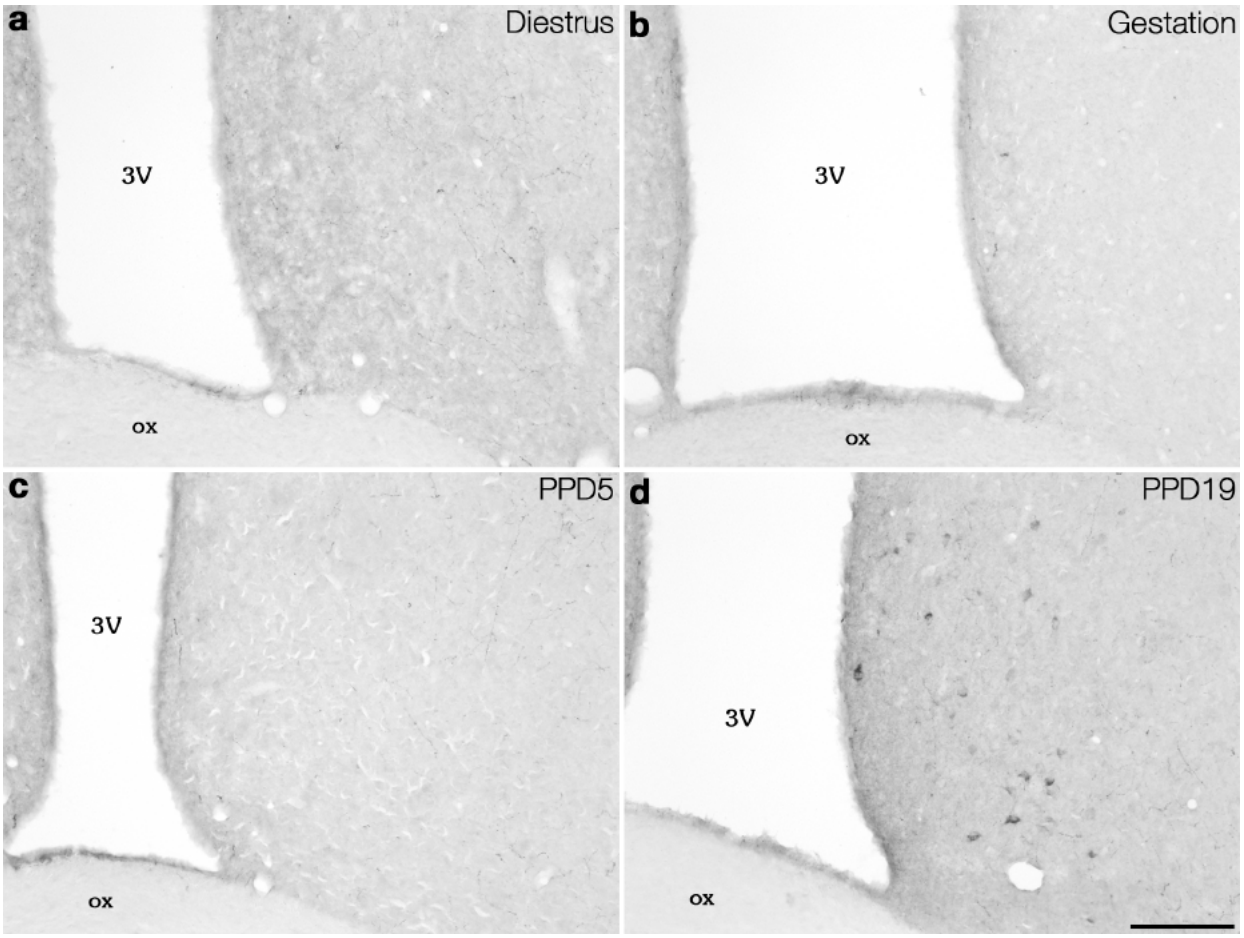

Figure 12.tiff

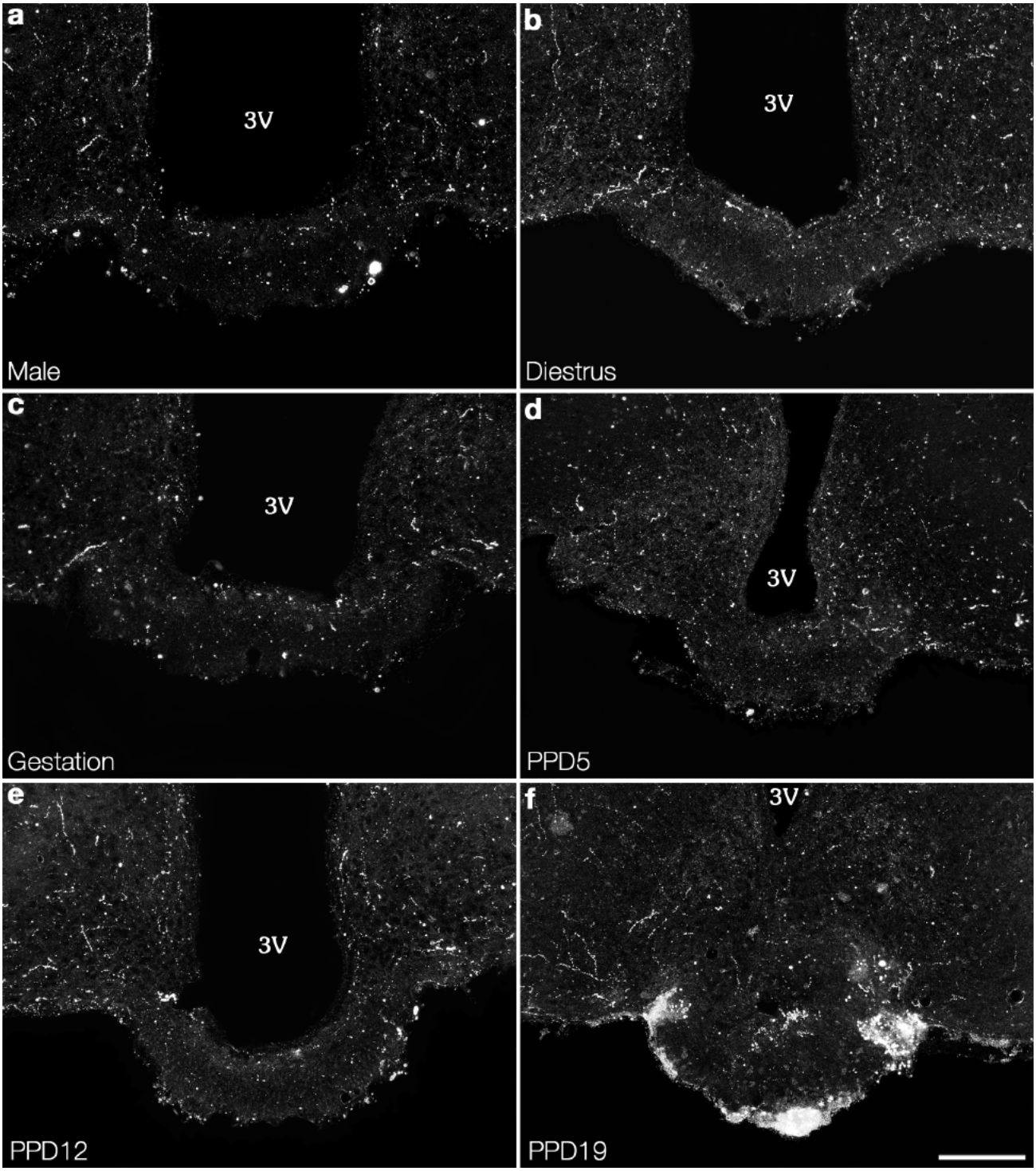

Figure 13.tiff

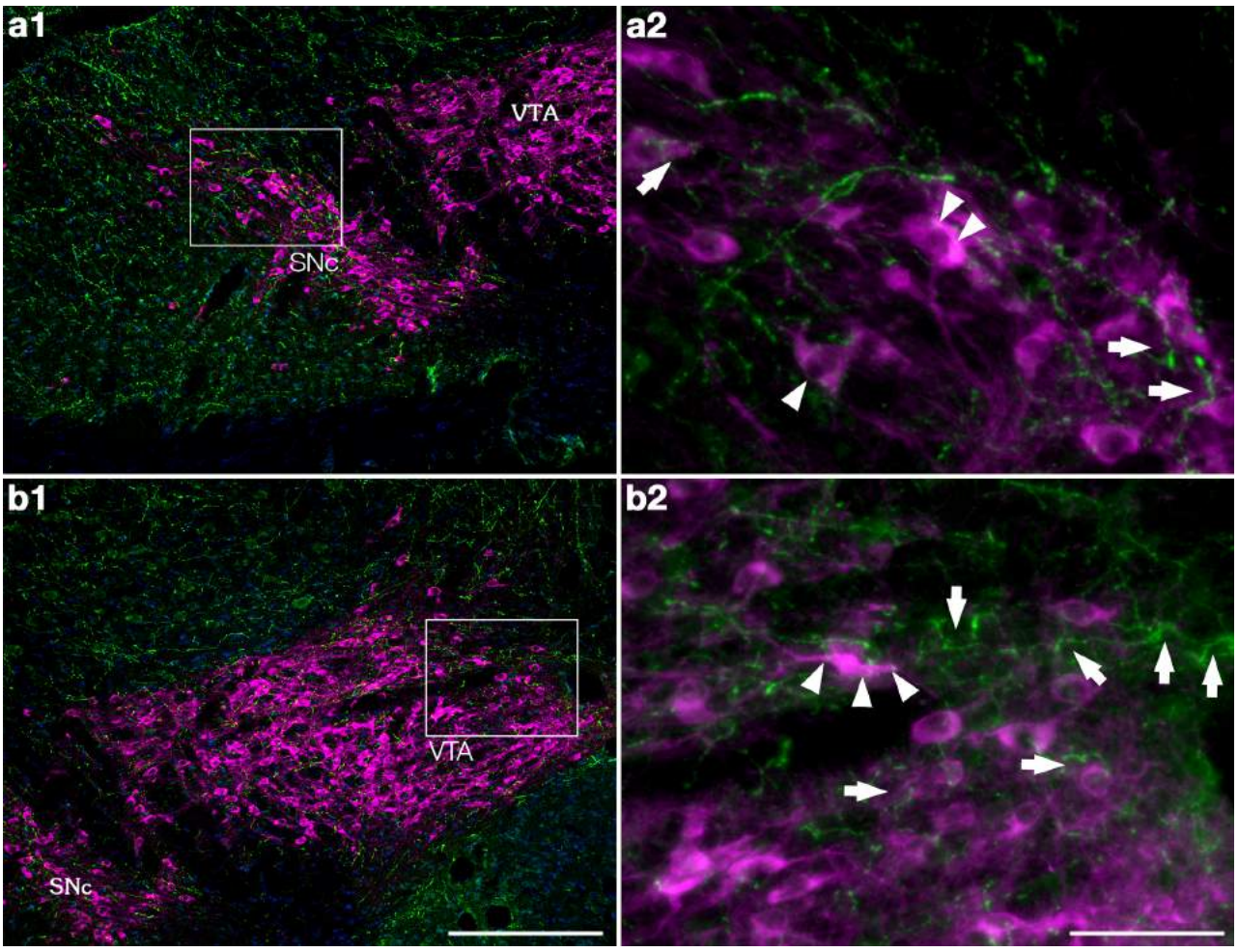

Figure 14.tiff

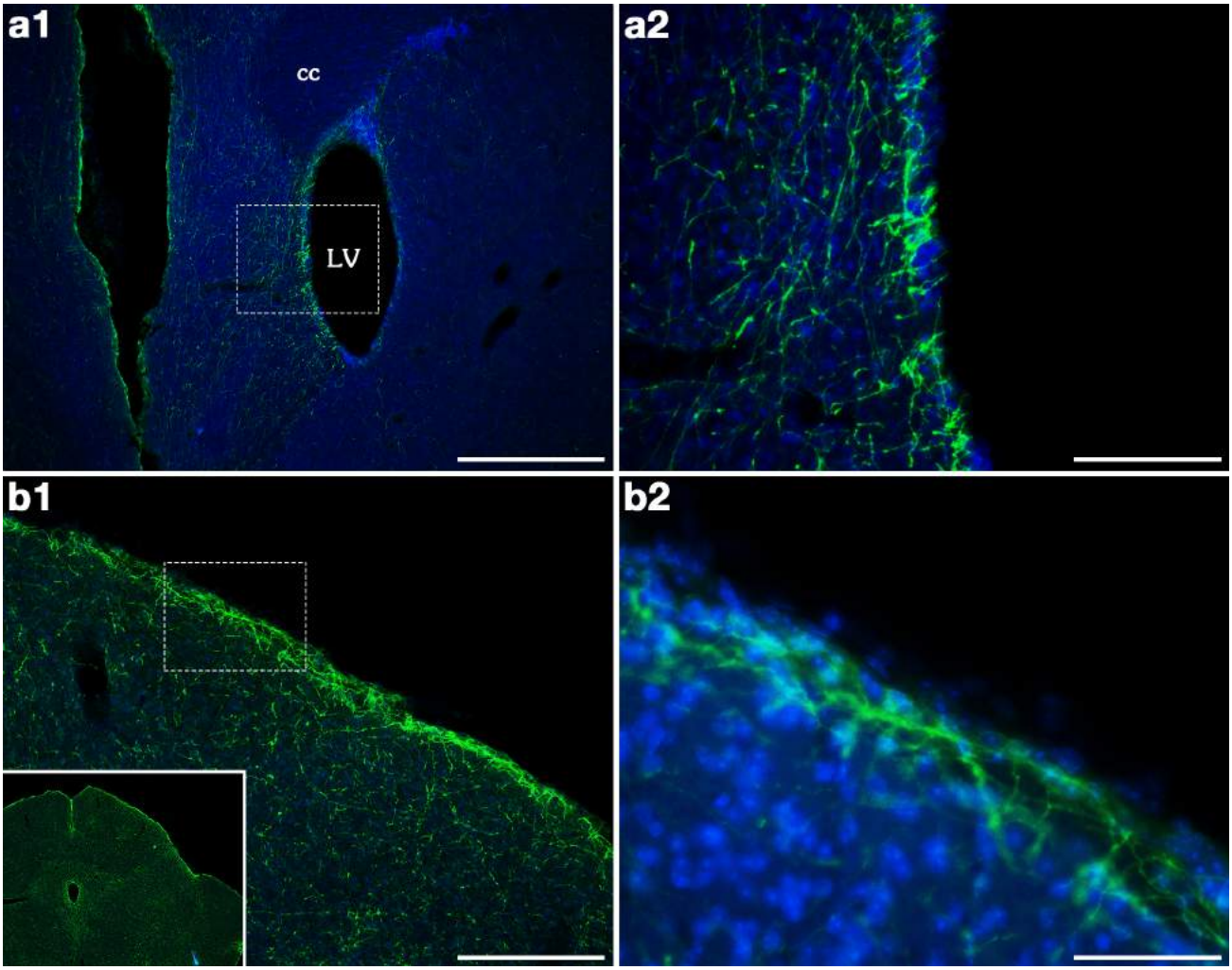

Figure 15.tiff

Lateral Hypothalamic Area		
• Highest number of MCH neurons • Lower density of MCH neurons in the LHAc • Low number of neurons in the PeF • Predominance of multipolar neurons	• Highest number of MCH neurons • Uniform density of MCH neurons • High number of neurons in the PeF • Predominance of multipolar neurons	• Highest number of MCH neurons • Uniform density of MCH neurons • High number of neurons in the PeF • Predominance of multipolar neurons
Zona Incerta		
• Intermediate number of MCH neurons	• Intermediate number of MCH neurons • Predominance of bipolar neurons	• Intermediate number of MCH neurons • Predominance of bipolar neurons
Incerto-Hypothalamic Area		
• Intermediate number of MCH neurons • Neurons intermingled with TH-ir neurons • Juxtaposed to the AHA group of MCH neurons • Predominance of bipolar neurons	• Intermediate number of MCH neurons • Neurons intermingled with TH-ir neurons • Separated from the AHA group of MCH neurons • Predominance of bipolar neurons	• Unclear number of MCH neurons • Overlaid by the AHA group of MCH neurons
Periventricular Nucleus		
• Non-existent	• Low number of MCH neurons • Present on the whole extent of the tuberal hypothalamus • Third ventricle dorsal cap	• Few scattered cells • Poorly-defined third ventricle dorsal cap
Other Areas		
• High number of MCH neurons in the AHA • No MCH neurons in the dorsal tuberomammilary nucleus • No MCH neurons in the posterior hypothalamic area	• Low number of MCH neurons in the AHA • MCH neurons in the dorsal tuberomammilary nucleus • MCH neurons in the posterior hypothalamic area	• High number of MCH neurons in the AHA • No MCH neurons in the dorsal tuberomammilary nucleus • MCH neurons in the posterior hypothalamic area

Chapter 4

The distribution of neuronal primary cilia immunoreactive to melanin-concentrating hormone receptor 1 (MCHR1) in the murine prosencephalon

Diniz GB, Battagello DS, Ferreira JGP, Klein MO, Motta-Teixeira LC, Duarte JCG, Presse F, Nahon J-L, Adamantidis A, Sita LV and Bittencourt JC

To be submitted for publication

The distribution of neuronal primary *cilia* immunoreactive to melanin-concentrating hormone receptor 1 (MCHR1) in the murine prosencephalon

Giovanne B. Diniz[a], Daniella S. Battagello[a], Jozélia G. P. Ferreira[a], Marianne O. Klein[a], Livia C. Motta-Teixeira[a], Jéssica C. G. Duarte[a], Françoise Presse[b,c], Jean-Louis Nahon[b,d], Antoine Adamantidis[e, f], Luciane V. Sita[a] and Jackson C. Bittencourt[a, g, *]

[a] Universidade de Sao Paulo, Instituto de Ciencias Biomedicas, Sao Paulo, SP, Brazil.
[b] CNRS/UNS UMR 7275, Institut de Pharmacologie Moléculaire et Cellulaire, Sophia Antipolis, Valbonne, France.
[c] Université Côte d'Azur, Nice, France.
[d] Station de Primatologie UPS846 CNRS, Rousset-sur-Arc, France.
[e] Center for Experimental Neurology, Department of Neurology, Inselspital University Hospital, University of Bern, Bern, Switzerland.
[f] Department for BioMedical Research, University of Bern, Bern, Switzerland.
[g] Universidade de Sao Paulo, Institute of Psychology, Sao Paulo, SP, Brazil.

* Corresponding author:
Jackson Cioni Bittencourt, M.D., Ph.D.
Laboratory of Chemical Neuroanatomy
Department of Anatomy
Institute of Biomedical Sciences
University of São Paulo
São Paulo, Brazil – ZIP: 05508-000
Phone: +55 (11) 3091 7300
E-mail: jcbitten@icb.usp.br

Working title: Ciliary MCHR1 in murines

Keywords: MCH; volume transmission; olfactory integration; neurochemical characterization; GPCR.

Funding: Financial support for this study was provided in the form of grants from the Fundação de Amparo à Pesquisa do Estado de São Paulo (FAPESP, São Paulo Research Foundation; Grants # 2016/02748-0 to G.B.D., 2017/17998-5 to M.O.K., 2014/22313-3 and 2016/18941-4 to L.C.M.-T., and 2016/02224-1 and 2017/16293-8 to J.C.B.). We are thankful for the support provided by the Brazilian Coordenação de Aperfeiçoamento de Pessoal de Nível Superior (CAPES, Office for the Advancement of Higher Education, Grant # 848/15). D.S.B. is a fellowship recipient of PNPD/CAPES, Brazil). J.C.B. is an Investigator with the Brazilian Conselho Nacional de Desenvolvimento Científico e Tecnológico (CNPq, National Council for Scientific and Technological Development, grant # 426378/2016-4).

Abstract

Melanin-concentrating hormone (MCH) is a ubiquitous vertebrate neuropeptide predominantly synthesized by neurons of the diencephalon that can act through two G protein-coupled receptors, called MCHR1 and MCHR2. The expression of *Mchr1* has been investigated in both rats and mice, but its synthesis remains poorly described. After identifying an antibody that detects MCHR1 with high specificity, we employed immunohistochemistry to map the distribution of MCHR1 in the CNS of rats and mice. Multiple neurochemical markers were also employed to characterize some of the neuronal populations that synthesize MCHR1. Our results show that MCHR1 is abundantly found in a sensory subcellular structure called the neuronal primary *cilium*, which has been associated with the detection of free neurochemical agents released to act through volume transmission. Ciliary MCHR1 was found in a wide range of areas, including the olfactory bulb, cortical mantle, *striatum*, hippocampal formation, amygdala, midline thalamic nuclei, periventricular hypothalamic nuclei, and midbrain areas. No differences were observed between male and female mice, and rats and mice diverged in two key areas: the caudate-putamen nucleus and the subgranular zone of the dentate gyrus. Ciliary MCHR1 was found in close association to several neurochemical markers, including tyrosine hydroxylase, calretinin, kisspeptin, estrogen receptor, oxytocin, vasopressin, and corticotropin-releasing factor. Given the role of neuronal primary *cilia* in sensing free neurochemical messengers in the extracellular fluid, the widespread distribution of ciliary MCHR1, and the diverse neurochemical populations who synthesize MCHR1, our data indicates that volume transmission may play a prominent role in the normal function of the MCH system.

1. Introduction

Melanin-concentrating hormone (MCH) is a ubiquitous vertebrate neuropeptide, synthesized predominantly by neurons of the diencephalon and, in particular, of the lateral hypothalamic area (Bittencourt & Diniz 2018; Bittencourt *et al.* 1992). The MCH neuropeptidergic system has been involved in several physiological roles, including the integration and promotion of motivated behaviors (Diniz & Bittencourt 2017), sleep (Ferreira *et al.* 2017a; Gao 2018), ventricular homeostasis (Conductier *et al.* 2013b; Conductier *et al.* 2013a), and autonomic function modulation (Brown *et al.* 2007; Messina & Overton 2007). It has also been implicated in sexual physiology (Naufahu *et al.* 2013), including the release of luteinizing hormone (Chiocchio *et al.* 2001; Murray *et al.* 2000b), the promotion of sexual behavior (Gonzalez *et al.* 1996), and parental behavior (Alachkar *et al.* 2016; Benedetto *et al.* 2014).

The mammalian MCH peptidergic system is composed by three peptides produced from a single precursor, encoded by the *Pmch* gene. In addition to MCH, neuropeptide E-I (NEI) and neuropeptide G-E (NGE) are cleaved by prohormone convertases and may have biological activities that are independent of MCH (Bittencourt & Celis 2008). This system is also composed by two receptors that bind with specificity to MCH, called MCH receptor 1 (MCHR1) and receptor 2 (MCHR2) (reviewed in Presse *et al.* (2014) and Bittencourt and Diniz (2018)). While MCHR1 is present in a wide range of vertebrates, MCHR2 has been lost after the divergence of the *Glires* clade, what resulted in the loss of a working MCHR2 receptor in rabbits, guinea pigs, hamsters, rats and mice (Tan *et al.* 2002). As a result, the amount of information amassed about MCHR1 is significantly higher than that about MCHR2.

Despite the focus on MCHR1, there are a few important aspects of this receptor that are not well understood. After the discovery of MCH as the ligand of MCHR1 (Bächner *et al.* 1999; Chambers *et al.* 1999; Saito *et al.* 1999; Shimomura *et al.* 1999), the distributions of *Mchr1* gene expression and MCHR1 immunoreactivity were described in rats (Saito *et al.* 2001; Hervieu *et al.* 2000). In both cases, only male specimens were used, and both works describe widespread expression/synthesis of MCHR1. The next wave of works then focused on mice, through the use of gene reporters (Chee *et al.* 2013; Engle *et al.* 2018). Despite an exhaustive investigation and detailed description of the gene reporter distribution, the experimental model of gene reporters cannot inform the subcellular localization of the protein product that results from the investigated gene. It is unclear, therefore, what is the precise subcellular localization of MCHR1 *in vivo*.

The first hint that the subcellular localization of MCHR1 may be important for its function came in the work of Berbari *et al.* (2008), who described MCHR1 immunoreactivity in the primary *cilia* of cultured cells, and in a few areas of the central nervous system. Primary *cilia* are non-motile structures, found within the CNS exclusively in neurons, and first described in humans (Mandl & Megele 1989). The main role of primary *cilia* is chemical sensing and signal transducing (Pazour & Witman 2003; Berbari *et al.* 2009), as they are covered in receptors (Händel *et al.* 1999; Brailov *et al.* 2000; Loktev & Jackson 2013; Koemeter-Cox *et al.* 2014; Siljee *et al.* 2018), and participate in several signaling pathways (Breunig *et al.* 2008; Rohatgi *et al.* 2007; Corbit *et al.* 2005). Neuronal primary *cilia* may be an integral part of volume transmission (VT), a neuronal method of communication that involves the use of neurochemical messengers outside the synapse (Agnati *et al.* 1986; Agnati *et al.* 1995; Agnati *et al.* 2010), including the release of neuroactive substances in the extracellular space (ECS) and the cerebrospinal fluid (CSF) (Fuxe *et al.* 2007; Agnati & Fuxe 2014).

Mapping the areas where MCHR1 is associated to primary *cilia* in the CNS may help us understand its mechanisms of action. It has recently been demonstrated that MCH acts in a VT paradigm to exert a modulatory role in feeding (Noble *et al.* 2018; Jiang & Brüning 2018). Areas linked to feeding behavior where MCHR1 is ciliary are the likely target for this effect. Furthermore, areas unrelated to feeding behavior that contain ciliary MCHR1 may reveal clues about other actions exerted by

MCH that depend on VT. With that in mind, we mapped the presence of MCHR1 immunoreactivity in *cilia* in the prosencephalon of adult rats and mice. Since MCH has been implicated in sexual regulation (Gonzalez *et al.* 1996; Murray *et al.* 2000b; Murray *et al.* 2006; Wu *et al.* 2009), and female models have been poorly explored in the literature concerning MCH, we included females in all four estrous cycle stages to evaluate possible changes in the receptor distribution linked to reproductive status. The results found in mice were then compared to rats to inform us about possible interspecies differences in the distribution of MCHR1.

2. Materials and Methods

2.1. Animals

Adult male and female virgin C57BL/6 mice (n = 25) were bred and raised in the animal facility of the Department of Anatomy, Institute of Biomedical Sciences of the University of São Paulo. At the beginning of the experiments, animals were approximately three months old and weighed between 20 and 30g. Females were housed five per cage, while males were housed individually after they reached sexual maturity, in a room with 12/12h light/dark cycle (lights on at 6:00 AM), controlled temperature (22±2ºC), and *ad libitum* access to water and standard chow. All experiments were carried out in accordance with the Guidelines for the Care and Use of Mammals in Neuroscience and Behavioral Research established by the Brazilian National Research Council (CONCEA, 2016), as well as with those established by the Ethics Committee on the Animal Use of the Institute of Biomedical Sciences (Protocol CEUA #096/2014). No effort was spared to minimize the number of animals employed in this study and any incidental suffering caused to them. To evaluate the possibility that interspecies differences exist in the distribution of MCHR1, adult male Sprague-Dawley rats (n = 5) were bred and raised as described above. To test antibody specificity, we employed *Mchr1*$^{-/-}$ mice (Adamantidis *et al.* 2005), as well as their heterozygous and WT littermates. These animals were bred and raised in the animal facility of the University Hospital, Inselspital, in Bern, Switzerland in conditions similar as above.

To determine the day of euthanasia, females had their estrous cycle followed daily at 10:00 AM by the method of vaginal cytology (Byers *et al.* 2012). To that end, 50µl of saline were inserted in the vaginal channel with a pipette and gel-loading tips. Care was taken so the tip did not touch the vagina to avoid unintended stimulation and pseudopregnancy. The liquid was then collected, spread on glass slides, and examined under the light microscope (Nikon Corporation; Minato, Tokyo, Japan). Estrous cycle determination was based on the relative densities of epithelial, cornified, and leucocyte cell populations (Byers *et al.* 2012).

2.2. Tissue collection

At the day of euthanasia, animals were anesthetized with an excess of Xylazine, Ketamine and Acepromazine. Once verified the loss of reflexes, animals were thoracotomized and transcardially perfused. For mice, approximately 20ml of cold 0.9% saline solution were perfused to clean the vascular bed, followed by 240ml of 4% formaldehyde solution in borate buffer (pH 9.5). In rats, the volume was 100ml of cold 0.9% saline and 750 ml of 4% formaldehyde solution in borate buffer (pH 9.5). After perfusion, the heads were separated from the body, the cranium opened, and the brain removed and post-fixed in the same fixative solution with 20% sucrose for four hours. At the end of the postfixation time, brains were transferred to 0.02M potassium-phosphate buffered saline (KPBS, pH 7.4) with 20% sucrose until slicing. Slicing of the brains was performed in the frontal plane in a sliding microtome. One-in-five series of 20µm slices were obtained from mice and one-in-five series of 40µm were obtained from rats. Slices were kept in antifreeze solution at -30ºC until immunohistochemistry.

2.3. Immunohistochemistry

2.3.1. Antibody selection

To identify an antibody that selectively labels MCHR1, we tested six brands of commercially-available antibodies. The details of each antibody are listed in Table 1. Each antibody was used for immunoperoxidase staining in six different dilutions (1:1,000, 1:3,000, 1:10,000, 1:30,000, 1:100,000 and 1:300,000), as described by Hoffman *et al.* (2016) for antibody titration. In some cases, where no signal whatsoever could be detected, we tested more concentrated titers (not shown). The concentration of antibody found to be optimal for immunoperoxidase staining was then used for immunofluorescence procedures. Primary and secondary antibody suppression tests were performed for all antibodies (not shown). The antibody that resulted in the best labeling was then further tested on tissue from knockout animals, negative control test described as the gold standard of antibody validation by Saper and Sawchenko (2003).

2.3.2. Immunoperoxidase

For immunoperoxidase staining, slices were extensively rinsed in KPBS for antifreeze solution removal and incubated with a 0.3% solution of hydrogen peroxidase in KPBS for 15 minutes. Slices were then rinsed again in KPBS and incubated with primary antibody in a KPBS solution of 3% normal goat serum (Vector Laboratories; Burlingame, CA, USA; AB_2336615) and 0.3% Triton X-100 for membrane permeabilization. In the following day, slices were rinsed in KPBS and incubated with biotinylated goat anti-rabbit IgG (1:800, Vector; AB_2313606) for one hour at room temperature. After new rinses, slices were incubated with an avidin-biotin-horseradish peroxidase solution (1:333, Vector; AB_2336819) for one hour. For chromogen deposition, slices were transferred to a solution of 3,3'-diaminobenzidine tetrahydrochloride (DAB, 0.02% - Sigma Chemical; St. Louis, MO, USA) with 0.003% hydrogen peroxide and 2.5% nickel ammonium sulfate diluted in 0.2M sodium acetate buffer (pH 6.5). Reactions were stopped by transferring slices to clean sodium acetate buffer and then rinsing them with KPBS. Sections were then mounted on gelatin-coated glass slides in rostrocaudal order, dehydrated, defatted and coverslipped with a hydrophobic mounting medium (DPX; Sigma).

2.3.3. Immunofluorescence

For immunofluorescence staining of MCHR1, a protocol similar to that described by Hoffman et al (2016) was employed. Briefly, slices were rinsed in KPBS and incubated with a 0.3% solution of hydrogen peroxidase in KPBS for 20 minutes. After new rinses, slices were incubated with primary antibody in a KPBS solution of 3% normal donkey serum (Jackson ImmunoResearch; West Grove, PA, USA; AB_2337258) and 0.3% Triton X-100 for membrane permeabilization. In the following day, slices were incubated with biotinylated donkey anti-rabbit IgG antibody (1:5000, Jackson ImmunoResearch; AB_2340593) for one hour at room temperature and then incubated with avidin-biotin-horseradish peroxidase solution (1:833, Vector; AB_2336819) for 30 minutes at room temperature. Slices were then washed and incubated with a 0.5% biotinylated (EZ-Link sulfo-NHS-LC-biotin; ThermoFisher Scientific, Waltham, MA, USA) tyramine (Sigma-Aldrich; Sigma Chemical; St. Louis, MO, USA) and hydrogen peroxide (0.005%) solution for 20 minutes, and then incubated with AlexaFluor 594-conjugated streptavidin (1:200, Invitrogen; Carlsbad, CA, USA). Slices were then rinsed in KPBS, incubated with DAPI (1:10'000, Invitrogen) for 10 minutes and mounted in glass slides or used in following labeling experiments.

To label other markers, MCHR1-immunolabeled slices were rinsed with KPBS and incubated with primary antibodies for different neurochemical markers (Table 1) in KPBS containing 3% normal donkey serum (Jackson ImmunoResearch; AB_2337258) and 0.3% Triton X-100. In the following day, slices were rinsed and incubated with AlexaFluor 488-conjugated donkey anti-IgG antibodies (1:200, Invitrogen; AB_2556546, AB_2534082, AB_2556542, AB_2534102) for two hours at room

temperature. After final rinses with KPBS, slices were mounted in glass slides. After a brief period of air drying, the slides were then covered with antifade mounting medium (Invitrogen) and coverslipped.

2.4. Imaging and Data Analysis

Immunoperoxidase-labeled slices were examined with brightfield microscopy in a Nikon 80i microscope (Nikon) coupled to a digital camera (CX3000 - MBF Bioscience Co.; Williston, VT, USA) and operating under the software Microlucida 3.03 (MBF Bioscience). Immunofluorescence-labeled slices were examined with widefield and confocal fluorescence microscopy in an AxioImager Z2 motorized upright microscope (Carl Zeiss; Wetzlar, Germany). Widefield illumination was obtained with an HXP 120V illuminator (Carl Zeiss) and photomicrographs were produced with an AxioCam 506c (Carl Zeiss). Each fluorophore was imaged separately in emulated monochromatic mode in separate channels and then merged. Confocal microscopy was performed using a laser unit as light source and the LSM800 scan unit with two metal halide detectors (Carl Zeiss). All images had adjustments in their brightness, contrast, and sharpness applied to every pixel in the picture, and the changes did not alter the information illustrated in the figures. The plates were assembled, and off-tissue background/methodological artifacts were cleared by means of Adobe Photoshop CC 2017.0.1 software (Adobe Systems Inc; San Jose, CA, USA; SCR_014199).

Mapping of MCHR1 immunoreactivity was performed by comparing the cytoarchitectonic characteristics of each slice, as evidenced by DAPI staining (when applicable), to the atlas of Paxinos and Franklin (2012) and Paxinos and Watson (2006). In some cases, additional information was obtained using neurochemical markers to delineate specific areas. The comparison of relative densities between male and female and between different estrous cycle stages was performed using a semi-quantitative method. After analysis of random slices, a scale of *cilia* density was developed. An investigator blind to the experimental condition of the animals then used the scale to rate the presence of immunoreactive *cilia* in each area examined with a number ranging from 0-8, with 0 corresponding to complete absence of immunoreactivity and 8 corresponding to the highest density found. The same procedure was performed for all animals and the average density of *cilia* was obtained for each area and each sexual status. To facilitate the presentation of these results, the number system was then converted to a system of crosses with less discrimination but better noise suppression.

3. Results

3.1. The antibody used targets ciliary MCHR1 with high specificity

From the six antibodies tested for MCHR1 detection (Table 1), only one resulted in consistent labeling at the tested concentrations: antibody PA5-24182 from Invitrogen. Antibody Santa Cruz C-17 (Table 1) also resulted in staining, but the lower signal/background *ratio* and the discontinuation of this antibody by its manufacturer led us to use antibody PA5-24182 in the rest of the experiments. Because antibody PA5-24182 has never been used in the literature, we proceeded to verify its specificity by employing standard omission tests and using tissue from *Mchr1*$^{-/-}$ and *Mchr1*$^{+/-}$ mice (Saper & Sawchenko 2003). As expected, antibody and fluorophore omission tests were successful, with no staining observed in the antibody suppression cases (Fig. 1 A'-A''). Using the antibody on tissue from *Mchr1*$^{+}$ animals resulted in the regular pattern of staining observed during titrations (Fig. 1 A, B). No staining could be observed on slices from *Mchr1*$^{-/-}$ animals (Fig. 1 B''). Interestingly, *Mchr1*$^{+/-}$ animals displayed an intermediate pattern of staining, with scattered labeling found in areas otherwise heavily labeled in *Mchr1*$^{+}$ animals (Fig. 1 B'). These tests show that the used MCHR1 antibody labels its target with high specificity.

To confirm the labeling observed using the PA5-24182 was ciliary, we performed double immunohistochemistry in series of some animals using an anti-adenylate cyclase III (AC3) antibody. Adenylate cyclase III has been shown to be a marker of neuronal primary *cilia* (Bishop *et al.* 2007). As expected, we found widespread staining for AC3, agreeing to the distribution described by Bishop et al (2007). In several areas, colocalization between MCHR1 and AC3 was almost complete, such as in the

pyramidal layer of the hippocampus proper (Fig. 2 A), while in others there was no signal of MCHR1 colocalizing with the AC3-positive labeling, such as in the granular layer of the dentate gyrus (Fig. 2 B). Upon closer inspection, it was observed that MCHR1 labeling seldom covers the whole *cilia*, in most cases forming a patched pattern upon the ciliary surface (Fig. 2 A'). As an additional control, we performed simultaneous MCHR1 and NeuN (neuronal marker) or GFAP (glial marker) labeling. Since neuronal primary *cilia* are not found in glial cells, we expected no clear pattern of co-distribution between MCHR1 and GFAP. As expected, no clear pattern was observed, while MCHR1 was found codistributed with NeuN in several areas (Supplementary Material 01).

3.2. MCHR1 is widely distributed within the murine prosencephalon

To map the distribution of MCHR1 in the mouse prosencephalon, we developed a grading scale that went from 0 (complete absence of staining) to 8 (maximum density of weight) (Fig. 3). Each area identified using the mouse brain atlas by Paxinos and Franklin (2012) from each animal was then scored based on that grading scale by a single experimenter, who was blind to the group of each animal. Upon comparison, there were no consistent differences between male and female and the different stages of the estrous cycle, and therefore only a stereotypical distribution contemplating all groups will be presented in this paper (Table 2). The distribution of MCHR1 in rats and mice was also highly similar, and therefore the mouse will be used to elaborate the description of the results, and differences between the two species will be highlighted at the end of this section. To simplify the description of the results, the numerical system implemented in the first analysis was simplified to a cross system, where a dash represents no staining and four crosses represent maximum staining (Fig. 3). Highlights of the morphological distribution of MCHR1-ir *cilia* in adult mice will be provided in this section, and some areas are illustrated in Fig. 4. For an exhaustive description, we ask the reader to refer to Table 2.

Labeling could be abundantly observed in olfactory areas, such as the olfactory bulb, including the glomerular and granular layers, internal plexiform layer and mitral cell layer; layer 2 of the piriform cortex; dorsal and ventral *taenia tecta*; dorsal and intermediate endopiriform nucleus; and olfactory tubercle. Albeit in a smaller density, we also observed labeling in the medial aspect of the anterior olfactory nucleus. Other subcortical areas were also rich in labeling. The region with the densest immunolabeling for MCHR1 was the shell of the *nucleus accumbens*, with a moderate density found in the core subdivision of this nucleus. The neighboring *ventral pallidum* also displayed high levels of MCHR1 immunoreactivity. In the caudate-putamen nucleus, a mediolateral gradient was observed in the matrix, with a high density found medially, close to the lateral ventricle walls. No staining was observed in the striasomes. Likewise, no staining was observed in the *globus pallidus*. In the adjoining septal nuclei, only sparse immunoreactivity was seen in the ventral part of the lateral septal nucleus, with no labeling detected in other subdivisions of the lateral septal nucleus or in the medial septal nucleus.

In the amygdaloid complex, scattered MCHR1 immunoreactivity was observed in the basolateral, basomedial, medial and central nuclei. The hippocampal formation displayed a very characteristic pattern of staining, with a high density of immunolabeled *cilia* in the pyramidal stratum of CA1, CA2, and to a lesser extent, CA3 of the hippocampus proper. Scattered immunoreactivity was found in *strata Oriens* and *Radiatum*. The cortical distribution of MCHR1 followed a clear layer-specific distribution, with high densities of MCHR1 found in layers 2, 3 and 5, lower densities found in layers 4 and 6, and no staining found in layer 1 (Supplementary Material 01). Among the cortical regions containing MCHR1-ir *cilia* elements are: orbital, granular and agranular insular cortex; primary and secondary somatosensory cortices; primary and secondary motor cortices; frontal, perirhinal and entorhinal cortices; temporal, visual and auditory cortices. In the cingulate cortex, we observed a decreased density of MCHR1-ir *cilia* in layers 2 and 3 when compared to other cortical areas.

In the diencephalon, MCHR1-ir *cilia* were observed in several thalamic areas, such as the parataenial nucleus, the paraventricular thalamic nucleus, medial thalamic nuclei, and the medial habenular nucleus. We did not observe immunoreactivity in the *zona incerta*. In the hypothalamus, scattered *cilia* can be found in the lateral zone, in addition to strong clusters of immunoreactive material in the preoptic periventricular nucleus, paraventricular hypothalamic nucleus, and arcuate nucleus. Average densities of *cilia* were found in the medial preoptic area, anterior hypothalamic area and the posterior hypothalamic area, while medial zone nuclei were mostly devoid of labeling, such as the dorsomedial hypothalamic nucleus and the ventromedial hypothalamic nucleus.

At first glance, the distribution of MCHR1-ir *cilia* appeared to be complementary to that of MCH- and NEI-ir fibers, with areas rich in immunoreactive fibers virtually devoid of MCHR1-ir *cilia*, while areas rich in the receptor receive sparse innervation (Diniz *et al.* 2019). To confirm this pattern, we performed double immunohistochemistry to visualize MCHR1 and MCH-ir fibers in the same slices. The resulting pattern of labeling confirmed the segregation between some MCH-ir fibers-rich areas and areas containing large amounts of MCHR1-ir *cilia*, such as the nucleus accumbens/medial septal nucleus boundary (Fig. 5), or the medial/lateral *globus pallidus* (not shown).

In rats, the general outline of staining was very similar to the one found in mice, including abundant staining in olfactory regions, chiefly the olfactory bulb and anterior olfactory nuclei, piriform cortex, olfactory tubercle, ventral *pallidum* and the islands of Calleja; the shell of the *nucleus accumbens*; layers 2, 3 and 5 of numerous cortical fields; the pyramidal stratum of the hippocampal formation; medial and central amygdaloid nuclei; midline thalamic nuclei and the periventricular and medial zones of the hypothalamus. Two notable differences, however, could be found between rats and mice. While mouse has a moderate-to-high staining of MCHR1 in the caudate putamen, rats were almost devoid of immunoreactivity is this area, with a very high background observed in the matrix. On the other hand, a negligible amount of MCHR1 immunoreactivity is observed in the mouse granular layer of the dentate gyrus, while a layer of stained *cilia* can be discerned in the subgranular zone of the rat dentate gyrus (Fig. 6).

3.3. Defined neurochemical populations display ciliary MCHR1

Because MCHR1-ir *cilia* were found in areas with heterogeneous neurochemical populations, we employed double immunohistochemistry to characterize some of those populations. In the olfactory bulb, MCHR1-ir *cilia* were found in a pattern that closely resembled the distribution of tyrosine hydroxylase-ir cells, bordering the glomeruli (Fig. 7 A, A'). To a lesser extent, MCHR1-ir *cilia* are found associated to calretinin-ir cells (Fig. 7 B, B'). On the other hand, no MCHR1-ir *cilia* were found within range of calbindin-ir cells (not shown). In the preoptic hypothalamus, we found MCHR1-ir *cilia* associated with kisspeptin-ir cells (Fig. 8 A, A') but not with gonadotropin-releasing hormone (GnRH)-ir cells. In the periventricular and medial preoptic nuclei, MCHR1-ir *cilia* were also encountered in close proximity to estrogen receptor α cells (Fig. 8 B, B').

In the paraventricular nucleus of the hypothalamus, MCHR1-ir *cilia* were densest in the parvicellular subdivisions, but immunoreactive *cilia* were also found in the magnocellular subdivisions. While there is no clear overlap on the MCHR1 and vasopressin distributions, MCHR1is largely codistributed with oxytocin, mainly in the fringes of the magnocellular nuclei (Fig. 8 C, C'). A higher degree of colocalization was seen between MCHR1-ir *cilia* and corticotropin-releasing factor (CRF) in the parvicellular paraventricular nucleus (Fig. 8 D, D'). In the supraoptic nucleus, a different pattern was observed, with almost complete colocalization between MCHR1-ir *cilia* and vasopressinergic neurons, while only partial colocalization was found between MCHR1 and oxytocinergic neurons (Fig. 8 E, E').

In the arcuate nucleus, we found no colocalization between MCHR1 and α-melanocyte-stimulating hormone (α-MSH) or cocaine- and amphetamine-regulated transcript (CART). The only clear codistribution observed in the arcuate nucleus was between MCHR1 and tyrosine hydroxylase (TH), a dopaminergic marker. The arcuate nucleus, however, was not the only area where TH and MCHR1 were extensively codistributed, as virtually every TH-ir neuron in the incerto-hypothalamic area has a corresponding MCHR1-ir *cilium* (Fig. 8 F, F'). Neurons immunoreactive to CART in the incerto-hypothalamic area and in the lateral hypothalamus did not contain MCHR1-ir *cilia*, and there was no clear codistribution of MCHR1 and orexin in the lateral hypothalamus. Finally, no colocalization was observed between doublecortin and MCHR1 in the canonical sites of adult neurogenesis in the mouse brain.

4. Discussion

The presence of ciliary MCHR1 in the prosencephalon of murines is more extensive than previously known. In this work, we identified a commercial antibody that is able to stain ciliary MCHR1 with high specificity, and we employed it to map the presence of MCHR1 in neuronal primary *cilia* of both rats and mice, including female mice in all four stages of the reproductive cycle. Our results show a ciliary MCHR1 distribution that includes a wide range of structures, from the olfactory bulb to the hypothalamic mammillary nuclei. Our results are in agreement to most of what has been published up to this point in terms of *Mchr1* gene expression, suggesting ciliary MCHR1 is at least as abundant as, if not even more abundant, than other subcellular locations of MCHR1. The wide range of areas in which MCHR1 is found opens up the possibility that volume transmission may be a very important aspect of MCH cellular communication within the CNS, and an important aspect of neurochemical communication in vertebrate systems as a whole.

Up to this point, the staining of MCHR1 has been limited to a few works. Hervieu *et al.* (2000) were the first to use antibodies to map MCHR1, but there is no mention as to the subcellular localization of the labeling obtained by those authors. The other two published works that employed immunohistochemistry for MCHR1 were Berbari *et al.* (2008) and Niño-Rivero *et al.* (2019), who used a now discontinued antibody to demonstrate the presence of MCHR1 in the neuronal primary *cilia* of specific areas within the CNS of mice and rats. We demonstrated in this work that antibody PA5-24182 is a suitable replacement for the labeling of MCHR1, generating negative results in antibody omission tests, not labeling tissue from *Mchr1*$^{-/-}$, and specifically labeling MCHR1 in neuronal primary *cilia*, as demonstrated by the colocalization with AC3. An additional benefit of the identified antibody is its target epitope. Directed at the last 27 residues of MCHR1, within the intracellular C-terminal portion of this receptor, this sequence is highly conserved between mammals, with a single conservative substitution in humans when compared to rodents, suggesting it may be successfully used to label MCHR1 in other mammals.

The distribution of MCHR1 obtained in this work is mostly similar, but not identical, to what has been described before. With respect to the immunohistochemical mapping of Hervieu *et al.* (2000) and the *in situ* hybridization mapping of Saito *et al.* (2001), several areas of the rat brain were also stained with antibody PA5-24182, including the olfactory tubercle, piriform cortex, endopiriform nuclei, hippocampal formation, amygdala, periventricular and paraventricular hypothalamic nuclei, arcuate nucleus, the cortical mantle and the midline thalamic nuclei. We also observed labeling in the olfactory bulb, islands of Calleja and in the medial habenular nucleus, areas that were also labeled in Hervieu *et al.* (2000), but not in Saito *et al.* (2001). On the other hand, Hervieu *et al.* (2000) described intense labeling of the medial septal nucleus and similar labeling of the hippocampus proper and the dentate gyrus, while this work and that of Saito *et al.* (2001) found an absence of MCHR1 synthesis and *Mchr1* expression in the medial septal nucleus, and a much lower presence of MCHR1/*Mchr1* in the dentate gyrus when compared to the hippocampus proper.

The differences in MCHR1 density between rats and mice observed in this work are partially coherent with previous works. Hervieu *et al.* (2000) found a medium density of MCHR1 in the caudate-putamen of rats, while Saito *et al.* (2001) found a low expression of Mchr1 in this area. Chee *et al.* (2013) found a medium-high density of *Mchr1* reporter expression in mice. Our results align well with those of Chee *et al.* (2013) and Saito *et al.* (2001), as the mouse has a much more pronounced presence of MCHR1 *cilia* in the caudate-putamen. This is also the case with the dentate gyrus, as Saito *et al.* (2001) report a restricted presence of *Mchr1* expression in this structure, and Chee *et al.* (2013) found no *Mchr1* mRNA expression. To what extent these interspecies differences results in physiological differences is still unknown. Rats and mice have different profiles in terms of generation of new neurons in the hippocampus and their integration into functional circuits (Snyder *et al.* 2009), and the site of MCHR1 synthesis in rats found in this work is the subgranular zone, area thoroughly implicated in adult neurogenesis (Eriksson *et al.* 1998). Rats and mice also show different social responses to cocaine (Kummer *et al.* 2014), what could have as substrate differences in the caudate-putamen nucleus. To determine to what extent MCHR1 is involved in those differences more studies will be necessary.

Gene reporters and *in situ* hybridization have been used to investigate the expression of *Mchr1* in the mouse brain (Chee *et al.* 2013; Engle *et al.* 2018). Our distribution of MCHR1 immunoreactivity is mostly similar to what has been described in those works, including the olfactory areas, a similar pattern of cortical distribution, very dense labeling of the islands of Calleja, preeminent labeling in the pyramidal layer of the hippocampal formation and *induseum griseum*, no labeling of the medial septal nucleus, low labeling of thalamic nuclei, and weak to moderate labeling of the *zona incerta* and amygdala. The major disagreement between our work and that of Chee *et al.* (2013) concerns the relative density of synthesis/expression in some hypothalamic nuclei: while gene expression was highest in the arcuate nucleus and only moderate in the paraventricular and supraoptic nuclei, we found average synthesis in the arcuate nucleus and a very dense labeling density in the paraventricular and supraoptic nuclei. Curiously, Engle *et al.* (2018) report that the level of *Mchr1* expression in the arcuate and paraventricular nuclei varied significantly between animals with inducible versus constitutive *Mchr1-Cre* alleles, suggesting that transient expression of *Mchr1* may occur during development at critical windows, possibly resulting in the variations observed between our animals and previous studies.

The labeling obtained in this work was entirely ciliary, as revealed by the full colocalization between MCHR1 and AC3 in all areas examined. It is unclear, at this moment, if this results from all MCHR1 being found solely at primary *cilia*, or if the antibody targets ciliary MCHR1 selectively, either due to slight post-translational differences between ciliary and non-ciliary MCHR1 or due to facilitated antibody access to its epitope in the *cilium* as compared to the membrane or synaptic space. Hervieu *et al.* (2000) found labeling with anti-MCHR1 to be confined to the plasma membrane, indicating that the antibody used in that work targets specifically membrane MCHR1, while both Berbari *et al.* (2008) and Niño-Rivero *et al.* (2019) found labeling to be exclusively ciliary. Regardless of the case, our work demonstrates that MCHR1 presence in the *cilium* is widespread, what has important functional implications. Neuronal primary *cilia* are believed to function as sensory organs for the cell (Pazour & Witman 2003). The existence of primary *cilia* as sensory organs can be explained through an evolutionary perspective: neuronal surface components tend to interfere with the homogenization of the ECS due to electrostatic interactions between the cellular membrane and ECS proteins. An appendicular structure that projects into the ECS, distancing itself from the cellular membrane, provides an adaptive advantage by better sensing subtle changes in the extracellular matrix composition (Marshall & Nonaka 2006). One direct inference that can be made from the fact that MCHR1 is found in the primary *cilia* is that MCH must be found in the ECS, outside the synaptic space, what is commonly associated with the concept of VT (Agnati *et al.* 1986; Agnati *et al.* 2010; Agnati *et al.* 1995).

Volume transmission concerns the communication between neurons that happens through pathways that are structurally poorly defined, occurs in a tridimensional space, and generally has multiple targets. Mechanisms of VT include the extrasynaptic spilling of neurotransmitters, release of neurochemical messengers in the ECS and CSF, and vesicle release, as opposed to wiring transmission, which includes synapses and gap junctions (Agnati & Fuxe 2014; Fuxe *et al.* 2007). Particularly relevant for ciliary receptors is the release of neurochemical messengers in the ECS and CSF. This release can occur in several ways, including peptide vesicle release at axonal non-synaptic domains (Golding 1994), reverse-uptake release of neurotransmitters (Attwell *et al.* 1993), and exocytotic and non-exocytotic somatodendritic release of peptides (Pow & Morris 1989). Once the signal is released, it can bind to receptors in the parent neurons, diffuse to neighbor neurons through the ECS, or travel to distant sites through the paravascular fluid circulation (Rennels *et al.* 1985), fiber bundle convection (Bjelke *et al.* 1995) or CSF flow.

Volume transmission mechanisms of communication have been demonstrated or suggested for a wide range of monoaminergic and peptidergic systems, including serotonin, norepinephrine, acetylcholine, dopamine, oxytocin, vasopressin, gonadotropin-releasing hormone, dynorphin, neurokinin A, substance P, cholecystokinin, enkephalin, and beta-endorphin, corticotropin-releasing factor, and orexin (Alpár *et al.* 2019; Agnati *et al.* 2010). Morphological aspects of those systems are often used as indicatives of VT, such as the presence of fiber plexuses close to the ventricle, fiber varicosities that lack synaptic specializations, somatodendritic release, and fiber-receptor mismatches. Recently, Noble *et al.* (2018) added MCH to the list of neuropeptides that use VT, by demonstrating that: MCH-ir fibers contact the ventricular space; 2. Levels of MCH in the CSF fluctuate tethered to MCH neuronal activation; 3. Activation of CSF-contacting fibers modulates feeding behavior. We recently demonstrated that the intimate relationship between MCH fibers and the ventricular space is a common feature of muroids, suggesting some degree of phylogenetic conservation, and that not only the ventricular *lumen*, but the subleptomeningeal space, may be used as a vehicle for the transport of MCH (Diniz *et al.* 2019). Given that MCH and NEI are found in different subcellular compartments, this opens up the possibility that the two peptides may be differentially released to act on wiring and VT paradigms (Diniz *et al.* 2019).

It was unclear, up to this point, what are the targets of the CSF-released MCH described by Noble *et al.* (2018). The results obtained in our work indicate that multiple regions are equipped to respond to free MCH, and that functions beyond the modulation of feeding behavior may be impacted. The two most likely targets for ingestive behavior modulation by free MCH are the arcuate nucleus and the paraventricular nucleus of the hypothalamus. Both structures have been thoroughly implicated in feeding behavior (Stanley & Leibowitz 1985; Bouret *et al.* 2004), and injections of MCH in these areas have been shown to modulate ingestion (Abbott *et al.* 2003). These two areas have some of the highest densities of ciliary MCHR1 in the murine diencephalon, making them particularly apt to detect free MCH, in particular the paraventricular nucleus due to its intimate association with the third ventricle. Although not as close the lateral ventricles as the paraventricular nucleus, numerous varicose MCH- and NEI-ir fibers are observed adjacent to the nucleus accumbens, suggesting MCH may be released by those fibers in the ECS and then diffuse to bind to ciliary MCHR1 in the *nucleus accumbens*. Although the arcuate nucleus would also be a possible target for ingestive modulation, we did not detect MCHR1 in the neurochemical populations of this area that have been related to feeding behavior.

Morphofunctional correlated indicate that several functions previously associated with MCH may be modulated through VT, in addition to the aforementioned role in feeding behavior. The widespread distribution of ciliary MCHR1 in the cortical mantle, including the motor and cingulate cortices, allows MCH to play a role in motor function (Segal-Lieberman *et al.* 2003) and the animal emotional state (Borowsky *et al.* 2002). The high density of MCHR1 in the caudate-putamen also allows

MCH to act on reward circuits through the mesolimbic pathway (Domingos *et al.* 2013). Through the pyramidal layer of the hippocampus proper, MCH may act on learning, novelty, spatial and contextual memory retrieval, and anxiety (Sita *et al.* 2016; Monzon *et al.* 1999; Blanco-Centurion *et al.* 2019; Oh *et al.* 2019; Jimenez *et al.* 2018), with important ramifications for animal behavior. The presence of ciliary MCHR1 on dopaminergic neurons of the incerto-hypothalamic area may be the nexus for an MCH role on reproductive behavior and hormone secretion (Murray *et al.* 2000a), while through tuberoinfundibular dopaminergic neurons it may interface with prolactin secretion (Hökfelt & Fuxe 1972).

The arcuate nucleus is not the only pathway through which free MCH may modulate the adenohypophyseal release of hormones. Through the preoptic periventricular nucleus, free MCH from the CSF may act on kisspeptin neurons to modulate GnRH release (Wu *et al.* 2009), and in the PVH it may act to modulate the function of CRF neurons. While the former is likely related to a reproductive role (Murray *et al.* 2000b; Murray *et al.* 2000c; Murray *et al.* 2006), the modulation of CRF neurons may be related to control of stress responses and emotion (Lagos *et al.* 2011; Kennedy *et al.* 2003; Smith *et al.* 2006). A modulation of sexual function may also be achieved through estrogen receptor α neurons of the medial preoptic area and periventricular hypothalamus. The presence of MCHR1 in the medial preoptic area may also be important for the display of maternal behavior (Alachkar *et al.* 2016; Benedetto *et al.* 2014), if the lactation-generated MCH neurons of the medial preoptic area (Knollema *et al.* 1992; Rondini *et al.* 2010; Alvisi *et al.* 2016; Costa *et al.* 2019; Ferreira *et al.* 2017b) release MCH in a paracrine mode. Finally, another major function that may be played by MCH through VT is olfactory integration. One of the densest areas of ciliary MCHR1 is the olfactory bulb, where MCHR1 is found in several key layers, in addition to other ancillary areas important for olfactory processing, including the piriform cortex, anterior olfactory nucleus, olfactory tubercle, and *taenia tecta*. The presence of MCHR1 in two very important populations of the glomerular layer, dopamine and calbindin cells, in particular, indicates that those cells are the way through which MCH acts on olfactory integration, a role previously suggested for MCH (Adams *et al.* 2011; Alhassen *et al.* 2019).

In conclusion, we mapped for the first time the distribution of ciliary MCHR1 immunoreactivity in the brain of rats and mice. To do that, we evaluated a panel of commercial antibodies and identified one that has high specificity, good signal/background *ratio*, and that identifies an epitope that has been well conserved among mammals. All immunoreactivity detected with this antibody is ciliary, given the colocalization between MCHR1 and a specific neuronal primary *cilium* marker in all areas examined. Given the role of the neuronal primary *cilia* in sensing of the extracellular space, this colocalization suggests MCH can be found outside the synaptic space, and that free MCH may have an important role in VT modes of neuromodulatory signaling. Given the widespread distribution of ciliary MCHR1, it is fundamental that further studies are conducted to better understand how volume transmission affects the MCH system, what may open the possibility to new venues of pharmacological intervention targeting MCHR1 in the future.

References

Abbott, C. R., Kennedy, A. R., Wren, A. M. et al. (2003) Identification of hypothalamic nuclei involved in the orexigenic effect of melanin-concentrating hormone. *Endocrinology* **144,** 3943-3949.

Adamantidis, A., Thomas, E., Foidart, A. et al. (2005) Disrupting the melanin-concentrating hormone receptor 1 in mice leads to cognitive deficits and alterations of NMDA receptor function. *European journal of neuroscience* **21,** 2837-2844.

Adams, A. C., Domouzoglou, E. M., Chee, M. J., Segal-Lieberman, G., Pissios, P. and Maratos-Flier, E. (2011) Ablation of the hypothalamic neuropeptide melanin concentrating hormone is associated with behavioral abnormalities that reflect impaired olfactory integration. *Behavioural Brain Research* **224,** 195-200.

Agnati, L. F. and Fuxe, K. (2014) Extracellular-vesicle type of volume transmission and tunnelling-nanotube type of wiring transmission add a new dimension to brain neuro-glial networks. *Philosophical Transactions of the Royal Society B: Biological Sciences* **369,** 1-13.

Agnati, L. F., Fuxe, K., Zoli, M., Zini, I., Toffano, G. and Ferraguti, F. (1986) A correlation analysis of the regional distribution of central enkephalin and β-endorphin immunoreactive terminals and of opiate receptors in adult and old male rats. Evidence for the existence of two main types of communication in the central nervous system: the volume transmission and the wiring transmission. *Acta Physiologica Scandinavica* **128,** 201-207.

Agnati, L. F., Guidolin, D., Guescini, M., Genedani, S. and Fuxe, K. (2010) Understanding wiring and volume transmission. *Brain research reviews* **64,** 137-159.

Agnati, L. F., Zoli, M., Strömberg, I. and Fuxe, K. (1995) Intercellular communication in the brain: wiring versus volume transmission. *Neuroscience* **69,** 711-726.

Alachkar, A., Alhassen, L., Wang, Z., Wang, L., Onouye, K., Sanathara, N. and Civelli, O. (2016) Inactivation of the melanin concentrating hormone system impairs maternal behavior. *European Neuropsychopharmacology* **26,** 1826-1835.

Alhassen, L., Phan, A., Alhassen, W., Nguyen, P., Lo, A., Shaharuddin, H., Sanathara, N., Civelli, O. and Alachkar, A. (2019) The role of Olfaction in MCH-regulated spontaneous maternal responses. *Brain research* **1719,** 71-76.

Alpár, A., Benevento, M., Romanov, R. A., Hökfelt, T. and Harkany, T. (2019) Hypothalamic cell diversity: non-neuronal codes for long-distance volume transmission by neuropeptides. *Current opinion in neurobiology* **56,** 16-23.

Alvisi, R. D., Diniz, G. B., Da-Silva, J. M., Bittencourt, J. C. and Felicio, L. F. (2016) Suckling-induced Fos activation and melanin-concentrating hormone immunoreactivity during late lactation. *Life sciences* **148,** 241-246.

Attwell, D., Barbour, B. and Szatkowski, M. (1993) Nonvesicular release of neurotransmitter. *Neuron* **11,** 401-407.

Bächner, D., Kreienkamp, H.-J., Weise, C., Buck, F. and Richter, D. (1999) Identification of melanin concentrating hormone (MCH) as the natural ligand for the orphan somatostatin-like receptor 1 (SLC-1). *FEBS letters* **457,** 522-524.

Benedetto, L., Pereira, M., Ferreira, A. and Torterolo, P. (2014) Melanin-concentrating hormone in the medial preoptic area reduces active components of maternal behavior in rats. *Peptides* **58,** 20-25.

Berbari, N. F., Johnson, A. D., Lewis, J. S., Askwith, C. C. and Mykytyn, K. (2008) Identification of ciliary localization sequences within the third intracellular loop of G protein-coupled receptors. *Molecular Biology of the Cell* **19,** 1540-1547.

Berbari, N. F., O'Connor, A. K., Haycraft, C. J. and Yoder, B. K. (2009) The primary cilium as a complex signaling center. *Current Biology* **19,** R526-R535.

Bishop, G. A., Berbari, N. F., Lewis, J. and Mykytyn, K. (2007) Type III adenylyl cyclase localizes to primary cilia throughout the adult mouse brain. *Journal of Comparative Neurology* **505,** 562-571.

Bittencourt, J. C. and Celis, M. E. (2008) Anatomy, function and regulation of neuropeptide EI (NEI). *Peptides* **29,** 1441-1450.

Bittencourt, J. C. and Diniz, G. B. (2018) Neuroanatomical Structure of the MCH System. In: *Melanin-Concentrating Hormone and Sleep,* pp. 1-46. Springer.

Bittencourt, J. C., Presse, F., Arias, C., Peto, C. A., Vaughan, J. M., Nahon, J.-L., Vale, W. and Sawchenko, P. E. (1992) The melanin-concentrating hormone system of the rat brain: an immuno- and hybridization histochemical characterization. *The Jorunal of Comparative Neurology* **319,** 218-245.

Bjelke, B., England, R., Nicholson, C., Rice, M. E., Lindberg, J., Zoli, M., Agnati, L. F. and Fuxe, K. (1995) Long distance pathways of diffusion for dextran along fibre bundles in brain. Relevance for volume transmission. *Neuroreport* **6,** 1005-1009.

Blanco-Centurion, C., Luo, S., Spergel, D. J., Vidal-Ortiz, A., Oprisan, S. A., Van den Pol, A. N., Liu, M. and Shiromani, P. J. (2019) Dynamic Network Activation of Hypothalamic MCH Neurons in REM Sleep and Exploratory Behavior. *Journal of Neuroscience* **39,** 4986-4998.

Borowsky, B., Durkin, M. M., Ogozalek, K. et al. (2002) Antidepressant, anxiolytic and anorectic effects of a melanin-concentrating hormone-1 receptor antagonist. *Nature medicine* **8,** 825.

Bouret, S. G., Draper, S. J. and Simerly, R. B. (2004) Formation of projection pathways from the arcuate nucleus of the hypothalamus to hypothalamic regions implicated in the neural control of feeding behavior in mice. *Journal of Neuroscience* **24,** 2797-2805.

Brailov, I., Bancila, M., Brisorgueil, M.-J., Miquel, M.-C., Hamon, M. and Vergé, D. (2000) Localization of 5-HT6 receptors at the plasma membrane of neuronal cilia in the rat brain. *Brain research* **872,** 271-275.

Breunig, J. J., Sarkisian, M. R., Arellano, J. I. et al. (2008) Primary cilia regulate hippocampal neurogenesis by mediating sonic hedgehog signaling. *PNAS* **105,** 13127-13132.

Brown, S. N., Chitravanshi, V. C., Kawabe, K. and Sapru, H. N. (2007) Microinjections of melanin concentrating hormone into the nucleus tractus solitarius of the rat elicit depressor and bradycardic responses. *Neuroscience* **150,** 796-806.

Byers, S. L., Wiles, M. V., Dunn, S. L. and Taft, R. A. (2012) Mouse estrous cycle identification tool and images. *PloS one* **7,** e35538.

Chambers, J., Ames, R. S., Bergsma, D. et al. (1999) Melanin-concentrating hormone is the cognate ligand for the orphan G-protein-coupled receptor SLC-1. *Nature* **400,** 261-265.

Chee, M. J. S., Pissios, P. and Maratos-Flier, E. (2013) Neurochemical characterization of neurons expressing melanin-concentrating hormone receptor 1 in the mouse hypothalamus. *Journal of Comparative Neurology* **521,** 2208-2234.

Chiocchio, S. R., Gallardo, M. a. G. P., Louzan, P., Gutnisky, V. and Tramezzani, J. H. (2001) Melanin-concentrating hormone stimulates the release of luteinizing hormone-releasing hormone and gonadotropins in the female rat acting at both median eminence and pituitary levels. *Biology of Reproduction* **64,** 1466-1472.

Conductier, G., Brau, F., Viola, A. et al. (2013a) Melanin-concentrating hormone regulates beat frequency of ependymal cilia and ventricular volume. *Nature neuroscience* **16,** 845-847.

Conductier, G., Martin, A. O., Risold, P.-Y., Jego, S., Lavoie, R., Lafont, C., Mollard, P., Adamantidis, A. and Nahon, J.-L. (2013b) Control of ventricular ciliary beating by the melanin concentrating hormone-expressing neurons of the lateral hypothalamus: a functional imaging survey. *Frontiers in Endocrinology* **4,** 1-9.

Corbit, K. C., Aanstad, P., Singla, V., Norman, A. R., Stainier, D. Y. R. and Reiter, J. F. (2005) Vertebrate Smoothened functions at the primary cilium. *Nature* **437,** 1018.

Costa, H. C., Da-Silva, J. M., Diniz, G. B. et al. (2019) Characterization and origins of melanin-concentrating hormone immunoreactive fibers of the posterior lobe of the pituitary and median eminence during lactation in Long-Evans rat. *Journal of Neuroendocrinology* **00:e12723**.

Diniz, G. B., Battagello, D. S., Cherubini, P. M. et al. (2019) Melanin-concentrating hormone peptidergic system: comparative morphology between muroid species. *Journal of Comparative Neurology* **In press**

Diniz, G. B. and Bittencourt, J. C. (2017) The Melanin-Concentrating Hormone as an Integrative Peptide Driving Motivated Behaviors. *Frontiers in Systems Neuroscience* **11,** 1-32.

Domingos, A. I., Sordillo, A., Dietrich, M. O. et al. (2013) Hypothalamic melanin concentrating hormone neurons communicate the nutrient value of sugar. *eLife* **2,** e01462.

Engle, S. E., Antonellis, P. J., Whitehouse, L. S., Bansal, R., Emond, M. R., Jontes, J. D., Kesterson, R. A., Mykytyn, K. and Berbari, N. F. (2018) A CreER mouse to study melanin concentrating hormone signaling in the developing brain. *genesis* **56,** e23217.

Eriksson, P. S., Perfilieva, E., Björk-Eriksson, T., Alborn, A.-M., Nordborg, C., Peterson, D. A. and Gage, F. H. (1998) Neurogenesis in the adult human hippocampus. *Nature medicine* **4,** 1313.

Ferreira, J. G. P., Bittencourt, J. C. and Adamantidis, A. (2017a) Melanin-concentrating hormone and sleep. *Current Opinion in Neurobiology* **44,** 152-158.

Ferreira, J. G. P., Duarte, J. C. G., Diniz, G. B. and Bittencourt, J. C. (2017b) Litter size determines the number of melanin-concentrating hormone neurons in the medial preoptic area of Sprague Dawley lactating dams. *Physiology & Behavior* **181,** 75-79.

Fuxe, K., Dahlström, A., Höistad, M. et al. (2007) From the Golgi–Cajal mapping to the transmitter-based characterization of the neuronal networks leading to two modes of brain communication: wiring and volume transmission. *Brain Research Reviews* **55,** 17-54.

Gao, X.-B. (2018) The Role of Melanin-Concentrating Hormone in the Regulation of the Sleep/Wake Cycle: Sleep Promoter or Arousal Modulator? In: *Melanin-Concentrating Hormone and Sleep : Molecular, Functional and Clinical Aspects*, (S. R. Pandi-Perumal, P. Torterolo and J. M. Monti eds.), pp. 57-74. Springer International Publishing, Cham.

Golding, D. W. (1994) A pattern confirmed and refined–synaptic, nonsynaptic and parasynaptic exocytosis. *Bioessays* **16,** 503-508.

Gonzalez, M. I., Vaziri, S. and Wilson, C. A. (1996) Behavioral effects of alpha-MSH and MCH after central administration in the female rat. *Peptides* **17,** 171-177.

Händel, M., Schulz, S., Stanarius, A., Schreff, M., Erdtmann-Vourliotis, M., Schmidt, H., Wolf, G. L. and Höllt, V. (1999) Selective targeting of somatostatin receptor 3 to neuronal cilia. *Neuroscience* **89,** 909-926.

Hervieu, G., Cluderay, J., Harrison, D., Meakin, J., Maycox, P., Nasir, S. and Leslie, R. A. (2000) The distribution of the mRNA and protein products of the melanin-concentrating hormone (MCH) receptor gene, slc-1, in the central nervous system of the rat. *European Journal of Neuroscience* **12,** 1194-1216.

Hoffman, G. E., Murphy, K. J. and Sita, L. V. (2016) The importance of titrating antibodies for immunocytochemical methods. *Current Protocols in Neuroscience* **76,** 2.12.11-12.12.37.

Hökfelt, T. and Fuxe, K. (1972) Effects of prolactin and ergot alkaloids on the tubero-infundibular dopamine (DA) neurons. *Neuroendocrinology* **9,** 100-122.

Jiang, H. and Brüning, J. C. (2018) Melanin-Concentrating Hormone-Dependent Control of Feeding: When Volume Matters. *Cell Metabolism* **28,** 7-8.

Jimenez, J. C., Su, K., Goldberg, A. R. et al. (2018) Anxiety cells in a hippocampal-hypothalamic circuit. *Neuron* **97,** 670-683. e676.

Kennedy, A. R., Todd, J. F., Dhillo, W. S. et al. (2003) Effect of direct injection of melanin-concentrating hormone into the paraventricular nucleus: further evidence for a stimulatory role in the adrenal axis via SLC-1. *Journal of Neuroendocrinology* **15,** 268-272.

Knollema, S., Brown, E. R., Vale, W. and Sawchenko, P. E. (1992) Novel hypothalamic and preoptic sites of prepro-melanin-concentrating hormone messenger ribonucleic Acid and Peptide expression in lactating rats. *Journal of Neuroendocrinology* **4,** 709-717.

Koemeter-Cox, A. I., Sherwood, T. W., Green, J. A. et al. (2014) Primary cilia enhance kisspeptin receptor signaling on gonadotropin-releasing hormone neurons. *PNAS***,** 201403286.

Kummer, K. K., Hofhansel, L., Barwitz, C. M., Schardl, A., Prast, J. M., Salti, A., El Rawas, R. and Zernig, G. (2014) Differences in social interaction-vs. cocaine reward in mouse vs. rat. *Frontiers in behavioral neuroscience* **8,** 363.

Lagos, P., Urbanavicius, J., Scorza, M. C., Miraballes, R. and Torterolo, P. (2011) Depressive-like profile induced by MCH microinjections into the dorsal raphe nucleus evaluated in the forced swim test. *Behavioural brain research* **218,** 259-266.

Loktev, A. V. and Jackson, P. K. (2013) Neuropeptide Y family receptors traffic via the Bardet-Biedl syndrome pathway to signal in neuronal primary cilia. *Cell Reports* **5,** 1316-1329.

Mandl, L. and Megele, R. (1989) Primary cilia in normal human neocortical neurons. *Zeitschrift fur mikroskopisch-anatomische Forschung* **103,** 425-430.

Marshall, W. F. and Nonaka, S. (2006) Cilia: tuning in to the cell's antenna. *Current Biology* **16,** R604-R614.

Messina, M. M. and Overton, J. M. (2007) Cardiovascular effects of melanin-concentrating hormone. *Regulatory Peptides* **139,** 23-30.

Monzon, M. E., de Souza, M. M., Izquierdo, L. A., Izquierdo, I., Barros, D. M. and de Barioglio, S. R. (1999) Melanin-concentrating hormone (MCH) modifies memory retention in rats. *Peptides* **20,** 1517-1519.

Murray, J., Mercer, J., Adan, R., Datta, J., Aldairy, C., Moar, K., Baker, B., Stock, M. and Wilson, C. (2000a) The effect of leptin on luteinizing hormone release is exerted in the zona incerta and mediated by melanin-concentrating hormone. *Journal of neuroendocrinology* **12,** 1133-1139.

Murray, J. F., Adan, R. A. H., Walker, R., Baker, B. I., Thody, A. J., Nijenhuis, W. A., Yukitake, J. and Wilson, C. A. (2000b) Melanin-concentrating hormone, melanocortin receptors and regulation of luteinizing hormone release. *Journal of Neuroendocrinology* **12,** 217-223.

Murray, J. F., Baker, B. I., Levy, A. and Wilson, C. A. (2000c) The influence of gonadal steroids on pre-pro melanin-concentrating hormone mRNA in female rats. *Journal of Neuroendocrinology* **12,** 53-59.

Murray, J. F., Hahn, J. D., Kennedy, A. R., Small, C. J., Bloom, S. R., Haskell-Luevano, C., Coen, C. W. and Wilson, C. A. (2006) Evidence for a Stimulatory Action of Melanin-Concentrating Hormone on Luteinising Hormone Release Involving MCH1 and Melanocortin-5 Receptors. *Journal of Neuroendocrinology* **18,** 157-167.

Naufahu, J., Cunliffe, A. D. and Murray, J. F. (2013) The roles of melanin-concentrating hormone in energy balance and reproductive function: are they connected? *Reproduction* **146,** R141-R150.

Niño-Rivero, S., Torterolo, P. and Lagos, P. (2019) Melanin-concentrating hormone receptor-1 is located in primary cilia of the dorsal raphe neurons. *Journal of chemical neuroanatomy* **98,** 55-62.

Noble, E. E., Hahn, J. D., Konanur, V. R. et al. (2018) Control of Feeding Behavior by Cerebral Ventricular Volume Transmission of Melanin-Concentrating Hormone. *Cell metabolism* **28,** 55-68.e57.

Oh, S. T., Liu, Q. F., Jeong, H. J. et al. (2019) Nasal Cavity Administration of Melanin-Concentrating Hormone Improves Memory Impairment in Memory-Impaired and Alzheimer's Disease Mouse Models. *Molecular Neurobiology*.

Paxinos, G. and Franklin, K. (2012) *The Mouse Brain in Stereotaxic Coordinates*. Academic Press.

Paxinos, G. and Watson, C. (2006) *The rat brain in stereotaxic coordinates: hard cover edition*. Elsevier.

Pazour, G. J. and Witman, G. B. (2003) The vertebrate primary cilium is a sensory organelle. *Current Opinion in Cell Biology* **15,** 105-110.

Pow, D. and Morris, J. (1989) Dendrites of hypothalamic magnocellular neurons release neurohypophysial peptides by exocytosis. *Neuroscience* **32,** 435-439.

Presse, F., Conductier, G., Rovere, C. and Nahon, J. (2014) The melanin-concentrating hormone receptors: neuronal and non-neuronal functions. *International journal of obesity supplements* **4,** S31.

Rennels, M. L., Gregory, T. F., Blaumanis, O. R., Fujimoto, K. and Grady, P. A. (1985) Evidence for a 'paravascular' fluid circulation in the mammalian central nervous system, provided by the rapid distribution of tracer protein throughout the brain from the subarachnoid space. *Brain Res* **326,** 47-63.

Rohatgi, R., Milenkovic, L. and Scott, M. P. (2007) Patched1 regulates hedgehog signaling at the primary cilium. *Science* **317,** 372-376.

Rondini, T. A., Donato, J., Rodrigues, B. C., Bittencourt, J. C. and Elias, C. F. (2010) Chemical identity and connections of medial preoptic area neurons expressing melanin-concentrating hormone during lactation. *Journal of chemical neuroanatomy* **39,** 51-62.

Saito, Y., Cheng, M., Leslie, F. M. and Civelli, O. (2001) Expression of the melanin-concentrating hormone (MCH) receptor mRNA in the rat brain. *Journal of Comparative Neurology* **435,** 26-40.

Saito, Y., Nothacker, H.-P., Wang, Z., Lin, S. H. S., Leslie, F. and Civelli, O. (1999) Molecular characterization of the melanin-concentrating-hormone receptor. *Nature* **400,** 265-269.

Saper, C. B. and Sawchenko, P. E. (2003) Magic peptides, magic antibodies: guidelines for appropriate controls for immunohistochemistry. *Journal of Comparative Neurology* **465,** 161-163.

Segal-Lieberman, G., Bradley, R. L., Kokkotou, E. et al. (2003) Melanin-concentrating hormone is a critical mediator of the leptin-deficient phenotype. *Proceedings of the National Academy of Sciences* **100,** 10085-10090.

Shimomura, Y., Mori, M., Sugo, T. et al. (1999) Isolation and identification of melanin-concentrating hormone as the endogenous ligand of the SLC-1 receptor. *Biochemical and Biophysical Research Communications* **261,** 622-626.

Siljee, J. E., Wang, Y., Bernard, A. A., Ersoy, B. A., Zhang, S., Marley, A., Von Zastrow, M., Reiter, J. F. and Vaisse, C. (2018) Subcellular localization of MC4R with ADCY3 at neuronal primary cilia underlies a common pathway for genetic predisposition to obesity. *Nature Genetics* **50,** 180-185.

Sita, L. V., Diniz, G. B., Canteras, N. S., Xavier, G. F. and Bittencourt, J. C. (2016) Effect of intrahippocampal administration of anti-melanin-concentrating hormone on spatial food-seeking behavior in rats. *Peptides* **76,** 130-138.

Smith, D. G., Davis, R. J., Rorick-Kehn, L., Morin, M., Witkin, J. M., McKinzie, D. L., Nomikos, G. G. and Gehlert, D. R. (2006) Melanin-concentrating hormone-1 receptor modulates neuroendocrine, behavioral, and corticolimbic neurochemical stress responses in mice. *Neuropsychopharmacology* **31,** 1135-1145.

Snyder, J. S., Choe, J. S., Clifford, M. A., Jeurling, S. I., Hurley, P., Brown, A., Kamhi, J. F. and Cameron, H. A. (2009) Adult-born hippocampal neurons are more numerous, faster maturing, and more involved in behavior in rats than in mice. *Journal of Neuroscience* **29,** 14484-14495.

Stanley, B. G. and Leibowitz, S. F. (1985) Neuropeptide Y injected in the paraventricular hypothalamus: a powerful stimulant of feeding behavior. *Proceedings of the National Academy of Sciences* **82,** 3940-3943.

Tan, C. P., Sano, H., Iwaasa, H. et al. (2002) Melanin-concentrating hormone receptor subtypes 1 and 2: species-specific gene expression. *Genomics* **79,** 785-792.

Wu, M., Dumalska, I., Morozova, E., van den Pol, A. N. and Alreja, M. (2009) Melanin-concentrating hormone directly inhibits GnRH neurons and blocks kisspeptin activation, linking energy balance to reproduction. *Proceedings of the National Academy of Sciences* **106,** 17217-17222.

Tables

Table 1. Primary antibodies employed in this work

Antiboby	Manufacturer	Man. ID	RRID	Antiboby	Manufacturer	Man. ID	RRID
Rabbit anti melanin-concentrating hormone receptor 1 (anti-hMCHR1)	ThermoFisher Scientific	PA5-24182	AB_2541682	Rabbit gonadotropin-releasing hormone (anti-GnRH)	ImmunoStar	20075	AB_572248
Rabbit anti melanin-concentrating hormone receptor 1 (anti-hMCHR1)	Abcam	Ab97509	AB_10680290	Rabbit anti kisspeptin (anti-KiSS)	Millipore (Chemicon)	AB9754	AB_2296529
Rabbit anti melanin-concentrating hormone receptor 1 (anti-hMCHR1)	SantaCruz Biotechnology	sc-25667	AB_2143948	Rabbit anti estrogen receptor α (anti-ERα)	Millipore (Upstate)	06-935	AB_310305
Rabbit anti melanin-concentrating hormone receptor 1 (anti-hMCHR1)	SantaCruz Biotechnology	Sc-5534	AB_2143957	Rabbit anti vasopressin (anti-AVP)	ImmunoStar (DiaSorin)	20069	AB_572219
Rabbit anti melanin-concentrating hormone receptor 1 (anti-hMCHR1)	Sigma-Aldrich/Atlas	HPA004149	AB_1079363	Guinea-pig anti oxytocin (anti-OT)	Peninsula	T-5021.0050	AB_518526
Rabbit anti melanin-concentrating hormone receptor 1 (anti-rMCHR1)	Alomone Labs	AMR-041	AB_11218957	Rabbit anti corticotropin-releasing factor (anti-CRF)	Peptide Biology Laboratory, The Salk Institute	rC70	AB_2650437
Rabbit anti adenylate cyclase III (anti-AC3)	ThermoFisher Scientific	PA5-35382	AB_2552692	Sheep anti α -melanocyte-stimulating hormone (anti-α MSH)	Millipore (Chemicon)	AB5087	AB_91683
Rabbit anti melanin-concentrating hormone (anti-MCH)	Peptide Biology Laboratory, The Salk Institute	PBL #234	AB_2650444	Rabbit anti cocaine- and amphetamine-regulated transcript (anti-CART)	Peptide Biology Laboratory, The Salk Institute	6838	AB_2650446
Mouse anti tyrosine hydroxylase (anti-TH)	ImmunoStar	#22941	AB_572268	Mouse anti neuron-specific nuclear protein (anti-NeuN)	Millipore (Chemicon)	MAB377	AB_2298772
Mouse anti calbindin D-28k	Swant	300	AB_10000347	Mouse anti glial fibrillary acidic protein (anti-GFAP)	Sigma-Aldrich	G3893	AB_477010
Goat anti (rat, mouse, human) calretinin	Swant	CG1	AB_10000342	Mouse anti doublecortin (anti-DCX)	Santa Cruz	Sc-8066	AB_2088494

Table 2. Relative density of MCHR1-ir *cilia* in the mouse CNS

Cell group	MCHR1-ir *cilia*
A. Olfactory areas	
1. Main olfactory bulb	
Glomerular layer	++
Juxtaglomerular layer	-
External plexiform layer	-
Mitral layer	+
Internal plexiform layer	-/+
Granule cells layer	
External part	+++
Internal part	++++
2. Accessory olfactory bulb	
Accessory granule cells layer	++++
Accessory mitral layer	-
Accessory external plexiform layer	-
3. Anterior olfactory nucleus	
Medial part	+
Dorsal part	++
Lateral part	++
Ventral part	++
External part	+
4. Olfactory Cortex	
Ventral *tenia tecta*	
Layer 1	-
Layer 2	++
Layer 3	-/+
Dorsal *tenia tecta*	
Layer 1	-
Layer 2	+
Layer 3	-
Piriform cortex	
Layer 1	-
Layer 2	+++
Layer 3	-
Endopiriform nucleus	
Dorsal part	-/+
Internal part	-/+
Olfactory tubercle	
Layer 1	-
Layer 2	++
Layer 3	-/+
B. Septofimbrial area	
1. Septal nucleus	
Lateral septal nucleus	
Ventral part	++
Dorsal part	-/+
Intermediate part	+
Medial septal nucleus	
Medial column	-
Lateral column	-/+
Lambdoid Septal Zone	-/+
2. Diagonal band of Broca	
Vertical limb	-
Horizontal limb	-
3. Transitional nuclei	
Septohippocampal nucleus	+
Septofimbrial nucleus	++
Septohypothalamic nucleus	-
4. Bed nucleus of the *stria terminalis*	
Rostromedial region	+
Rostrolateral region	+
Posteromedial region	+
Posterolateral region	-/+
5. *Indusium griseum*	++++
6. Islands of Calleja	-/+
7. Triangular septal nucleus	+
8. Bed nucleus of the anterior commissure	+
C. Basal nuclei and associated structures	
1. Caudate-putamen nucleus	
Matrix	
Medial part	++++
Lateral part	+++
Striosomes	-
2. *Nucleus accumbens*	
Core part	++++
Shell part	++++
Lateral *accumbens (fundus* of *striatum)*	+++
3. Ventral *pallidum*	++
4. *Globus pallidus*	-
5. Subthalamic nucleus	-

Table 2. Relative density of MCHR1-ir *cilia* in the mouse CNS, continued

Cell group	MCHR1-ir *cilia*
D. Cortical mantle	
Layer I	-
Layer II	++
Layer III	-/+
Layer IV	-
Layer V	+
Layer VI	+
Claustrum	
Anterior	-/+
Posterior	+
E. Hippocampal formation	
1. *Fasciola Cinerea*	++++
2. Hippocampus proper	
CA1	
Stratum oriens	-
Stratum pyramidale	++++
Stratum radiatum	-
Stratum lacunosum-moleculare	-
CA2	
Stratum oriens	-
Stratum pyramidale	++
CA3	
Stratum oriens	-
Stratum pyramidale	+
Stratum radiatum	-
Stratum lacunosum-moleculare	-
3. Dentate gyrus	
Polymorphic layer	-
Granule cells layer	-
Subgranular zone	-
Molecular layer	-
4. Subiculum	
Dorsal part	++
Ventral part	+++
F. Amygdaloid complex	
1. Cortex-amygdala transition zone	
Layer 1	-
Layer 2	++
Layer 3	-/+
2. Nucleus of the lateral olivary tract	-
3. Anterior division	
Anterior cortical amygdaloid nucleus	+
Anterior amygdaloid nucleus	+
Extension of the amygdala	++
4. Intercalated nucleus of the amygdala	++
5. Basolateral division	
Anterior basolateral nucleus	+
Ventral basolateral nucleus	+
6. Central nucleus	
Central part	++
Medial part	++
Lateral part	++
7. Medial division	
Anterodorsal medial nucleus	-/+
Anteroventral medial nucleus	-/+
Posterodorsal medial nucleus	+
Posteroventral medial nucleus	+
8. Basomedial division	
Posterior basomedial nucleus	+
Anterior basomedial nucleus	++
G. Hypothalamus	
1. Periventricular zone	
Anteroventral periventricular nucleus	+
Median preoptic nucleus	+
Preoptic periventricular nucleus	
Dorsal part	+
Ventral part	++
Suprachiasmatic nucleus	-
Paraventricular hypothalamic nucleus	
Anterior parvicellular part	+
Medial parvicellular part	+
Medial magnocellular part	+++
Ventral part	+++
Lateral magnocellular part	+++
Subparaventricular area	-/+
Posterior part	+
Arcuate nucleus	
Anterior	+
Intermediate	+++

Table 2. Relative density of MCHR1-ir *cilia* in the mouse CNS, continued

Cell group	MCHR1-ir *cilia*
2. Medial zone	
Ventromedial preoptic nucleus	+
Medial preoptic area	-
Medial preoptic nucleus	
Medial part	+
Lateral part	-/+
Anterior hypothalamic nucleus	
Anterior part	+
Central part	+
Posterior part	+
Retrochiasmatic area	-
Incerto-hypothalamic area	++
Subincertal nucleus	+
Ventromedial hypothalamic nucleus	-
Dorsomedial hypothalamic nucleus	+
Posterior hypothalamic area	+
Dorsal tuberomammilary nucleus	+
Premammillary nucleus	
Dorsal part	++
Ventral part	++
Retromammillary nucleus	+
Median mammillary nucleus	-
Medial mammillary nucleus	
Medial part	-
Lateral part	-/+
Lateral mammillary nucleus	-/+
3. Lateral zone	
Lateral preoptic area	-/+
Ventrolateral preoptic nucleus	-
Lateral hypothalamic area	
Anterior level	-
Tuberal level	-/+

Cell group	MCHR1-ir *cilia*
Anterodorsal thalamic nucleus	-
Interoanteromedial thalamic nucleus	-/+
Interoanterodorsal thalamic nucleus	-
4. Mediodorsal nucleus	
MD	-/+
MDM	-
5. Laterodorsal nucleus	
Dorsomedial part	-
Ventrolateral part	-
6. Midline group	
Paraventricular thalamic nucleus	+
Paratenial thalamic nucleus	-
Nucleus *reuniens*	+
Xifoid nucleus	+
Rhomboid nucleus	-/+
Intermediodorsal thalamic nucleus	+
7. Intralaminar nuclei	
Paracentral thalamic nucleus	-/+
Centromedial thalamic nucleus	+
Centrolateral thalamic nucleus	-
Parafascicular thalamic nucleus	-
8. Ventral group	
Ventrolateral thalamic nucleus	-
Ventromedial thalamic nucleus	-/+
Ventral posterolateral thalamic nucleus	-
Ventral posteromedial thalamic nucleus	-
9. Posterior complex	-
10. Medial geniculate	+
11. Lateral geniculate	+
12. Reticular nucleus	
Subparafascicular thalamic nucleus	++
Parasubthalamic nucleus	+

H. Thalamus	
1. Medial habenula	
Dorsal part	+++
Ventral part	-/+
2. Lateral habenula	-/+
3. Anterior group	
Anteromedial thalamic nucleus	-/+
Anteroventral thalamic nucleus	-

I. Circumventricular organs	
1. Vascular organ of the lamina terminalis	-
2. Subfornical organ	-
3. Median eminence	
Internal	-/+
External	-
4. Area postrema	-

Figure Legends

Figure 1 – Specificity controls for the MCHR1 antibody employed in this work. Widefield fluorescence photomicrographs of frontal brain slices obtained from male mice with different genotypes submitted to immunohistochemistry with or without antibodies and counterstained with DAPI (blue). A) Reaction in the presence of primary and secondary antibodies results in ample labeling of the *nucleus accumbens*; A') Omitting the primary antibody results in no labeling of *cilia* in the *nucleus accumbens*. Note that red fluorescence on the anterior commissure and matrix of the caudate-putamen are caused by overexposure of the red channel, and do not represent specific labeling; A'') As is the case with the primary antibody, omitting the secondary biotinylated antibody also resulted in abolished labeling; B) The use of antibody PA5-24182 results in ample labeling of *cilia* in WT C57BL/6 mice; B') In heterozygous mice, a clear reduction in the number of labeled *cilia* is observed; B'') In homozygous Mchr1$^{-/-}$ mice, no labeling can be observed. Abbreviations: ac – anterior commissure; lCj – islands of Calleja; LV – lateral ventricle. Scale bar: 100µm.

Figure 2 – The subcellular localization of MCHR1. Widefield fluorescence photomicrographs of frontal male mouse brain slices submitted to immunohistochemistry for adenylate cyclase III (green) and MCHR1 (red) and counterstained with DAPI (blue). A) In the pyramidal layer of the hippocampus, there is a large degree of colocalization between MCHR1 and AC3, as revealed by the merged yellow-orange labeling; A') Higher magnification of A. Immunoreactivity to MCHR1 is found in restricted areas of the AC3-positive *cilia*, varying in terms of coverage of the ciliary surface; B) Other areas, such as the granular layer of the dentate gyrus, are rich in AC3-ir *cilia*, but lack any MCHR1. Abbreviations: cc – *corpus callosum*; Ctx – cortex; GrDG – granular layer of the dentate gyrus; LMol – *stratum lacunosum moleculare* of the hippocampus; MoDG – molecular layer of the dentate gyrus; Or – *stratum oriens* of the hippocampus; Rad – *stratum radiatum* of the hippocampus. Scale bar: A, B = 100 µm; A' = 50µm.

Figure 3 – Scale of MCHR1 immunoreactivity density. Widefield fluorescence photomicrographs of frontal mice brain slices submitted to immunohistochemistry for MCHR1 (red) and counterstained with DAPI (blue). The areas used to elaborate this scale are: accessory olfactory bulb (0 | -), central medial thalamic nucleus (1 | -/+), arcuate nucleus (2 | +), basolateral nucleus of the amygdala (3 | ++), cortical layers 2 and 3 (4 | ++), paraventricular nucleus (5 | +++), caudate-putamen (6 | +++), pyramidal layer of the hippocampus proper (7 | ++++), and shell of the *nucleus accumbens* (8 | ++++). Scale bar: 100µm.

Figure 4 – MCHR1 immunoreactivity in discrete prosencephalic areas. Widefield fluorescence photomicrographs of frontal mice brain slices submitted to immunohistochemistry for MCHR1 (red) and counterstained with DAPI (blue). A) The olfactory bulb contains one of the highest densities of ciliary MCHR1 in the mouse prosencephalon; B) Moderate to high densities of ciliary MCHR1 are found in layers 2, 3 and 5 of several cortical areas. A high density of labeling is observed in the caudate-putamen nucleus at this same level; C) A moderate density of *cilia* is observed in the preoptic periventricular nucleus of the hypothalamus. Some labeled *cilia* are also observed in the medial preoptic area; D) the paraventricular hypothalamic nucleus harbors one of the highest numbers of MCHR1-labeled *cilia* in the hypothalamus; E) Although only a few neurons contain neurons with MCHR1-harboring *cilia* in the incerto-hypothalamic area, this area can be clearly identified due to the lack of labeled *cilia* around it; F) The arcuate nucleus also contains a large number of immunolabeled *cilia* when compared to other hypothalamic nuclei, in particular in its ventromedial portion. Abbreviations: 3V – third ventricle; AHA – anterior hypothalamic area;

Arc – arcuate nucleus; cc – *corpus callosum*; CPu – caudate-putamen; EPL – external plexiform layer of the olfactory bulb; GrA – granular layer of the accessory olfactory bulb; GrO – granular layer of the olfactory bulb; IPL – internal plexiform layer of the olfactory bulb; IHy – incerto-hypothalamic area; LV – lateral ventricle; MPOA – medial preoptic area; Pe – periventricular preoptic nucleus; PVH – paraventricular hypothalamic nucleus; VMH – ventromedial hypothalamic nucleus; ZI – *zona incerta*. Scale bar: 100µm.

Figure 5 – Segregation of MCH and MCHR1 fields. Widefield fluorescence photomicrographs of a frontal male mouse brain slice submitted to immunohistochemistry for MCH (green) and MCHR1 (red), and counterstained with DAPI (blue). A) The septal area shows a clear segregation between MCH-ir fibers and MCHR1-ir *cilia*. A high number of fibers occupy the medial septal nucleus and only sparely innervate the shell of the *nucleus accumbens*, while MCHR1-ir *cilia* are found in the *nucleus accumbens* but not in the medial septal nucleus; A') Higher magnification of the delineated area in A. A clear MCH/MCHR1 boundary can be seen. Abbreviations: Acb – *nucleus accumbens*; CPu caudate-putamen; ICj – islands of Calleja; LSv – lateral septal nucleus, ventral part; LV – lateral ventral; MS – medial septal nucleus. Scale bar: A = 100µm; A' = 50µm.

Figure 6 – Differences between rats and mice concerning the distribution of MCHR1-ir *cilia*. Widefield fluorescence photomicrographs of frontal mice brain slices submitted to immunohistochemistry for MCHR1 (red). A, B) While the rat caudate-putamen displays a very high background and a very low number of immunoreactive *cilia*, the mouse caudate-putamen has a high number of immunoreactive *cilia*. C, D) The opposite is observed in the subgranular zone of the dentate gyrus. Although not abundant, rats display a strip of immunoreactive *cilia* in the subgranular zone, between the granular and polymorphic layers of the dentate gyrus. On the other hand, similar *cilia* are not observed in the mouse subgranular zone; C', D') Higher magnification of the delineated areas in C and D. Abbreviations: CPu – caudate-putamen; GP – *globus pallidus*; GrDG – granular layer of the dentate gyrus; MoDG – molecular layer of the dentate gyrus; PoDG – polymorphic layer of the dentate gyrus; SGZ – subgranular zone. Scale bar: A-D = 200µm; C', D' = 100µm.

Figure 7 – Neurochemistry identity of ciliary MCHR1-containing neurons in the glomerular layer of olfactory bulb. Confocal fluorescence photomicrographs of frontal mice brain slices submitted to immunohistochemistry for MCHR1 (red) and various neurochemical markers (green). A, A') Ample colocalization between MCHR1 and tyrosine hydroxylase in the glomerular layer of the olfactory bulb; B, B') Some colocalization is observed between calbindin and MCHR1, although in fewer numbers than MCHR1 and dopaminergic cells. Scale bar: A, B = 40µm; A', B' = 20µm.

Figure 8 – Neurochemistry identity of ciliary MCHR1-containing neurons in the hypothalamus. Widefield fluorescence photomicrographs of frontal mice brain slices submitted to immunohistochemistry for MCHR1 (red) and various neurochemical markers (green) counterstained with DAPI (blue). A, A') In the periventricular nucleus, some kisspeptin-ir cells have MCHR1-ir *cilia*; B, B') MCHR1-ir *cilia* are also seen in proximity to nuclei immunoreactive to estrogen receptor alpha in the periventricular nucleus; C – D') In the paraventricular nucleus, MCHR1-ir *cilia* are found in oxytocin-ir and corticotropin-releasing factor-ir neurons; E, E') In the supraoptic nucleus, the largest colocalization is between MCHR1-ir *cilia* and vasopressinergic cells; F, F') In the incerto-hypothalamic area, virtually every dopaminergic cell has a MCHR1-ir *cilium*. Abbreviations: 3V – third ventricle; AHA – anterior hypothalamic area; IHy – incerto-hypothalamic area; LPO – lateral preoptic area; MeA – medial nucleus of the amygdala; MnPO – median

preoptic nucleus; MPOA – medial preoptic nucleus; ot – optic tract; Pe – periventricular preoptic nucleus; PVH – paraventricular hypothalamic nucleus; Re – *nucleus reuniens*; SO -supraoptic nucleus. Scale bar: A-C, F = 100µm; D, E = 40µm; A'-F' = 20µm.

Supplementary Material 01 – Colocalization between MCHR1-ir *cilia* and NeuN in the cortex. Widefield fluorescence photomicrographs of frontal mice brain slices submitted to immunohistochemistry for MCHR1 (red) and NeuN or DCX (green) counterstained with DAPI (blue). A, A') *Cilia* immunoreactive to MCHR1 largely colocalizes with NeuN, reinforcing that primary *cilia*-containing cells are neurons. B, B') There is no colocalization between MCHR1 and new neurons originated at the subgranular zone of the dentate gyrus. Abbreviations: 1 – cortical layer 1; 4 – cortical layer 4; 6 – cortical layer 6; cc – *corpus callosum*; GrDG – granular layer of the dentate gyrus; MoDG – molecular layer of the dentate gyrus; PoDG – polymorphic layer of the dentate gyrus. Scale bar: A = 100µm; B = 40µm; A', B' = 20µm.

FIGURE 1.tiff

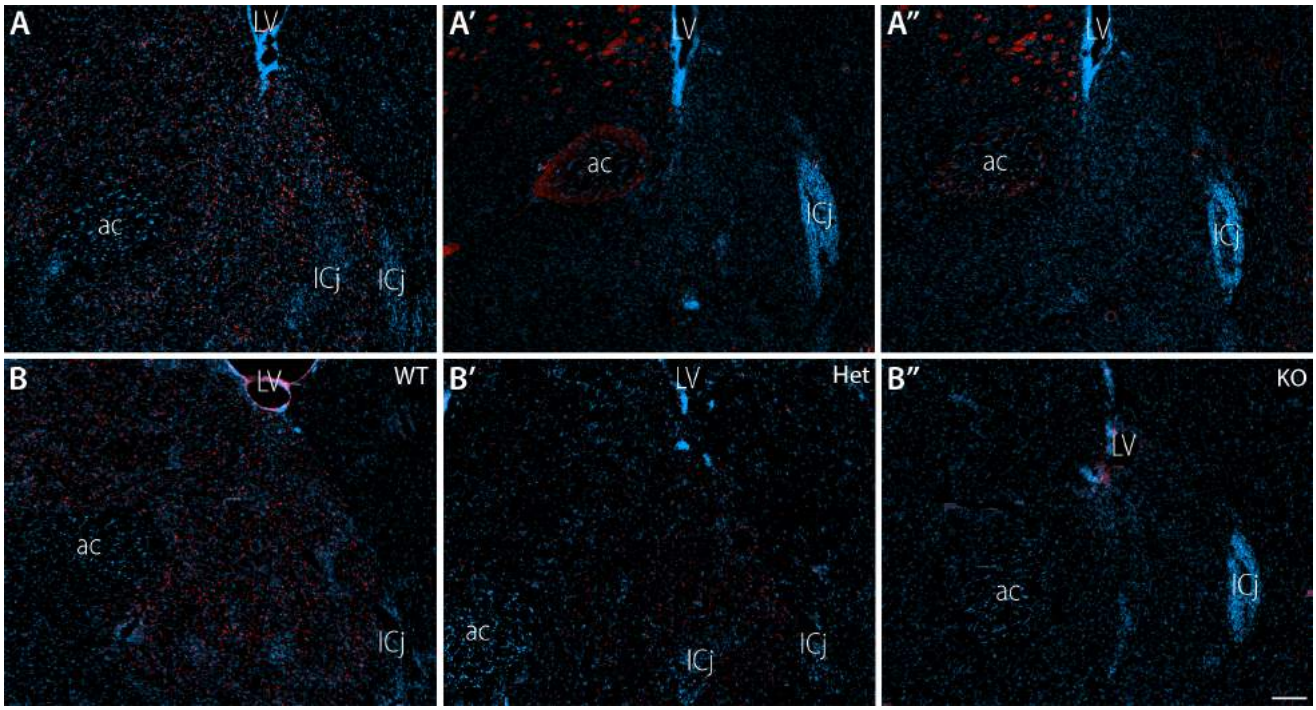

FIGURE 02.tiff

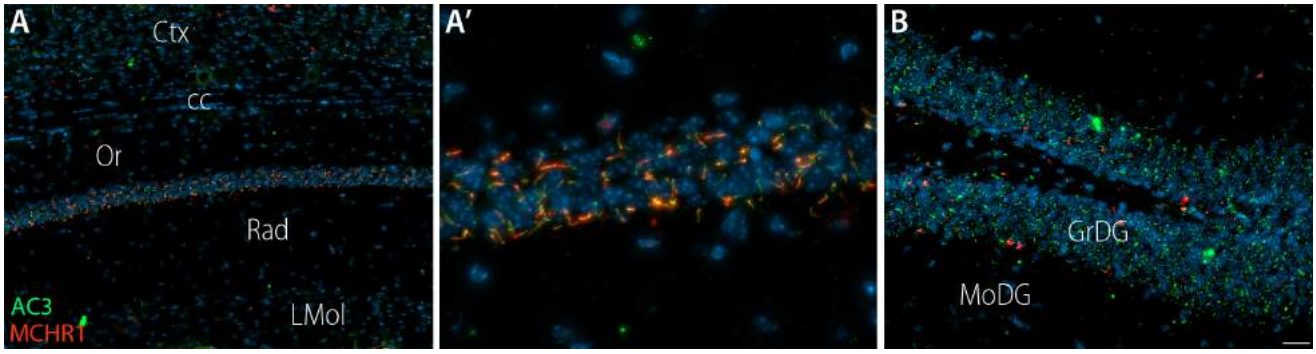

FIGURE 03.tiff

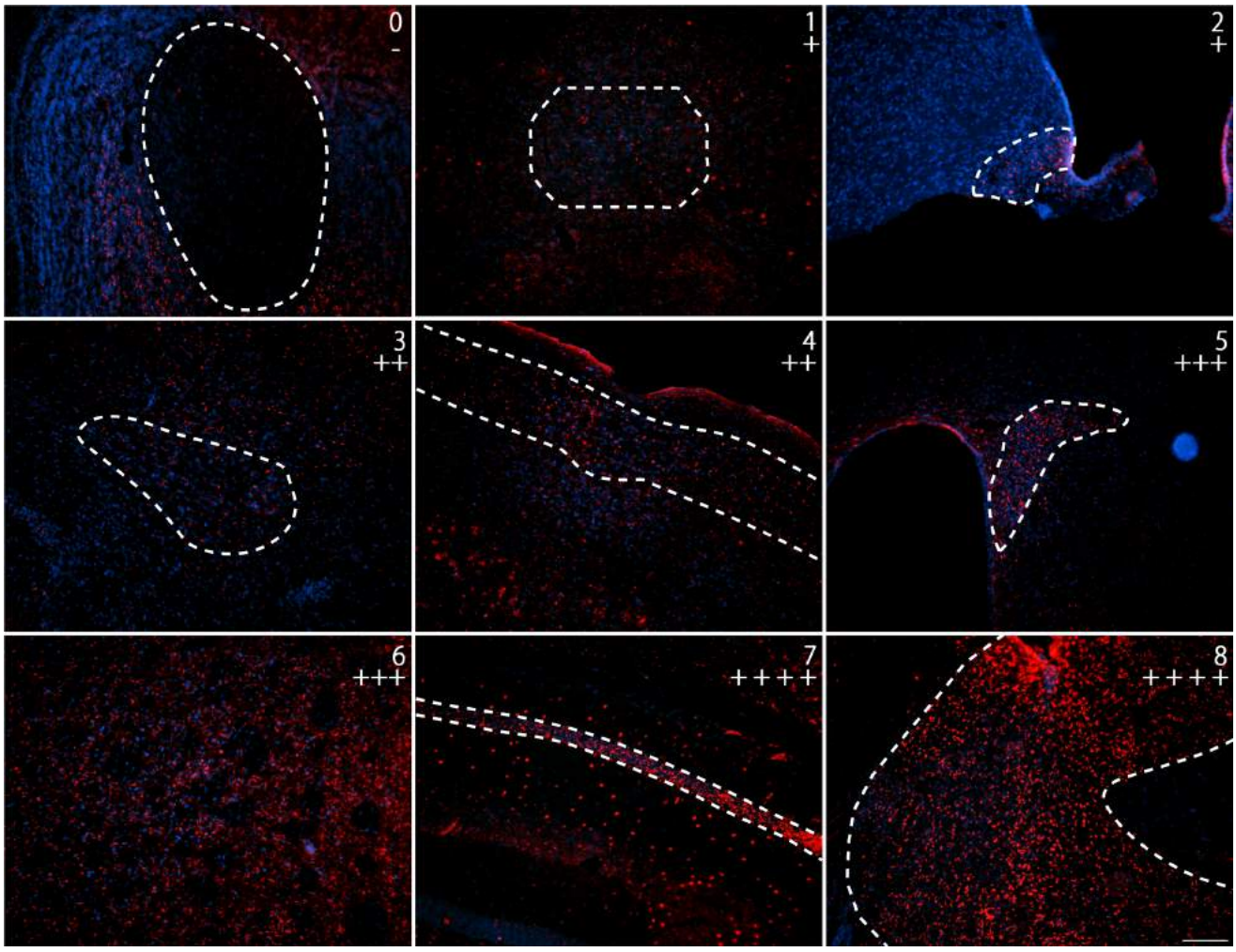

FIGURE 04.tiff

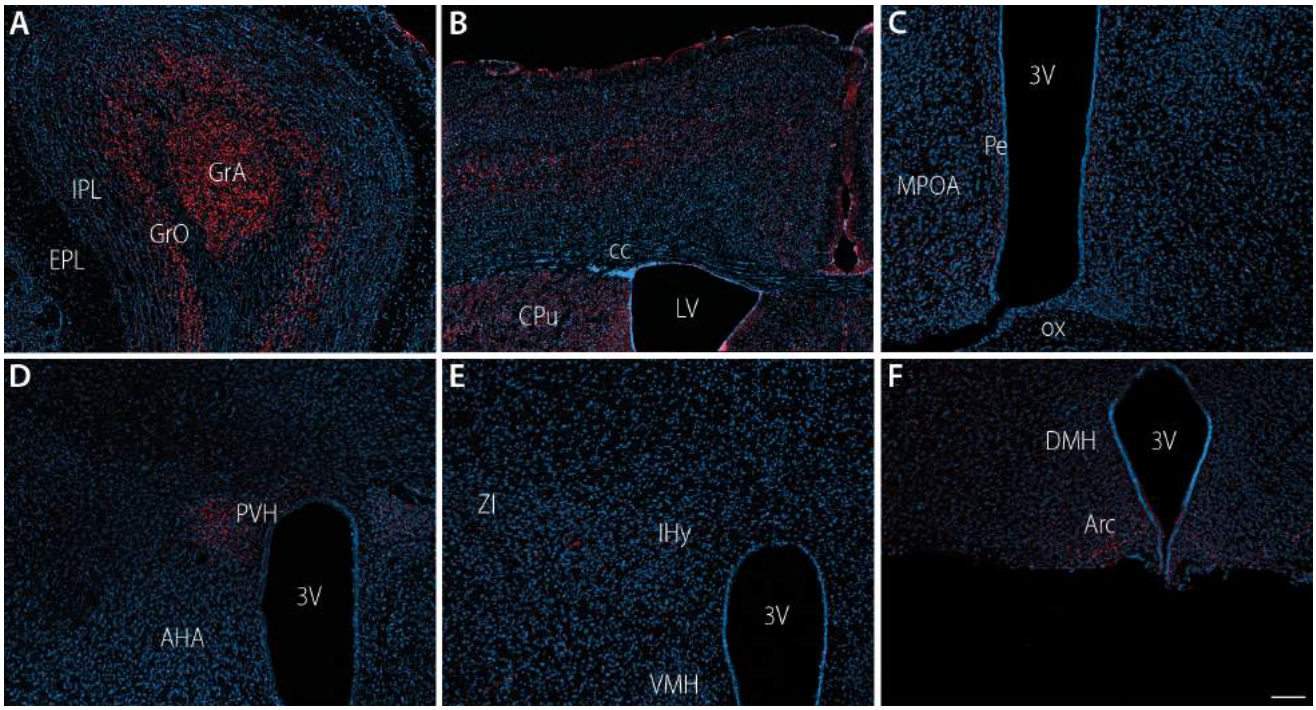

FIGURE 05.tiff

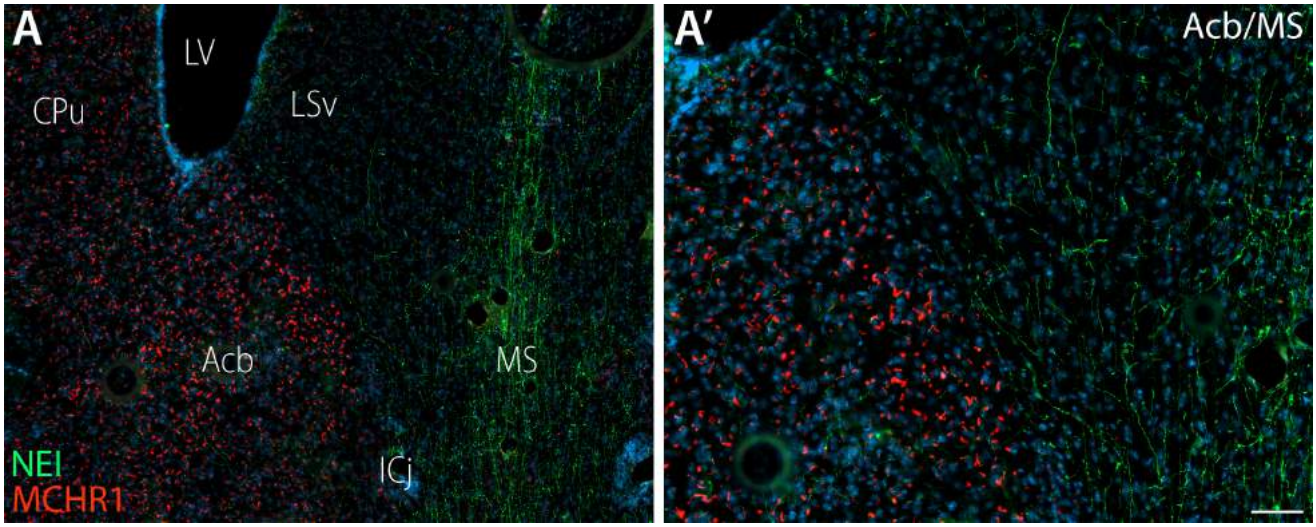

FIGURE 06.tiff

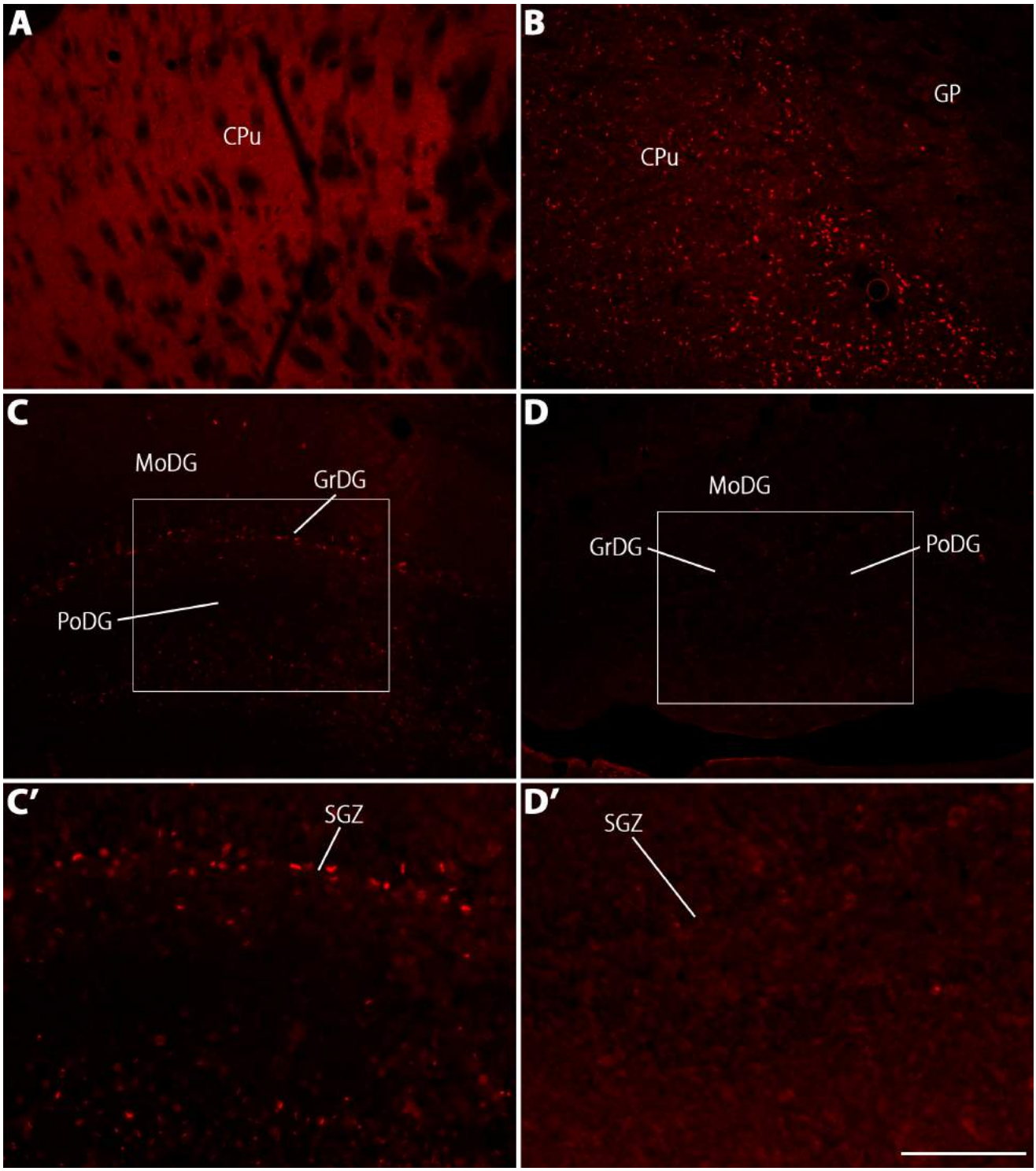

FIGURE 07.tiff

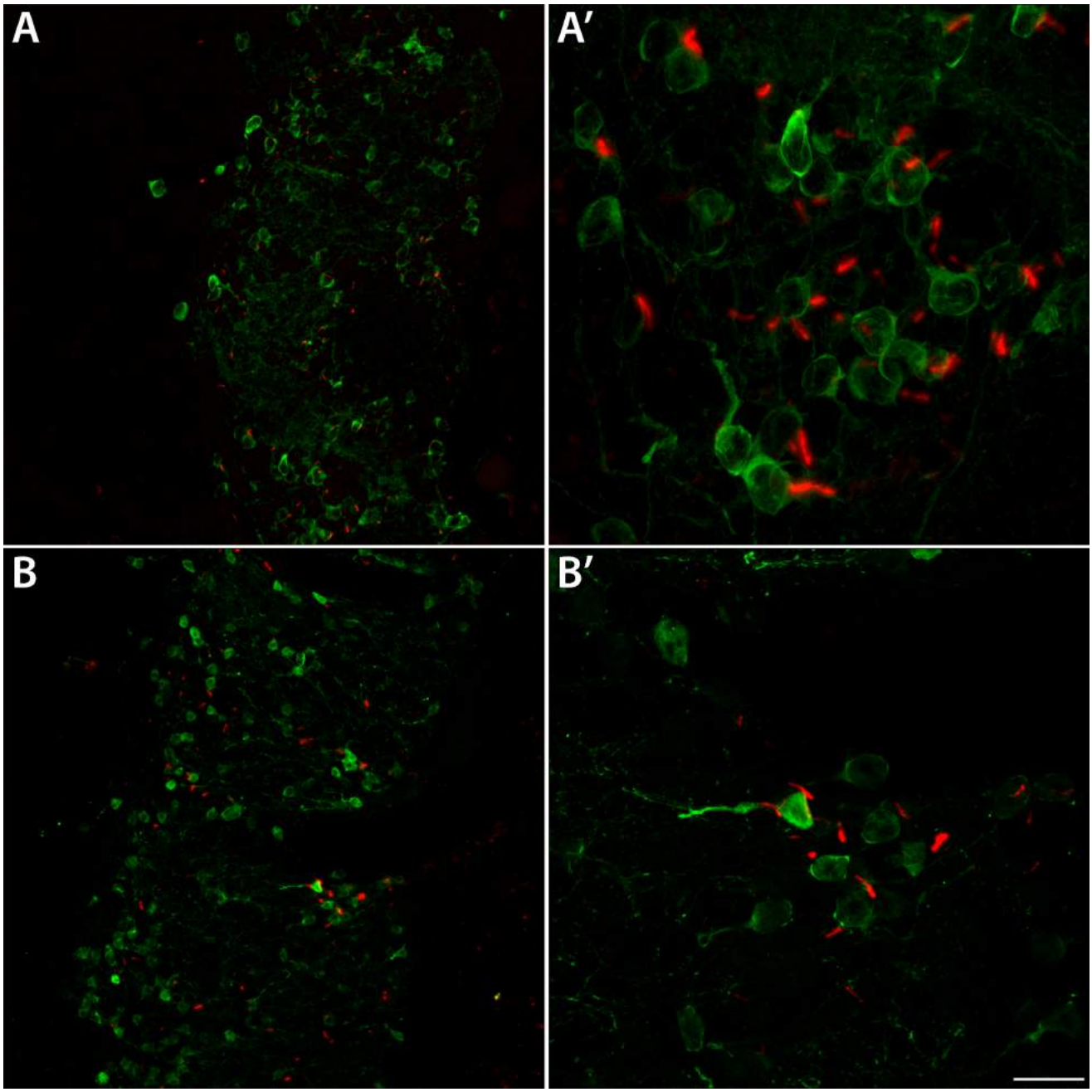

FIGURE 08.tiff

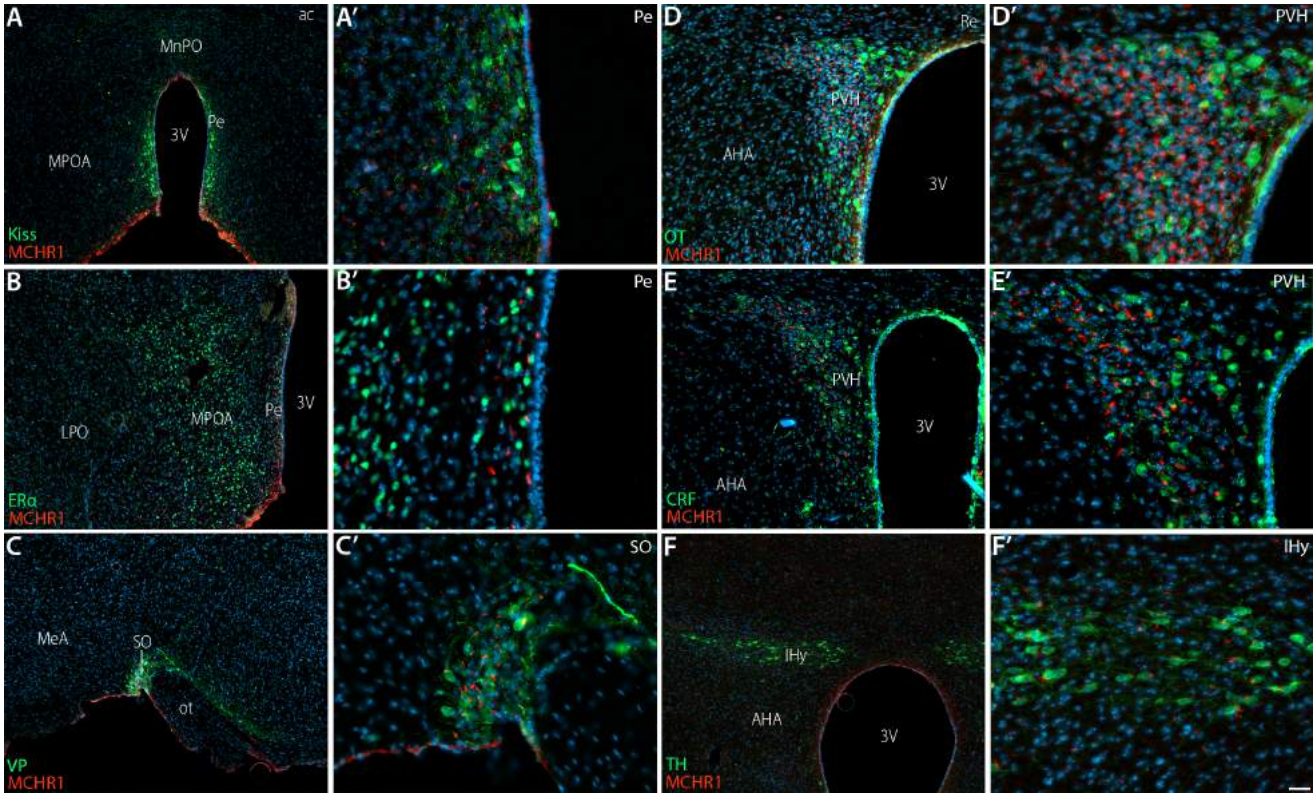

SUPPLEMENTARY_MATERIAL 01.tiff

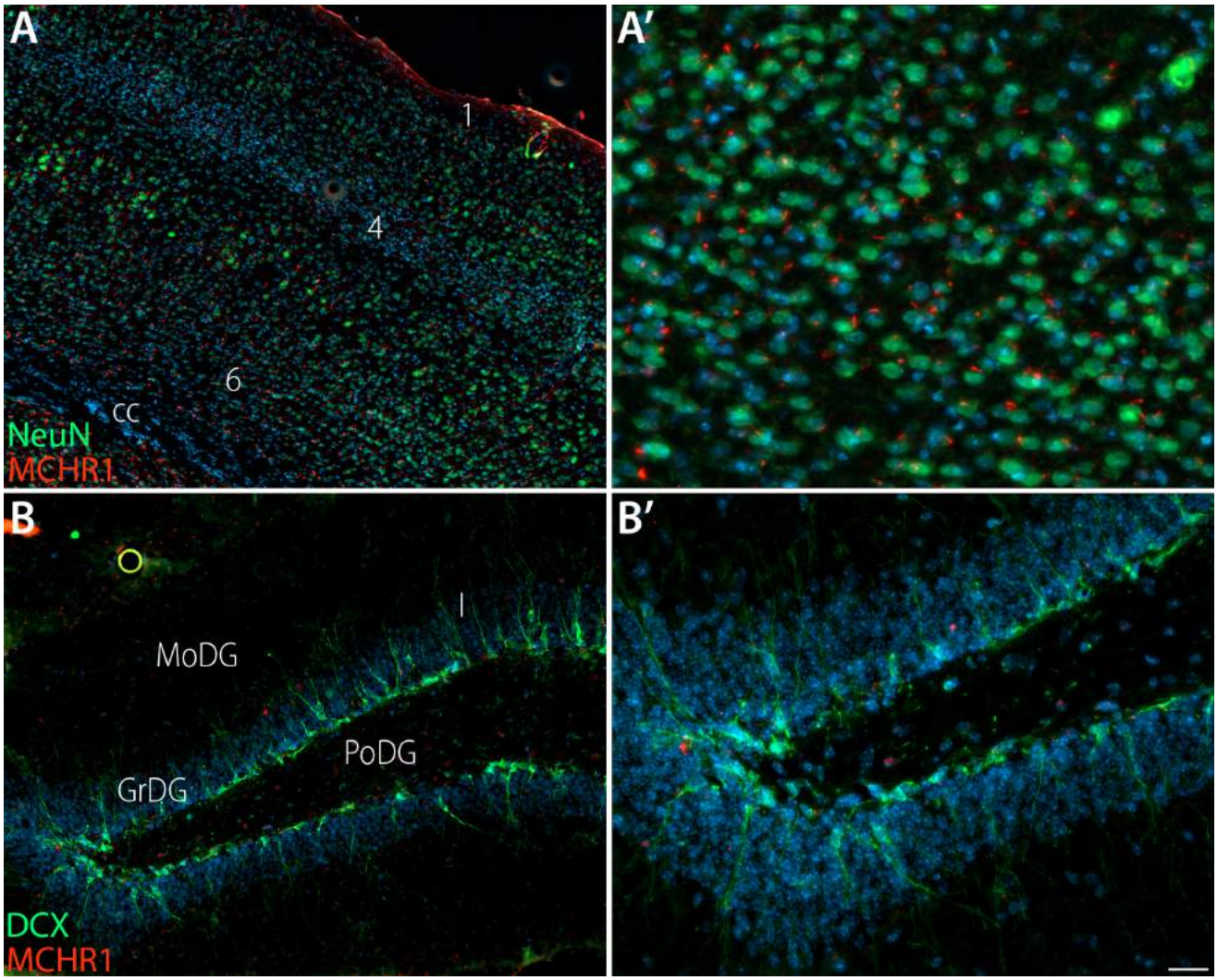

Chapter 5

The melanin-concentrating hormone (MCH) system: a tale of two peptides

Diniz GB and **Bittencourt** JC

Submitted for consideration in: Front. Neurosci. | Research Topic: The Phylogenetic History of Hypothalamic Neuromodulators

The melanin-concentrating hormone (MCH) system: a tale of two peptides

Giovanne B. Diniz[a,b] and Jackson C. Bittencourt[b, c, *]

[a] Department of Neurosurgery, Yale School of Medicine, New Haven, CT, USA
[b] Laboratory of Chemical Neuroanatomy, Department of Anatomy, Institute of Biomedical Sciences, University of São Paulo [USP], 05508-000, São Paulo, Brazil
[c] Center for Neuroscience and Behavior, Institute of Psychology, University of São Paulo [USP], 05508-030, São Paulo, Brazil

*Corresponding author:
Jackson Cioni Bittencourt, M.D., Ph.D.
E-mail: jcbitten@icb.usp.br

Working title: Phylogenetic history of MCH

Keywords: NEI, MCHR1, MCHR2, lateral hypothalamus, neuropeptides, vertebrates

Funding: Financial support for this study was provided in the form of grants from the Fundação de Amparo à Pesquisa do Estado de São Paulo (FAPESP, São Paulo Research Foundation; Grant no. 2010/52068-0 and 2016/02224-1 to JCB and 2016/02748-0 to GBD). We are thankful for the support provided by the Brazilian Coordenação de Aperfeiçoamento de Pessoal de Nível Superior CAPES, Office for the Advancement of Higher Education, Grant #848/15. JCB is an Investigator with the Brazilian Conselho Nacional de Desenvolvimento Científico e Tecnológico (CNPq, National Council for Scientific and Technological Development, Grant # 426378/2016-4).

Acknowledgements: We would like to thank the colleagues who read and provided critical commentary on this work: Dr. Anthony N. van den Pol (Yale School of Medicine) and Dr. Luciane V. Sita (University of São Paulo).

Conflict of Interest: The Authors declare that the research was conducted in the absence of any commercial or financial relationships that could be construed as a potential conflict of interest.

Role of Authors: Both GD and JB contributed with the writing of this article and approved it for publication.

Article Type: Review – part of Special Topic "The Phylogenetic History of Hypothalamic Neuromodulators"

Word Count: 11.706

Total Figures and Tables: 9

List of Abbreviations

3V – third ventricle
A13 – dopaminergic group A13
aa – amino acids
ACTH – adrenocorticotropic hormone
AH – adenohypophysis
AHA – anterior hypothalamic area
AROM – antisense RNA overlapping MCH
CNS – central nervous system
CRF – corticotropin-releasing factor
CSF – cerebrospinal fluid
DHA – dorsal hypothalamic area
DHN - dorsomedial hypothalamic nucleus (non-mammalian)
DHM – dorsomedial hypothalamic nucleus (mammalian)
GH – growth hormone
GPR24 – G protein-coupled receptor 24
IHy – incerto-hypothalamic area
IR – immunoreactivity
LHA – lateral hypothalamic area
LVR – lateral ventricular recess
MCH – melanin-concentrating hormone
MCHR1 – melanin-concentrating hormone receptor 1
MCHR2 – melanin-concentrating hormone receptor 2
ME – median eminence
mfb – medial forebrain bundle
MGOP – MCH gene-overprinted polypeptide
MGRP – MCH gene-related peptide
MYA – million years ago
NEI – neuropeptide glutamic acid-isoleucine
NGE – neuropeptide glycine-glutamic acid
NH – neurohypophysis
NLT – lateral tuberal nucleus (nucleus lateralis tuberis)
ORX- orexin
PCR – proximal neurosecretory contact region
PHA – posterior hypothalamic area
Pmch/pmch/PMCH – melanin-concentrating hormone precursor (gene)
Pmch/PMCH - melanin-concentrating hormone precursor (protein)
PMCHL1 – *PMCH*-Linked 1 gene
PMCHL2 – *PMCH*-Linked 2 gene
PVO – paraventricular organ
SCP_A – small cardioactive peptide A
SL - somatolactin
SLC-1 – somatostatin-like receptor 1
STT – somatostatin
STTR – somatostatin receptor(s)
VMH – ventromedial hypothalamic nucleus
WGD – whole-genome duplication
ZI -zona incerta
α-MSH – α-melanocyte-stimulating hormone

Abstract

The melanin-concentrating hormone (MCH) system is a robust integrator of exogenous and endogenous information, modulating arousal and energy balance. While MCH has been strongly associated with the integration of exogenous and endogenous inputs to inform motivated behaviors in mammals, its predominant function in teleosts is to disperse melanin, contributing to the adaptive color change observed in several teleost species. These contrasting functions result from the teleost whole-genome duplication, which resulted in the generation of two MCH-coding genes in this clade, which acquired distinctive sequences, distribution, and functions. The teleost whole-genome duplication, however, was not the only large-scale genomic event to have an impact on MCH. While not found in invertebrates, immunoreactivity to MCH can be located in the earliest Chordates, positioning the appearance of MCH around the same time as the first whole-genome duplication event common for all vertebrates. Here we propose that MCH originated from a paralog of the invertebrate small cardioactive peptide A, which was positively selected for its capacity to interact with somatostatin receptors. We also describe here the distribution of MCH immunoreactivity and gene expression in a large number of species, in an attempt to identify its core elements. While initially originated as a periventricular peptide, with an intimate relationship with the third ventricle, multiple events of later migration occurred during evolution, making the ventrolateral and dorsolateral hypothalamus the predominant sites of MCH in teleosts and mammals, respectively. Substantial differences between species are observed, likely reflecting differences in habitat and behavior. This aligns well with the idea that MCH is a major integrator of internal and external information, ensuring an appropriate response to ensure the organism homeostasis. New studies on the MCH system in species that have not yet been investigated will help us understand more precisely how these habitat changes are connected to the hypothalamic neurochemical circuits, paving the way to new intervention strategies that may be used with pharmacological purposes.

1. Introduction

1.1. The melanin-concentrating hormone system

The melanin-concentrating hormone (MCH) system is a robust integrator of exogenous and endogenous information, modulating arousal, promoting motivated behaviors, and controlling energy balance (Diniz and Bittencourt, 2017), contributing to the appropriate sleep architecture (Ferreira et al., 2017a), and tethering energy status and reproductive function (Naufahu et al., 2013). While certain aspects of this system have been explored in length, such as its neuroanatomical aspects (Bittencourt and Diniz, 2018), several others are still open to investigation, such as its precise role in reproductive physiology (Naufahu et al., 2013) and in parental behavior (Benedetto et al., 2014; Alachkar et al., 2016; Alhassen et al., 2019), or the mechanisms through which MCH is used to convey information within the CNS (Noble et al., 2018). Although MCH is strongly linked to the roles above, its discovery, and hence its name, is linked to an additional function performed in Teleosts: the control of skin color through the modulation of chromatophore activity (Kawauchi et al., 1983). By concentrating melanin within melanophores, MCH promotes pallor, necessary for adaptive color change. Since neurons of the Teleost hypothalamus synthesize MCH and release it in the bloodstream through the neurohypophysis, it has received the *status* of neurohormone. Although only isolated in 1983, its existence was predicted almost 50 years prior, by Hogben and Slome (1931).

The identification of MCH in the chum salmon pituitary was the gateway for a plethora of discoveries regarding this system. Just six years after the salmon description, Nahon et al. (1989) identified the mammalian *Pmch* gene, as well as other predicted peptides that originate from the *Pmch*-coded precursor, PMCH: neuropeptide E-I (NEI) and neuropeptide G-E (NGE), following the nomenclature scheme of Tatemoto and Mutt (1981). In that same year, Vaughan et al. (1989) isolated and sequenced the mammalian MCH peptide. In parallel, different peptides were identified originating from the teleost *Pmch* gene, such as neuropeptide E-V (Minth et al., 1989). Three years later, Bittencourt et al. (1992) published the first complete mapping of *Pmch* expression and MCH and NEI immunoreactivity (IR) in the rat brain. The next major breakthrough in the field came at the turn of the century, when reverse pharmacology studies identified GPR24/SLC-1 as the selective receptor for MCH, now known as MCHR1 (Bächner et al., 1999; Chambers et al., 1999; Lembo et al., 1999; Saito et al., 1999; Shimomura et al., 1999). Homology searches in genomic databases then revealed a second MCH receptor in 2001, now known as MCHR2 (An et al., 2001; Hill et al., 2001; Mori et al., 2001; Rodriguez et al., 2001; Sailer et al., 2001; Wang et al., 2001).

In addition to the canonical MCH system, there are non-canonical transcripts that originate from the *Pmch*/*PMCH* genes. Toumaniantz et al. (1996) discovered an alternative-splicing product originating from those genes, the MCH-gene-overprinted-polypeptide (MGOP). In the antisense strand of the *Pmch/PMCH* genes, Borsu et al. (2000) identified the antisense-RNA-overlapping-MCH (AROM), a complex gene that originated coding and non-coding transcripts that may modulate gene expression (Moldovan et al., 2012). Finally, exclusively in the hominid lineage, two chimeric genes originated from *PMCH, PMCH-Linked* 1 and 2 (*PMCHL1/PMCHL2*), with putative transcription modulation activity (Courseaux and Nahon, 2001).

As just a glance reveals, MCH is part of a complex system, involved in numerous functions and with multiple canonical and non-canonical elements. This complexity stems from a rich evolutionary history, as significant genomic events influenced the *Pmch* gene and its ancillary elements. The MCH system, therefore,

provides us with a window to look at those evolutionary events and how they shaped the vertebrate hypothalamus and its circuits. In this review, the canonical MCH peptidergic system will be reviewed, including the orthologs and paralogs of the *Pmch* gene, and the distribution of the *Pmch*-coded peptides within the nervous system. Due to the abundance of data, we will not include the MCH receptors and the non-canonical elements, except when they help us understand the peptidergic family. A brief description of the phylogenetic relationship between major clades is included in each section to help readers contextualize the information.

1.2. Unknown origins

While the phylogenetic history of some neuropeptidergic families have clear roots in invertebrate species, such as the corticotropin-releasing factor (CRF) system (Lovejoy and de Lannoy, 2013), the origins of MCH are less clear. Analogies to other peptidergic systems, however, can help us understand how MCH has originated in the vertebrate lineage, with two candidates most likely to have contributed to the emergence of MCH in vertebrates. The first is the precursor of the small cardioactive peptide A (SCP_A), found in the sea slug *Aplysia californica*. According to Nahon et al. (1989), there is significant sequence similarity between rat PMCH and the SCP_A precursor, with mature MCH corresponding to an acidic peptide found in the C-terminal of the SCP_A precursor. Synthesis of SCP_A occurs in motoneurons that innervate the heart, gut and mouth muscles, contributing to cardiovascular homeostasis and feeding behavior modulation (Lloyd et al., 1984; Lloyd et al., 1985; Lloyd, 1986). The motor activity of SCP_A is crucial at the accessory radula closer muscle, which participates in *A. californica*'s behavioral response to feeding, akin to the complex feeding behavior of higher vertebrates (Cropper et al., 2018). In the mouth motoneurons, SCP_A acts as a neuromodulator to enhance cholinergic activity at the postsynaptic neuromuscular junction, as well as through an independent mechanism (Cropper et al., 1988; Vilim et al., 1996). In addition to motor/feeding roles, SCP_A is also able to elicit chromatophore expansion in the cuttlefish *Sepia officinalis*, suggesting it may play a role in the adaptive color change of invertebrates (Loi et al., 1996). It should be noted, however, that despite SCP_A's effect in the cuttlefish being the opposite of that of MCH in teleosts in terms of chromatophore response, MCH also has a pigment dispersion effect in frogs and lizards (Wilkes et al., 1984; Ide et al., 1985), indicating that adaptive color change roles can switch between species.

It is noteworthy, however, that despite sequence similarity, there is structurally little in common between MCH and the acidic peptide of SCP_A. Mature MCH displays a complex three-dimensional structure that relies on a dicysteine bridge to form a ring shape necessary for binding (Macdonald et al., 2000; Audinot et al., 2001), while the acidic peptide is a linear peptide. Another neuromodulatory system, however, matches the structural features of MCH: the somatostatin (STT) system. The STT family of peptides is widely found in vertebrate species, with several peptides and at least five receptor isoforms (as reviewed in Tostivint et al. (2008)). Somatostatin-like immunoreactivity has been described in invertebrate species, but genome analyses do not support the existence of STT in non-Vertebrates. Possible orthologs of SST receptors (STTRs), however, have been described in invertebrate species, including the Arthropod *Drosophila melanogaster*, where STTRs bind to allatostatins (Kreienkamp et al., 2002). Vertebrate STT is a 14 amino acids (aa) peptide, with a circular structure resulting from a cysteine bridge encompassing 12 aa, including two positively-charged residues. Melanin-concentrating hormone is also a cyclic neuropeptide resulting from a cysteine bridge, with two positively-charged residues found in the circular part of this peptide. Another link between MCH and SST are their receptors, which share substantial sequence similarity. Initially identified as the somatostatin-like coupled receptor 1, MCHR1 shares over 40% identity with STTRs in the transmembrane domains, in addition to residues that are important for the SST-

SSTR binding being found in similar positions (Kolakowski Jr et al., 1996; Lakaye et al., 1998). Despite these similarities, SST does not bind to MCHR1, with MCH acting as its only specific ligand. The level of similarity between MCHR1 and STTRs is comparable to the identity between the paralogs MCHR1 and MCHR2, which share 44% identity in the transmembrane domain (An et al., 2001).

How could the acidic peptide of SCP_A and SST/SSTR combine to produce MCH? The 2R hypothesis postulates that two rounds of whole-genome duplication (WGD) occurred at the base of the jawed vertebrates, creating multiple gene paralogs that were then lost or modified (Ohno, 2013). The first WGD event may have duplicated an ancestral vertebrate SCP_A ortholog, resulting in less constraint over the copies' structure due to redundancy (Figure 1). While one copy was lost, successive mutations led the acidic peptide of the other copy to assume a tertiary structure that resembled that of SST, allowing this modified peptide to interact with newly duplicated paralogs of one of the SST receptors. The modified STTR paralog was then positively selected to better bind the modified acidic peptide, at the expense of losing its ability to bind SST. The modified acidic peptide then became what we now identify as MCH, and the receptor became MCHR1. The second round of genome duplication then originated a paralog of MCHR1, MCHR2, while the copy of MCH was lost. This theory for the origin of MCH fits well with the lack of evidence for the presence of MCH or MCHR in Cephalochordates and Tunicates, while both MCH immunoreactivity (MCH-IR) and automatic annotations for single MCH receptors can be found in Cyclostomes (Al-Yousuf and Mizuno, 1991), establishing the formation of vertebrate MCH in between 800 and 600 million years ago (MYA), at around the same time the cranium and hypophysis developed, and preceding the emergence of a jaw in the vertebrate lineage (Kumar et al., 2017).

2. The MCH system in early Chordates

2.1. Chordata > Petromyzontidae

Lampreys and hagfishes were the first vertebrate to diverge (Figure 2), at an estimated time of 797 MYA (Kumar et al., 2017). Together, these two groups form superclass Cyclostomata, clade characterized by the lack of a jaw and internal branchial arches. Due to the very early divergence of Cyclostomata, species belonging to this clade are often considered models for the common vertebrate ancestor. Two major extant clades form Cyclostomata: Petromyzontidae, containing lamprey species, and Myxinidae, containing hagfish species. Four species of lamprey have been used to study MCH: the European river lamprey (*Lampetra fluviatilis*), sea lamprey (*Petromyzon marinus*), brook lamprey (*Lampetra planeri*), and pouched lamprey (*Geotria australis*). Morphological data has been obtained in all species using a salmon MCH-directed antibody (Al-Yousuf and Mizuno, 1991; Bird et al., 2001).

In Petromyzontids, MCH-immunoreactive cells are predominantly restricted to a single hypothalamic *locus*, the dorsomedial hypothalamic nucleus (DHN) of the posterior hypothalamus, occupying parts of the ependyma and subependyma, with only a few scattered neurons found scattered towards the lateral hypothalamus (Al-Yousuf and Mizuno, 1991; Bird et al., 2001). The position of MCH cells in the hypothalamus is illustrated in Figure 3. The DHN is found bordering the third ventricle (3V) and is part of the paraventricular organ (PVO), an ubiquitous nonmammalian structure that contains a myriad of neuroactive substances (Nozaki et al., 1983; Brodin et al., 1990; Tobet et al., 1995), plays a role in hypothalamic integration (Vigh-Teichmann and Vigh, 1989; Meurling and Rodríguez, 1990), has no blood-brain barrier, and is highly vascularized (Röhlich and Vigh, 1967). Exclusively in sexually maturing *L. petromizon*, a weakly-labeled group of neurons is found in the anterior

basal telencephalon. Neurons immunoreactive to MCH in the petromyzontid DHN are frequently bipolar, with one axon projecting into the 3V *lumen*, and the other axon extending laterally towards the lateral hypothalamus.

In addition to local lateral projections, three major innervation pathways are observed: anterior, towards the olfactory lobes; dorsal, towards the habenular nucleus; and posterior, towards the spinal cord (Bird et al., 2001). In *L. fluviatilis* and *L. planeri*, an additional innervation pathway is observed: ventral, towards the hypophysis. In lamprey, the hypophysis is continuous with the hypothalamic floor, as there is no portal system or *infundibulum*. In *L. fluviatilis*, immunoreactive fibers are observed in the proximal neurosecretory contact region (PCR) - the Petromyzontid homolog of the tetrapod median eminence (ME) - and in the proximal neurohypophysis (NH). Some immunolabeled axon terminals are also found close to the basement membrane that separates the NH and the *pars distalis* of the adenohypophysis (AH) (Al-Yousuf and Mizuno, 1991). It should be mentioned, however, that Baker and Rance (1983) did not find evidence of MCH activity in a bioassay using *L. fluviatilis* hypophyses.

Based on these data, Bird et al. (2001) make a series of morphofunctional correlates that, as it will be described later in this work, are extremely relevant for the understanding of MCH in mammals. These authors suggest that: 1. the 3V-contacting axon of MCH neurons, and their position near the ependyma and subependyma, could allow those neurons to sense biomarkers in the cerebrospinal fluid (CSF), or release MCH directly in the *lumen* to act on distant sites; 2. The ample distribution of laterally-projecting axons allows MCH neurons to exert widespread modulation within the CNS; 3. The moderate presence of MCH-ir terminals in the NH could be the substrate through which MCH modulates the release of other neuropeptides in a paracrine fashion, or influences the secretory action of the AH; 4. The NH MCH fibers observed in *L. petromizon* could originate from the telencephalic group of cells observed only in sexually maturing individuals of that species, and those neurons could play a role in physiological adaptation towards reproduction.

2.2. Chordata > Gnathostomata > Chondrichthyes

Cartilaginous fish, members of the Chondrichthyes class, are the earliest diverging class of living jawed vertebrates (Gnathostomata), splitting from bony vertebrates (Osteichthyes) between 475 and 450 MYA (Venkatesh et al., 2014; Kumar et al., 2017) (Figure 2). Extant animals are divided into two subclades, Holocephali (chimeras) and Elasmobranchii (sharks and rays), which split about 421 MYA (Renz et al., 2013).

Chondrichthyans have a single *pmch* gene composed of three exons, encoding a Pmch precursor that is 172 aa-long in the Holocephalan Australian ghost shark (*Callorhinchus milii*) or 165 aa-long in the Elasmobranch scalloped hammerhead (*Sphyrna lewini*). At the N-terminus of this precursors sits a signal peptide that varies in length according to the species, and at the C-terminus is a mature 19 aa-long MCH that can be released by proteolytic activity through a dibasic Arg-Arg site (Mizusawa et al., 2012). In *C. milii*, it is possible that a second 14 aa-long peptide (Neuropeptide G-T) is cleaved from another dibasic pair upstream from the MCH-originating pair, but in *S. lewini* this peptide is 33 aa in length (Neuropeptide T-V). Since there is significant variation in the other peptides that may be produced from the *pmch* gene in addition to MCH, these peptides will all be grouped under an umbrella term: MCH gene-related peptides (MGRPs), a term borrowed from Gröneveld et al. (1993). The Chondrichthyan *pmch* gene is a perfect blueprint for the mammalian *PMCH*. Both human and *S. lewini* precursors have the same length (165 aa), a signal peptide in its N-terminus (which varies in length depending on the species), and a 19 aa-long mature MCH in the C-terminus that can be cleaved from an Arg-Arg pair. There is a

single substitution between mammalian MCH and Chondrichthyes MCH (Val[19] in mammals, Asn[19] in *S. lewini*, Ile[19] in *C. milii*), but the ring structure between Cys[7]-Cys[16] is wholly preserved.

Regarding the distribution of immunoreactivity in Chondrichthyes, labeled cells are found in the dorsal wall of the posterior hypothalamus, and fibers were found exclusively inside the hypothalamus (Mizusawa et al., 2012) (Figure 3). This distribution of MCH-synthesizing neurons is similar to what has been described for Cyclostomes, further reinforcing the dorsomedial posterior hypothalamus as the original *locus* of MCH synthesis in the chordate brain. No fibers are found in the hypophysis, and it is unclear if the hypothalamic-restricted distribution of fibers is a feature of the species or a methodological artifact.

3. The MCH system in the ray-finned fish lineage

3.1. Gnathostomata > Osteichthyes > Actinopterygii

The superclass Osteichthyes contains all vertebrates with bony skeletons, splitting from Chondrichthyans at around 450 MYA (Venkatesh et al., 2014). Osteichtyans split early into two major clades, Actinopterygii (the ray-finned fishes) and Sarcopterygii (lobe-finned fishes), at around 435 MYA (Figure 2) (Kumar et al., 2017). Actinopterygians then diverged into more than 25.000 known extant species, making it the most specious vertebrate clade, partially thanks to the Teleost radiation that occurred at the Cretaceous-Paleogene transition (Friedman, 2010; Sibert and Norris, 2015). Actinopterygians split into five clades: Polypteriformes, Ascipenseriformes, Lepisosteiformes, Amiiformes, and Teleostei (Figure 2). There is uncertainty in the literature regarding the exact relationship between the clades of Actinopterygii (Kumar et al., 2017), but for this work it is only relevant that Polypteriformes, Ascinpenseriformes, Lepisosteiformes, Amiiformes are all considered ancient with respect to Teleostei. Due to the importance of the latter to the understanding of MCH, those animals will be described in a separate section.

Regarding the makeup of *pmch* genes, there are no significant changes in non-Teleost Actinopterygii. The genes with available data are comprised of three introns, giving origin to 167 to 170 aa-long precursors. Mature MCH is 19 aa in length, with some divergence observed in the last residue (Val[19] in *Lepisosteus oculatus*, Ile[19] in *Erpetoichthys calabaricus*), with a 13 aa-long MGRP possibly cleaved at an upstream Arg-Arg pair. Contrasting to the relatively unchanged genomic structure, the Actinopterygii divergence was a period of change in terms of the neuroanatomy of the MCH system. In the brain of the Polypteriform *E. calabaricus*, MCH IR is remarkably similar to what has been described for Petromyzontids. All immunoreactivity resides in the periependymal area, over the dorsal surface of the lateral ventricular recesses (LVR) and in the lateral wall of the 3V (Figure 3). These neurons are found within the PVO, close to the blood capillaries and contacting the ventricular cavity. Abundant fibers are found in the PCR, but not in the hypophysis (Baker and Bird, 2002). The distribution of immunoreactivity in the Ascipenseriform starry sturgeon (*Acipenser stellatus*) is similar to that of *E. calabaricus*, with one striking difference: instead of stopping at the PCR, fibers continued towards the NH (Baker and Bird, 2002) (Figure 3).

In the brain of the Lepisosteriform longnose gar (*Lepisosteus osseus)*, a significant change occurred. Instead of being concentrated in a single area, MCH neurons are found in two separate groups: the dorsomedial ventricular group, similar to what has been described previously, and a new group of neurons within the *nucleus lateralis tuberis* (NLT). Neurons in the ventricular group follow the same pattern as described for MCH neurons so far: predominantly bipolar, in association with the PVO, with one axon contacting the ventricular cavity and

another branching in the lateral hypothalamus and other areas of the SNC. Fibers from the NLT, on the other hand, are found coursing through the basal hypothalamus towards the pituitary stalk, forming a plexus around blood capillaries of the PCR and NH (Baker and Bird, 2002).

The morphological aspects of the MCH system in the three aforementioned species are in accordance to some models of Actinopterygii divergence. Polypteriforms were likely the first clade to split, at around 407 MYA (Kumar et al., 2017), and the distribution of MCH-immunoreactivity in these animals closely resemble that of Petromyzontids and Elasmobranchii. The next clade to split was likely the Ascipenseriforms, since *A. stellatus* has a very similar distribution of cellular bodies but differs from Polypteriforms by having a dense direct innervation of the NH. Since the lamprey *L. planari* also has a direct innervation of the NH, it is possible that this feature appeared independently in Petromyzontids and the common ancestor between Ascipenseriforms and Lepisosteriforms. Alternatively, the innervation of the NH by MCH fibers may have first appeared in Petromyzontids as a plastic feature, becoming then fixed by the time of Ascipenseriform divergence. An evolutive advantage in having the NH innervated directly by MCH (interpreted as MCH release directly in the bloodstream) may have paved the way for the split between periventricular/dorsomedial and tuberal lateral groups to be positively selected, with NLT neurons becoming a magnocellular group that preferentially innervates the NH, which was then itself followed by the acquisition of adaptive color change.

3.2. Actinopterygii > Teleostei

The infraclass Teleostei split from other Actinopterygii at around 320 MYA (Kumar et al., 2017). Teleosts can be divided into four major clades: Osteoglossomorpha, Elopomorpha, Otocephala, and Euteleostei (Figure 2). Most teleost species are part of Euteleostei, with extant members of the other three clades including bonytongues (Osteoglossomorpha), eels (Elopomorpha), and catfishes (Otocephala). Although there is some controversy regarding the exact phylogenetic relationship between Teleost clades, molecular and morphological data suggest that Osteoglossomorpha may have been the first clade to split, at 285 MYA, followed by Elopomorpha (265 MYA), and finally Otocephala and Euteleostei (230 MYA) (Kumar et al., 2017). Since several developments occurred in the MCH system shortly after the Teleostei split, and Euteleosts have been extensively used to probe the MCH system, they will be examined in the following section, with this section focusing on non-Euteleost Teleosts.

3.2.1. Genome

Considerable changes in terms of genomic makeup marked the divergence of Teleosts. The 3R theory postulates that a third WGD occurred in the common ancestor of Teleosts (Meyer and Van de Peer, 2005) (Figure 2). This duplication was then followed by rounds of genomic loss or modification of the copies that were under a positive pressure to be maintained. The MCH system reflects this WGD event, with two *pmch* genes found in most Teleost species. This duplication,when compounded with the historical order of MCH discoveries, creates substantial clutter in the nomenclature of *pmch* orthologs and paralogs. Therefore, we will use in this review a nomenclature that adheres to the prescribed gene nomenclature guidelines for the various species examined, at the expense of not using some of the original nomenclature used in the literature. A table of normalized terms is provided (Table 1). Henceforth, the gene most commonly identified as “pmch2” will be designated as *pmcha*, and “pmch1” will be designated as *pmchb*.

The *pmcha* gene has a similar structure to both Elasmobranch and Mammalian *pmch/Pmch*, being comprised of three exons, having a 3' splice site of intron 2 in the same position, and displaying similar synteny. The Pmcha prepropeptide ranges from 148 to 156 aa in length, and through a dibasic cleavage site originates a mature MCH_A that is 19 aa-long and 84.2% identical and 89.5% similar to mammalian MCH. Three substitutions are observed in the mature MCH_A, Ile^2 replaces Phe^2, Val^9 replaces Leu^9, and Ala^{19} replaces Asn^{19}/Ile^{19} in Elasmobranchii or Val^{19} in Mammals. An additional aa substitution occurred in the common carp, *Cyprinus carpio* (Ile^4 replaces Met^4). These changes are all conservative, and only the Val^9 substitution has occurred in the bioactive zone of MCH_A. The *pmchb* gene, on the other hand, is intronless and codes a Pmchb precursor that is 124 aa-long in all described species. There is a remarkably low similarity between *pmcha* and *pmchb*. At the C-terminus of Pmchb is a mature MCH_B that is 17 aa-long (two residues shorter in the N-terminus), has two substitutions on the N-terminal stretch before the ring structure (Thr^2 replaces Met^4, and Met^3 replaces Leu^5), the same substitution as MCH_A inside the ring, and one non-conservative substitution in the C-terminal sequence outside the ring (Glu^{16} replaces Gln^{18}).

Two aspects of the formation of MCH_A and MCH_B in the Teleost ancestor are worth noting. The first is the remarkable capability of neuromodulators to change shortly after being duplicated. Given the uniform distribution of *pmchb* in early Teleosts, it is clear that this newly generated copy underwent its substitutions before there were any significant splits in the Teleost lineage. The second remarkable aspect is how genomic duplications affect phylogenetic constraints. As the only source of MCH in non-Teleosts, the *pmch/Pmch* gene remained remarkably conserved from Elasmobranchs to Mammals. In the Teleost lineage, however, *pmcha* became a very dynamic neuropeptide, while *pmchb* became the most conserved paralog, even though its sequence differs significantly from non-Teleost *pmch/Pmch,* probably due to the acquisition of an adaptive color change role for MCH, which then acted to impose a phylogenetic constraint over *pmchb*.

It should be mentioned that attempts to clone the transcripts of *pmch* genes in some Otocephala species have not always resulted in the identification of two paralogs. In the goldfish *Carassius auratus*, two paralogs encoding highly similar *pmch* were found (Cerdá-Reverter et al., 2006), and a single paralog was found in *Schizothorax prenati* (Wang et al., 2016) and *C. carpio* (Xu et al., 2019). This apparent contradiction between the genomic databases and the attempts to clone *pmch* transcripts can be explained by a very low expression of *pmcha,* coupled to a high dissimilarity between *pmcha* and *pmchb*. Since most probes have been designed based on the well-known salmon sequence (of *pmchb*), it is easy to imagine that most probes would fail to identify *pmcha* transcripts. Furthermore, as we will see in the next section, the use of different antibodies to map MCH in goldfish is supportive of the existence of two structurally dissimilar MCH peptides.

3.2.2. Anatomy

In the Osteoglossomorphs goldeye (*Hiodon alosoides*) and freshwater butterflyfish (*Pantodon buchholzi*), the bulk of MCH neurons is found in the basal hypothalamus, but instead of forming a neuronal sheet in the NLT area, neurons are found in the mid-hypothalamic region (Figure 3). Despite this difference, these neurons project to the NH, similar to the NLT group of other Actinopterygians. A second group of small neurons is found in the periventricular area of the LVR, clustered around the PVO. As the other periventricular groups described here, these neurons project to the ependyma and the ventricular cavity (Baker and Bird, 2002). In the Elopomorph European eel (*Anguilla anguilla*), 80% of MCH neurons are large and located in the NLT at the ventrolateralhypothalamus, below the LVR, with dense projections to the NH. This is the first significant shift of

cells to the ventral hypothalamus from the periventricular area, a transitional stage that will be repeated in several other species. A small group of neurons still resides at the dorsal surface of the LVR, but there is no apparent contact with the PVO (Baker and Bird, 2002). In Otocephala, the dominant group of MCH neurons is located in the NLT, with dense projections to the hypophysis, in addition to projections to the thalamus, pretectal region, preoptic area, and telencephalon. A second, small group of neurons is observed close to the LVR, near the junction between the LVR and 3V. The axons of those neurons course towards the vicinity of the PVO, but no direct contact with the ventricular cavity is observed (Bird et al., 1989; Baker and Bird, 2002). These descriptions were made using a salmon MCH-directed antibody; therefore, those descriptions are likely more relevant to MCH_B than to MCH_A in those species. Fortunately, some works provide some insight into the differences between MCH_A and MCH_B in terms of distribution.

In zebrafish (*Danio rerio)*, *pmchb* mRNA expression is found in the lateral and posterior NLT, in a group dorsal to the LVR, and the caudal zone of the periventricular hypothalamus. The distribution of *pmcha*, on the other hand, is more restricted, with *pmcha*-expressing neurons found exclusively in the anterior NLT. There is no overlap in the expression of the two *pmch* paralogs. Immunoreactivity to MCH_A and MCH_B was determined to follow a similar pattern, as revealed by the use of salmon MCH- and mammalian MCH-directed antibodies. An extensive network of MCH_A-ir fibers was found, including immunoreactivity in the dorsal nucleus of the ventral telencephalic area, the thalamus, the habenula, the periventricular nucleus of the posterior tuberculum, the posterior tuberal nucleus, and the torus lateralis. In the hypothalamus, fibers were found in the lateral and periventricular zones, the ventral hypothalamus close to the ME, and the hypophysis. In the mesencephalon, the periventricular gray zone of the optic *tectum* and the *torus semicircularis*, and in the rhombencephalon fibers were found in the *griseum centrale* and *locus coeruleus* (Berman et al., 2009). This widespread distribution of fibers, covering regions from the anterior telencephalon to the rhombencephalon will be found in mammals and other species. A similar dichotomy between *pmcha*/MCH_A and *pmchb*/MCH_B is observed in the goldfish (Huesa et al., 2005; Cerdá-Reverter et al., 2006; Matsuda et al., 2006; Tanaka et al., 2009).

These observations of MCH immunoreactivity in Teleostei leading to Euteleostei show a consolidation of the pattern that emerged in ancient Actinopterygii and, in particular, at the time of Lepisosteriform divergence. The NTS group of MCH neurons became the dominant group, and a strong innervation of the ME and the hypophysis developed. On the other hand, the periventricular group started drifting away of the periependymal area and the PVO, and lost contact with the ventricular cavity, but remained in the posteromedial part of the hypothalamus. The duplication of the *pmch* gene also impacted the anatomy of the system. While *pmchb* was retained in all previously described groups of MCH neurons, projections from MCH_B-synthesizing neurons became concentrated in the hypophysis. On the other hand, *pmcha* became restricted to a small group of neurons in the NLT, but those neurons have widespread fibers in the CNS.

3.3. Teleostei > Euteleostei > Protacanthopterygii

The Euteleosts have been extensively investigated, due to the initial discovery of MCH happening in the chum salmon pituitary. The Euteleosts can be split into two clades: Protacanthopterygii and Neoteleostei, which includes Acanthopterygii (Figure 2). Order Salmoniformes, which includes trout and salmons, is part of the Protacanthopterygii, and will be the focus of this section. The members of the *Oncorhynchus* genus played a historical role in the discovery of MCH since the peptide was first isolated from the hypophysis of the chum salmon (*Oncorhynchus keta*) by Kawauchi et al. (1983).

3.3.1. Genome

Another major genetic shift occurred after the divergence of the Salmoniformes. In these animals, an additional duplication of the *pmch* genes occurred, conforming to the 4R theory, which states that a fourth WGD event occurred in the Salmoniform lineage, between 25 and 100 MYA (Allendorf and Thorgaard, 1984), and this is reflected in gene databases (Figure 2). The nomenclature employed by the automated computational analyses, however, is often confusing and should be interpreted with care. In this review, the two copies of *pmcha* will be called *pmcha1* and *pmcha2*, and the two copies of *pmchb* will be called *pmchb1* and *pmchb2*. Detailed information is available for three species of Salmonids, the rainbow trout (*Oncorhynchus mykiss*), the coho salmon (*Oncorhynchus kisutch*), and the Chinook salmon (*Oncorhynchus tshawytscha*), with minimal variation between species. Both *pmcha1* and *pmcha2* are composed of three exons that encode Pmcha precursors that are 144 aa-long for *pmcha2* and 146 or 147 aa-long for *pmcha1*. At the C-terminus is a mature MCHA that is 21 residues-long due to the insertion of two residues at the N-terminal (Glu^{1} and Ala^{2}). There are also two conservative substitutions in the N-terminal stretch before the cysteine ring (Leu^{4} replaces Ile^{2} and Glu^{5} replaces Asp^{3}) when compared to the carp MCH_{A}. A single substitution differentiates MCH_{A1} from MCH_{A2} (Ser^{19} replaces Trp^{19}). The *pmchb1* and *pmchb2* genes, on the other hand, are very similar: both are intronless genes that code for 132 aa-long Pmchb. At the C-terminus of those preprohormones is a 17 aa mature MCH, with sequence identical to Otocephala MCH_{B}.

Attempts to clone MCH transcripts in salmonids, however, did not reproduce what is observed in the automatic annotation of gene databases. Most attempts to identify *pmch* genes in salmonids resulted in the identification of only *pmchb1* and *pmchb2* transcripts (Masao et al., 1988; Minth et al., 1989; Takayama et al., 1989; Nahon et al., 1991; Baker et al., 1995). Genes identified by library cloning agree well to the independent information available at the online repositories. It is unclear, at this point, if all the salmonid *pmch* genes are expressed. One report in *O. tshawitscha* found similar patterns of expression for both *pmchb1* and *pmchb2* (Masao et al., 1988), while in *O. kisutch* and *O. mykiss* only *pmchb2* was found to be expressed, while *pmchb1* appears to be a silent gene (Nahon et al., 1991; Baker et al., 1995; Suzuki et al., 1995; Suzuki et al., 1997). Further studies are necessary to validate the automatic annotation reports of *pmcha1* and *pmcha2* in salmonids, and to detect if those genes are expressed.

3.3.2. Anatomy

The distribution of MCH_{B}-ir cells has been reported for *O. mykiss* and *O. keta*. In these animals, the main group of MCH_{B}-ir neurons is found in the NLT, encircling the pituitary stalk (Figure 3). A dense network of fibers is directed to the hypophysis, while a few projections are found in the telencephalon, preoptic area, thalamus, and pretectal region. In the hypophysis, fibers predominantly innervated the NH, but could also be found in the AH. Smaller groups of neurons were found behind the pituitary stalk, extending between the basal hypothalamus and the LVR, and medially over the dorsal surface of the LVR, in close contact with the PVO (Figure 3) (Naito et al., 1985; Bird et al., 1989; Baker et al., 1995; Suzuki et al., 1995; Baker and Bird, 2002). *In situ* hybridization supports the presence of cell bodies in the NLT and dorsal to the LVR (Baker et al., 1995). This distribution is highly compatible with that described for MCH_{B} in zebrafish and other species of Otocephala.

3.4. Teleostei > Euteleostei > Neoteleostei

The Neoteleostei is a large and complex clade of Euteleosts. Regarding the MCH system, all works have concentrated in a single clade, Acanthomorpha and, inside that clade, in clade Percomorpha of the superorder

Acanthopterygii. The animals evaluated regarding the MCH system can be divided into two major clades, the Carangimorpharia, and Percomorpharia. Inside Carangimorpharia, order Pleuronectiforme was the first to diverge, followed then by the closely related orders Beloniformes and Cyprinodontiformes (Figure 2). Inside order Percomorpha, all species studies were part of order Perciformes.

3.4.1. Genome

The idea that the second duplication of MCH occurred specifically in the Salmonid lineage is reinforced by the observation of only two copies of *pmch* in Neoteleosts. Neoteleost *pmcha* encodes Pmcha precursors that range from 146 to 150 aa in length. The mature MCH_A contained in these precursors also has a variable length, ranging from 21 aa (winter flounder, *Platichthys americanus*) to 25 aa (barfin flounder, *Verasper moseri*). There is no indication that an MGRP can be originated from Pmcha (Tuziak and Volkoff, 2012; Kang and Kim, 2013; Mizusawa et al., 2015). On the other hand, *pmchb* is an intronless gene, encoding a Pmchb protein that is shorter than Pmcha, ranging from 129 aa (*starry flounder, Platichthys stellatus*) to 136 aa (Nile tilapia, *Oreochromis niloticus*). In all available described and predicted cases, MCH_B is 17 aa long and mostly conserved: tilapia MCH_B is identical to Otocephala MCH_B, while other Neoteleosts have a single conservative substitution (Asn^2 replaces Thr^2), and the winter flounder has an additional substitution inside the ring sequence (Gly^7 replaces Val^7). In most cases, a large 22 or 23 aa-long MGRP precedes mature MCH, potentially cleaved in a single basic locus to originate smaller peptides (Gröneveld et al., 1993; Takahashi et al., 2004; Pérez-Sirkin et al., 2012; Tuziak and Volkoff, 2012; Kang and Kim, 2013; Hosomi et al., 2015). It should be noted, however, that Takahashi et al. (2004) found no evidence of MGRP synthesis using mass spectroscopy in *V. moseri* samples.

3.4.2. Anatomy

The distribution of MCH has been examined in Pleuronectiformes (Baker and Bird, 2002; Amano et al., 2003; Amiya et al., 2008a; Amiya et al., 2008b), Cyprinodontiformes (Batten and Baker, 1988; Batten et al., 1999) and Perciformes (Mancera and Fernández-Llebrez, 1995; Batten et al., 1999; Duarte et al., 2001; Baker and Bird, 2002; Pandolfi et al., 2003; Cánepa et al., 2008). The overall distribution of MCH neurons remains mostly the same, with the main group of cells found in the NLT and a second, smaller group found close to the LVR (Figure 3). The principal group of fibers courses towards the hypophysis, with fibers reaching not only the NH but also the AH junction in the rostral and proximal *pars distalis*. Within the hypophysis, MCH-ir fibers contact multiple cellular types. A large number of fibers contain stained vesicles in the posterior neurohypophysis, making contact with pituicytes or the basement membrane of capillaries. Discontinuities within the neuro-intermediate basement membrane allow MCH-ir fibers to contact *pars intermedia* endocrine cells, including α-melanocyte-stimulating hormone (α-MSH) and somatolactin (SL) cells. In some instances, MCH fibers are observed in the adrenocorticotropic hormone (ACTH) cell zone and contacting growth hormone (GH) cells. Other cell types do not appear to be contacted by MCH-ir fibers (Batten and Baker, 1988; Batten et al., 1999). Smaller numbers of fibers are found projecting to other areas, such as the preoptic hypothalamus, thalamus, pretectal region, and telencephalon. In the sailfin molly (*Poecilia latipinna*), fibers are also found in the ventral telencephalon and olfactory bulb (Batten and Baker, 1988). Neurons in the LVR appear to project preferentially to non-hypophyseal targets. At least in Pleuronectiforms, neurons in the NLT are contacted by both gonadotropin-releasing hormone (GnRH)-ir and orexin-ir fibers, but reciprocal connections are only made to orexin neurons (Amiya et al., 2008a; Amiya et al., 2008b).

One interesting aspect of the MCH anatomy in Neoteleostei is the description of time-sensitive neurons during development. These neurons appear not to be present in Pleuronectiformes (Amano et al., 2003), but they are found in at least two Perciform species, the gilt-head bream (*Sparus aurata*) and the Cichlid *Cichlastoma dimerus*. In *S. auratus*, cells were found in the periventricular area of the medial hypothalamus from days 4 through 23 after hatching, disappearing after this time frame (Mancera and Fernández-Llebrez, 1995). In *C. dimerus*, the transient neurons were found in the *nucleus periventricularis* posterior, starting at day 6 and disappearing by day 42 after hatching (Pandolfi et al., 2003).

4. The MCH system in the tetrapod lineage

4.1. Osteichthyes > Sarcopterygii > Dipnoi

As mentioned before, Actinopterygii and Sarcopterygii diverged at approximately 435 MYA (Kumar et al., 2017). The Sarcopterygii clade includes the tetrapod lineage, in addition to the clade containing their closest extant relatives, the lungfish, grouped in Subclass Dipnoi (Figure 4). Limited information is available about MCH in lungfish, as a single work has examined the distribution of MCH-ir elements in the West African lungfish (*Protopterus annectens*) (Vallarino et al., 1998). In this animal, diencephalic MCH neurons are found in two groups: a main group, located in the periventricular tuberal hypothalamus, and a second group described in the peripheral layers of the ventral hypothalamus (Figure 5). According to Croizier et al. (2013), this peripheral group of neurons corresponds to a migrated sheet of cells in contact with the dorsal periventricular hypothalamus. Another two groups have been found in lungfish: in the *subpallium* and the *pars intermedia* of the hypophysis. It is unclear, at this moment, if those extra-diencephalic groups represent actual *loci* of MCH neurons, with further studies necessary to ascertain their specificity. Regarding the fiber distribution, immunoreactive projections are found throughout the telencephalon, including the anterior olfactory nucleus, medial *subpallium*, and medial *pallium*. The preoptic, suprachiasmatic and caudal hypothalamus contain large numbers of fibers, while the thalamus receives a moderate-to-low number of fibers. The mesencephalon and rhombencephalon contain average numbers of fibers, except for the mesencephalic *tectum*, which received a large input, agreeing to what has been described for Actinopterygii. No fibers were observed in the ME or the hypophysis (Vallarino et al., 1998).

4.2. Sarcopterygii > Tetrapoda > Lissamphibia

Tetrapods diverged from lungfish at approximately 413 MYA, and Lissamphibia was the first group to diverge, including all extant amphibians, at approximately 350 MYA (Figure 4) (Kumar et al., 2017). Amphibians, also classified as anamniotes, are semiaquatic, laying their eggs in the water. Subclass Lissamphibia is composed of three major groups: Gymnophiona (caecilians), Anura (frogs), and Caudata (salamanders). In terms of genetic composition, there are no major changes in Lissamphibians when compared to non-Teleost groups. A single *pmch* gene is found, encoding a Pmch precursor that ranges from 167 to 180 aa in length. At the C-terminus of this Pmch is a mature MCH identical to mammalian MCH, which can be cleaved from a dibasic Arg-Arg pair. MGRPs can potentially be cleaved from a dibasic pair upstream of mature MCH, but they vary in length and sequence.

The distribution of MCH neurons in Lissamphibians follows a particular pattern that is not observed in other clades (Andersen et al., 1986; Francis and Baker, 1995; Lázár et al., 2002; Croizier et al., 2013). The major cluster of MCH neurons occurs in the dorsal periventricular nucleus, arranged as a subependymal sheet of cells. Although these neurons are found close to the PVO, they do not invade its limits. A second group of cells has

been described in the ventral tuberal nucleus, at least in the common frog (*Rana temporaria*) (Figure 5). The lateral hypothalamus appears not to contain MCH neurons, at least in Anurans. Andersen et al. (1986) describe MCH-ir neurons in the ventral thalamic area of the marsh frog (*Rana ridibunda*), and Lázár et al. (2002) found MCH-IR in the posterior *tuberculum*, which Croizier et al. (2013) insightfully pointed out as harboring dopaminergic neurons. It is possible that these two groups represent the basis of what later became the zona incerta (ZI) and incerto-hypothalamic area (IHy) in mammals. There appears to be substantial plasticity in the MCH system of Anurans, with an enlargement of certain subsets of neurons upon the transition from tadpole to adult and the appearance of neurons in the preoptic hypothalamus linked to the reproductive period (Francis and Baker, 1995). Areas that receive MCH input in Lissamphibia include the olfactory lobe, the habenular nucleus, the optic *tectum*, the ME, and the spinal cord. In addition to those areas, Andersen et al. (1986) found a dense plexus of fibers in the NH.

4.3. Tetrapoda > Amniota > Sauropsida

Amniota is a group of vertebrates who have developed adaptations to lay their eggs in a terrestrial environment. The amnion membrane that gives name to the clade is a structure in the egg that forms a cavity filled with fluids around the embryo, providing the necessary hydration during development. This adaptation occurred at approximately 350 MYA and was a key development in the transition from an aquatic to a fully terrestrial life for vertebrates (Kumar et al., 2017). At approximately 320 MYA, the Amniota lineage split into Diapsida, who then later originated the Mammalia clade, and Sauropsida, which contains all extant reptiles and birds. Within the Sauropsida clade, order Squamata was the first to split, at approximately 280 MYA, and contains the extant lizards and snakes. The next split within Sauropsida was between Testudines and Archosauria, at approximately 250 MYA. Testudines contains the extant turtles, while Archosauria contains orders Crocodilia and Aves, which split at around 240 MYA (Figure 4) (Kumar et al., 2017).

The genetic makeup of the MCH system remains strongly conserved in Sauropsida. Among Squamata, most animals from this clade have a single *pmch* formed by three exons that codes for a PMCH that is 164 aa-long in Serpentes, and between 166 and 174 aa in other clades. At the C-terminus of PMCH is a 19 aa-long mature MCH, which is identical to mammals in the common wall lizard (*Podarcis muralis*) and Schlegel's Japanese gecko (*Gekko japonicus*), or have a single substitution in residue 19 when compared to both humans and Elasmobranchs (Ala^{19} replaces Ile^{19} or Val^{19}). An additional substitution is observed in family Elapidae of serpents, where Leu^{4} replaces Met^{4}. In Testudines and Crocodilia, PMCH is similar to Squamata PMCH, 167 aa in length and with an MCH sequence that is identical to mammalian MCH. In most species within Aves, the mature MCH structure is similar to the other Sauropsids, with occasional changes occurring in individual lineages, especially in positions 4 (Ile^{4}, Thr^{4} or Lys^{4} replacing Met^{4}) and 19 (Ile^{19} or Ala^{19} replacing Val^{19}). It is likely, therefore, that positions 4 and 19 represent "hotspots" that were frequently interchanges during evolution. In non-Avian Sauropsids, an MGRP that is 13 aa in length can be produced from a dibasic site, but in Aves, one of the Arg residues of this cleavage locus was replaced by a Glu residue. It is still possible that an MGRP may be produced from a single basic residue by different prohormone convertases, but this seems unlikely (Cardot et al., 1999).

Immunoreactivity to MCH has been described in a few Squamata and Testudines species: the common wall lizard (*P. muralis*), the grass and viperine snakes (*Natrix natrix* and *Natrix maura*), and the water turtle (*Chrysemis scripta elegans*), by Cardot et al. (1994). In Aves, species examined include chicken (*Gallus gallus domesticus*), guinea hens (*Numida meleagris*), quails (*Coturnix coturnix japonica*), gosling (*Anser domesticus*), ducks (*Cairina moschata*), and coots (*Fulica atra*) (Cardot et al., 1999). Cells immunoreactive to MCH were found in two

major groups: at the dorsomedial periventricular nucleus, ventrolateral to the PVO, and in the lateral hypothalamic area. In some cases, a few cells were observed within the PVO. In the lateral hypothalamus, cells were described to form an arc shape (Figure 5).

Regarding the distribution of fibers, non-avian Sauropsids are very similar to what is observed in mammals. Fibers are found in olfactory areas, such as the olfactory bulb, the olfactory *tuberculum*, and the piriform cortex; the septum, the diagonal band of Broca, the *paleostriatum*, the amygdala, parts of the cortex, the preoptic hypothalamus, the lateral zone of the hypothalamus, the pretectal area, the optic lobes and in several areas of the brainstem and spinal cord (Cardot et al., 1994). Immunoreactivity was also observed in the same areas when an anti-NEI antiserum was used, confirming the synthesis of an MGRP in non-avian Sauropsids. In Aves, the same basic plan was observed, but a few key differences are noted: projections to the olfactory system are more restricted in birds, the hippocampus receives less MCH fibers, the thalamus receives less dense projections, and although dense, projections to the brainstem are more constrained to specific areas, as opposed to the more diffuse projections observed in other Sauropsids. No staining was observed when an anti-NEI antibody was used (Cardot et al., 1999).

Summarizing these observations, non-avian Sauropsids developed a very similar pattern of projections to mammals, an example of convergent evolution facilitated by a shared common plan first observed in Lissamphibia. In the Aves lineage, however, projections were trimmed in some areas, while developed in others, likely to better work for the different needs of birds. Another important event was the loss of an MGRP in the Aves lineage, which combined to the great variability in the sequence of those peptides in other *phyla*, raises questions about the extent of functions performed by those peptides. We cannot discard the possibility, however, that the loss of an MGRP in the base of Aves has facilitated the involution of that system in areas where its interaction with MCH was important.

4.4. Tetrapoda > Amniota > Mammalia

Mammals originated from the sister clade of Sauropsida, Synapsida. Mammals are characterized by the acquisition of several morphological traits, including mammary glands, three bones in the inner ear, and hair. Another important development was the acquisition of a placenta, after 160MYA, which separates the Eutherians from Prototherians (*e.g.,* Platypus and Echidna) and Metatherians (*e.g.* modern marsupials) (Figure 4) (Kumar et al., 2017). Among Eutherians, geographically distinct clades developed in between 105 and 100 MYA, including Xenarthra (*e.g.,* anteaters and armadillos), Afrotheria (*e.g.,* moles, shrews, tenrecs, manatees and elephants), and Boroeutheria (*e.g.,* rodents, primates, carnivores, ungulates), which likely split almost simultaneously (Figure 4) (Nishihara et al., 2009). To us, the exact relationship between these groups is of little importance, as almost no information is available for Xenarthra and Afrotheria regarding the MCH system.

Regarding the *Pmch* gene, mammals have a very homogenous composition. The *Pmch* gene is formed by three exons and two introns, which contribute similarly to PMCH formation as in other vertebrates. Mature MCH is 19 aa-long, processed from a dibasic (Arg-Arg) pair, ending with a Val^{19} in most mammals, but a few species have an Ile^{19} (similar to Elasmobranchs), such as the platypus (*Ornithorhynchus anatinus*), the pangolin (*Manis javanica*), and a few primate species, such as the northern white-cheeked gibbon (*Nomaseus leucogenys*) and the white-tufted-ear marmoset (*Callithrix jacchus*). The only exception to that rule are some species of bats, where Ile^{5} replaced Leu^{5}. All substitution observed are conservative and happened outside the loop between Cys

residues. Two MGRPs appear to be encoded in mammalian *Pmch*. Mature NEI is 13 aa-long and precedes MCH in the PMCH sequence. The sequence of NEI has been mostly conserved in mammals, with some variation observed in the first three residues, in particular in position 2. These changes are conservative in all cases, except for the rhinoceros (*Ceratotherium simun simun*), where Glu^{1} was replaced by a Gly^{1}. While NEI is produced from a dibasic Arg-Arg pair in Prototheria and Metatheria, Eutheria has a single substitution on the first Arg of the pair, allowing NEI to be cleaved from a Lys-Arg pair instead. Finally, NGE may be cleaved from a single basic residue, but evidence of its actual synthesis is lacking (for a review, see Bittencourt and Diniz (2018)).

The distribution of MCH-ir perikarya among mammals is familiar but distinctive. Here, we observe a significant shift of MCH cells, which now are more numerously found in the lateral hypothalamus, rather than the periventricular zone. This later migration is similar to what happened during the Actinopterygii differentiation and represents a second, independent shift in the position of MCH cells. Similar shifts occurred with less intensity in other clades, such as Dipnoi and Sauropsida, but the number of cells in lateral areas never surpassed the density of cells in the periventricular area in those groups. While the later migration of MCH cells in Actinopterygii occurred in parallel to an increase of MCH innervation of the hypophysis, the lateral migration observed in Mammals occurred concomitant to an expansion of MCH innervation throughout the CNS. These movements are strongly linked to hodological characteristics of the lateral areas: while the NLT has an intimate relationship with the *infundibulum*, the lateral hypothalamic area (LHA) of mammals acts as the bed nucleus of the medial forebrain bundle (*mfb*), a massive fiber bundle that connects the basal telencephalon to the hindbrain through ascending and descending fibers (Nieuwenhuys et al., 1982). The presence of MCH neurons in the LHA serves a double purpose: it allows these neurons to receive a massive amount of information, at the same time granting access to distant areas of the CNS.

The Mammalian LHA is a large structure, with a very intricate pattern of parcellation based on its connections and neurochemistry (Swanson et al., 2005; Hahn, 2010). Melanin-concentrating hormone-ir neurons are found in the LHA of all studied Mammals, but its relative position within this structure varies. This is likely related to the particular area of the *mfb* that needs to be accessed by MCH neurons, since the *mfb* has a well-defined topographical distribution within the LHA. The LHA group of cells also varies substantially in its rostrocaudal and mediolateral extent among Mammalian clades. Usually, a second diencephalic group is present, in the form of a dorsomedial cluster of cells, which varies among species in terms of its proximity to the ventricle and rostrocaudal position and extent. A ventral thalamic group is often observed, corresponding to the *zona incerta* (ZI). Other groups besides these three will be highlighted for the appropriate species in the next sections.

4.5. Boreoeutheria > Laurasiatheria

Approximately 10 million years after the divergence of Boroeutheria, this clade split again into two groups: Laurasiatheria and Euarchontoglires. Laurasiatheria contains a diverse group of animals, including ungulates, bats, whales, and carnivores. There are only three species of Laurasiatherians with a described distribution of MCH neurons: the domestic cat (*Felis catus*), a Carnivore, and the Euungulates domestic pig (*Sus scrofa domesticus*) and sheep (*Ovis aries*) (Figure 4).

In Euungulates, MCH neurons have an extensive distribution in the rostrocaudal axis (Tillet et al., 1996; Chaillou et al., 2003; Chometton et al., 2014). This large extent results from the combination of the lateral group starting in the anterior hypothalamus, and the dorsomedial group prolonging into the anterior level of the ventral

tegmental nucleus. The main group of MCH neurons in the LHA is found in its ventral part, between the ventral margin of the internal capsule, the fornix, and the optic tract (Figure 6). Fewer MCH neurons are observed dorsal to the fornix, in the lateral part of the LHA. In the medial zone, a few immunoreactive cells are found in the internuclear space between the dorsomedial (DMH) and ventromedial (VMH) hypothalamic nuclei, while the periventricular zone is mostly devoid of labeling. The dorsomedial periventricular group of MCH cells is first observed within the posterior hypothalamic area (PHA). The most significant difference between pigs and sheep concerns the subthalamic area, as no cells were reported in the sheep ZI, while both the rostromedial and ventral ZI were reported to contain immunoreactive cells in pigs (Tillet et al., 1996; Chaillou et al., 2003; Chometton et al., 2014).

The distribution of fibers in Euungulates is extensive, and the primary projection pathways resemble those observed in Lissamphibians and Sauropsids. The anterior pathway conducts fibers to ventral telencephalic and subtelencephalic structures, including the cortical fields ventral to the rhinal sulcus, the dorsal *subiculum*, the *taenia tecta*, the amygdala, and the medial *septum*. Only a light innervation is observed in the hippocampus proper, and the dentate gyrus is mostly devoid of fibers. A dorsal pathway allows a sparse innervation of the midline thalamic nucleus, the habenular nuclei, and the *subthalamus*. A dense descending pathway takes fibers to most of the midbrain and hindbrain, including the optic *tectum*, the *substantia nigra*, the reticular formation and the periventricular gray matter, up to the dorsal horn of the spinal cord. Local dense hypothalamic projections are also observed, mostly restricted to the lateral zone in sheep, but more widespread in pigs. Some fibers are observed in the external layer of the ME (Tillet et al., 1996; Chaillou et al., 2003; Chometton et al., 2014).

The domestic cat, a Carnivore, shows several distinctive characteristics in its distribution of MCH-ir perikarya when compared to Euungulates. The large rostrocaudal extent is not observed, with neurons restricted to the tuberal and mammillary levels of the diencephalon. At tuberal levels, the largest group of neurons is found in the LHA, and, within it, in the perifornical nucleus. These neurons are mostly found in the medial LHA, directly dorsal and ventral to the fornix, making the distribution of MCH neurons in the cat substantially more dorsal than what is observed in Euungulates. Some neurons are also observed in the ventral ZI. In the medial hypothalamus, neurons are found in the dorsal hypothalamic area (DHA), dorsal to the DMH, and these neurons appear to be contiguous with neurons in the PHA (Figure 6). Immunoreactive neurons are not found at the level of the mammillary bodies (Torterolo et al., 2006; Badami et al., 2010).

While a pattern is easily observed for Euungulates, it is harder to discern an overarching pattern for Laurasiatherians. The two main group of cells observed in Lissamphibians are likely represented here, the LHA cells corresponding to the ventrolateral group, while the DHA/PHA group corresponds to the dorsal infundibular nucleus surrounding the 3V. In cats, however, the LHA cells migrated dorsally, occupying a dorsomedial position within the LHA. It is hard to determine, however, how representative of the Carnivores as a whole the distribution of cats is, as it is the only species of carnivore mapped to this point. The difference between Carnivora and Euungulata could correspond to the difference between feeding habits between these two clades, but more information is necessary to confirm this.

4.6. Boreoeutheria > Euarchontoglires > Rodentia

At approximately 90 MYA, the Euarchontoglires clade split into two major groups: Glires, containing rabbits, hares, and Rodents; and Primates, which includes lemurs, monkeys, and humans. Glires then split into

two major orders: Lagomorpha and Rodentia, at approximately 82 MYA (Kumar et al., 2017). The Glires clade is marked by the loss of one of the MCH receptor paralogs, making MCHR1 the only receptor found in those animals (Figure 4) (Tan et al., 2002). No information about the MCH system is available for Lagomorphs, while Rodents have been amply investigated due to their popularity as animal models. Rodentia is a complex order, with several molecular techniques employed to try to define the relationships between members of this order (Figure 7). Although order Rodentia is composed of several groups, only Muroidea has been investigated in terms of MCH distribution, leaving animals like beavers, squirrels, guinea pigs, and jerboas still to be studied. The two largest groups of Muroids are the Murids and the Cricetids, with these two groups splitting at approximately 33 MYA. The Muroids include the traditional laboratory models, the brown rat (*Rattus norvegicus*) and the house mouse (*Mus musculus*), which split at approximately 21 MYA (Kumar et al., 2017). Both rats and mice have been used to describe the distribution of MCH-ir elements (Bittencourt et al., 1992; Elias et al., 2001; Diniz et al., 2019b). The Cricetids include a diverse group of species, including voles (Arvicolinae), hamsters (Cricetinae), and deer mice (Neotominae) (Figure 7). The MCH system has been described in two hamsters, the golden hamster (*Mesocricetus auratus*) and the Siberian hamster (*Phodopus sungorus*) (Khorooshi and Klingenspor, 2005; Vidal et al., 2005), in addition to the Neotomine Mexican volcano mouse (*Neotomodon alstoni*) (Diniz et al., 2019b).

As mentioned before, the presence of MCH in the LHA is shared among all Mammals, and Rodents are no exception. In all cases, the largest cluster of MCH neurons is found in the dorsolateral tuberal LHA, lateral to the medial part of the internal capsule and cerebral peduncle (Figure 6). In *R. norvegicus*, *N. alstoni*, and *P. sungorus*, a large number of MCH neurons is observed within the limits of the perifornical nucleus, while *M. musculus* and *M. auratus* have only scattered cells in this area. The mediolateral extent of MCH cells within the LHA is also variable, with a continuous band of neurons from the pericapsular part to the medial hypothalamus observed in *R. norvegicus*, while in *M. musculus* MCH cells are mostly restricted to the areal lateral to the fornix. Dorsal to the LHA is a group of cells in the ventral ZI, observed in all Rodent species. The lateral cells are observed until the tuberomammillary level and disappear before the mammillary nuclei are fully formed. A comparison on the three-dimensional distribution of MCH cells in rats, mice, and volcano mice is available in Figure 8.

The medial zone of the hypothalamus, on the other hand, shows more variability between species. At the dorsalmost part of the medial zone of the hypothalamus rests a small group of MCH neurons intermingled with dopaminergic neurons the A13 group, corresponding to the IHy (Sita et al., 2003; 2007). The existence of a neurochemically defined IHy has been demonstrated in *R. norvegicus* (Sita et al., 2003; 2007) and *M. musculus* (Diniz et al., 2019b), and has been suggested in *N. alstoni* and *M. auratus* (Vidal et al., 2005; Diniz et al., 2019b). Ventral to the IHy is one of the two dorsomedial groups of MCH cells found in Rodents, the anterior hypothalamic area group (AHA). In *R. norvegicus*, these cells are scarce and separated from the IHy, while numerous neurons are found in the AHA of *M. musculus* and *N. alstoni*, and this group is virtually continuous with the IHy. The second group of dorsomedial MCH cells is found in the PHA, in close association with the 3V. This group is observed in *R. norvegicus*, *N. alstoni*, and *P. sungorus*, but not in *M. musculus* or *M. auratus*. In addition to those groups, rats and mice have been shown to have an additional time-sensitive group of MCH neurons that is detectable only in the medial preoptic area, preoptic periventricular nucleus, and anterior paraventricular hypothalamic area of lactating animals (Knollema et al., 1992; Rondini et al., 2010; Alvisi et al., 2016; Ferreira et al., 2017b; Costa et al., 2019; Diniz et al., 2019b). Several extra-diencephalic groups of MCH neurons have been identified exclusively in rats. In the basal forebrain, MCH neurons are found in the olfactory tubercle, and in the brain stem, immunolabeling is found in the laterodorsal tegmental nucleus, only in females, and in the paramedian pontine reticular formation

(Bittencourt et al., 1992; Bittencourt and Diniz, 2018). Brainstem MCH neurons have also been observed in the cat (Costa et al., 2018). Regarding the distribution of fibers, almost all areas of the rat CNS receive MCH-ir fibers to some extent, except for some motor nuclei of the hindbrain (Bittencourt et al., 1992).

As the available data reveals, a substantial expansion of the MCH system occurred in Rodents. The LHA is the main group of neurons, as in other Mammals, but this group is the most extensive in Rodents, including the whole pericapsular LHA, and often the medial LHA and the perifornical nucleus. This distribution is more lateral than what is observed in Carnivores, and more dorsal than what is observed in Euungulates, and varies substantially among Rodents. As mentioned before, such variability may be linked to preferential access to some parts of the mfb, leading to richer innervations of some areas when compared to others. These differences may be linked to the vastly different habits and behaviors displayed by Mammals. The dorsomedial group of cells is also substantially variable within the rostrocaudal and mediolateral axes. In rats, dorsomedial MCH neurons are very close to the third ventricle, and neuroendocrine areas are densely innervated (Bittencourt et al., 1992; Diniz et al., 2019b), while in mice these neurons drifted away from the periventricular zone and neuroendocrine areas appear to receive fewer fibers (Diniz et al., 2019b).

Although the contact between MCH and the ventricular lumen first observed in Petromyzontids appears to have been lost in the early Sarcopterygii lineage, at least in Rodents, this contact appears to have been reacquired, resulting in a volume transmission mode of communication for MCH neurons (Noble et al., 2018). Other aspects of the distribution of MCH neurons in Rodents may have counterparts in distant species, including the time-sensitive appearance of MCH neurons linked to reproductive stage (Petromyzontids, Anurans), neurons in the basal forebrain (Dipnoi), neurons in the brainstem (Carnivora), and neurons in a transitional structure between the hypothalamus and the subthalamus, in proximity to dopaminergic neurons (Anurans). The multiple independent acquisitions of the same morphological aspects indicate that, despite the frequent occurrence of losses, it is likely that underlying properties of the peptidergic system facilitate the reacquisition of lost characteristics, despite substantial divergence in terms of habitat and behavior among species.

4.7. Boreoeutheria > Euarchontoglires > Primates

Only two species of Primates have been examined in terms of MCH morphology: the tufted capuchin monkey, of the *Sapajus* genus, and humans (Figure 4). *Sapajus spp.* are new-world monkeys, member of Family Cebidae, which diverged at approximately 43 MYA. Member of genus Homo are believed to have split from their closest relatives, Pan, at approximately 6.7 MYA (Kumar et al., 2017). It should be noted that, in the original description of MCH in a new world monkey, the species has been identified as *Cebus apella* (Bittencourt et al., 1998). The taxonomic identification of the monkeys used in that experiment has been revised, as those animals are now more closely identified with members of genus *Sapajus*, and there is some controversy in the precise species definition (for a brief discussion on this subject, see Battagello et al. (2017)). In *Sapajus spp.*, MCH neurons are found exclusively in the diencephalon. These neurons are found from the caudal levels of the paraventricular nucleus up to the level of the medial mammillary nucleus, a distribution in the rostrocaudal axis that is slightly longer than Rodents, but shorter than Laurasiatherians. In the anterior tuberal hypothalamus, cells were observed dorsal to the fornix and in the dorsal part of the periventricular nucleus, in addition to the lateral ZI, but there is no indication that cells are found in the IHy area. At more caudal levels, the main group of neurons is observed occupying the LHA, but the medial zone is devoid of neurons (Figure 6). At mammillary levels, neurons are found dorsal to the medial mammillary nucleus and ventral to the mesencephalic aqueduct. Fibers were found in the

medial mammillary nucleus, the external layer of the ME, and the lateral *globus pallidus*, but a complete mapping of fibers has not been published (Bittencourt et al., 1998).

Several authors investigated the distribution of MCH neurons in humans of male and female individuals, both through *in situ* hybridization for *PMCH* (Elias et al., 1998; Krolewski et al., 2010) or immunohistochemistry for MCH (Thannickal et al., 2007; Aziz et al., 2008). Due to how detailed is the description provided by Krolewski et al. (2010), it will be used as a base to describe the distribution of MCH in *H. sapiens*. Neurons expressing *PMCH* mRNA are first detected in the LHA, at the intermediate levels of the PVH. While Krolewski et al. (2010) identified these anterior neurons as belonging to the LHA, Elias et al. (1998) identified them as part of the rostromedial ZI, possibly corresponding to the Muroid IHy. As the PVH nears its caudal end, the distribution of *PMCH* mRNA-expressing neurons expands to the lateral aspects of the LHA, and two new groups are observed: the DMH and the DHA (Krolewski et al., 2010). Together, these groups give the impression that MCH neurons surround the whole tuberomammillary extent of the fornix (Figure 6) (Elias et al., 1998). A dense cluster of MCH neurons in the DHA forms a ring-shaped structure around a central core of non-labeled cells (Krolewski et al., 2010). This observation is particularly interesting, as Diniz et al. (2019b) recently proposed that, in *M. musculus*, MCH neurons form a ring-shaped structure in the LHA surrounding ORX neurons, a neurochemical division called the LHA shell. It is possible that a similar feature appears in humans, with MCH neurons surrounding another population of neurons. Finally, at the level of the mammillary bodies, the DHA continues into the PHA, which assumes a position close to the 3V.

In addition to the distribution of neurons, the number of MCH neurons has also been investigated, particularly in studies evaluating hypothalamic correlates in neurodegenerative diseases. Thannickal et al. (2007) report a loss of MCH neurons throughout the anteroposterior axis that is correlated with Parkinson's Disease stage, ranging from 12% of loss in Stage I to 74% of loss in Stage V. Aziz et al. (2008) performed a similar experiment in Huntington's Disease patients, but found no loss of MCH neurons in patients as compared to the controls. Regarding immunoreactive fibers, only Elias et al. (1998) reported fibers immunoreactivity, citing areas such as the cingulate and insular cortex, amygdala, hippocampus, anterior thalamic nucleus, preoptic hypothalamus, and mammillary bodies are recipients of fibers. These innervation fields are compatible with what has been described in other mapping studies for mammals.

Considering the data available, the distribution of MCH neurons in Primates appears to be mostly conserved. Both *S. apella* and *H. sapiens* share the same rostrocaudal extent, and the areas containing the most substantial numbers of neurons are the same. Some crucial questions are still open, however. It is unclear, at this point, if Primates have an IHy similar to Murids, where MCH neurons are found intermingled with tyrosine hydroxylase-synthesizing neurons. The second question is the presence of MCH neurons in the zona incerta, as Bittencourt et al. (1998) reported cells in the lateral ZI of *Sapajus spp.*, but the same has not been reported in humans (Elias et al., 1998; Krolewski et al., 2010). Furthermore, there is no complete mapping of MCH fibers in the human brain and no physical evidence that NEI is synthesized in Primates. The overall pattern observed in Primates appears to be unique to this clade, as the rostrocaudal extent of MCH neurons is longer in Primates than it is in Rodents but shorter than what has been described for Laurasiatherians. It is a common feature between Euarchontoglires, however, the predominance of neurons dorsal to the fornix, and a lateromedial presence of neurons that spans the lateral and medial zones, with only the rat presenting a dense cluster of cells in the periventricular nucleus. There is a high number of labeled neurons around the fornix in several Euarchontoglires species (with the exception of mice and golden hamsters), but it is possible that the neurons observed in humans

are actually part of other nuclei in the hypothalamus, compressed against the fornix due to the reduced lateromedial extent of the hypothalamus in the Primate lineage.

5. Conclusion

The melanin-concentrating hormone peptidergic system is a versatile neurochemical element, demonstrated to play a varied range of roles within the Rodent nervous system. Such functional diversity is only possible thanks to a complex morphological substrate, which has been investigated in a substantial number of species. This morphological substrate, however, is not a universal feature, varying among species and clades, likely reflecting differences in habitat and behavior. This interplay between MCH probably developed from the initial function of MCH: broadcaster of external stimuli. By contacting the ventricular lumen with fine projections while projecting to the lateral hypothalamus and thalamus, MCH neurons were able to coordinate metabolic signals present in the CSF with effector centers of the diencephalon. As vertebrates evolved to display more complex behaviors and a richer relationship with their environment, MCH neurons that could integrate not only endogenous signals, but also external inputs were selected, and this is reflected in a drift of MCH cells away from the ventricle. This aligns well with the idea that MCH is a major integrator of internal and external information, ensuring an appropriate response to ensure the organism homeostasis. It would not be possible, however, if all organisms shared identical MCH organizations, given the different challenges imposed by different aquatic/terrestrial environments, food chain positions, and reproductive strategies. New studies of the MCH system in species that have not been investigated yet will help us understand more precisely how these habitat changes are connected to the hypothalamic neurochemical circuits, paving the way to new intervention strategies that may be used with pharmacological purposes.

Perhaps even more important than knowledge about the MCH system, however, is a better understanding of how large-scale genomic events have impacted neurochemical systems. In this article, we propose that MCH developed right after the first round of whole-genome duplication that occurred in the Chordate lineage, from a newly formed paralog of an invertebrate peptide combined with ancestral somatostatin receptors. While the second round of genome duplication resulted in the formation of two MCH receptor paralogs, the third round (specific to the Teleost lineage) developed two MCH peptides, which evolved to acquire different sequences, distributions within the SNC, and functions. This is telling of how plastic even the most essential neurochemical systems can be, and the potential that results from loosened evolutionary constraints secondary to whole-genome duplications. It is likely that the duplication of hypothalamic neuropeptides allowed vertebrates to developed increasingly complex circuits, which then led to a successful colonization of new habitats.

References

Al-Yousuf, S.a., and Mizuno, N. (1991). Electron microscopic identification of axons containing melanin-concentrating hormone in the lamprey, Lampetra fluviatilis L. *Neuroscience letters* 128(2)**,** 249-252. doi: 10.1016/0304-3940(91)90272-U.

Alachkar, A., Alhassen, L., Wang, Z., Wang, L., Onouye, K., Sanathara, N., et al. (2016). Inactivation of the melanin concentrating hormone system impairs maternal behavior. *European Neuropsychopharmacology* 26(11)**,** 1826-1835. doi: 10.1016/j.euroneuro.2016.08.014.

Alhassen, L., Phan, A., Alhassen, W., Nguyen, P., Lo, A., Shaharuddin, H., et al. (2019). The role of Olfaction in MCH-regulated spontaneous maternal responses. *Brain research* 1719**,** 71-76.

Allendorf, F., and Thorgaard, G. (1984). Evolutionary genetics of fishes. *Tetraploidy and the Evolution of Salmonid Fishes***,** 55-93.

Alvisi, R.D., Diniz, G.B., Da-Silva, J.M., Bittencourt, J.C., and Felicio, L.F. (2016). Suckling-induced Fos activation and melanin-concentrating hormone immunoreactivity during late lactation. *Life sciences* 148**,** 241-246. doi: 10.1016/j.lfs.2016.02.038.

Amano, M., Takahashi, A., Oka, Y., Yamanome, T., Kawauchi, H., and Yamamori, K. (2003). Immunocytochemical localization and ontogenic development of melanin-concentrating hormone in the brain of a pleuronectiform fish, the barfin flounder. *Cell and tissue research* 311(1)**,** 71-77.

Amiya, N., Amano, M., Iigo, M., Yamanome, T., Takahashi, A., and Yamamori, K. (2008a). Interaction of orexin/hypocretin-like immunoreactive neurons with melanin-concentrating hormone and α-melanocyte-stimulating hormone neurons in brain of a pleuronectiform fish, barfin flounder. *Fisheries science* 74(5)**,** 1040-1046. doi: 10.1111/j.1444-2906.2008.01622.x.

Amiya, N., Amano, M., Yamanome, T., Yamamori, K., and Takahashi, A. (2008b). Effects of background color on GnRH and MCH levels in the barfin flounder brain. *General and comparative endocrinology* 155(1)**,** 88-93. doi: 10.1016/j.ygcen.2007.03.007.

An, S., Cutler, G., Zhao, J.J., Huang, S.-G., Tian, H., Li, W., et al. (2001). Identification and characterization of a melanin-concentrating hormone receptor. *Proceedings of the National Academy of Sciences* 98(13)**,** 7576-7581. doi: 10.1073/pnas.131200698.

Andersen, A.C., Pelletier, G., Eberle, A.N., Leroux, P., Jegou, S., and Vaudry, H. (1986). Localization of melanin-concentrating hormone-like immunoreactivity in the brain and pituitary of the frog Rana ridibunda. *Peptides* 7(6)**,** 941-951.

Audinot, V., Beauverger, P., Lahaye, C., Suply, T., Rodriguez, M., Ouvry, C., et al. (2001). Structure-activity relationship studies of melanin-concentrating hormone (MCH)-related peptide ligands at SLC-1, the human MCH receptor. *Journal of Biological Chemistry* 276(17)**,** 13554-13562. doi: 10.1074/jbc.M010727200.

Aziz, A., Fronczek, R., Maat-Schieman, M., Unmehopa, U., Roelandse, F., Overeem, S., et al. (2008). Hypocretin and melanin-concentrating hormone in patients with Huntington disease. *Brain pathology* 18(4)**,** 474-483.

Bächner, D., Kreienkamp, H.-J., Weise, C., Buck, F., and Richter, D. (1999). Identification of melanin concentrating hormone (MCH) as the natural ligand for the orphan somatostatin-like receptor 1 (SLC-1). *FEBS letters* 457(3)**,** 522-524. doi: 10.1016/S0014-5793(99)01092-3.

Badami, V.M., Rice, C.D., Lois, J.H., Madrecha, J., and Yates, B.J. (2010). Distribution of hypothalamic neurons with orexin (hypocretin) or melanin concentrating hormone (MCH) immunoreactivity and multisynaptic connections with diaphragm motoneurons. *Brain research* 1323**,** 119-126. doi: 10.1016/j.brainres.2010.02.002.

Baker, B., Levy, A., Hall, L., and Lightman, S. (1995). Cloning and expression of melanin-concentrating hormone genes in the rainbow trout brain. *Neuroendocrinology* 61(1)**,** 67-76. doi: 10.1159/000126814.

Baker, B.I., and Bird, D.J. (2002). Neuronal organization of the melanin-concentrating hormone system in primitive actinopterygians: Evolutionary changes leading to teleosts. *Journal of Comparative Neurology* 442(2)**,** 99-114. doi: 10.1002/cne.10074.

Baker, B.I., and Rance, T.A. (1983). Further observations on the distribution and properties of teleost melanin concentrating hormone. *General and comparative endocrinology* 50(3)**,** 423-431. doi: 10.1016/0016-6480(83)90263-0.

Battagello, D.S., Diniz, G.B., Candido, P.L., da Silva, J.M., de Oliveira, A.R., Torres da Silva, K.R., et al. (2017). Anatomical Organization of Urocortin 3-Synthesizing Neurons and Immunoreactive Terminals in the Central Nervous System of Non-Human Primates [Sapajus spp.]. *Frontiers in Neuroanatomy* 11**,** 57. doi: 10.3389/fnana.2017.00057.

Batten, T.F.C., and Baker, B.I. (1988). Melanin-concentrating hormone (MCH) immunoreactive hypophysial neurosecretory system in the teleost Poecilia latipinna: light and electron microscopic study. *General and comparative endocrinology* 70(2)**,** 193-205. doi: 10.1016/0016-6480(88)90140-2.

Batten, T.F.C., Moons, L., and Vandesande, F. (1999). Innervation and control of the adenohypophysis by hypothalamic peptidergic neurons in teleost fishes: EM immunohistochemical evidence. *Microscopy research and technique* 44(1)**,** 19-35. doi: 10.1002/(SICI)1097-0029(19990101)44:1<19::AID-JEMT4>3.0.CO;2-L.

Benedetto, L., Pereira, M., Ferreira, A., and Torterolo, P. (2014). Melanin-concentrating hormone in the medial preoptic area reduces active components of maternal behavior in rats. *Peptides* 58**,** 20-25. doi: 10.1016/j.peptides.2014.05.012.

Berman, J.R., Skariah, G., Maro, G.S., Mignot, E., and Mourrain, P. (2009). Characterization of two melanin-concentrating hormone genes in zebrafish reveals evolutionary and physiological links with the mammalian MCH system. *Journal of Comparative Neurology* 517(5)**,** 695-710. doi: 10.1002/cne.22171.

Bird, D.J., Baker, B.I., and Kawauchi, H. (1989). Immunocytochemical demonstration of melanin-concentrating hormone and proopiomelanocortin-like products in the brain of the trout and carp. *General and comparative endocrinology* 74(3)**,** 442-450. doi: 10.1016/S0016-6480(89)80042-5.

Bird, D.J., Potter, I.C., Sower, S.A., and Baker, B.I. (2001). The distribution of melanin-concentrating hormone in the lamprey brain. *General and comparative endocrinology* 121(3)**,** 232-241. doi: 10.1006/gcen.2001.7609.

Bittencourt, J.C., and Diniz, G.B. (2018). "Neuroanatomical Structure of the MCH System," in *Melanin-Concentrating Hormone and Sleep*. 1st ed: Springer), 1-46.

Bittencourt, J.C., Frigo, L., Rissman, R.A., Casatti, C.A., Nahon, J.-L., and Bauer, J.A. (1998). The distribution of melanin-concentrating hormone in the monkey brain (Cebus apella). *Brain Research* 804(1)**,** 140-143. doi: 10.1016/S0006-8993(98)00662-3.

Bittencourt, J.C., Presse, F., Arias, C., Peto, C.A., Vaughan, J.M., Nahon, J.-L., et al. (1992). The melanin-concentrating hormone system of the rat brain: an immuno- and hybridization histochemical characterization. *The Jorunal of Comparative Neurology* 319(2)**,** 218-245. doi: 10.1002/cne.903190204.

Blake, J.A., Eppig, J.T., Kadin, J.A., Richardson, J.E., Smith, C.L., Bult, C.J., et al. (2016). Mouse Genome Database (MGD)-2017: community knowledge resource for the laboratory mouse. *Nucleic acids research* 45(D1)**,** D723-D729.

Borsu, L., Presse, F., and Nahon, J.-L. (2000). The AROM gene, spliced mRNAs encoding new DNA/RNA-binding proteins are transcribed from the opposite strand of the melanin-concentrating hormone gene in mammals. *Journal of Biological Chemistry* 275(51)**,** 40576-40587. doi: 10.1074/jbc.M006524200.

Braschi, B., Denny, P., Gray, K., Jones, T., Seal, R., Tweedie, S., et al. (2018). Genenames. org: the HGNC and VGNC resources in 2019. *Nucleic acids research* 47(D1)**,** D786-D792.

Brodin, L., Theordorsson, E., Christenson, J., Cullheim, S., Hökfelt, T., Brown, J.C., et al. (1990). Neurotensin-like peptides in the CNS of lampreys: chromatographic characterization and immunohistochemical localization with reference to aminergic markers. *European Journal of Neuroscience* 2(12)**,** 1095-1109.

Burt, D.W., Carrë, W., Fell, M., Law, A.S., Antin, P.B., Maglott, D.R., et al. (Year). "The chicken gene nomenclature committee report", in: *BMC genomics*: BioMed Central), S5.

Cánepa, M., Pozzi, A., Astola, A., Maggese, M.C., and Vissio, P. (2008). Effect of salmon melanin-concentrating hormone and mammalian gonadotrophin-releasing hormone on somatolactin release in pituitary culture of Cichlasoma dimerus. *Cell and tissue research* 333(1)**,** 49. doi: 10.1007/s00441-008-0622-8.

Cardot, J., Fellmann, D., and Bugnon, C. (1994). Melanin-concentrating hormone-producing neurons in reptiles. *General and comparative endocrinology* 94(1)**,** 23-32. doi: 10.1006/gcen.1994.1056.

Cardot, J., Griffond, B., Risold, P.Y., Blähser, S., and Fellmann, D. (1999). Melanin-concentrating hormone-producing neurons in birds. *Journal of Comparative Neurology* 411(2)**,** 239-256. doi: 10.1002/(SICI)1096-9861(19990823)411:2<239::AID-CNE5>3.0.CO;2-7.

Cerdá-Reverter, J.M., Canosa, L.F., and Peter, R.E. (2006). Regulation of the hypothalamic melanin-concentrating hormone neurons by sex steroids in the goldfish: possible role in the modulation of luteinizing hormone secretion. *Neuroendocrinology* 84(6)**,** 364-377.

Chaillou, E., Baumont, R., Fellmann, D., Tramu, G., and Tillet, Y. (2003). Sensitivity of Galanin-and Melanin-Concentrating Hormone-Containing Neurones to Nutritional Status: An Immunohistochemical Study in the Ovariectomized Ewe. *Journal of neuroendocrinology* 15(5)**,** 459-467. doi: 10.1046/j.1365-2826.2003.00998.x.

Chambers, J., Ames, R.S., Bergsma, D., Muir, A., Fitzgerald, L.R., Hervieu, G., et al. (1999). Melanin-concentrating hormone is the cognate ligand for the orphan G-protein-coupled receptor SLC-1. *Nature* 400(6741)**,** 261-265. doi: 10.1038/22313.

Chometton, S., Franchi, G., Houdayer, C., Mariot, A., Poncet, F., Fellmann, D., et al. (2014). Different distributions of preproMCH and hypocretin/orexin in the forebrain of the pig (Sus scrofa domesticus). *Journal of chemical neuroanatomy* 61**,** 72-82. doi: 10.1016/j.jchemneu.2014.08.001.

Costa, A., Castro-Zaballa, S., Lagos, P., Chase, M.H., and Torterolo, P. (2018). Distribution of MCH-containing fibers in the feline brainstem: Relevance for REM sleep regulation. *Peptides* 104**,** 50-61. doi: 10.1016/j.peptides.2018.04.009.

Costa, H.C., Da-Silva, J.M., Diniz, G.B., Da-Silva Pereira, L., Gobbo, D.R., Da-Silva, R.J., et al. (2019). Characterization and origins of melanin-concentrating hormone immunoreactive fibers of the posterior lobe of the pituitary and median eminence during lactation in Long-Evans rat. *Journal of Neuroendocrinology* 00:e12723. doi: 10.1111/jne.12723.

Courseaux, A., and Nahon, J.-L. (2001). Birth of two chimeric genes in the Hominidae lineage. *Science* 291(5507)**,** 1293-1297. doi: 10.1126/science.1057284.

Croizier, S., Cardot, J., Brischoux, F., Fellmann, D., Griffond, B., and Risold, P. (2013). The vertebrate diencephalic MCH system: a versatile neuronal population in an evolving brain. *Frontiers in neuroendocrinology* 34(2)**,** 65-87.

Cropper, E.C., Jing, J., Vilim, F.S., Barry, M.A., and Weiss, K.R. (2018). Multifaceted expression of peptidergic modulation in the feeding system of Aplysia. *ACS chemical neuroscience* 9(8)**,** 1917-1927. doi: 10.1021/acschemneuro.7b00447.

Cropper, E.C., Miller, M.W., Tenenbaum, R., Kolks, M.A.G., Kupfermann, I., and Weiss, K.R. (1988). Structure and action of buccalin: a modulatory neuropeptide localized to an identified small cardioactive peptide-containing cholinergic motor neuron of Aplysia californica. *Proceedings of the National Academy of Sciences* 85(16)**,** 6177-6181. doi: 10.1073/pnas.85.16.6177.

[Dataset] Diniz, G.B., Battagello, D.S., Cherubini, P.M., Reyes-Mendoza, J.D., Luna-Illades, C., Klein, M.O., et al. (2019a). *Melanin- concentrating hormone peptidergic system: Comparative morphology between muroid species - dataset 1.* Open Society Foundations. doi: https://doi.org/10.17605/OSF.IO/ZRK2V.

Diniz, G.B., Battagello, D.S., Cherubini, P.M., Reyes-Mendoza, J.D., Luna-Illades, C., Klein, M.O., et al. (2019b). Melanin-concentrating hormone peptidergic system: comparative morphology between muroid species. *Journal of Comparative Neurology* In press

Diniz, G.B., and Bittencourt, J.C. (2017). The Melanin-Concentrating Hormone as an Integrative Peptide Driving Motivated Behaviors. *Frontiers in Systems Neuroscience* 11**,** 1-32. doi: 10.3389/fnsys.2017.00032.

Duarte, G., Segura-Noguera, M., Del Río, M.M., and Mancera, J. (2001). The hypothalamo-hypophyseal system of the white seabream Diplodus sargus: immunocytochemical identification of arginine-vasotocin, isotocin, melanin-concentrating hormone and corticotropin-releasing factor. *The Histochemical Journal* 33(9-10)**,** 569-578. doi: 10.1023/A:1014912110318.

Elias, C.F., Lee, C.E., Kelly, J.F., Ahima, R.S., Kuhar, M., Saper, C.B., et al. (2001). Characterization of CART neurons in the rat and human hypothalamus. *Journal of Comparative Neurology* 432(1)**,** 1-19. doi: 10.1002/cne.1085.

Elias, C.F., Saper, C.B., Maratos-Flier, E., Tritos, N.A., Lee, C., Kelly, J., et al. (1998). Chemically defined projections linking the mediobasal hypothalamus and the lateral hypothalamic area. *Journal of Comparative Neurology* 402(4)**,** 442-459. doi: 10.1002/(SICI)1096-9861(19981228)402:4<442::AID-CNE2>3.0.CO;2-R

Fabre, P.-H., Hautier, L., Dimitrov, D., and Douzery, E.J.P. (2012). A glimpse on the pattern of rodent diversification: a phylogenetic approach. *BMC Evolutionary Biology* 12**,** 88. doi: 10.1186/1471-2148-12-88.

Ferreira, J.G.P., Bittencourt, J.C., and Adamantidis, A. (2017a). Melanin-concentrating hormone and sleep. *Current Opinion in Neurobiology* 44**,** 152-158. doi: 10.1016/j.conb.2017.04.008.

Ferreira, J.G.P., Duarte, J.C.G., Diniz, G.B., and Bittencourt, J.C. (2017b). Litter size determines the number of melanin-concentrating hormone neurons in the medial preoptic area of Sprague Dawley lactating dams. *Physiology & Behavior* 181**,** 75-79. doi: j.physbeh.2017.08.028.

Francis, K., and Baker, B.I. (1995). Developmental changes in melanin-concentrating hormone in Rana temporaria. *General and comparative endocrinology* 98(2)**,** 157-165.

Friedman, M. (2010). Explosive morphological diversification of spiny-finned teleost fishes in the aftermath of the end-Cretaceous extinction. *Proceedings of the Royal Society B: Biological Sciences* 277(1688)**,** 1675-1683. doi: 10.1098/rspb.2009.2177.

Gröneveld, D., Hut, M.J., Balm, P.H.M., Martens, G.J.M., and Bonga, S.E.W. (1993). Cloning and sequence analysis of hypothalamus cDNA encoding tilapia melanin-concentrating hormone. *Fish physiology and biochemistry* 11(1-6)**,** 117. doi: 10.1007/BF00004557.

Hahn, J.D. (2010). Comparison of melanin-concentrating hormone and hypocretin/orexin peptide expression patterns in a current parceling scheme of the lateral hypothalamic zone. *Neuroscience Letters* 468(1)**,** 12-17. doi: 10.1016/j.neulet.2009.10.047.

Hill, J., Duckworth, M., Murdock, P., Rennie, G., Sabido-David, C., Ames, R.S., et al. (2001). Molecular cloning and functional characterization of MCH2, a novel human MCH receptor. *Journal of Biological Chemistry* 276(23)**,** 20125-20129. doi: 10.1074/jbc.M102068200.

Hogben, L.T., and Slome, D. (1931). The pigmentary effector system. VI. The dual character of endocrine co-ordination in amphibian colour change. *Proceedings of the Royal Society of London. Series B, Containing Papers of a Biological Character* 108(755)**,** 10-53. doi: 10.1098/rspb.1931.0020.

Hosomi, N., Masumoto, T., and Fukada, H. (2015). Yellowtail melanin-concentrating hormone 1: molecular cloning, tissue distribution, and response to fasting and feeding. *Aquaculture Science* 63(2)**,** 169-178. doi: 10.11233/aquaculturesci.63.169.

Huesa, G., van den Pol, A.N., and Finger, T.E. (2005). Differential distribution of hypocretin (orexin) and melanin-concentrating hormone in the goldfish brain. *Journal of Comparative Neurology* 488(4)**,** 476-491. doi: 10.1002/cne.20610.

Ide, H., Kawazoe, I., and Kawauchi, H. (1985). Fish melanin-concentrating hormone disperses melanin in amphibian melanophores. *General and comparative endocrinology* 58(3)**,** 486-490. doi: 10.1016/0016-6480(85)90123-6.

Kang, D.-Y., and Kim, H.-C. (2013). Functional characterization of two melanin-concentrating hormone genes in the color camouflage, hypermelanosis, and appetite of starry flounder. *General and comparative endocrinology* 189**,** 74-83. doi: 10.1016/j.ygcen.2013.04.025.

Karimi, K., Fortriede, J.D., Lotay, V.S., Burns, K.A., Wang, D.Z., Fisher, M.E., et al. (2017). Xenbase: a genomic, epigenomic and transcriptomic model organism database. *Nucleic acids research* 46(D1)**,** D861-D868.

Kawauchi, H., Kawazoe, I., Tsubokawa, M., Kishida, M., and Baker, B.I. (1983). Characterization of melanin-concentrating hormone in chum salmon pituitaries. *Nature* 305(5932)**,** 321-323. doi: 10.1038/305321a0.

Khorooshi, R.M.H., and Klingenspor, M. (2005). Neuronal distribution of melanin-concentrating hormone, cocaine-and amphetamine-regulated transcript and orexin B in the brain of the Djungarian hamster

(Phodopus sungorus). *Journal of Chemical Neuroanatomy* 29(2), 137-148. doi: 10.1016/j.jchemneu.2004.10.003.

Knollema, S., Brown, E.R., Vale, W., and Sawchenko, P.E. (1992). Novel hypothalamic and preoptic sites of prepro-melanin-concentrating hormone messenger ribonucleic Acid and Peptide expression in lactating rats. *Journal of Neuroendocrinology* 4(6), 709-717. doi: 10.1111/j.1365-2826.1992.tb00222.x.

Kolakowski Jr, L.F., Jung, B.P., Nguyen, T., Johnson, M.P., Lynch, K.R., Cheng, R., et al. (1996). Characterization of a human gene related to genes encoding somatostatin receptors. *FEBS letters* 398(2-3), 253-258.

Kreienkamp, H.-J., Larusson, H.J., Witte, I., Roeder, T., Birgül, N., Hönck, H.-H., et al. (2002). Functional annotation of two orphan G-protein-coupled receptors, Drostar1 and-2, from Drosophila melanogaster and their ligands by reverse pharmacology. *Journal of Biological Chemistry* 277(42), 39937-39943.

Krolewski, D.M., Medina, A., Kerman, I.A., Bernard, R., Burke, S., Thompson, R.C., et al. (2010). Expression patterns of corticotropin-releasing factor, arginine vasopressin, histidine decarboxylase, melanin-concentrating hormone, and orexin genes in the human hypothalamus. *Journal of Comparative Neurology* 518(22), 4591-4611.

Kumar, S., Stecher, G., Suleski, M., and Hedges, S.B. (2017). TimeTree: a resource for timelines, timetrees, and divergence times. *Molecular biology and evolution* 34(7), 1812-1819. doi: 10.1093/molbev/msx116.

Kusumi, K., Kulathinal, R.J., Abzhanov, A., Boissinot, S., Crawford, N.G., Faircloth, B.C., et al. (2011). Developing a community-based genetic nomenclature for anole lizards. *BMC genomics* 12(1), 554.

Lakaye, B., Minet, A., Zorzi, W., and Grisar, T. (1998). Cloning of the rat brain cDNA encoding for the SLC-1 G protein-coupled receptor reveals the presence of an intron in the gene. *Biochimica et Biophysica Acta (BBA)-Molecular Cell Research* 1401(2), 216-220.

Lázár, G., Maderdrut, J.L., and Merchenthaler, I. (2002). Distribution of melanin-concentrating hormone-like immunoreactivity in the central nervous system of Rana esculenta. *Brain research bulletin* 57(3-4), 401-407.

Lembo, P.M.C., Grazzini, E., Cao, J., Hubatsch, D.A., Pelletier, M., Hoffert, C., et al. (1999). The receptor for the orexigenic peptide melanin-concentrating hormone is a G-protein-coupled receptor. *Nature cell biology* 1(5), 267. doi: 10.1038/12978.

Lloyd, P.E. (1986). The small cardioactive peptides: a class of modulatory neuropeptides in Aplysia. *Trends in Neurosciences* 9, 428-432. doi: 10.1016/0166-2236(86)90138-4.

Lloyd, P.E., Kupfermann, I., and Weiss, K.R. (1984). Evidence for parallel actions of a molluscan neuropeptide and serotonin in mediating arousal in Aplysia. *Proceedings of the National Academy of Sciences* 81(9), 2934-2937. doi: 10.1073/pnas.81.9.2934.

Lloyd, P.E., Mahon, A., Kupfermann, I., Cohen, J., Scheller, R., and Weiss, K.R. (1985). Biochemical and immunocytological localization of molluscan small cardioactive peptides in the nervous system of Aplysia californica. *Journal of Neuroscience* 5(7), 1851-1861. doi: 10.1073/pnas.81.9.2934.

Loi, P.K., Saunders, R.G., Young, D.C., and Tublitz, N.J. (1996). Peptidergic regulation of chromatophore function in the European cuttlefish Sepia officinalis. *Journal of experimental biology* 199(5), 1177-1187.

Lovejoy, D.A., and de Lannoy, L. (2013). Evolution and phylogeny of the corticotropin-releasing factor (CRF) family of peptides: expansion and specialization in the vertebrates. *Journal of chemical neuroanatomy* 54, 50-56. doi: 10.1016/j.jchemneu.2013.09.006.

Macdonald, D., Murgolo, N., Zhang, R., Durkin, J.P., Yao, X., Strader, C.D., et al. (2000). Molecular characterization of the melanin-concentrating hormone/receptor complex: identification of critical residues involved in binding and activation. *Molecular Pharmacology* 58(1), 217-225. doi: 10.1124/mol.58.1.217.

Mancera, J., and Fernández-Llebrez, P. (1995). Development of melanin-concentrating hormone-immunoreactive elements in the brain of gilthead seabream (Sparus auratus). *Cell and tissue research* 282(3), 523-526. doi: 10.1007/BF00318885.

Masao, O., Chieki, W., Ikuo, O., Ichiro, K., and Hiroshi, K. (1988). Structures of two kinds of mRNA encoding the chum salmon melanin-concentrating hormone. *Gene* 71(2)**,** 433-438. doi: 10.1016/0378-1119(88)90060-1.

Matsuda, K., Shimakura, S.-I., Maruyama, K., Miura, T., Uchiyama, M., Kawauchi, H., et al. (2006). Central administration of melanin-concentrating hormone (MCH) suppresses food intake, but not locomotor activity, in the goldfish, Carassius auratus. *Neuroscience letters* 399(3)**,** 259-263. doi: 10.1016/j.neulet.2006.02.005.

Meurling, P., and Rodríguez, E.M. (1990). The paraventricular and posterior recess organs of elasmobranchs: A system of cerebrospinal fluid-contacting neurons containing immunoreactive serotonin and somatostatin. *Cell and Tissue Research* 259(3)**,** 463-473. doi: 10.1007/BF01740772.

Meyer, A., and Van de Peer, Y. (2005). From 2R to 3R: evidence for a fish-specific genome duplication (FSGD). *Bioessays* 27(9)**,** 937-945. doi: 10.1002/bies.20293.

Minth, C.D., QIu, H., Akil, H., Watson, S.J., and Dixon, J.E. (1989). Two precursors of melanin-concentrating hormone: DNA sequence analysis and in situ immunochemical localization. *Proceedings of the National Academy of Sciences* 86(11)**,** 4292-4296. doi: 10.1073/pnas.86.11.4292.

Mizusawa, K., Amiya, N., Yamaguchi, Y., Takabe, S., Amano, M., Breves, J.P., et al. (2012). Identification of mRNAs coding for mammalian-type melanin-concentrating hormone and its receptors in the scalloped hammerhead shark Sphyrna lewini. *General and comparative endocrinology* 179(1)**,** 78-87. doi: 10.1016/j.ygcen.2012.07.023.

Mizusawa, K., Kawashima, Y., Sunuma, T., Hamamoto, A., Kobayashi, Y., Kodera, Y., et al. (2015). Involvement of melanin-concentrating hormone 2 in background color adaptation of barfin flounder Verasper moseri. *General and comparative endocrinology* 214**,** 140-148. doi: 10.1016/j.ygcen.2014.07.008.

Moldovan, G.-L., Dejsuphong, D., Petalcorin, M.I.R., Hofmann, K., Takeda, S., Boulton, S.J., et al. (2012). Inhibition of homologous recombination by the PCNA-interacting protein PARI. *Molecular cell* 45(1)**,** 75-86. doi: 10.1016/j.molcel.2011.11.010.

Mori, M., Harada, M., Terao, Y., Sugo, T., Watanabe, T., Shimomura, Y., et al. (2001). Cloning of a novel G protein-coupled receptor, SLT, a subtype of the melanin-concentrating hormone receptor. *Biochemical and Biophysical Research Communications* 283(5)**,** 1013-1018. doi: 10.1006/bbrc.2001.4893.

Nahon, J.-L., Presse, F., Bittencourt, J.C., Sawchenko, P.E., and Vale, W. (1989). The rat melanin-concentrating hormone messenger ribonucleic acid encodes multiple putative neuropeptides coexpressed in the dorsolateral hypothalamus. *Endocrinology* 125(4)**,** 2056-2065. doi: 10.1210/endo-125-4-2056.

Nahon, J.L., Presset, F., Schoepfer, R., and Vale, W. (1991). Identification of a single melanin-concentrating hormone messenger ribonucleic acid in coho salmon: structural relatedness with 7SL ribonucleic acid. *Journal of neuroendocrinology* 3(2)**,** 173-183. doi: 10.1111/j.1365-2826.1991.tb00260.x.

Naito, N., Nakai, Y., Kawauchi, H., and Hayashi, Y. (1985). Immunocytochemical identification of melanin-concentrating hormone in the brain and pituitary gland of the teleost fishes Oncorhynchus keta and Salmo gairdneri. *Cell and tissue research* 242(1)**,** 41-48.

Naufahu, J., Cunliffe, A.D., and Murray, J.F. (2013). The roles of melanin-concentrating hormone in energy balance and reproductive function: are they connected? *Reproduction* 146(5)**,** R141-R150. doi: 10.1530/REP-12-0385.

Nieuwenhuys, R., Geeraedts, L.M.G., and Veening, J.G. (1982). The medial forebrain bundle of the rat. I. General introduction. *Journal of Comparative Neurology* 206(1)**,** 49-81. doi: 10.1002/cne.902060106

Nishihara, H., Maruyama, S., and Okada, N. (2009). Retroposon analysis and recent geological data suggest near-simultaneous divergence of the three superorders of mammals. *Proceedings of the National Academy of Sciences* 106(13)**,** 5235-5240. doi: 10.1073/pnas.0809297106.

Noble, E.E., Hahn, J.D., Konanur, V.R., Hsu, T.M., Page, S.J., Cortella, A.M., et al. (2018). Control of Feeding Behavior by Cerebral Ventricular Volume Transmission of Melanin-Concentrating Hormone. *Cell metabolism* 28(1)**,** 55-68.e57. doi: 10.1016/j.cmet.2018.05.001.

Nozaki, M., Tsukahara, T., and Kobayashi, H. (1983). An immunocytochemical study on the distribution of neuropeptides in the brain of certain species of fish. *BIOMEDICAL RESEARCH-TOKYO* 4**,** 135-143.

Ohno, S. (2013). *Evolution by gene duplication.* Springer Science & Business Media.

Pandolfi, M., Cánepa, M., Ravaglia, M., Maggese, M., Paz, D., and Vissio, P. (2003). Melanin-concentrating hormone system in the brain and skin of the cichlid fish Cichlasoma dimerus: anatomical localization, ontogeny and distribution in comparison to α-melanocyte-stimulating hormone-expressing cells. *Cell and tissue research* 311(1)**,** 61-69. doi: 10.1007/s00441-002-0654-4.

Pérez-Sirkin, D., Cánepa, M., Fossati, M., Fernandino, J., Delgadin, T., Canosa, L., et al. (2012). Melanin concentrating hormone (MCH) is involved in the regulation of growth hormone in Cichlasoma dimerus (Cichlidae, Teleostei). *General and comparative endocrinology* 176(1)**,** 102-111. doi: 10.1016/j.ygcen.2012.01.002.

Platt, R.N., Amman, B.R., Keith, M.S., Thompson, C.W., and Bradley, R.D. (2015). What Is Peromyscus? Evidence from nuclear and mitochondrial DNA sequences suggests the need for a new classification. *Journal of mammalogy* 96(4)**,** 708-719. doi: 10.1093/jmammal/gyv067.

Renz, A.J., Meyer, A., and Kuraku, S. (2013). Revealing less derived nature of cartilaginous fish genomes with their evolutionary time scale inferred with nuclear genes. *PLoS One* 8(6)**,** e66400. doi: 10.1371/journal.pone.0066400.

Rodriguez, M., Beauverger, P., Naime, I., Rique, H., Ouvry, C., Souchaud, S., et al. (2001). Cloning and molecular characterization of the novel human melanin-concentrating hormone receptor MCH2. *Molecular pharmacology* 60(4)**,** 632-639.

Röhlich, P., and Vigh, B. (1967). Electron microscopy of the paraventricular organ in the sparrow (Passer domesticus). *Zeitschrift für Zellforschung und Mikroskopische Anatomie* 80(2)**,** 229-245.

Rondini, T.A., Donato, J., Rodrigues, B.C., Bittencourt, J.C., and Elias, C.F. (2010). Chemical identity and connections of medial preoptic area neurons expressing melanin-concentrating hormone during lactation. *Journal of Chemical Neuroanatomy* 39(1)**,** 51-62. doi: 10.1016/j.jchemneu.2009.10.005.

Sailer, A.W., Sano, H., Zeng, Z., McDonald, T.P., Pan, J., Pong, S.-S., et al. (2001). Identification and characterization of a second melanin-concentrating hormone receptor, MCH-2R. *Proceedings of the National Academy of Sciences* 98(13)**,** 7564-7569. doi: 10.1073/pnas.121170598.

Saito, Y., Nothacker, H.-P., Wang, Z., Lin, S.H.S., Leslie, F., and Civelli, O. (1999). Molecular characterization of the melanin-concentrating-hormone receptor. *Nature* 400(6741)**,** 265-269. doi: 10.1038/22321.

Shimomura, Y., Mori, M., Sugo, T., Ishibashi, Y., Abe, M., Kurokawa, T., et al. (1999). Isolation and identification of melanin-concentrating hormone as the endogenous ligand of the SLC-1 receptor. *Biochemical and Biophysical Research Communications* 261(3)**,** 622-626. doi: 10.1006/bbrc.1999.1104.

Sibert, E.C., and Norris, R.D. (2015). New Age of Fishes initiated by the Cretaceous− Paleogene mass extinction. *Proceedings of the National Academy of Sciences* 112(28)**,** 8537-8542. doi: 10.1073/pnas.1504985112.

Sita, L.V., Elias, C.F., and Bittencourt, J.C. (2003). Dopamine and melanin-concentrating hormone neurons are distinct populations in the rat rostromedial zona incerta. *Brain Research* 970(1-2)**,** 232-237. doi: 10.1016/S0006-8993(03)02345-X.

Sita, L.V., Elias, C.F., and Bittencourt, J.C. (2007). Connectivity pattern suggests that incerto-hypothalamic area belongs to the medial hypothalamic system. *Neuroscience* 148(4)**,** 949-969. doi: 10.1016/j.neuroscience.2007.07.010.

Sprague, J., Bayraktaroglu, L., Clements, D., Conlin, T., Fashena, D., Frazer, K., et al. (2006). The Zebrafish Information Network: the zebrafish model organism database. *Nucleic acids research* 34(suppl_1)**,** D581-D585.

Suzuki, M., Bennett, P., Levy, A., and Baker, B.I. (1997). Expression of MCH and POMC genes in rainbow trout (Oncorhynchus mykiss) during ontogeny and in response to early physiological challenges. *General and comparative endocrinology* 107(3)**,** 341-350. doi: 10.1006/gcen.1997.6936.

Suzuki, M., Narnaware, Y., Baker, B.I., and Levy, A. (1995). Influence of environmental colour and diurnal phase on MCH gene expression in the trout. *Journal of neuroendocrinology* 7(4)**,** 319-328. doi: 10.1111/j.1365-2826.1995.tb00764.x.

Swanson, L.W., Sanchez-Watts, G., and Watts, A.G. (2005). Comparison of melanin-concentrating hormone and hypocretin/orexin mRNA expression patterns in a new parceling scheme of the lateral hypothalamic zone. *Neuroscience Letters* 387(2)**,** 80-84. doi: 10.1016/j.neulet.2005.06.066.

Takahashi, A., Tsuchiya, K., Yamanome, T., Amano, M., Yasuda, A., Yamamori, K., et al. (2004). Possible involvement of melanin-concentrating hormone in food intake in a teleost fish, barfin flounder. *Peptides* 25(10)**,** 1613-1622. doi: 10.1016/j.peptides.2004.02.022.

Takayama, Y., Wada, C., Kawauchi, H., and Ono, M. (1989). Structures of two genes coding for melanin-concentrating hormone of chum salmon. *Gene* 80(1)**,** 65-73. doi: 10.1016/0378-1119(89)90251-5.

Tan, C.P., Sano, H., Iwaasa, H., Pan, J., Sailer, A.W., Hreniuk, D.L., et al. (2002). Melanin-concentrating hormone receptor subtypes 1 and 2: species-specific gene expression. *Genomics* 79(6)**,** 785-792. doi: 10.1006/geno.2002.6771.

Tanaka, M., Azuma, M., Nejigaki, Y., Saito, Y., Mizusawa, K., Uchiyama, M., et al. (2009). Melanin-concentrating hormone reduces somatolactin release from cultured goldfish pituitary cells. *Journal of Endocrinology* 203(3)**,** 389. doi: 10.1677/JOE-09-0330.

Tatemoto, K., and Mutt, V. (1981). Isolation and characterization of the intestinal peptide porcine PHI (PHI-27), a new member of the glucagon--secretin family. *Proceedings of the National Academy of Sciences* 78(11)**,** 6603-6607.

Thannickal, T.C., Lai, Y.-Y., and Siegel, J.M. (2007). Hypocretin (orexin) cell loss in Parkinson's disease. *Brain* 130(6)**,** 1586-1595.

Tillet, Y., Batailler, M., and Fellmann, D. (1996). Distribution of melanin-concentrating hormone (MCH)-like immunoreactivity in neurons of the diencephalon of sheep. *Journal of chemical neuroanatomy* 12(2)**,** 135-145. doi: 10.1016/S0891-0618(96)00195-0.

Tobet, S., Nozaki, M., Youson, J., and Sower, S. (1995). Distribution of lamprey gonadotropin-releasing hormone-III (GnRH-III) in brains of larval lampreys (Petromyzon marinus). *Cell and tissue research* 279(2)**,** 261-270.

Torterolo, P., Sampogna, S., Morales, F.R., and Chase, M.H. (2006). MCH-containing neurons in the hypothalamus of the cat: searching for a role in the control of sleep and wakefulness. *Brain research* 1119(1)**,** 101-114. doi: 10.1016/j.brainres.2006.08.100.

Tostivint, H., Lihrmann, I., and Vaudry, H. (2008). New insight into the molecular evolution of the somatostatin family. *Molecular and cellular endocrinology* 286(1-2)**,** 5-17. doi: 10.1016/j.mce.2008.02.029.

Toumaniantz, G., Bittencourt, J.C., and Nahon, J.-L. (1996). The rat melanin-concentrating hormone gene encodes an additional putative protein in a different reading frame. *Endocrinology* 137(10)**,** 4518-4521. doi: 10.1210/en.137.10.4518.

Tuziak, S.M., and Volkoff, H. (2012). A preliminary investigation of the role of melanin-concentrating hormone (MCH) and its receptors in appetite regulation of winter flounder (Pseudopleuronectes americanus). *Molecular and cellular endocrinology* 348(1)**,** 281-296. doi: 10.1016/j.mce.2011.09.015.

Vallarino, M., Trabucchi, M., Chartrel, N., Jäggin, V., Eberle, A.N., and Vaudry, H. (1998). Melanin-concentrating hormone system in the brain of the lungfish Protopterus annectens. *Journal of Comparative Neurology* 390(1)**,** 41-51. doi: 10.1002/(SICI)1096-9861(19980105)390:1<41::AID-CNE4>3.0.CO;2-Q Ci.

Vaughan, J.M., Fischer, W.H., Hoeger, C., Rivier, J., and Vale, W. (1989). Characterization of melanin-concentrating hormone from rat hypothalamus. *Endocrinology* 125(3)**,** 1660-1665. doi: 10.1210/endo-125-3-1660.

Venkatesh, B., Lee, A.P., Ravi, V., Maurya, A.K., Lian, M.M., Swann, J.B., et al. (2014). Elephant shark genome provides unique insights into gnathostome evolution. *Nature* 505(7482)**,** 174. doi: 10.1038/nature12826.

Vidal, L., Blanchard, J.H., and Morin, L.P. (2005). Hypothalamic and zona incerta neurons expressing hypocretin, but not melanin concentrating hormone, project to the hamster intergeniculate leaflet. *Neuroscience* 134(3)**,** 1081-1090. doi: 10.1016/j.neuroscience.2005.03.062.

Vigh-Teichmann, I., and Vigh, B. (1989). The cerebrospinal fluid-contacting neuron: a peculiar cell type of the central nervous system. Immunocytochemical aspects. *Archives of histology and cytology* 52(Supplement)**,** 195-207. doi: 10.1679/aohc.52.Suppl_195.

Vilim, F., Cropper, E., Price, D., Kupfermann, I., and Weiss, K. (1996). Release of peptide cotransmitters in Aplysia: regulation and functional implications. *Journal of Neuroscience* 16(24)**,** 8105-8114. doi: 10.1523/JNEUROSCI.16-24-08105.1996.

Wang, S., Behan, J., O'Neill, K., Weig, B., Fried, S., Laz, T., et al. (2001). Identification and pharmacological characterization of a novel human melanin-concentrating hormone receptor, mch-r2. *Journal of Biological Chemistry* 276(37)**,** 34664-34670. doi: 10.1074/jbc.M102601200.

Wang, T., Yuan, D., Zhou, C., Lin, F., Wei, R., Chen, H., et al. (2016). Molecular characterization of melanin-concentrating hormone (MCH) in Schizothorax prenanti: cloning, tissue distribution and role in food intake regulation. *Fish physiology and biochemistry* 42(3)**,** 883-893. doi: 10.1007/s10695-015-0182-2.

Wilkes, B.C., Hruby, V.J., Sherbrooke, W.C., Castrucci, A.M.d.L., and Hadley, M.E. (1984). Synthesis and biological actions of melanin concentrating hormone. *Biochemical and biophysical research communications* 122(2)**,** 613-619. doi: 10.1016/S0006-291X(84)80077-7.

Xu, J., Hou, F., Wang, D., Li, J., and Yang, G. (2019). Characterization and expression of melanin-concentrating hormone (MCH) in common carp (Cyprinus carpio) during fasting and reproductive cycle. *Fish physiology and biochemistry* 45(2)**,** 805-817. doi: 10.1007/s10695-018-0586-x.

Figure Legends

Figure 1 - A hybrid model for the origination of the MCH system. The precise origin of MCH in Vertebrates remains unknown, but it may have arisen during the Invertebrate-Vertebrate transition, facilitated by whole-genome duplication (WGD) events combined with interactions between to invertebrate systems. 1. The acidic peptide contained in the precursor for the small cardioactive peptide A from *Aplysia californica* bears significant residue similarity to MCH. Identical residues are indicated in dark red, and conservative substitutions are indicated in light red. Somatostatin-like receptors are believed to be present in Invertebrate species, here modelled after the Drostar-1 and Drostar-2 receptors of Drosophila melanogaster, in green and blue. 2. After the first round of WGD, constraints were loosened over the acidic peptide due to redundancy, what allowed one of the copies to mutate and acquire a three-dimensional structure that resembled that of somatostatin, with a dicysteine bridge formed between residues 7 and 16 (indicated in purple). The newly acquired cyclic structure allowed this new acidic peptide to interact with one or multiple forms of the somatostatin receptor homologs also duplicated at this point. Over time, one of these somatostatin receptor homologs lost its ability to bind to somatostatin and became an exclusive MCH receptor (indicated in yellow). 3. The second WGD event then resulted in two paralogs of MCH receptors and five paralogs of somatostatin receptor, due to the loss of one additional somatostatin receptor. Only one copy of MCH was maintained at this point.

Figure 2 – Phylogenetic relationship between early-diverging Chordates and Actinopterygians. Illustrative tree showing the main phylogenetic relationship between clades with available information about MCH. Several clades have been omitted for clarity, and the tree is not meant to represent the absolute order of relationship between these groups, but rather the most probable organization based on current molecular data and information about the MCH system. The multiple whole-genome duplication (WGD) events believed to have occurred in the Vertebrate lineage are indicated in the tree. Under each clade name are the pmch genes annotated or cloned for that clade, with the "conserved" *pmch/pmcha* genes indicated with red colors and the Teleost derived *pmchb* indicated in blue.

Figure 3 – Diagrammatic representation of the main morphological features of the MCH distribution in early-diverged Chordates and Actinopterygians. Major clades are indicated in bold font, while clade-wide events are represented in red. The diagrams for each clade are not meant to represent a single species or a single hypothalamic level, but rather a visual summary of what has been described for animals belonging to that clade. In Petromyzontids and Elasmobranchs, the majority of MCH neurons is found in the ependymal and subependymal layers of the third ventricle. While there is no indication of hypophyseal innervation in Elasmobranchs, there are mixed reports about the presence of MCH in the proximal neurosecretory contact region (PCR) and neurohypophysis of Petromyzontids. After the Actinopterygii divergence, two major changes occurred in the MCH system. First, the periventricular neurons were divided in two groups by the emerging lateral recess, separating them into dorsal and ventral groups. Second, a clear innervation of the PCR and adenohypophysis becomes perceptible, indicating the acquisition of a modulatory role by MCH neurons at this stage, followed then by direct innervation of the neurohypophysis, suggesting a neurosecretory role. Around the time of the Teleost split, the final large-scale changes in the MCH system occurred. A lateral migration process started, with large, neurosecretory MCH neurons moving towards the nucleus lateralis tuberis and densely projecting to the hypophysis from this ventrolateral position. This change occurred contemporaneously to the acquisition of a role in adaptive color change by MCH. Based on data from Baker and Bird (2002), Duarte et al. (2001) and Amano et al. (2003).

Figure 4 – Phylogenetic relationship between Sarcopterygians. Illustrative tree showing the main phylogenetic relationship between clades with available information about MCH. Several clades have been

omitted for clarity, and the tree is not meant to represent the absolute order of relationship between these groups, but rather the most probable organization based on current molecular data and information about the MCH system. Two changes in the MCH system are indicated in the tree: the loss of an MCH gene-related peptide (MGRP) in birds and the loss of the MCH receptor subtype 2 (MCHR2) in Glires. Under each clade name is the standardized nomenclature for the pmch gene that respective clade.

Figure 5 – Diagrammatic representation of the main morphological features of the MCH distribution in non-Mammalian Sarcopterygians. Major clades are indicated in bold font, while clade-wide events are represented in red. The diagrams for each clade are not meant to represent a single species or a single hypothalamic level, but rather a visual summary of what has been described for animals belonging to that clade. Lungfish (Dipnoi) have a distribution of cells that closely resembles that of Elasmobranchs and early Actinopterygians, with neurons concentrated around the ventricle, and only scattered cells found in lateral areas. In Lissamphibians, neurons are still concentrated in the dorsomedial hypothalamus, but these cells are not as close to the ventricle as in other species, and some of the extend dorsally towards the ventral thalamus. There is no consensus about the presence of MCH neurons in the ventral tuberal nucleus, represented by open circles, or about the innervation of the hypophysis. In Sauropsids, a lateral migration event occurred, with some neurons found forming an arc shaped in the lateral hypothalamus. These neurons do not surpass the number of periventricular neurons, however, making this a minor lateral migration event. Based on data from Vallarino et al. (1998), Cardot et al. (1994), Cardot et al. (1999), Francis and Baker (1995), and Lázár et al. (2002).

Figure 6 – Diagrammatic representation of the main morphological features of the MCH distribution in Mammals. Major clades are indicated in bold font, while clade-wide events are represented in red. The diagrams for each clade are not meant to represent a single species or a single hypothalamic level, but rather a visual summary of what has been described for animals belonging to that clade. The rat was chosen to represent rodents, to avoid the complexity that representing intra-Muroid variations would bring. In the Laurasiatheria branch, numerous MCH neurons are found in the ventrolateral hypothalamus, representing a ventral shift in this group when compared to Euarchontoglires. In Carnivora, there is a substantial group of labeled neurons in the medial hypothalamus, while the lateral part of the lateral hypothalamic area (LHA) is less densely populated. A very dense distribution of neurons in the ventral hypothalamus is observed in Euungulates. In Euarchontoglires, the dorsolateral LHA becomes the main locus of MCH neurons, with fewer neurons found in the medial hypothalamus. In all Mammals, there is a strong association of MCH neurons and the fornix and a dorsomedial group of neurons, possible representing the ancestral group of periependymal neurons seen in Petromyzontids. Based on data from Torterolo et al. (2006), Tillet et al. (1996), Chometton et al. (2014), Bittencourt et al. (1992), Bittencourt et al. (1998), and Krolewski et al. (2010).

Figure 7 – Phylogenetic relationship between Muroids. Illustrative tree showing the phylogenetic relationship between members of Superfamily Muroidea, with several groups omitted for clarity. Commonly used animal models are indicated at the top of the tree, and species with available morphological data for MCH are indicated in green and red. Molecular data to build the tree comes from Fabre et al. (2012) and Platt et al. (2015). Reproduced with permission from Diniz et al. (2019b).

Figure 8 –The three-dimensional distribution of MCH neurons in Muroids. Hypothalamic reconstructions from *R. norvegicus, M. musculus and N. alstoni*. Each neuron is indicated by a magenta dot. Notable differences are observed when the three species are compared. The distribution of MCH neurons occupies virtually the whole medio-lateral extent of the tuberal hypothalamus, with neurons ranging from the ventricle border to the internal margin of the internal capsule. Only a small number of neurons is found ventral to the fornix. In contrast, the mouse periventricular nucleus and the medial part of the lateral hypothalamic area (LHA) are mostly devoid of neurons, with the anterior hypothalamic area and the dorsolateral LHA representing the largest groups. In *N.*

alstoni, an intermediate profile is observed, with moderate numbers of neurons observed in the medial LHA and the periventricular area. The Mexican volcano mouse, however, distinguishes itself for a substantial presence of MCH neurons ventral to the fornix, in the perifornical area. Animated versions of these reconstructions can be found in Diniz et al. (2019a). Structures: 3V, third ventricle (orange); f, fornix (yellow); ic, internal capsule (purple); mt, mammillothalamic tract (green); opt, optic tract (blue). Reproduced with permission from Diniz et al. (2019b).

Table

Table 1 – Standardized nomenclature of *pmch* genes across Vertebrate species. The gene nomenclature guidelines used to compose this table are: Sprague et al. (2006), Karimi et al. (2017), Kusumi et al. (2011), Burt et al. (2009), Blake et al. (2016) and Braschi et al. (2018).

Gene abbreviation	Protein abbreviation
Petromyzontid	
pmch	Pmch
Elasmobranchii	
pmch	Pmch
Actinopterygii (non-Teleost)	
pmch	Pmch
Teleost (non-Salmonids)	
pmcha	Pmcha
pmchb	Pmchb
Salmonids	
pmcha1	Pmcha1
pmcha2	Pmcha2
pmchb1	Pmchb1
pmchb2	Pmchb2
Dipnoi	
pmch	Pmch
Lissamphibian	
pmch	Pmch
Sauropsid (non-Aves)	
pmch	Pmch
Aves	
PMCH	PMCH
Mammalian (non-Primate)	
Pmch	PMCH
Primate	
PMCH	PMCH

Figure 1.tiff

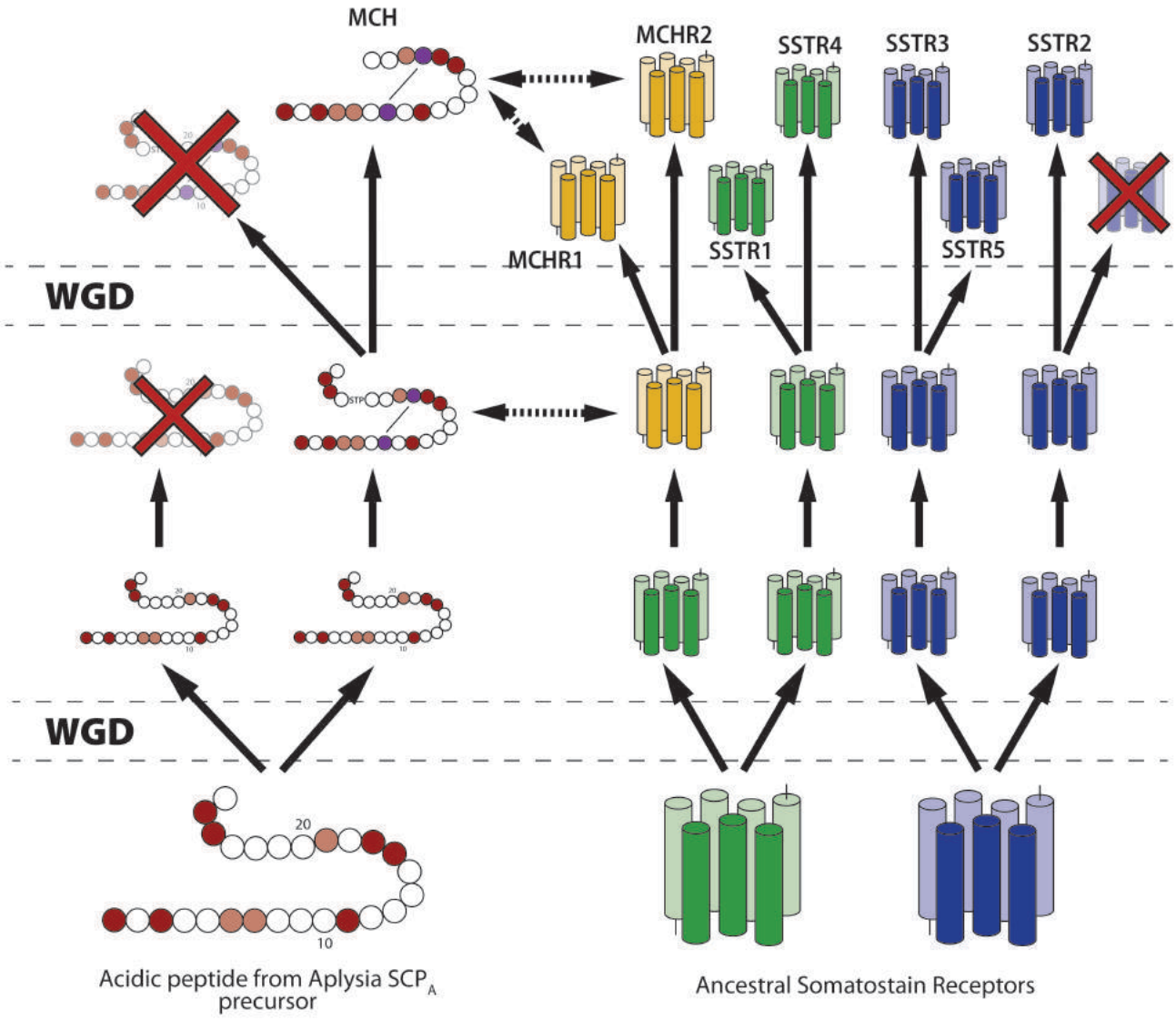

Figure 2.tiff

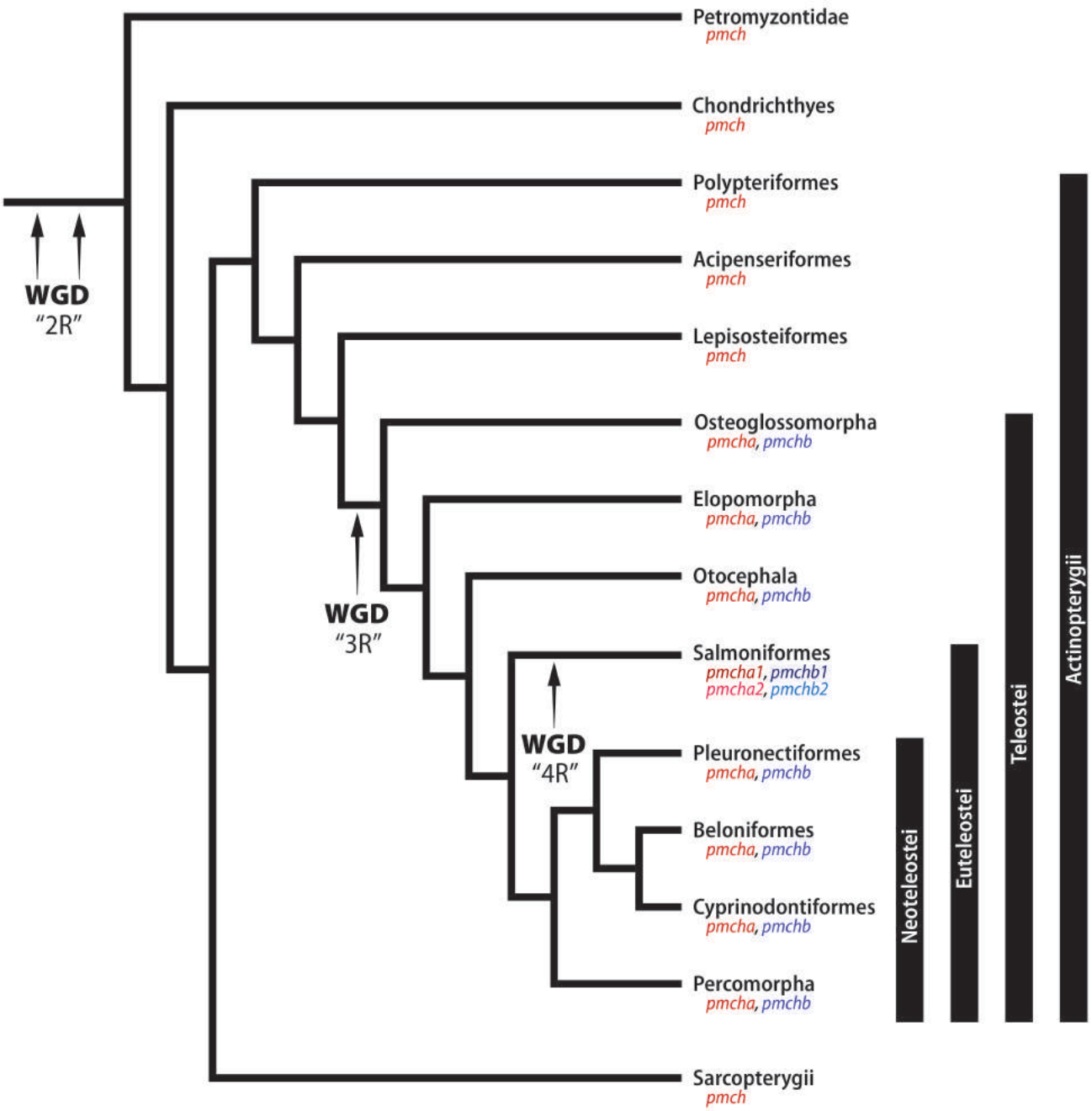

Figure 3.tiff

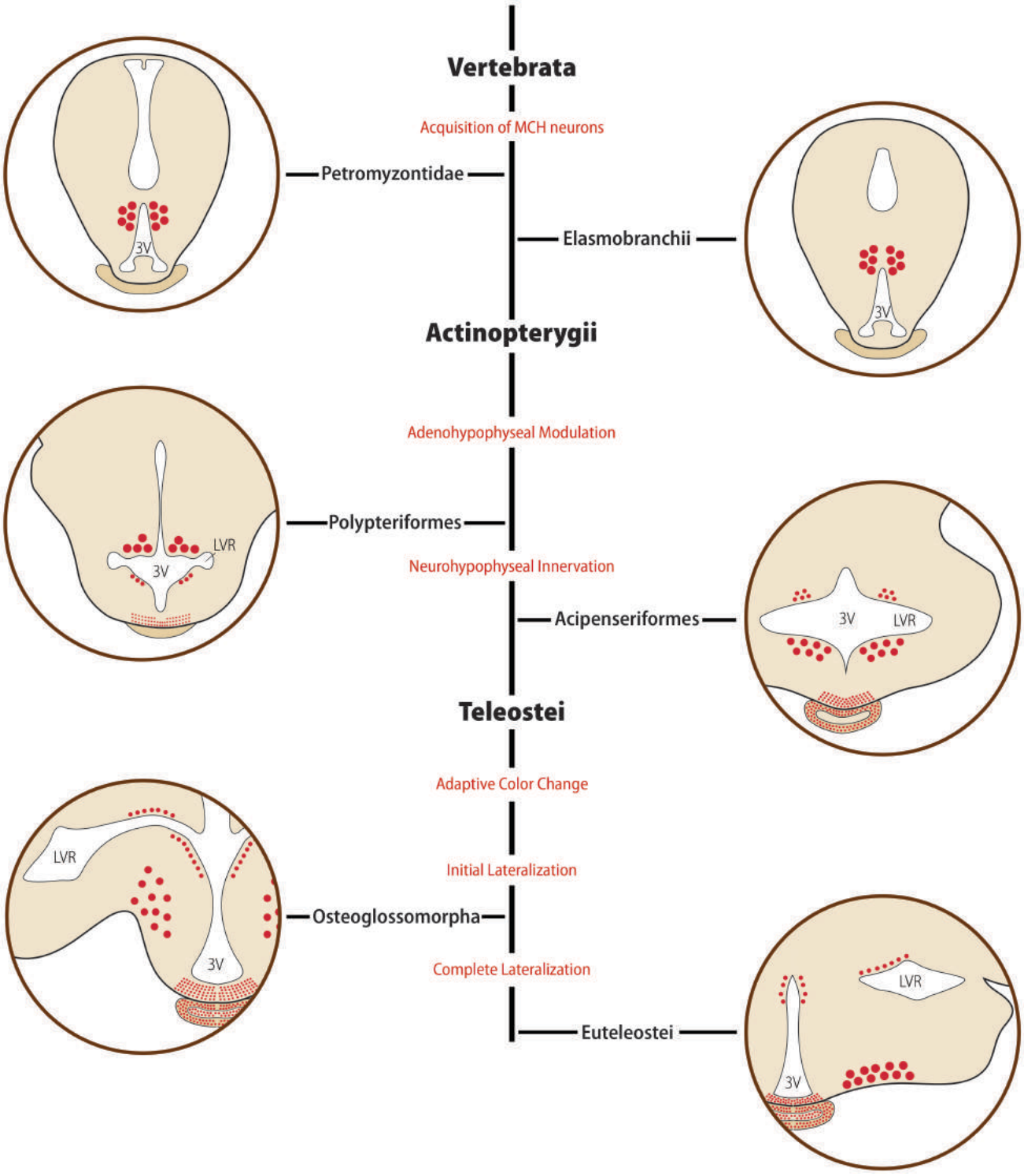

Figure 4.tiff

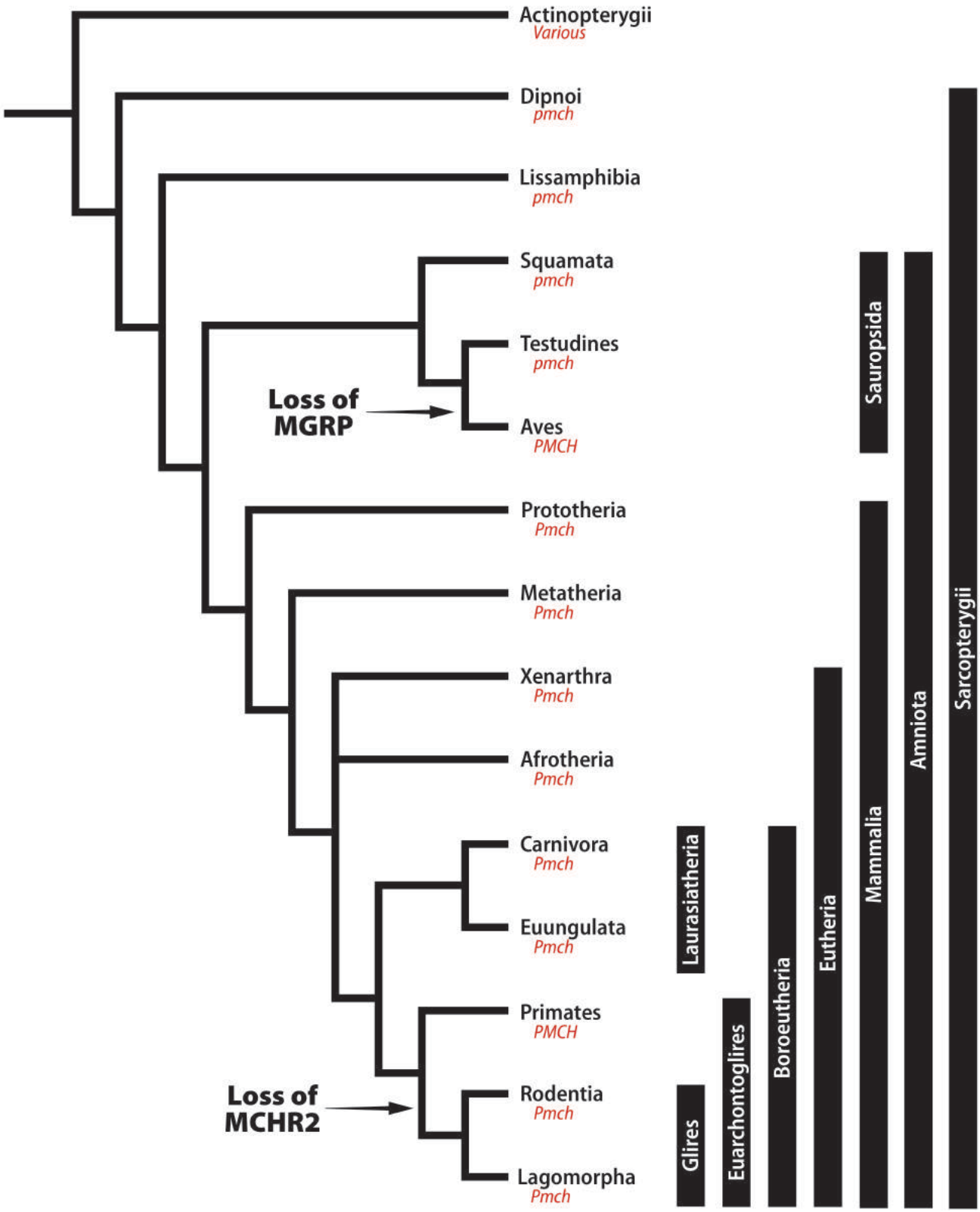

Figure 5.tiff

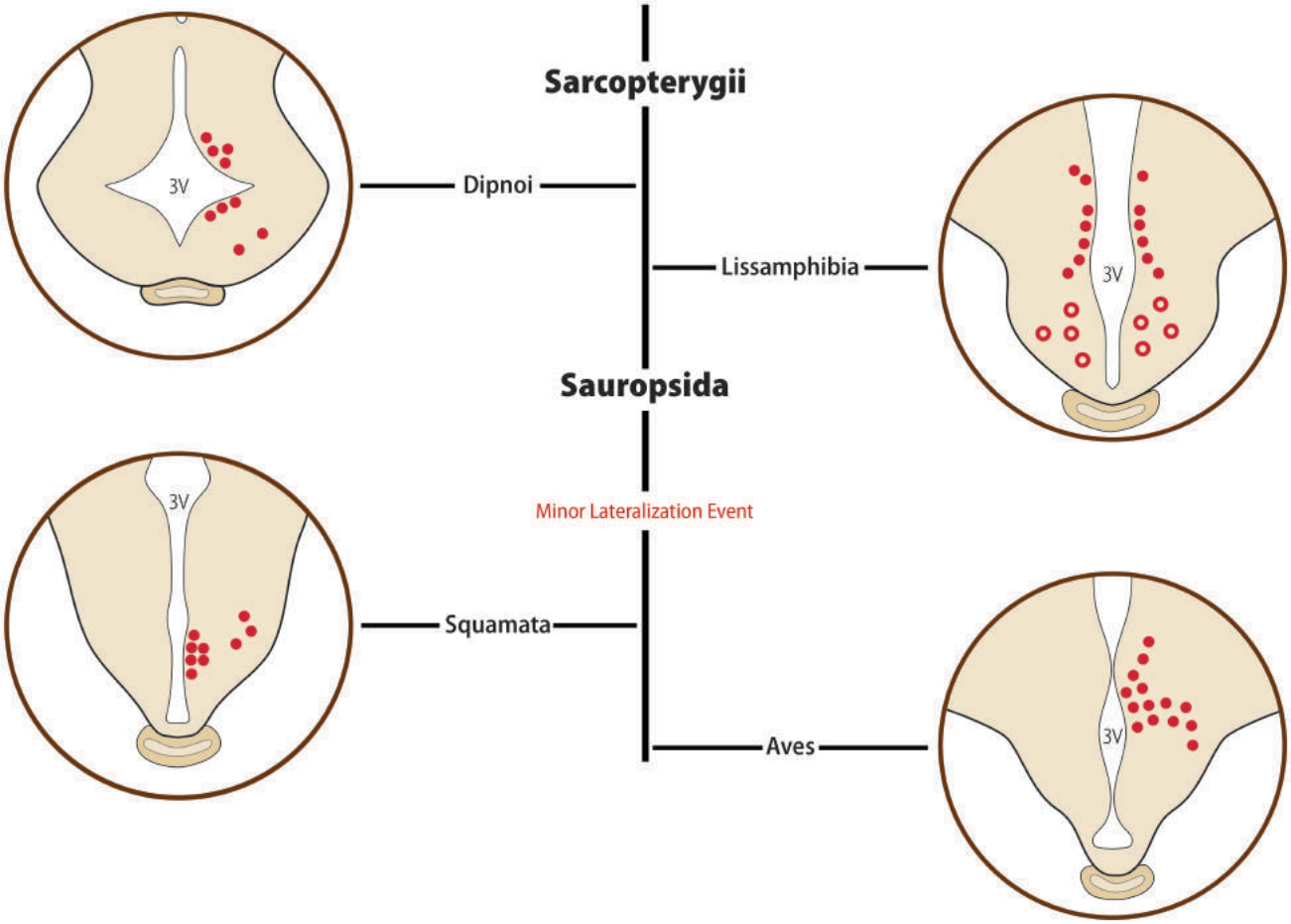

Figure 6.tiff

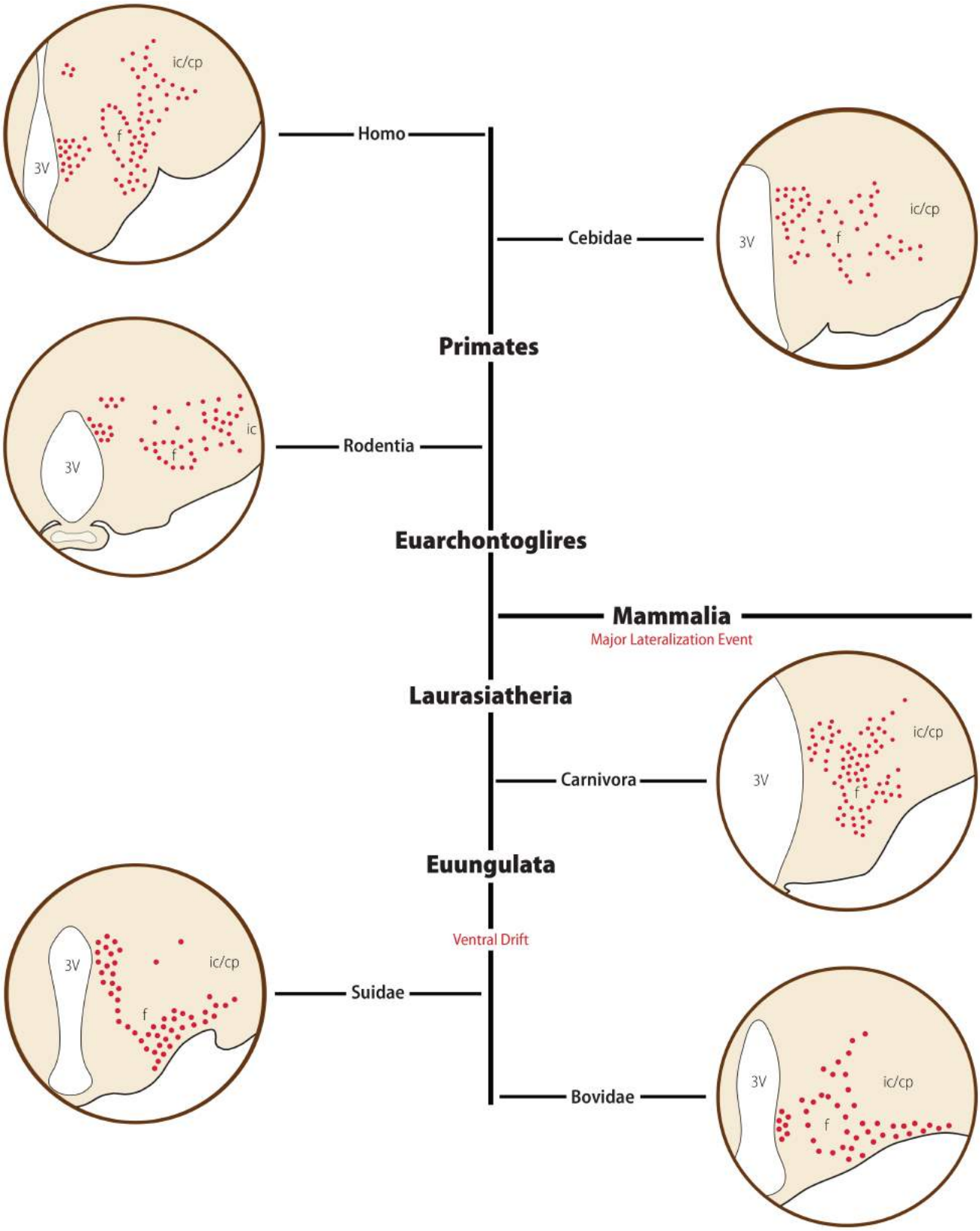

Figure 7.tiff

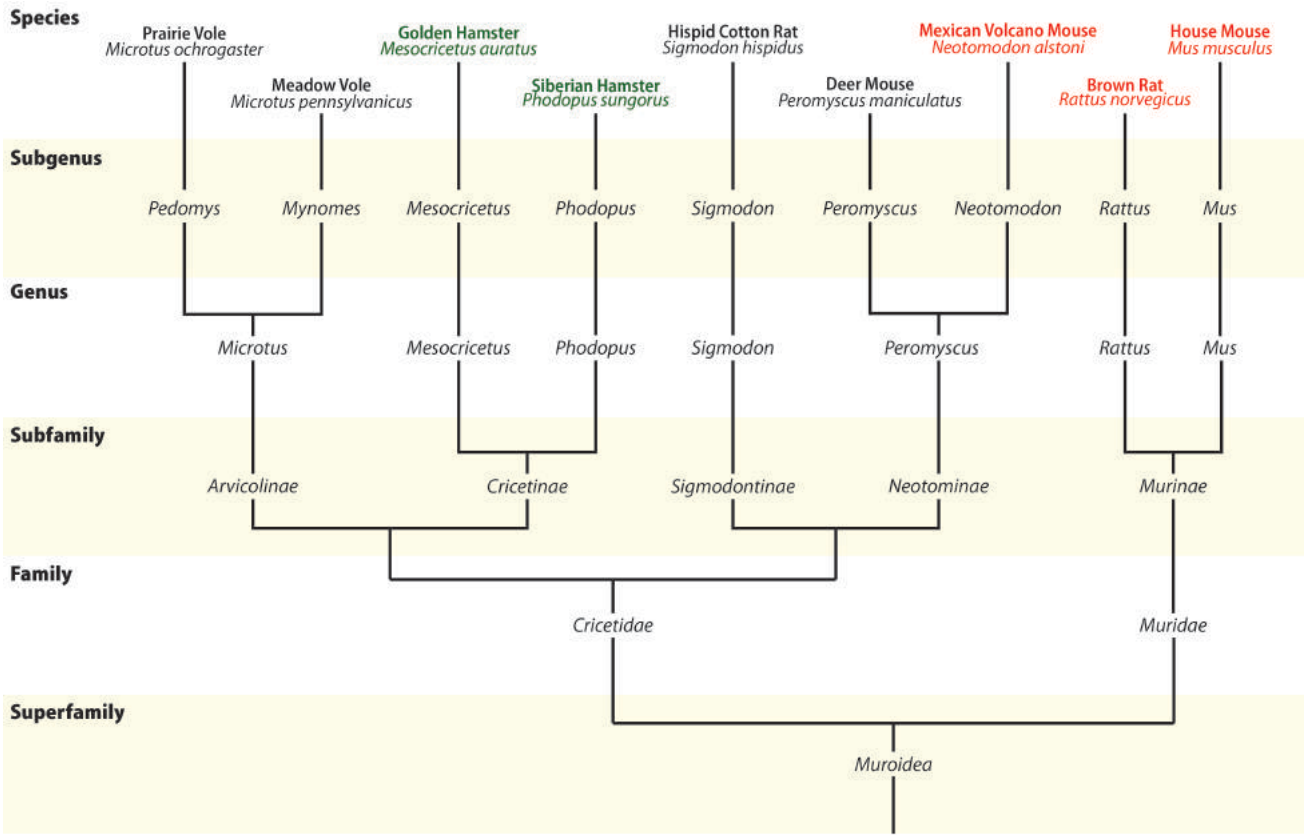

Figure 8.tiff

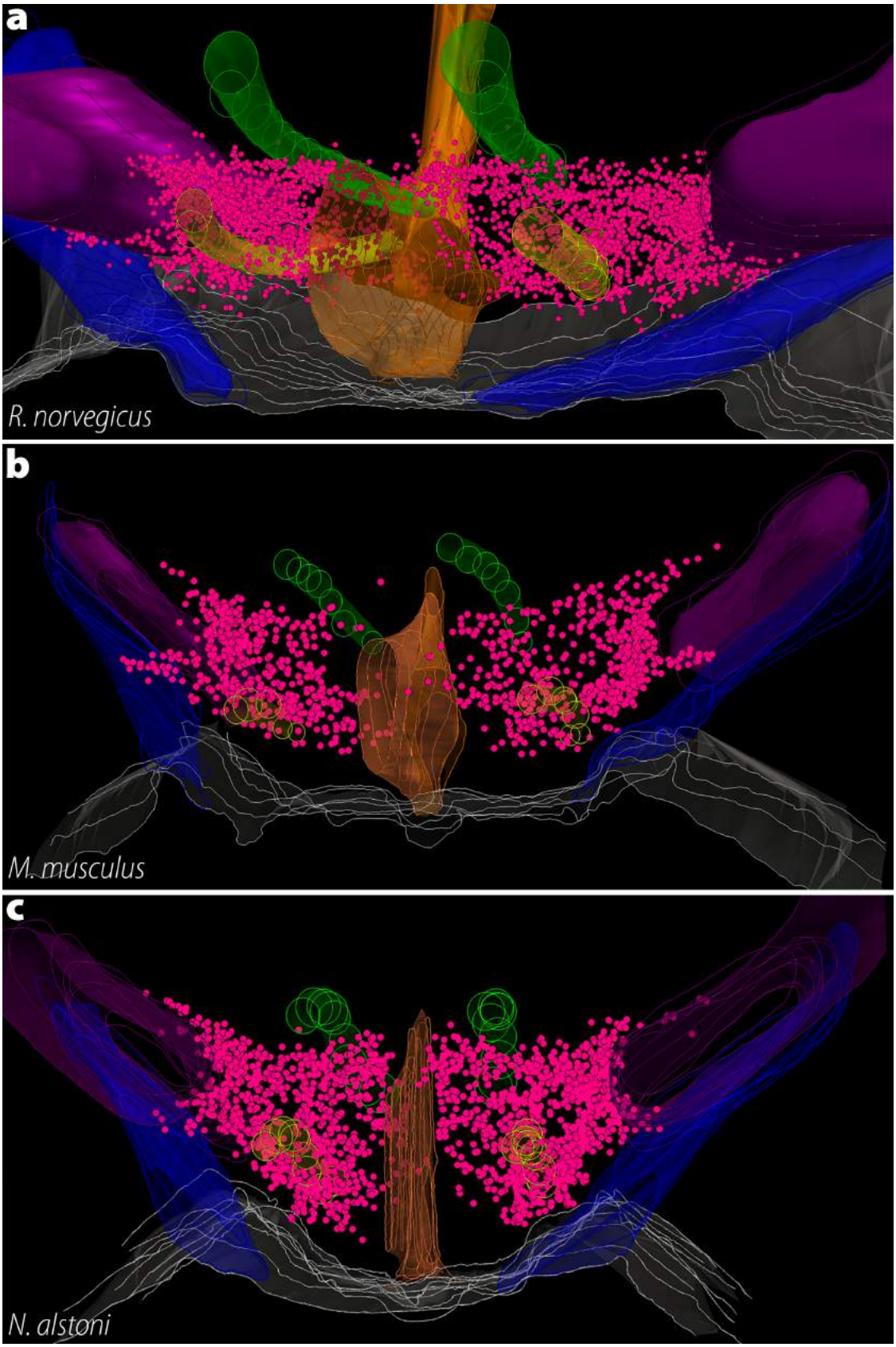

Chapter 6
Conclusion

6 CONCLUSION

By comparing the MCH system between multiple species, both through the generation of new data and through the analysis of gene databases and the literature, we were able to draw meaningful conclusions about this system. Here, we proposed a model for its origin in vertebrates; we identified changes in the MCH system linked to whole-genome alterations that occurred in the vertebrate lineage; we proposed a model to explain the two major events of lateral migration of MCH neurons that occurred during evolution; we showed significant plasticity in the distribution of MCH neurons, even between closely related species; we demonstrated the conservation of cellular characteristics; we identified a new antibody for the localization of MCHR1 and employed it to map the distribution of ciliary MCHR1 in the murine nervous system; and we provided overwhelming evidence towards the existence of an anatomical basis for volume transmission in the MCH system. We believe the data produced in this work will be of value to the scientific literature, as we hope the questions raised in this work may encourage others to pursue the fascinating MCH system.

A better understanding of the MCH system is paramount to our knowledge of the human brain, not only due to the actions of MCH in mammalian physiology, but because it serves as a model for different neuromodulatory systems. While its phylogenetic history tells us about the events that shaped the brain of extant species as we know them, the conserved/diverged aspects of MCH cells between different species serves as a cautionary tale about the limitations of extrapolating data obtained in one model to other animal species, even closely related ones. More than an interesting topic, comparative morphology is an essential aspect of translational research, equipping us with the knowledge necessary to make appropriate interspecies considerations.

Finally, our discovery of a strong basis for volume transmission in the MCH system of multiple rodent species is a starting point for numerous other works necessary to fully comprehend how MCH operates. It is vital that we understand how released MCH travels within the brain, and how does it operate outside the synapse. It is insufficient for an MCHR1 agonist or antagonist to bind to the receptor in the same way MCH does. To fully mimic or block MCH actions, these substances must have a half-life and a transport system that imitates that of volume transmission MCH. By screening substances that have this broader range of similarities with MCH, we may be able to identify compounds with practical use for the treatment of human pathologies.

REFERENCES

1. Moret F, Guilland JC, Coudouel S, Rochette L, Vernier P. Distribution of tyrosine hydroxylase, dopamine, and serotonin in the central nervous system of amphioxus (Branchiostoma lanceolatum): implications for the evolution of catecholamine systems in vertebrates. Journal of Comparative Neurology. 2004;468(1):135-50.
2. Swanson LW. Brain Maps - Structure of the Rat Brain. 3rd ed. San Diego: Academic Press; 2004. 215 p.
3. Paxinos G, Watson C. The Rat Brain in Stereotaxic Coordinates. 7th ed: Academic Press; 2013 24th October 2013. 472 p.
4. Paxinos G, Franklin K. The Mouse Brain in Stereotaxic Coordinates. 4th Edition ed: Academic Press; 2012 25th October 2012. 360 p.
5. Gurdjian ES. The diencephalon of the albino rat. Studies on the brain of the rat. no. 2. J Comp Neurol. 1927;43(1):1-114.
6. Veening JG, Swanson LW, Cowan WM, Nieuwenhuys R, Geeraedts LM. The medial forebrain bundle of the rat. II. An autoradiographic study of the topography of the major descending and ascending components. J Comp Neurol. 1982;206(1):82-108.
7. Nieuwenhuys R, Geeraedts LMG, Veening JG. The medial forebrain bundle of the rat. I. General introduction. Journal of Comparative Neurology. 1982;206(1):49-81.
8. Geeraedts LM, Nieuwenhuys R, Veening JG. Medial forebrain bundle of the rat: III. Cytoarchitecture of the rostral (telencephalic) part of the medial forebrain bundle bed nucleus. J Comp Neurol. 1990;294(4):507-36.
9. Geeraedts LM, Nieuwenhuys R, Veening JG. Medial forebrain bundle of the rat: IV. Cytoarchitecture of the caudal (lateral hypothalamic) part of the medial forebrain bundle bed nucleus. J Comp Neurol. 1990;294(4):537-68.
10. Simerly R. Organization of the hypothalamus. The rat nervous system Fourth Edition San Diego: Elsevier. 2015:267-88.
11. Bonnavion P, Mickelsen LE, Fujita A, De Lecea L, Jackson AC. Hubs and spokes of the lateral hypothalamus: cell types, circuits and behaviour. The Journal of physiology. 2016;594(22):6443-62.
12. Bittencourt JC, Presse F, Arias C, Peto CA, Vaughan JM, Nahon J-L, et al. The melanin-concentrating hormone system of the rat brain: an immuno- and hybridization histochemical characterization. The Jorunal of Comparative Neurology. 1992;319(2):218-45.
13. Peyron C, Tighe DK, Van Den Pol AN, De Lecea L, Heller HC, Sutcliffe JG, et al. Neurons containing hypocretin (orexin) project to multiple neuronal systems. Journal of Neuroscience. 1998;18(23):9996-10015.
14. Koylu EO, Couceyro PR, Lambert PD, Ling NC, DeSouza EB, Kuhar MJ. Immunohistochemical localization of novel CART peptides in rat hypothalamus, pituitary and adrenal gland. Journal of neuroendocrinology. 1997;9(11):823-33.
15. Warden MK, Young III WS. Distribution of cells containing mRNAs encoding substance P and neurokinin B in the rat central nervous system. Journal of Comparative Neurology. 1988;272(1):90-113.
16. Skofitsch G, Jacobowitz DM. Immunohistochemical mapping of galanin-like neurons in the rat central nervous system. Peptides. 1985;6(3):509-46.
17. Gao XB, van den Pol AN. Melanin concentrating hormone depresses synaptic activity of glutamate and GABA neurons from rat lateral hypothalamus. The Journal of physiology. 2001;533(1):237-52.

18. Bittencourt JC, Diniz GB. Neuroanatomical Structure of the MCH System. Melanin-Concentrating Hormone and Sleep. 1st ed: Springer; 2018. p. 1-46.
19. Vaughan JM, Fischer WH, Hoeger C, Rivier J, Vale W. Characterization of melanin-concentrating hormone from rat hypothalamus. Endocrinology. 1989;125(3):1660-5.
20. Nahon J-L, Presse F, Bittencourt JC, Sawchenko PE, Vale W. The rat melanin-concentrating hormone messenger ribonucleic acid encodes multiple putative neuropeptides coexpressed in the dorsolateral hypothalamus. Endocrinology. 1989;125(4):2056-65.
21. Viale A, Ortola C, Hervieu G, Furuta M, Barbero P, Steiner DF, et al. Cellular localization and role of prohormone convertases in the processing of pro-melanin concentrating hormone in mammals. Journal of Biological Chemistry. 1999;274(10):6536-45.
22. Rondini TA, Rodrigues BC, de Oliveira AP, Bittencourt JC, Elias CF. Melanin-concentrating hormone is expressed in the laterodorsal tegmental nucleus only in female rats. Brain research bulletin. 2007;74(1-3):21-8.
23. Knollema S, Brown ER, Vale W, Sawchenko PE. Novel hypothalamic and preoptic sites of prepro-melanin-concentrating hormone messenger ribonucleic Acid and Peptide expression in lactating rats. Journal of Neuroendocrinology. 1992;4(6):709-17.
24. Rondini TA, Donato J, Rodrigues BC, Bittencourt JC, Elias CF. Chemical identity and connections of medial preoptic area neurons expressing melanin-concentrating hormone during lactation. Journal of chemical neuroanatomy. 2010;39(1):51-62.
25. Alvisi RD, Diniz GB, Da-Silva JM, Bittencourt JC, Felicio LF. Suckling-induced Fos activation and melanin-concentrating hormone immunoreactivity during late lactation. Life sciences. 2016;148:241-6.
26. Ferreira JGP, Duarte JCG, Diniz GB, Bittencourt JC. Litter size determines the number of melanin-concentrating hormone neurons in the medial preoptic area of Sprague Dawley lactating dams. Physiology & Behavior. 2017;181:75-9.
27. Costa HC, Da-Silva JM, Diniz GB, Da-Silva Pereira L, Gobbo DR, Da-Silva RJ, et al. Characterization and origins of melanin-concentrating hormone immunoreactive fibers of the posterior lobe of the pituitary and median eminence during lactation in Long-Evans rat. Journal of Neuroendocrinology. 2019;00:e12723.
28. Elias CF, Bittencourt JC. Study of the origins of melanin-concentrating hormone and neuropeptide EI immunoreactive projections to the periaqueductal gray matter. Brain Research. 1997;755(2):255-71.
29. Bittencourt J, Elias C. Melanin-concentrating hormone and neuropeptide EI projections from the lateral hypothalamic area and zona incerta to the medial septal nucleus and spinal cord: a study using multiple neuronal tracers. Brain research. 1998;805(1-2):1-19.
30. Elias CF, Sita L, Zambon B, Oliveira E, Vasconcelos L, Bittencourt JC. Melanin-concentrating hormone projections to areas involved in somatomotor responses. Journal of chemical neuroanatomy. 2008;35(2):188-201.
31. Casatti C, Elias CF, Sita L, Frigo L, Furlani V, Bauer JA, et al. Distribution of melanin-concentrating hormone neurons projecting to the medial mammillary nucleus. Neuroscience. 2002;115(3):899-915.
32. Lima FF, Sita LV, Oliveira AR, Costa HC, da Silva JM, Mortara RA, et al. Hypothalamic melanin-concentrating hormone projections to the septo-hippocampal complex in the rat. Journal of chemical neuroanatomy. 2013;47:1-14.
33. Haemmerle C, Campos A, Bittencourt J. Melanin-concentrating hormone inputs to the nucleus accumbens originate from distinct hypothalamic sources and are apposed to

GABAergic and cholinergic cells in the Long-Evans rat brain. Neuroscience. 2015;289:392-405.
34. Diniz GB, Bittencourt JC. The Melanin-Concentrating Hormone as an Integrative Peptide Driving Motivated Behaviors. Frontiers in Systems Neuroscience. 2017;11:1-32.
35. Ferreira JGP, Bittencourt JC, Adamantidis A. Melanin-concentrating hormone and sleep. Current Opinion in Neurobiology. 2017;44:152-8.
36. Gao X-B. The Role of Melanin-Concentrating Hormone in the Regulation of the Sleep/Wake Cycle: Sleep Promoter or Arousal Modulator? In: Pandi-Perumal SR, Torterolo P, Monti JM, editors. Melanin-Concentrating Hormone and Sleep : Molecular, Functional and Clinical Aspects. Cham: Springer International Publishing; 2018. p. 57-74.
37. Torterolo P, Scorza C, Lagos P, Urbanavicius J, Benedetto L, Pascovich C, et al. Melanin-concentrating hormone (MCH): role in REM sleep and depression. Frontiers in neuroscience. 2015;9:475.
38. Naufahu J, Cunliffe AD, Murray JF. The roles of melanin-concentrating hormone in energy balance and reproductive function: are they connected? Reproduction. 2013;146(5):R141-R50.
39. Adamantidis A, Thomas E, Foidart A, Tyhon A, Coumans B, Minet A, et al. Disrupting the melanin-concentrating hormone receptor 1 in mice leads to cognitive deficits and alterations of NMDA receptor function. European journal of neuroscience. 2005;21(10):2837-44.
40. Sita LV, Diniz GB, Canteras NS, Xavier GF, Bittencourt JC. Effect of intrahippocampal administration of anti-melanin-concentrating hormone on spatial food-seeking behavior in rats. Peptides. 2016;76:130-8.
41. Conductier G, Brau F, Viola A, Langlet F, Ramkumar N, Dehouck B, et al. Melanin-concentrating hormone regulates beat frequency of ependymal cilia and ventricular volume. Nature neuroscience. 2013;16:845-7.
42. Méndez-Andino JL, Wos JA. MCH-R1 antagonists: what is keeping most research programs away from the clinic? Drug discovery today. 2007;12(21-22):972-9.
43. Cheon HG. Antiobesity effects of melanin-concentrating hormone receptor 1 (MCH-R1) antagonists. Appetite Control: Springer; 2012. p. 383-403.
44. Kawauchi H, Kawazoe I, Tsubokawa M, Kishida M, Baker BI. Characterization of melanin-concentrating hormone in chum salmon pituitaries. Nature. 1983;305(5932):321-3.
45. Baker BI, Bird DJ, Buckingham JC. Effects of chronic administration of melanin-concentrating hormone on corticotrophin, melanotrophin, and pigmentation in the trout. General and Comparative Endocrinology. 1986;63(1):62-9.
46. Baker BI, Bird DJ. Neuronal organization of the melanin-concentrating hormone system in primitive actinopterygians: Evolutionary changes leading to teleosts. Journal of Comparative Neurology. 2002;442(2):99-114.
47. Kolakowski LF, Jr., Jung BP, Nguyen T, Johnson MP, Lynch KR, Cheng R, et al. Characterization of a human gene related to genes encoding somatostatin receptors. FEBS Lett. 1996;398(2-3):253-8.
48. Lakaye B, Minet A, Zorzi W, Grisar T. Cloning of the rat brain cDNA encoding for the SLC-1 G protein-coupled receptor reveals the presence of an intron in the gene. Biochim Biophys Acta. 1998;1401(2):216-20.
49. Hawes BE, Kil E, Green B, O'Neill K, Fried S, Graziano MP. The melanin-concentrating hormone receptor couples to multiple G proteins to activate diverse intracellular signaling pathways. Endocrinology. 2000;141(12):4524-32.

50. Pissios P, Trombly DJ, Tzameli I, Maratos-Flier E. Melanin-concentrating hormone receptor 1 activates extracellular signal-regulated kinase and synergizes with G(s)-coupled pathways. Endocrinology. 2003;144(8):3514-23.
51. Tan CP, Sano H, Iwaasa H, Pan J, Sailer AW, Hreniuk DL, et al. Melanin-concentrating hormone receptor subtypes 1 and 2: species-specific gene expression. Genomics. 2002;79(6):785-92.
52. Chen Y, Hu C, Hsu CK, Zhang Q, Bi C, Asnicar M, et al. Targeted disruption of the melanin-concentrating hormone receptor-1 results in hyperphagia and resistance to diet-induced obesity. Endocrinology. 2002;143(7):2469-77.
53. Shimada M, Tritos NA, Lowell BB, Flier JS, Maratos-Flier E. Mice lacking melanin-concentrating hormone are hypophagic and lean. Nature. 1998;396(6712):670-4.
54. Marsh DJ, Weingarth DT, Novi DE, Chen HY, Trumbauer ME, Chen AS, et al. Melanin-concentrating hormone 1 receptor-deficient mice are lean, hyperactive, and hyperphagic and have altered metabolism. Proceedings of the National Academy of Sciences. 2002;99(5):3240-5.
55. Borowsky B, Durkin MM, Ogozalek K, Marzabadi MR, DeLeon J, Lagu B, et al. Antidepressant, anxiolytic and anorectic effects of a melanin-concentrating hormone-1 receptor antagonist. Nat Med. 2002;8(8):825-30.
56. Hervieu G, Cluderay J, Harrison D, Meakin J, Maycox P, Nasir S, et al. The distribution of the mRNA and protein products of the melanin-concentrating hormone (MCH) receptor gene, slc-1, in the central nervous system of the rat. European Journal of Neuroscience. 2000;12(4):1194-216.
57. Saito Y, Cheng M, Leslie FM, Civelli O. Expression of the melanin-concentrating hormone (MCH) receptor mRNA in the rat brain. Journal of Comparative Neurology. 2001;435(1):26-40.
58. Chee MJS, Pissios P, Maratos-Flier E. Neurochemical characterization of neurons expressing melanin-concentrating hormone receptor 1 in the mouse hypothalamus. Journal of Comparative Neurology. 2013;521(10):2208-34.
59. Engle SE, Antonellis PJ, Whitehouse LS, Bansal R, Emond MR, Jontes JD, et al. A CreER mouse to study melanin concentrating hormone signaling in the developing brain. genesis. 2018;56(8):e23217.
60. Berbari NF, Johnson AD, Lewis JS, Askwith CC, Mykytyn K. Identification of ciliary localization sequences within the third intracellular loop of G protein-coupled receptors. Molecular Biology of the Cell. 2008;19(4):1540-7.
61. Niño-Rivero S, Torterolo P, Lagos P. Melanin-concentrating hormone receptor-1 is located in primary cilia of the dorsal raphe neurons. Journal of chemical neuroanatomy. 2019;98:55-62.
62. Pazour GJ, Witman GB. The vertebrate primary cilium is a sensory organelle. Current Opinion in Cell Biology. 2003;15(1):105-10.
63. Agnati LF, Zoli M, Strömberg I, Fuxe K. Intercellular communication in the brain: wiring versus volume transmission. Neuroscience. 1995;69(3):711-26.
64. Noble EE, Hahn JD, Konanur VR, Hsu TM, Page SJ, Cortella AM, et al. Control of Feeding Behavior by Cerebral Ventricular Volume Transmission of Melanin-Concentrating Hormone. Cell metabolism. 2018;28(1):55-68.e7.
65. Qu D, Ludwig DS, Gammeltoft S, Piper M, Pelleymounter MA, Cullen MJ, et al. A role for melanin-concentrating hormone in the central regulation of feeding behaviour. Nature. 1996;380(6571):243-7.

66. Vallarino M, Trabucchi M, Chartrel N, Jäggin V, Eberle AN, Vaudry H. Melanin-concentrating hormone system in the brain of the lungfish Protopterus annectens. Journal of Comparative Neurology. 1998;390(1):41-51.
67. Adams AC, Domouzoglou EM, Chee MJ, Segal-Lieberman G, Pissios P, Maratos-Flier E. Ablation of the hypothalamic neuropeptide melanin concentrating hormone is associated with behavioral abnormalities that reflect impaired olfactory integration. Behavioural Brain Research. 2011;224:195-200.
68. Alhassen L, Phan A, Alhassen W, Nguyen P, Lo A, Shaharuddin H, et al. The role of Olfaction in MCH-regulated spontaneous maternal responses. Brain research. 2019;1719:71-6.
69. Bird DJ, Potter IC, Sower SA, Baker BI. The distribution of melanin-concentrating hormone in the lamprey brain. General and Comparative Endocrinology. 2001;121(3):232-41.
70. Mizusawa K, Amiya N, Yamaguchi Y, Takabe S, Amano M, Breves JP, et al. Identification of mRNAs coding for mammalian-type melanin-concentrating hormone and its receptors in the scalloped hammerhead shark Sphyrna lewini. General and comparative endocrinology. 2012;179(1):78-87.
71. Lázár G, Maderdrut JL, Merchenthaler I. Distribution of melanin-concentrating hormone-like immunoreactivity in the central nervous system of Rana esculenta. Brain research bulletin. 2002;57(3-4):401-7.
72. Nieuwenhuys R. An overview of the organization of the brain of actinopterygian fishes. American Zoologist. 1982;22(2):287-310.
73. Hofmann MH, Meyer DL. The extrabulbar olfactory pathway: primary olfactory fibers bypassing the olfactory bulb in bony fishes? Brain, behavior and evolution. 1995;46(6):378-88.
74. Paxinos G. The rat nervous system: Academic press; 2014.
75. Wu M, Dumalska I, Morozova E, van den Pol AN, Alreja M. Melanin-concentrating hormone directly inhibits GnRH neurons and blocks kisspeptin activation, linking energy balance to reproduction. Proceedings of the National Academy of Sciences. 2009;106(40):17217-22.
76. Smith DG, Davis RJ, Rorick-Kehn L, Morin M, Witkin JM, McKinzie DL, et al. Melanin-concentrating hormone-1 receptor modulates neuroendocrine, behavioral, and corticolimbic neurochemical stress responses in mice. Neuropsychopharmacology. 2006;31(6):1135-45.
77. Hökfelt T, Fuxe K. Effects of prolactin and ergot alkaloids on the tubero-infundibular dopamine (DA) neurons. Neuroendocrinology. 1972;9(2):100-22.
78. Brimblecombe KR, Cragg SJ. The striosome and matrix compartments of the striatum: a path through the labyrinth from neurochemistry toward function. ACS Chemical Neuroscience. 2016;8(2):235-42.
79. Segal-Lieberman G, Bradley RL, Kokkotou E, Carlson M, Trombly DJ, Wang X, et al. Melanin-concentrating hormone is a critical mediator of the leptin-deficient phenotype. Proceedings of the National Academy of Sciences. 2003;100(17):10085-90.
80. Sanchez M, Baker B, Celis M. Melanin-concentrating hormone (MCH) antagonizes the effects of α-MSH and neuropeptide EI on grooming and locomotor activities in the rat. Peptides. 1997;18(3):393-6.
81. Domingos AI, Sordillo A, Dietrich MO, Liu Z-W, Tellez LA, Vaynshteyn J, et al. Hypothalamic melanin concentrating hormone neurons communicate the nutrient value of sugar. eLife. 2013;2:e01462.

82. Alvarez-Buylla A, Garcıa-Verdugo JM. Neurogenesis in adult subventricular zone. Journal of Neuroscience. 2002;22(3):629-34.
83. Snyder JS, Choe JS, Clifford MA, Jeurling SI, Hurley P, Brown A, et al. Adult-born hippocampal neurons are more numerous, faster maturing, and more involved in behavior in rats than in mice. Journal of Neuroscience. 2009;29(46):14484-95.
84. Pan J, Snell W. The primary cilium: keeper of the key to cell division. Cell. 2007;129(7):1255-7.
85. Berbari NF, O'Connor AK, Haycraft CJ, Yoder BK. The primary cilium as a complex signaling center. Current Biology. 2009;19(13):R526-R35.
86. Contant C, Umbriaco D, Garcia S, Watkins K, Descarries L. Ultrastructural characterization of the acetylcholine innervation in adult rat neostriatum. Neuroscience. 1996;71(4):937-47.
87. Séguéla P, Watkins KC, Descarries L. Ultrastructural relationships of serotonin axon terminals in the cerebral cortex of the adult rat. Journal of Comparative Neurology. 1989;289(1):129-42.
88. Descarries L, Alain B, Watkins KC. Serotonin nerve terminals in adult rat neocortex. Brain Research. 1975;100(3):563-88.
89. Descarries L, Gisiger V, Steriade M. Diffuse transmission by acetylcholine in the CNS. Progress in Neurobiology. 1997;53(5):603-25.
90. Descarries L, Watkins KC, Lapierre Y. Noradrenergic axon terminals in the cerebral cortex of rat. III. Topometric ultrastructural analysis. Brain research. 1977;133(2):197-222.
91. Myers R, Hoch D. 14 C-dopamine microinjected into the brain-stem of the rat: dispersion kinetics, site content and functional dose. Brain research bulletin. 1978;3(6):601-9.
92. Jansson A, Descarries L, Cornea-Hébert V, Riad M, Vergé D, Bancila M, et al. Transmitter-receptor mismatches in central dopamine, serotonin, and neuropeptide systems. The neuronal environment: Springer; 2002. p. 83-108.
93. Fuxe K, Rivera A, Jacobsen K, Höistad M, Leo G, Horvath T, et al. Dynamics of volume transmission in the brain. Focus on catecholamine and opioid peptide communication and the role of uncoupling protein 2. Journal of neural transmission. 2005;112(1):65-76.
94. Agnati L, Zunarelli E, Genedani S, Fuxe K. On the existence of a global molecular network enmeshing the whole central nervous system: physiological and pathological implications. Current Protein and Peptide Science. 2006;7(1):3-15.
95. Jaffe EH, Marty A, Schulte A, Chow RH. Extrasynaptic vesicular transmitter release from the somata of substantia nigra neurons in rat midbrain slices. Journal of Neuroscience. 1998;18(10):3548-53.
96. Trueta C, De-Miguel FF. Extrasynaptic exocytosis and its mechanisms: a source of molecules mediating volume transmission in the nervous system. Frontiers in physiology. 2012;3:319.
97. Patel JC, Witkovsky P, Avshalumov MV, Rice ME. Mobilization of calcium from intracellular stores facilitates somatodendritic dopamine release. Journal of Neuroscience. 2009;29(20):6568-79.
98. Huang L-Y, Neher E. Ca 2+-dependent exocytosis in the somata of dorsal root ganglion neurons. Neuron. 1996;17(1):135-45.
99. Yao Y, Fu LY, Zhang X, van den Pol AN. Vasopressin and oxytocin excite MCH neurons, but not other lateral hypothalamic GABA neurons. Am J Physiol Regul Integr Comp Physiol. 2012;302(7):R815-24.

100. Parsons MP, Hirasawa M. GIRK channel-mediated inhibition of melanin-concentrating hormone neurons by nociceptin/orphanin FQ. Journal of neurophysiology. 2011;105(3):1179-84.
101. Hassani OK, Lee MG, Jones BE. Melanin-concentrating hormone neurons discharge in a reciprocal manner to orexin neurons across the sleep–wake cycle. Proceedings of the National Academy of Sciences. 2009;106(7):2418-22.
102. Konadhode RR, Pelluru D, Shiromani PJ. Neurons containing orexin or melanin concentrating hormone reciprocally regulate wake and sleep. Frontiers in systems neuroscience. 2015;8:244.

Appendix A

Copyright Permissions

The Journal of Comparative Neurology

Published by Wiley (the "Owner")

COPYRIGHT TRANSFER AGREEMENT

Date: May 31, 2019

Contributor name: JACKSON C. BITTENCOURT

Contributor address:

Manuscript number: JCN-19-0030.R2

Re: Manuscript entitled Melanin-concentrating hormone peptidergic system: comparative morphology between muroid species (the "Contribution")

for publication in The Journal of Comparative Neurology (the "Journal")

published by Wiley Periodicals, Inc. ("Wiley")

Dear Contributor(s):

Thank you for submitting your Contribution for publication. In order to expedite the editing and publishing process and enable the Owner to disseminate your Contribution to the fullest extent, we need to have this Copyright Transfer Agreement executed. If the Contribution is not accepted for publication, or if the Contribution is subsequently rejected, this Agreement shall be null and void.
Publication cannot proceed without a signed copy of this Agreement.

A. COPYRIGHT

1. The Contributor assigns to the Owner, during the full term of copyright and any extensions or renewals, all copyright in and to the Contribution, and all rights therein, including but not limited to the right to publish, republish, transmit, sell, distribute and otherwise use the Contribution in whole or in part in electronic and print editions of the Journal and in derivative works throughout the world, in all languages and in all media of expression now known or later developed, and to license or permit others to do so. For the avoidance of doubt, "Contribution" is defined to only include the article submitted by the Contributor for publication in the Journal and does not extend to any supporting information submitted with or referred to in the Contribution ("Supporting Information"). To the extent that any Supporting Information is submitted to the Journal for online hosting, the Owner is granted a perpetual, non-exclusive license to host and disseminate this Supporting Information for this purpose.

2. Reproduction, posting, transmission or other distribution or use of the final Contribution in whole or in part in any medium by the Contributor as permitted by this Agreement requires a citation to the Journal suitable in form and content as follows: (Title of Article, Contributor, Journal Title and Volume/Issue, Copyright © [year], copyright owner as specified in the Journal, Publisher). Links to the final article on the publisher website are encouraged where appropriate.

B. RETAINED RIGHTS

Notwithstanding the above, the Contributor or, if applicable, the Contributor's employer, retains all proprietary rights other than copyright, such as patent rights, in any process, procedure or article of manufacture described in the Contribution.

C. PERMITTED USES BY CONTRIBUTOR

1. Submitted Version. The Owner licenses back the following rights to the Contributor in the version of the Contribution as originally submitted for publication (the "Submitted Version"):

> **a.** The right to self-archive the Submitted Version on the Contributor's personal website, place in a not for profit subject-based preprint server or repository or in a Scholarly Collaboration Network (SCN) which has signed up to the STM article sharing principles [http://www.stm-assoc.org/stm-consultations/scn-consultation-2015/] ("Compliant SCNs"), or in the Contributor's company/ institutional repository or archive. This right extends to both intranets and the Internet. The Contributor may replace the Submitted Version with the Accepted Version, after any relevant embargo period as set out in paragraph C.2(a) below has elapsed. The Contributor may wish to add a note about acceptance by the Journal and upon publication it is recommended that Contributors add a Digital Object Identifier (DOI) link back to the Final Published Version.
>
> **b.** The right to transmit, print and share copies of the Submitted Version with colleagues, including via Compliant SCNs, provided that there is no systematic distribution of the Submitted Version, e.g. posting on a listserve, network (including SCNs which have not signed up to the STM sharing principles) or automated delivery.

2. Accepted Version. The Owner licenses back the following rights to the Contributor in the version of the Contribution that has been peer-reviewed and accepted for publication, but not final (the "Accepted Version"):

> **a.** The right to self-archive the Accepted Version on the Contributor's personal website, in the Contributor's company/institutional repository or archive, in Compliant SCNs, and in not for profit subject-based repositories such as PubMed Central, subject to an embargo period of 12 months for scientific, technical and medical (STM) journals and 24 months for social science and humanities (SSH) journals following publication of the Final Published Version. There are separate arrangements with certain funding agencies governing reuse of the Accepted Version as set forth at the following website: http://www.wileyauthors.com/funderagreements. The Contributor may not update the Accepted Version or replace it with the Final Published Version. The Accepted Version posted must contain a legend as follows: This is the accepted version of the following article: FULL CITE, which has been published in final form at [Link to final article]. This article may be used for non-commercial purposes in accordance with the Wiley Self-Archiving Policy [http://www.wileyauthors.com/self-archiving].
>
> **b.** The right to transmit, print and share copies of the Accepted Version with colleagues, including via Compliant SCNs (in private research groups only before the embargo and publicly after), provided that there is no systematic distribution of the Accepted Version, e.g. posting on a listserve, network (including SCNs which have not signed up to the STM sharing principles) or automated delivery.

3. Final Published Version. The Owner hereby licenses back to the Contributor the following rights with respect to the final published version of the Contribution (the "Final Published Version"):

> **a.** Copies for colleagues. The personal right of the Contributor only to send or transmit individual copies of the Final Published Version in any format to colleagues upon their specific request, and to share copies in private sharing groups in Compliant SCNs, provided no fee is charged, and further provided that there is no systematic external or public distribution of the Final Published Version, e.g. posting on a listserve, network or automated delivery.

b. Re-use in other publications. The right to re-use the Final Published Version or parts thereof for any publication authored or edited by the Contributor (excluding journal articles) where such re-used material constitutes less than half of the total material in such publication. In such case, any modifications must be accurately noted.

c. Teaching duties. The right to include the Final Published Version in teaching or training duties at the Contributor's institution/place of employment including in course packs, e-reserves, presentation at professional conferences, in-house training, or distance learning. The Final Published Version may not be used in seminars outside of normal teaching obligations (e.g. commercial seminars). Electronic posting of the Final Published Version in connection with teaching/training at the Contributor's company/institution is permitted subject to the implementation of reasonable access control mechanisms, such as user name and password. Posting the Final Published Version on the open Internet is not permitted.

d. Oral presentations. The right to make oral presentations based on the Final Published Version.

4. Article Abstracts, Figures, Tables, Artwork and Selected Text (up to 250 words).

a. Contributors may re-use unmodified abstracts for any non-commercial purpose. For online uses of the abstracts, the Owner encourages but does not require linking back to the Final Published Version.

b. Contributors may re-use figures, tables, artwork, and selected text up to 250 words from their Contributions, provided the following conditions are met:

(i) Full and accurate credit must be given to the Final Published Version.

(ii) Modifications to the figures and tables must be noted. Otherwise, no changes may be made.

(iii) The re-use may not be made for direct commercial purposes, or for financial consideration to the Contributor.

(iv) Nothing herein will permit dual publication in violation of journal ethical practices.

D. CONTRIBUTIONS OWNED BY EMPLOYER

1. If the Contribution was written by the Contributor in the course of the Contributor's employment (as a "work-made-for-hire" in the course of employment), the Contribution is owned by the company/institution which must execute this Agreement (in addition to the Contributor's signature). In such case, the company/institution hereby assigns to the Owner, during the full term of copyright, all copyright in and to the Contribution for the full term of copyright throughout the world as specified in paragraph A above.

2. In addition to the rights specified as retained in paragraph B above and the rights granted back to the Contributor pursuant to paragraph C above, the Owner hereby grants back, without charge, to such company/institution, its subsidiaries and divisions, the right to make copies of and distribute the Final Published Version internally in print format or electronically on the Company's internal network. Copies so used may not be resold or distributed externally. However, the company/institution may include information and text from the Final Published Version as part of an information package included with software or other products offered for sale or license or included in patent applications. Posting of the Final Published Version by the company/institution on a public access website may only be done with written permission, and payment of any applicable fee(s). Also, upon payment of the applicable reprint fee, the company/institution may distribute print copies of the Final Published Version externally.

E. GOVERNMENT CONTRACTS

In the case of a Contribution prepared under U.S. Government contract or grant, the U.S. Government may reproduce, without charge, all or portions of the Contribution and may authorize others to do so, for official U.S. Government purposes only, if the U.S. Government contract or grant so requires. (U.S. Government, U.K. Government, and other government employees: see notes at end.)

F. COPYRIGHT NOTICE

The Contributor and the company/institution agree that any and all copies of the Final Published Version or any part thereof distributed or posted by them in print or electronic format as permitted herein will include the notice of copyright as stipulated in the Journal and a full citation to the Journal.

G. CONTRIBUTOR'S REPRESENTATIONS

The Contributor represents that: (i) the Contribution is the Contributor's original work, all individuals identified as Contributors actually contributed to the Contribution, and all individuals who contributed are included; (ii) if the Contribution was prepared jointly, the Contributor has informed the co-Contributors of the terms of this Agreement and has obtained their signed written permission to execute this Agreement on their behalf; (iii) the Contribution is submitted only to this Journal and has not been published before, has not been included in another manuscript, and is not currently under consideration or accepted for publication elsewhere; (iv) if excerpts from copyrighted works owned by third parties are included, the Contributor shall obtain written permission from the copyright owners for all uses as set forth in the standard permissions form or the Journal's Author Guidelines, and show credit to the sources in the Contribution; (v) the Contribution and any submitted Supporting Information contains no libelous or unlawful statements, does not infringe upon the rights (including without limitation the copyright, patent or trademark rights) or the privacy of others, or contain material or instructions that might cause harm or injury and only utilize data that has been obtained in accordance with applicable legal requirements and Journal policies; (vi) there are no conflicts of interest relating to the Contribution, except as disclosed. Accordingly, the Contributor represents that the following information shall be clearly identified on the title page of the Contribution: (1) all financial and material support for the research and work; (2) any financial interests the Contributor or any co-Contributors may have in companies or other entities that have an interest in the information in the Contribution or any submitted Supporting Information (e.g., grants, advisory boards, employment, consultancies, contracts, honoraria, royalties, expert testimony, partnerships, or stock ownership); and (3) indication of no such financial interests if appropriate.

Wiley reserves the right, notwithstanding acceptance, to require changes to the Contribution, including changes to the length of the Contribution, and the right not to publish the Contribution if for any reason such publication would in the reasonable judgment of Wiley, result in legal liability or violation of journal ethical practices.

H. USE OF INFORMATION

The Contributor acknowledges that, during the term of this Agreement and thereafter, the Owner (and Wiley where Wiley is not the Owner) may process the Contributor's personal data, including storing or transferring data outside of the country of the Contributor's residence, in order to process transactions related to this Agreement and to communicate with the Contributor. By entering into this Agreement, the Contributor agrees to the processing of the Contributor's personal data (and, where applicable, confirms that the Contributor has obtained the permission from all other contributors to process their personal data). Wiley shall comply with all applicable laws, statutes and regulations relating to data protection and privacy and shall process such personal data in accordance with Wiley's Privacy Policy located at: https://www.wiley.com/en-us/privacy.

[X] I agree to the COPYRIGHT TRANSFER AGREEMENT as shown above, consent to execution and delivery of the Copyright Transfer Agreement electronically and agree that an electronic signature shall be given the same legal force as

a handwritten signature, and have obtained written permission from all other contributors to execute this Agreement on their behalf.

Contributor's signature (type name here): JACKSON CIONI BITTENCOURT

Date: May 31, 2019

SELECT FROM OPTIONS BELOW:

[X] Contributor-owned work

[ ] U.S. Government work

Note to U.S. Government Employees

*A contribution prepared by a U.S. federal government employee as part of the employee's official duties, or which is an official U.S. government publication, is called a "U.S. government work", and is in the public domain in the United States. If the Contribution was not prepared as part of the employee's duties or is not an official U.S. government publication, it is not a U.S. government work. If **all** authors are U.S. government employees, there is no copyright to transfer and Paragraph A.1 will not apply. Contributor acknowledges that the Contribution will be published in the United States and other countries. Please sign the form to confirm Contributor Representations. If at least one author is **not** a U.S. government employee, then the non-government author should also sign the form, indicating transfer of those rights which that author has and selecting the appropriate additional ownership selection option. If more than one author is not a U.S. government employee, one may sign on behalf of the others.*

[ ] U.K. Government work (Crown Copyright)

Note to U.K. Government Employees

For Crown Copyright this form should be signed in the Contributor's signatures section above by the appropriately authorised individual and uploaded to the Wiley Author Services Dashboard. For production editor contact details please visit the Journal's online author guidelines. *The rights in a contribution prepared by an employee of a UK government department, agency or other Crown body as part of his/her official duties, or which is an official government publication, belong to the Crown and must be made available under the terms of the Open Government Licence. Contributors must ensure they comply with departmental regulations and submit the appropriate authorisation to publish. If your status as a government employee legally prevents you from signing this Agreement, please contact the Journal production editor. If this selection does not apply to at least one author in the group, this author should also sign the form, indicating transfer of those rights which that author has and selecting the appropriate additional ownership selection option. If this applies to more than one author, one may sign on behalf of the others.*

[ ] Other

Including Other Government work or Non-Governmental Organisation work

Note to Non-U.S., Non-U.K. Government Employees or Non-Governmental Organisation Employees

For Other Government or Non-Governmental Organisation work this form should be signed in the Contributor's signatures section above by the appropriately authorised individual and uploaded to the Wiley Author Services Dashboard. For production editor contact details please visit the Journal's online author guidelines. *If you are employed by the Australian Government, the World Bank, the World Health Organization, the International Monetary Fund, the European Atomic Energy Community, the Jet Propulsion Laboratory at California Institute of Technology, the Asian Development Bank, the Bank of International Settlements, or are a Canadian Government civil servant, please download a copy of the license agreement from http://www.wileyauthors.com/licensingFAQ and upload the form to the Wiley Author Services Dashboard. If your*

status as a government or non-governmental organisation employee legally prevents you from signing this Agreement, please contact the Journal production editor. If this selection does not apply to at least one author in the group, this author should also sign the form, indicating transfer of those rights which that author has and selecting the appropriate additional ownership selection option. If this applies to more than one author, one may sign on behalf of the others.

Name of Government/Non-Governmental Organisation:

_____

[ ] Company/institution owned work (made for hire in the course of employment)

For "work made for hire" this form should be signed and uploaded to the Wiley Author Services Dashboard.

For production editor contact details please visit the Journal's online author guidelines. *If you are an employee of Amgen, please download a copy of the company addendum from http://www.wileyauthors.com/licensingFAQ and return your signed license agreement along with the addendum. If this selection does not apply to at least one author in the group, this author should also sign the form, indicating transfer of those rights which that author has and selecting the appropriate additional ownership selection option. If this applies to more than one author, one may sign on behalf of the others.*

Name of Company/Institution:

_____

Authorized Signature of Employer: _____

Date: _____

Signature of Employee: _____

Date: _____

2. Manuscript Guidelines

2.1. Open access and copyright

All Frontiers articles from July 2012 onwards are published with open access under the CC-BY Creative Commons attribution license (the current version is CC-BY, version 4.0 http://creativecommons.org/licenses/by/4.0/ (https://creativecommons.org/licenses/by/4.0/)). This means that the author(s) retain copyright, but the content is free to download, distribute and adapt for commercial or non-commercial purposes, given appropriate attribution to the original article.

Upon submission, author(s) grant Frontiers an exclusive license to publish, including to display, store, copy and reuse the content. The CC-BY Creative Commons attribution license enables anyone to use the publication freely, given appropriate attribution to the author(s) and citing Frontiers as the original publisher. The CC-BY Creative Commons attribution license does not apply to third-party materials that display a copyright notice to prohibit copying. Unless the third-party content is also subject to a CC-BY Creative Commons attribution license, or an equally permissive license, the author(s) must comply with any third-party copyright notices.

Preprint Policy

Frontiers' supportive preprint policy encourages full open access at all stages of a research paper, to share and generate the knowledge researchers need to support their work. Authors publishing in Frontiers journals may share their work ahead of submission to a peer-reviewed journal, as well as during the Frontiers review process, on repositories or pre-print servers

(such as ArXiv, PeerJ Preprints, OSF and others), provided that the server imposes no restrictions upon the author's full copyright and re-use rights. Also note that any manuscript files shared after submission to Frontiers journals, during the review process, must not contain the Frontiers logo or branding.

Correct attribution of the original source in repositories or pre-print servers must be included on submission, or added at re-submission if the deposition is done during the review process.

If the article is published, authors are then strongly encouraged to link from the preprint server to the Frontiers publication to enable readers to find, access and cite the final peer-reviewed version. Please note that we cannot consider for publication content that has been previously published, or is already under review, within a scientific journal, book or similar entity.

2.2. Registration with Frontiers

Please note that the corresponding and all submitting authors MUST register (https://www.frontiersin.org/Registration/Register.aspx) with Frontiers before submitting an article. You must be logged in to your personal Frontiers Account to submit an article.

For any co-author who would like his/her name on the article abstract page and PDF to be linked to a Frontiers profile on the Loop network (http://loop.frontiersin.org/about), please ensure to register (https://www.frontiersin.org/Registration/Register.aspx) before the final publication of the paper.

2.3. Manuscript Requirements and Style Guide